New Hampshire DOT

Research

Layer Coefficients for New Hampshire Department of Transportation Pavement Design

Final Report

Prepared by University of New Hampshire Department of Civil and Environmental Engineering
for the New Hampshire Department of Transportation, in cooperation with the
U.S. Department of Transportation, Federal Highway Administration

Technical Report Documentation Page

1. Report No.	2. Gov. Accession No.	3. Recipient's Catalog No.
FHWA-NH-RD-26962N		

4. Title and Subtitle	5. Report Date
Layer Coefficients for New Hampshire Department of Transportation Pavement Design	June 2019
	6. Performing Organization Code

7. Author(s)	8. Performing Organization Report No.
E.V. Dave, J.E. Sias, R. Nemati	

9. Performing Organization Name and Address	10. Work Unit No. (TRAIS)
University of New Hampshire College of Engineering and Physical Sciences Department of Civil and Environmental Engineering 33 Academic Way, Durham NH 03824	11. Contract or Grant No. 26962N, A004(533)

12. Sponsoring Agency Name and Address	13. Type of Report and Period Covered
New Hampshire Department of Transportation Bureau of Materials & Research Box 483, 5 Hazen Drive Concord, New Hampshire 03302-0483	FINAL REPORT
	14. Sponsoring Agency Code

15. Supplementary Notes

Conducted in cooperation with the U.S. DEPARTMENT OF TRANSPORTATION, FEDERAL HIGHWAY ADMINISTRATION

16. Abstract

At present, New Hampshire Department of Transportation (NHDOT) has adopted AASHTO empirical pavement design approach. This research focused on updating the layer coefficients (a-value) of the asphalt mixtures using different mechanistic and performance based measures. A set of 18 commonly used mixtures in New Hampshire were selected for performance testing and evaluation of structural contribution in terms of layer coefficients. In order to develop the layer coefficients, comprehensive research was performed on the performance and properties of the mixtures through different mechanistic based laboratory testing methods. In addition, mixtures from the New England region were used to develop and validate three novel performance index parameters for rutting, fatigue and transverse cracking. The developed parameters were incorporated with the field distress data such as International Roughness Index (IRI) in order to develop mechanistically informed layer coefficients for New Hampshire flexible pavement design approach.

17. Key Words	18. Distribution Statement
Asphalt, asphalt mixtures, layer coefficient, pavement, pavement design, performance based design. .	No Restrictions. This document is available to the public through the National Technical Information Service (NTIS), Springfield, Virginia, 22161.

19. Security Classif. (of this report)	20. Security Classif. (of this page)	21. No. of Pages	22. Price
UNCLASSIFIED	UNCLASSIFIED	163	

Layer Coefficients for New Hampshire Department of Transportation Pavement Design

Prepared by:
University of New Hampshire
College of Engineering and Physical Sciences
Department of Civil and Environmental Engineering
Durham, New Hampshire

Prepared for:
New Hampshire Department of Transportation
Bureau of Materials & Research
Concord, New Hampshire

DISCLAIMER

Layer Coefficients for New Hampshire Department of Transportation Pavement Design

FINAL REPORT

Prepared by:

Eshan V. Dave, Jo E. Sias and Rasool Nemati,
Department of Civil and Environmental Engineering
University of New Hampshire

June 2019

Published by:

New Hampshire Department of Transportation
Bureau of Materials and Research
5 Hazen Drive
Concord, NH 03302-0483

ACKNOWLEDGMENTS

This research study would not have been possible without the contribution of a number of individuals. We sincerely acknowledge significant efforts from Eric Thibodeau from Pavement Management section of the NHDOT Bureau of Materials and Research for his continuous input during the course of this study, organizing material sampling plans and for overseeing the pavement performance data gathering efforts. Authors would like to acknowledge all the efforts of Patrick Colburn (also from NHDOT Bureau of Materials and Research) for data-mining the NHDOT Pavement Management System to gather necessary data that was used in this research. Matt Courser (from Materials Section of the NHDOT Bureau of Materials and Research) played an instrumental role in this project as he coordinated the material sampling effort and made it possible for researchers to obtain the plant produced asphalt mixtures for evaluations. Support from Beran Black and Ryan Worsman in their technical inputs to the project is acknowledged.

We would also like to sincerely thank the NHDOT Research Section for their help in administration of this project. Specifically, Ann Scholz and Deirdre Nash (and formerly Beth Klemann) for all their insight and guidance during the course of project.

TABLE OF CONTENTS

CHAPTER 1: INTRODUCTION 1

1.1 BACKGROUND AND MOTIVATION 1

1.2 NEW HAMPSHIRE DEPARTMENT OF TRANSPORTATION PAVEMENT DESIGN APPROACH AND LAYER COEFFICIENTS 1

1.3 RESEARCH APPROACH 2

1.4 ORGANIZATION OF THE REPORT 3

1.5 REFERENCES 5

CHAPTER 2: LITERATURE REVIEW 6

2.1 AASHTO EMPIRICAL DESIGN GUIDE 6

2.2 AASHTO 1993 DESIGN VARIABLES 7

2.2.1 EQUIVALENT SINGLE AXLE LOAD (ESAL)- $\log_{w18}$ 7

2.2.2 RELIABILITY 7

2.2.3 PRESENT SERVICEABILITY INDEX (PSI) 7

2.2.4 STRUCTURAL NUMBER (SN) 8

2.2.5 SOIL RESILIENT MODULUS 8

2.3 LAYER COEFFICIENT 9

2.4 LAYER COEFFICIENT CALIBRATION 9

2.4.1 PAVEMENT EQUIVALENT STRUCTURAL RESPONSE 9

2.4.2 PAVEMENT PERFORMANCE 10

2.4.3 USE OF MECHANISTIC-EMPIRICAL PAVEMENT DESIGN GUIDE 10

2.4.4 MATERIAL CHARACTERIZATION 10

2.4.5 FALLING WEIGHT DEFLECTOMETER 12

2.5 REVIEW OF LAYER COEFFICIENTS USED BY OTHER AGENCIES 12

2.6 LITERATURE REVIEW SUMMARY 13

2.7 REFERENCES 14

CHAPTER 3: PROJECTS, MATERIALS AND TEST METHODS 16

3.1 PROJECTS AND MATERIALS 16

3.2 LABORATORY TEST METHODS 19

3.2.1 RESILIENT MODULUS TEST 19

3.2.2 COMPLEX MODULUS TEST 19

3.2.3 SEMI-CIRCULAR BEND (SCB) TEST 20

3.2.4 DIRECT TENSION CYCLIC FATIGUE TEST 21

3.2.5 DISK-SHAPED COMPACT TENSION TEST (DCT) 22

3.3 REFERENCES 23

CHAPTER 4: LABORATORY EVALUATION RESULTS AND ANALYSIS 25

4.1 INTRODUCTION 25

4.2 RESILIENT MODULUS (M_r) 27

4.3 COMPLEX MODULUS (|E*| AND PHASE ANGLE) 29

4.4 SEMI-CIRCULAR BEND TEST 31

4.5 DIRECT TENSION CYCLIC FATIGUE 34

4.6 DISK-SHAPED COMPACT TENSION TEST 37

4.7 STATISTICAL CORRELATION OF THE PERFORMANCE INDEX PARAMETERS 39

4.8 SUMMARY OF TEST RESULTS AND STATISTICAL ANALYSIS 41

4.9 REFERENCES 43

CHAPTER 5: PERFORMANCE INDICIES FOR ASPHALT MIXTURES 45

5.1 INTRODUCTION 45

5.2 DEVELOPMENT OF A COMPLEX MODULUS BASED RUTTING INDEX PARAMETER FOR ASPHALT MIXTURES 45

5.2.1 INTRODUCTION AND BACKGROUND 45

5.2.2 MATERIALS FOR MIX SET-1 49

5.2.3 COMPLEX MODULUS MASTER-CURVES 51

5.2.4 RESULTS AND DISCUSSION 54

5.2.5 EVALUATION OF THE RUTTING INDICES THROUGH FIELD RUTTING DATA (MIX SET-2) 55

5.2.6 EVALUATION OF THE RUTTING INDICES THROUGH MIXTURE DESIGN PROPERTIES VARIATIONS (MIX SET-3) 58

5.2.7 CORRELATION OF INDEX PARAMETERS WITH THE HWTT/FIELD RUT MEASUREMENTS 61

5.2.8 EVALUATION OF THE NHDOT PROJECT MIXTURES THROUGH THE DEVELOPED RUTTING INDEX PARAMETER 63

5.2.9 SUMMARY AND CONCLUSIONS FOR RUTTING PERFORMNCE INDEX 63

5.3 DEVELOPMENT OF A DAMAGE GROWTH RATE-BASED FATIGUE FAILURE CRITERION FOR ASPHALT MIXTURES USING SIMPLIFIED-VISCOELASTIC CONTINUUM DAMAGE THEORY 64

5.3.1 INTRODUCTION AND BACKGROUND 64

5.3.2 MATERIAL AND TESTING 65

5.3.3 FIELD CONDITIONS 65

5.3.4 RESULTS OF THE DIRECT TENSION CYCLIC FATIGUE 66

5.3.5 DEVELOPMENT OF THE DAMAGE-GROWTH RATE BASED FATIGUE FAILURE CRITERION 68

5.3.6 COMPARISON OF THE PROPOSED DAMAGE GROWTH RATE FATIGUE CRITERIA ($C_{N_f}^S$) WITH CURRENTLY AVAILABLE CRITERIA (N_f @ G^R=100, D^R AND S_{app}) 70

5.3.7 EVALUATION OF THE NHDOT PROJECT MIXTURES THROUGH THE PROPOSED FAILURE CRITERION ($C_{N_f}^S$) 73

5.3.8 EVALUATING THE FIELD PERFORMANCE OF THE NHDOT PROJECT MIXTURES THROUGH THE PROPOSED FAILURE CRITERION ($C_{N_f}^S$) 73

5.3.9 SUMMARY AND CONCLUSIONS FOR FATIGUE FAILURE CRITERION 75

5.4 DEVELOPMENT OF A RATE-DEPENDENT CUMULATIVE WORK AND INSTANTANEOUS POWER BASED ASPHALT CRACKING PERFORMANCE INDEX 75

5.4.1 INTRODUCTION AND BACKGROUND 75

5.4.2 DEVELOPMENT OF THE RATE DEPENDENT CRACKING INDEX (RDCI) 79

5.4.3 MATERIALS AND TESTING 83

5.4.4 RESULTS AND DISCUSSION 84

5.4.5 EVALUATION OF THE BINDER AND BASE COURSE MIXTURES FROM THIS STUDY USING RDCI PARAMETER 90

5.4.6 SUMMARY AND CONCLUSIONS FOR TRANSVERSE CRACKING PERFORMANCE INDEX 90

5.5 SUMMARY OF PERFORMANCE INDICES FOR ASPHALT MIXTURES 92

5.6 REFERENCES 94

CHAPTER 6: DEVELOPMENT OF LAYER COEFFICIENTS 99

6.1 INTRODUCTION 99

6.2 RESILIENT MODULUS BASED LAYER COEFFICIENTS 100

6.3 FIELD DISTRESS DATA ANALYSIS 100

6.4 BACK-CALCULATION OF LAYER COEFFICIENTS FROM FIELD IRI MEASUREMENTS 103

6.5 INCORPORATING THE LABORATORY PERFORMANCE TEST RESULTS IN DEVELOPMENT OF LAYER COEFFICIENTS FOR WEARING COURSE MIXTURES 109

6.6 CORRELATION OF LAYER COEFFICIENTS WITH MIXTURE PROPERTIES 113

6.7 MIXTURE PROPERTY BASED PREDICTIVE MODEL FOR LAYER COEFFICIENTS 117

6.8 DEVELOPMENT OF LAYER COEFFICIENTS FOR BINDER AND BASE COURSE MIXTURES 120

6.9 REFERENCES 123

CHAPTER 7: SUMMARY, CONCLUSIONS AND RECOMMENDATIONS 124

7.1 SUMMARY 124

7.2 CONCLUSIONS 125

7.3 RECOMMENDATIONS 126

7.3.1 RECOMMENDATIONS FOR MIXTURE DESIGN AND PERFORMANCE INDEX PARAMETERS 127

7.3.2 RECOMMENDATIONS FOR LAYER COEFFICIENTS 130

APPENDIX A TESTING RESULT 132

LIST OF FIGURES

Figure 1-1 Research approach to develop layer coefficients for NHDOT pavement design 3

Figure 2-1 Estimating layer coefficient of dense-graded asphalt concrete based on elastic resilient modulus a) Resilient modulus unit as psi b)resilient modulus unit as MPa 11

Figure 3-1 Resilient modulus test result and setup 19

Figure 3-2 Complex modulus test result and setup 20

Figure 3-3 Semi-circular bend test result and setup 21

Figure 3-4 Damage characteristic curve and direct tension cyclic fatigue test setup 22

Figure 3-5 Disk-shaped compact tension test result, setup and specimen geometry 23

Figure 4-1 M_r test results (error bars represent one standard deviation interval) 28

Figure 4-2 |E*|and phase angle master-curves constructed with shifted raw data 31

Figure 4-3 Fracture energy plots 32

Figure 4-4 Flexibility Index plots 33

Figure 4-5 N_f @G^R=100 fatigue failure criterion plots 34

Figure 4-6 D^R fatigue failure criterion plots 35

Figure 4-7 S_{app} fatigue failure criterion plots 35

Figure 4-8 DCT Fracture Energy (G_f) plots (number in box indicate test temperature in ˚C) 37

Figure 4-9 Fracture Strain Tolerance (FST) plots 38

Figure 4-10 Mahalanobis distance of the study mixtures 40

Figure 5-1 Typical dynamic modulus and phase angle master-curves for asphalt mixtures. Selected points on the master-curves to develop the rutting index parameters 48

Figure 5-2 HWTT test results for the first set of study mixtures 50

Figure 5-3 Fitted dynamic modulus master-curves of the first set of mixtures 52

Figure 5-4 Fitted phase angle master-curves of the first set of mixtures 52

Figure 5-5 Fitted |E*|master-curves of the second set of mixtures 57

Figure 5-6 Fitted phase angle master-curves of the second set of mixtures 57

Figure 5-7 Fitted |E*|master-curves of the third set of mixtures 59

Figure 5-8 Fitted phase angle master-curves of the third set of mixtures 60

Figure 5-9 Correlation between the index parameters and the measured rut depths 62

Figure 5-10 Evaluation of the NHDOT project mixtures through the developed rutting index parameter 63

Figure 5-11 Normalized field fatigue cracking 66

Figure 5-12 Damage characteristic curves (DCC) 67

Figure 5-13 N_f @ G^R =100 fatigue failure criteria 67

Figure 5-14 D^R fatigue failure criterion 68

Figure 5-15 S_{app} fatigue failure criterion 68

Figure 5-16 a) Pseudo stiffness versus damage accumulation (C vs S), b) Pseudo stiffness versus loading cycle (C vs N) 69

Figure 5-17 $C^S_{N_f}$ versus N_f plots 71

Figure 5-18 Statistical correlation between the field cracking length and the proposed fatigue criterion 72

Figure 5-19 Evaluation of the NHDOT project mixtures through the developed fatigue index parameter $N_f@C^S_{N_f} = 100$ 73

Figure 5-20 Normalized field crack length for different mixtures in terms of meter per kilometer 74

Figure 5-21 Normalized field fatigue cracking performance versus proposed fatigue failure threshold($N_f@C^S_{N_f} = 100$) 74

Figure 5-22 Typical Load-LLD curve 76

Figure 5-23 Determination of cumulative work between time at peak load and 0.1 of peak load 82

Figure 5-24 Comparison between RDCI and FI 85

Figure 5-25 Comparison of coefficient of variations (COV) determined by cracking index parameters 87

Figure 5-26 Percent difference in COV for RDCI and FI with respect to COV for FI 87

Figure 5-27 Evaluating the sensitivity of FI and RDCI to aging 88

Figure 5-28 Comparison of coefficient of variations of the index parameters at different long-term oven aged levels 90

Figure 5-29 RDCI and FI comparison plots for NHDOT binder and base course mixtures from this study 90

Figure 6-1 Resilient modulus based layer coefficients 100

Figure 6-2 IRI versus time for different mixtures and projects: a) ARGG mixtures, b) 12.5mm NMAS mixtures, c) 9.5 mm NMAS mixtures 103

Figure 6-3 Binder performance grade specification map for New Hampshire 105

Figure 6-4 Flowchart to back-calculate the layer coefficients from field IRI data 106

Figure 6-5. Schematic summary of steps 2,3 and 4 to incorporate performance index parameters in development of layer coefficients 110

Figure 6-6 Nominal property based predicted a_{ave}-value for all the study surface mixtures 119

Figure 7-1 CMRI versus rut depth for I-93 study mixtures 128

Figure 7-2 Normalized Crack length vs $N_f@C_{N_f}^S = 100$ for I-93 study mixtures 128

Figure 7-3 Correlation between RDCI and FI 129

Figure 7-4 Performance space diagrams for NHDOT mixtures 130

LIST OF TABLES

Table 1-1 Currently adopted layer coefficients by NHDOT 2

Table 2-1 Layer coefficients used by other agencies 13

Table 3-1 Selected projects and mixtures 17

Table 3-2 Study mixtures design properties 18

Table 4-1 Mixture design properties used for statistical analysis 27

Table 4-2 Significant mix design properties affecting resilient modulus (M_r) 29

Table 4-3 Significant mix design properties affecting SCB G_f and FI 33

Table 4-4 Significant mix design properties affecting Simplified Viscoelastic Continuum Damage based fatigue performance indices (N_f @ G^R = 100, D^R and S_{app}) 36

Table 4-5 Significant mix design properties affecting disk-shaped compact tension test performance indices (G_f and FST) 39

Table 4-6 Pearson's correlations among performance index parameters (Italics and (W) indicate weak correlation, (M) indicate medium correlation and, bold and (S) indicate strong correlation) 41

Table 5-1 Description of the selected points on the master-curves for rutting assessment 49

Table 5-2 Properties of the first set of mixtures used to develop the rutting index parameters 50

Table 5-3 Proposed complex modulus based rutting index (CMRI) parameters to evaluate the rutting performance 53

Table 5-4 Calculated value and ranking of individual rutting index parameters for the first set of mixtures 55

Table 5-5 Mixture design and properties of the second set of mixtures to verify the index parameters . 56

Table 5-6 Values of Rutting Index Parameters for High RAP Pooled Fund Study Mixtures 58

Table 5-7 Properties of the third set of mixtures used to examine the index parameters based on altering the mix design properties 59

Table 5-8 Ranking is based on the varying binder content at constant air void level 61

Table 5-9 Ranking is based on the varying air void level at constant binder content 61

Table 5-10 Field core air void of the mixtures 65

Table 5-11 Pearson's correlation coefficients for the S-VECD based parameters. 70

Table 5-12 Mixture ranking order in accordance to different failure criterion 72

Table 5-13 Summary of mixture used in RDCI development 84

Table 5-14 Results from each pair of student's t-test at significance level of 0.05 86

Table 5-15 Statistical evaluation of cracking indices to distinguish the aging levels 89

Table 6-1 Defining the initial serviceability value based on construction quality and IRI values one year after construction. 102

Table 6-2 General design assumptions to back-calculate a-values from field data 104

Table 6-3 Layer coefficients of the binder and base course mixtures used in back-calculations (resilient modulus based for HMA and conventional NHDOT value for CCPR mixtures) 104

Table 6-4 Back-calculated layer coefficients from the field IRI data 108

Table 6-5 Layer coefficients at different reliability levels for ARGG and non-ARGG wearing course asphalt mixtures based on field IRI data 109

Table 6-6 Development of averaged and minimum performance base incorporated a-values for the wearing course mixtures 112

Table 6-7 Correlation matrix including ARGG mixtures 115

Table 6-8 Correlation matrix including only non-ARGG mixtures 116

Table 6-9 a_{ave}-value and a_{min}-value for non-ARGG mixtures 117

Table 6-10 Prediction model for a_{ave}-value 119

Table 6-11 Development of averaged and minimum performance base incorporated a-values for the binder and base course mixtures 121

EXECUTIVE SUMMARY

Asphalt mixture as the top most layer in the pavement structure is prone to different types of structural distresses such as rutting, fatigue and thermal cracking. Depending on the loading and climatic conditions, the asphalt layer thickness in flexible pavements can vary from 5 cm to over 30 cm. It is well known that the type and magnitude of structural responses (deformations, stresses and strains) vary throughout the pavement. Therefore, there is need for different types of asphalt mixtures with different production methods, each designed to handle specific types and magnitude of responses within the structure. This not only increases the design reliability but can also result in considerable savings in financial resources by optimizing material properties in each layer.

Within the pavement structure, and depending on the design thickness, the asphalt course is generally divided into three sublayers as the base, binder and wearing layers. The wearing course is usually made of smaller aggregate size and higher binder content to prevent both functional and structural distresses. The binder and base courses contain relatively coarser aggregates and lower binder content. The binder layer is placed directly under the wearing course to facilitate the construction of the wearing course and to distribute the traffic loads onto a larger area. This layer increases the overall pavement structural capacity and helps prevent the wearing course from different types of premature distresses. The asphalt base layer is very similar to the binder course in terms of the performance expectations. Base layers are used in addition to the binder layer in cases where the load magnitudes and repetitions call for a relatively thicker pavement. In this case the base layer provides a strong foundation for the overlying lifts to prevent or reduce the risk of rutting and fatigue related distresses.

To enhance reliability of pavement designs and to ensure high return on investment for agencies, it is paramount to use performance driven design philosophies such as mechanistic-empirical (M-E) design methods. However, these methods require intensive field and laboratory performance data for locally calibrating the damage transfer functions. For this reason, many State highway agencies prefer to use the empirical design methods such as AASHTO empirical design approach due to its simplicity and relatively high reliability. One of the major drawbacks of empirical methods such as the AASHTO approach is the absence of fundamental material properties in the design equations. In order to quantify the material's properties, AASHTO empirical method uses regression based structural coefficients called as layer coefficients (a-values) developed through the AASHO road test in early 1960s. However, since the traffic loading as well as material's properties and production methods have significantly changed since initial development of layer coefficients, it is necessary to reevaluate these coefficients through implementing mechanistic mixture characterization methods. Therefore, this research project proposed laboratory performance-based informed asphalt mixture layer coefficients to improve reliability of AASHTO empirical pavement design system used by New Hampshire Department of Transportation (NHDOT).

In order to design the experimental plan of the research study, a wide range of ongoing projects that use different types of rehabilitation methods and mixtures were evaluated for use in this study. The objective was to select a variety of the commonly used mixtures in New Hampshire that include diverse mixture design properties. In addition, the selected projects and mixtures are needed to represent all the conventional traffic levels, climatic conditions, cross sectional designs, production methods, aggregate

size and binder types, recycled asphalt pavement (RAP) amount and recycled binder ratio (RBR) as well as gyration levels. Based on these investigations and criteria, a set of 18 asphalt mixtures were selected for evaluations and performance-based laboratory testing. The mixtures include two asphalt rubber gap graded (ARGG), four cold central plant recycled (CCPR) mixtures as well as other different types of conventional and polymer modified hot mixed asphalt (HMA) mixtures used in wearing, binder, and base course layers. The laboratory testing plan included resilient modulus (M_r), complex modulus (E*), direct tension cyclic fatigue (S-VECD), semi-circular bend (SCB) and disk-shaped compact tension (DCT) tests. The selection of the testing suite was based on capturing the linear viscoelastic properties of asphalt mixtures to represent full range of in-service temperatures and loading frequencies as well as to conduct laboratory cracking performance tests. Cracking has been the predominant distress for NH roadways in recent years and thus cracking performance tests were necessary to be incorporated in the development of pavement design coefficients.

On the basis of the test results and analysis, the effect of asphalt mixture constituents and different production methods (hot vs cold) on the predicted performance were evaluated through use of various statistical approaches. Also, the correlations between different performance index parameters were investigated to determine the indices that can be used interchangeably. In addition, using a separate database of over 30 mixtures (outside the study mixtures), the precision and applicability of the current laboratory performance index parameters were investigated in terms of their correlations with the field distress data and discriminating the effect of aging on mixtures. Based on these evaluations three new index parameters for rutting (CMRI based on complex modulus), Fatigue cracking ($C_{N_f}^S$base on S-VECD theory) and transverse cracking (RDCI based on SCB) were developed and applied to the mixtures studied in this project. All these parameters indicated high correlations with the mixtures' actual field performance to be reliably used in development of layer coefficients.

To develop the layer coefficients, the designated approach in this research was to incorporate the performance test results with the appropriate failure distress criteria such as International Roughness Index (IRI). Therefore, the IRI data for a set of seventeen cross sections on which similar mixtures to the study mixtures (similar binder type and mix design properties) have been placed, were selected for evaluations. Based on these analysis, and using available equations in the literature, the IRI data were converted into the Present Serviceability Index (PSI). Using the AASHTO 1993 design equation, and the available cross sections, the pavement structural number (SN) and consequently the IRI base layer coefficients (a_{IRI}-values) for wearing course mixtures were back-calculated. Using a normal distribution function, the average and standard deviation for wearing course a_{IRI}-values were determined to be 0.58 and 0.15 respectively. In order to incorporate the developed performance based index parameters with the IRI based layer coefficients, the values of the index parameters were calculated for each mixture separately. Then, using the normal distribution function, the average, standard deviation and consequently the level of reliability within each performance index was calculated for individual mixtures. This level of reliability was incorporated with the normal distribution of the a_{IRI}-values and performance based a-values were determined for each mixture. Based on the analysis, a set of average and minimum a-values at different levels of reliability have been proposed for future New Hampshire pavement designs.

CHAPTER 1: INTRODUCTION

1.1 BACKGROUND AND MOTIVATION

A variety of approaches are available to design pavement structures. These approaches are generally divided into two main categories: empirical and mechanistic-empirical (M-E) methods. The most widely used empirical method is the AASHTO 1993 design approach which uses material specific coefficients (layer coefficients) to quantify the structural capacity provided by each pavement layer. These coefficients are experimentally developed values from the AASHO road test which was conducted in the early 1960s and are based on statistical regressions. Almost no fundamental or engineering mixture properties or explicit failure criterion were used in the original development of layer coefficients. In addition, the empirical approaches are generally developed based on extensive field tests and statistically correlating different variables as part of the approach. On the other hand, the M-E approaches use fundamental mixture properties such as complex modulus (|E*| and phase angle) to determine the pavement's structural response and relate it to the distress through transfer functions. However, M-E approaches require extensive data for local calibrations as well as routine testing of mechanical properties for various pavement materials. Due to these challenges, many state transportation agencies have continued to use the empirical design approaches for routine design.

Recently, investigations have been conducted to improve the AASHTO 1993 design approach by updating the layer coefficients (a-values) for asphalt mixtures through different mechanistic and performance based measures. The layer coefficients significantly influence the determination of the layer thickness which translates into the structural contribution of the layers as well as the long term performance of the pavement and consequently the construction and maintenance costs. Therefore, it is critical to determine reliable a-values that are most relevant to the regional conditions and locally used materials. In addition, the asphalt mixtures in use today and vehicle loadings are substantially different from the ones characterized during the development of the design guide in the 1960s. With use of asphalt binder modification technologies, allowance for recycled materials (such as, recycled asphalt pavements, and ground tire rubber), and newer manufacturing and construction techniques (such as cold recycling), there is an urgent need to reevaluate the layer coefficients for materials that are currently being used in construction of pavements. Due to the lack of reliable layer coefficient values, there is high potential for over-design of pavements that could result in substantially higher costs for agencies. In order to promote sustainability and to maintain integrity through reliable pavement designs, this research study characterized asphalt mixtures that are currently used by the New Hampshire Department of Transportation (NHDOT) for determination of the appropriate layer coefficient values for those materials.

1.2 NEW HAMPSHIRE DEPARTMENT OF TRANSPORTATION PAVEMENT DESIGN APPROACH AND LAYER COEFFICIENTS

At present, the New Hampshire Department of Transportation (NHDOT) employs the AASHTO 1972 Empirical Pavement Design procedure for structural design of highways including new construction, reconstruction and major rehabilitations [1]. The current layer coefficients for asphalt mixtures used by

NHDOT (Table 1-1) were established using a combination of the original values proposed by AASHTO in the 1960s and research conducted by Janoo in 1994 (CRREL Special Report 94-30) [2]. The research by Janoo was primarily focused on layer coefficient characterization of subgrade soils and aggregate courses. The layer coefficients for the hot mixed asphalt are 0.38 for the wearing course and 0.34 for the binder and base course mixtures. In comparison to the layer coefficients values used by other states in the New England area that have similar traffic and climatic circumstances, the layer coefficients used by the NHDOT are relatively lower and are in need for reevaluation (discussed further in Chapter 2 of this report).

Table 1-1 Currently adopted layer coefficients by NHDOT

MATERIALS	**ASPHALT MIXTURES**				
LAYER COURSE	**WEARING**	**BINDER**	**BASE**		
PRODUCTION METHOD	Hot Mixed	Hot Mixed	Hot Mixed	Cold Mixed	Reclaimed Stabilized Base
LAYER COEFFICIENT	0.38	0.34	0.34	0.22	0.17

1.3 RESEARCH APPROACH

To develop the layer coefficients for the New Hampshire Department of Transportation (NHDOT) flexible pavement design, this research study was executed in four tasks:

- Task 1: Literature review and testing plan development
- Task 2: Laboratory characterization
- Task 3: Development of layer coefficients
- Task 4: Reporting

The overall research approach is outlined in Figure 1-1 and briefly discussed here. This research initiated with a comprehensive literature review that was performed to determine the recent approaches that have been used by different State highway agencies for development and calibration of the layer coefficients. Then, a variety of pavement rehabilitation projects from across the New Hampshire were reviewed to identify a wide range of mixtures commonly used by the NHDOT. As a result, a set of 18 different mixtures including wearing, binder and base courses with different production methods (hot and cold) were selected for characterization and development of layer coefficients. To characterize the mixtures, different mechanistic and performance tests including Resilient Modulus (M_r), Complex Modulus (E*), Semi-Circular Bend (SCB), Direct Tension Cyclic Fatigue (S-VECD) and Disk-Shaped Compact Tension (DCT) were conducted on the mixtures. As a result of the testing and analysis, three index parameters for rutting, fatigue and transverse cracking were developed during this study. To develop

reliable layer coefficients, field distress data in the form of International Roughness Index (IRI) values were obtained from the NHDOT pavement management system (PMS) for the study mixtures (and similar mixtures from previous years). Then, distress-based layer coefficients were back-calculated using the AASHTO 1993 design equation. Using statistical analysis, the three index parameters were combined with the distress based layer coefficients to determine the mechanistically informed layer coefficients for mixtures.

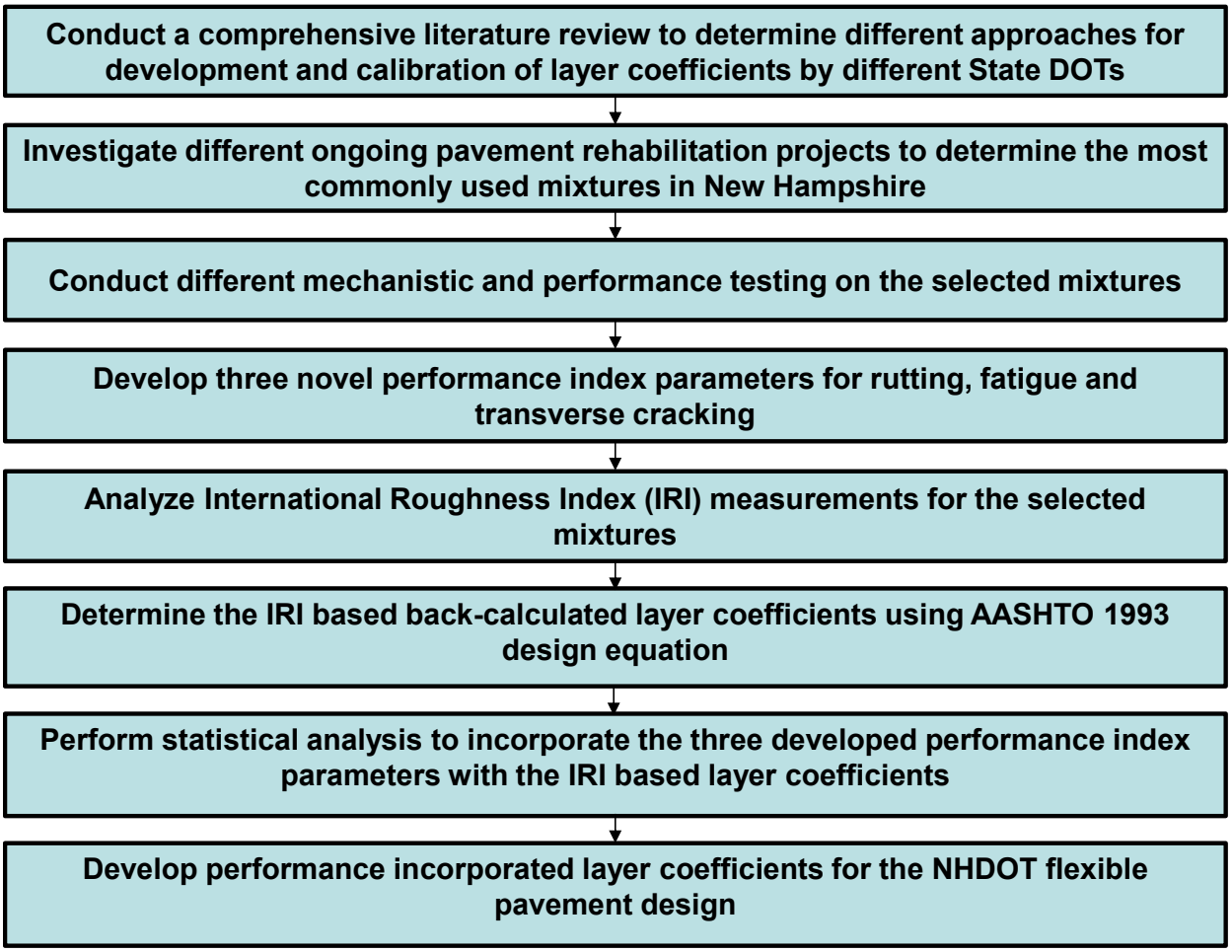

Figure 1-1 Research approach to develop layer coefficients for NHDOT pavement design

1.4 ORGANIZATION OF THE REPORT

This report is organized in seven chapters where Chapter 1 includes the background and motivation of this research study as well as the general research approach that was followed. Chapter 2 includes a comprehensive literature review that was performed to determine the layer coefficients that are used by different State highway agencies and to investigate the most recent approaches used by other states to develop or calibrate the layer coefficients of asphalt mixtures. The procedure of selection of the study mixtures and their properties as well as the experimental testing plan is discussed in Chapter 3. Chapter

4 includes the results of different mechanistic and performance based tests and description of the results in terms of comparative evaluation between different mixtures with respect to their characteristics. The procedure to develop three different performance index parameters for rutting, fatigue and transverse cracking and evaluation of the study mixtures by these indices is described in Chapter 5. Using the developed performance index parameters and the analysis of field distress data in terms of International Roughness Index (IRI), the procedure to construct a generalized methodology for developing mix specific mechanistically informed layer coefficients is described in Chapter 6. The summary, conclusions and overall recommendations of the study with respect to the newly developed layer coefficients along with some recommendations for future work are discussed in Chapter 7.

1.5 REFERENCES

[1]. New Hampshire Department of Transportation (NHDOT), Standard Specifications for Road and Bridge Construction, NHDOT, 7 Hazen Drive, Concord, N.H., September2010

[2]. Janoo, V. C. (1994). Layer Coefficients for NHDOT Pavement Materials (No. CRREL-SP-94-30). Cold Regions Research and Engineering Lab Hanover NH.

CHAPTER 2: LITERATURE REVIEW

2.1 AASHTO EMPIRICAL DESIGN GUIDE

There are several versions of AASHTO empirical design approach since it was first developed based on the American Association of State Highway Officials (AASHO) road test that was performed in the late 1950s and early 1960s in Ottawa, Illinois. The interim versions of this design guide are the AASHTO 1961, and AASHTO 1972. These design guides were then improved and released as AASHTO 1986 and AASHTO 1993 design guides.

The primary goal of the AASHO test was to develop a relationship between the number of axle load repetitions and the pavement performance during the pavement service life. The AASHO test was conducted on six different loops and the loading started in October 1958 and ended in November 1960 [1]. The main variables in this road test were the material thicknesses including hot mix asphalt, base and subbase along with the different axle configurations that were applied on the different test loops. The observations and data obtained from this test were converted into different parts of a design equation which relates the number of applied axle loads to the required thickness of the pavement. The AASHO road test resulted in major findings in pavement engineering science such as the relationship between the load and the damage called as Fourth Power Law. It also introduced important factors such as Serviceability, Equivalent Single Axle Load (ESAL) and the Structural Number (SN). The first AASHO design guide was published in 1961 as the "AASHO Interim Guide for the Design of Rigid and Flexible Pavements". Since the equations derived from AASHO test were based on limited data from two years of loading and only one climatic condition (Ottawa, Illinois), the design guide was significantly updated in 1972, 1986 and 1993 to meet different nationwide requirements and climatic conditions. The latter update is called as the AASHTO 1993 design guide and has not changed since then. Although major steps have been taken to switch from this empirical guide to a mechanistic-empirical pavement design guide (MEPDG) in the past three decades, the high costs and lack of available database for regionally calibrating this design guide has become an issue for many of the state DOTs. Therefore, AASHTO 1993 design equation (Equation 2.1) is still being used as a reliable pavement structure design tool in many states in the United States and other countries around the world [2].

$$log_{w18} = Z_R S_0 + 9.36 \log(SN+1) - 0.2 + \frac{\log\left[\frac{\Delta PSI}{4.2-1.5}\right]}{0.4+\frac{1094}{(SN+1)^{5.19}}} + 2.32 log M_r - 8.07 \quad \text{Equation (2.1)}$$

Where:

log_{w18}: Number of the allowable equivalent single axle loads (18kips) in design period

Z_R: z-statistic, determined based on level of reliability of the design

S_0: Standard deviation of the design, based on level of accuracy of data collection

SN: Structural Number, indicating the overall load bearing capacity of subgrade soil

ΔPSI: Loss in serviceability

M_r: Resilient modulus of subgrade soil

Currently, New Hampshire Department of Transportation (NHDOT) uses the AASHTO 1972 interim guide with some modifications to design the structure of pavements. This design guide uses variables such as Regional Factor (RF), Soil Support Value (S) and Average Daily Load (ADL) as the main inputs to determine the required SN and consequently the layers thicknesses. It is worth mentioning that, since the method of back-calculating the layer coefficients from structural number for the asphalt layers remains the same between AASHTO 1972 and AASHTO 1993 design guides, and due to the higher reliability of the latter approach (using more fundamental material properties such as resilient modulus), this method is used to develop the layer coefficients in this study. The variables of the AASHTO 1993 design approach are discussed in the next section.

2.2 AASHTO 1993 DESIGN VARIABLES

2.2.1 EQUIVALENT SINGLE AXLE LOAD (ESAL)- $\log_{w18}$

AASHTO 1993 design procedure for determining the thickness of different layers is based on the total number of applied wheel load over the design life of the pavement. Since the axle loads and configurations vary among different vehicle types, as a result, the damage induced by them would be different. One of the important achievements by the AASHO road test was the concept of Equivalent Axle Load Factor (EALF) which is used to convert the amount of induced damage to the pavement from any type of vehicle to the equivalent damage caused by an 18kip (80kN) single axle load. Then, the summation of equivalent damage over the pavement design life is considered as the Equivalent Single Axle Load (ESAL) which is the only traffic factor in the design [1].

2.2.2 RELIABILITY

This parameter is defined as the probability that the design will perform satisfactorily over the pavement design life and changes based on the type and importance of the road. Reliability is a factor of safety of the pavement design that is implemented in the AASHTO 1993 design guide. In other words, reliability of the design is used to ensure that the actual ESALs over the design life will not exceed the estimated ESALs. For instance, a 50% reliability means that the actual ESALs will be equal to the estimated ESALs at the end of the design period. In the AASTHO 1993, the factor of reliability is considered as the product of Z_R and S_0 in the equation.

2.2.3 PRESENT SERVICEABILITY INDEX (PSI)

The serviceability of a pavement is essentially evaluated by the ride quality experienced by the road users. By definition, serviceability is the ability of a specific section of a pavement to serve traffic in its existing condition. The Present Serviceability Index (PSI) which was developed during the AASHO Road Test, is based on the pavement roughness and distress conditions such as rutting, cracking and patching. The Present Serviceability Index is the mean of independent ratings by individuals to rate the ride quality of the pavement. This index ranges from 5 to 0 as the best and worst ride quality, respectively. This factor

can be used as a tool to determine the proper time for the correct type of maintenance, rehabilitation or even reconstruction of the pavement by the Pavement Management System (PMS). The initial serviceability of the pavement is a function of pavement type and construction quality and the typical value for the flexible pavements is considered as 4.2 whereas the adopted value for the terminal serviceability for this type of pavement is typically 2.5.

2.2.4 STRUCTURAL NUMBER (SN)

Structural number of pavement is defined as a criterion to measure the ability of pavement to withstand the applied load. The primary purpose of any pavement design is to protect the subgrade soil from excessive stresses due to the loading, as well as penetration of surface water into the subgrade soil that can significantly decrease its modulus and result in accelerated pavement damage. The structural number of a pavement is a function of type, quality, thickness, and drainage capability of different materials used in the pavement structure. The weaker the material the higher the required structural number will be for the same loading and climatic conditions. Equation (2.2) defines the structural number for a pavement structure with "n" layers. In this equation the layer coefficients (a-values) indicate the quality of the material and will be discussed in the next sections. However, the drainage coefficient (m-value) is defined based on the quality of drainage and can range from 0.4 to 1.40 depending on the material and moisture conditions. The drainage coefficient for the asphalt mixtures is usually considered to be as 1.0.

$$SN = \sum_{i=1}^{n} a_i \times D_i \times m_i \qquad \text{Equation (2.2)}$$

Where:

SN: Structural Number

a_i: Layer coefficient of the i^{th} layer

D_i: Thickness of the i^{th} layer

m_i: Drainage coefficient of the i^{th} layer

2.2.5 SOIL RESILIENT MODULUS

The resilient modulus of the soil is an important factor in AASHTO 1993 design guide. The temperature and moisture variations can significantly affect the resilient modulus of the materials. This could be even more evident for the cohesive soils and granular material with higher fraction of fines. Therefore, the resilient modulus of the subgrade soil can be affected by the changes in ground water table level, precipitation and seasonal temperature variations, especially during the freeze and thaw periods throughout the year. Therefore, the effective resilient modulus which is the representative modulus value for different weather conditions is calculated based on the damage that could occur to the pavement during different seasons with different subgrade soil moduli values throughout a year. The effective modulus value is essentially an equivalent resilient modulus that can cause the same amount of damage to the pavement if actual seasonal modulus values were used in the design. This value is the only subgrade soil property that is considered in AASHTO 1993 and is highly influential in determining the structural number (SN) of the overall design.

2.3 LAYER COEFFICIENT

The AASHTO design guide defines the layer coefficient as the empirical relationship between the structural number of a pavement structure and the layer thickness, indicating the relative ability of a material to function as a structural component of a pavement [2]. Layer coefficients (in this report will be denoted as a-value) were originally derived as the regression coefficients in relating the SN to the thickness of different layers in the AASHTO road test. In other words, for a given pavement structure the SN value was first determined through using Equation 2.1 and then based on the configuration of the pavement the calculated SN value was correlated to different layer thicknesses through Equation 2.2. and finally, the regression coefficients (a-values) were determined. The main factors affecting the a-value are:

1- Material type and properties
2- Layer thickness and location
3- Failure criterion
4- Loading level

The layer coefficient of asphalt materials is not only based on the asphalt material properties and thickness but it is also affected by the underlying material's properties.

2.4 LAYER COEFFICIENT CALIBRATION

Research conducted at the National Center for Asphalt Technology (NCAT) revealed that the layer coefficient followed by traffic level and resilient modulus are the most influential factors in determination of the pavement thickness using the AASHTO 1993 design equation [3]. Although the original layer coefficients from the AASHTO road test are reliable, they are applicable only to the types of material, traffic and the environmental conditions under which they have been generated. Since the layer coefficient has a significant influence in determining the layer thickness and consequently on the construction expenses as well as the long term performance of the pavement, it is essential to determine reliable a-values for different regions and materials. For this purpose, a number of the states that implement AASHTO 1993 design procedure or use layer coefficients as part of their specific design methodology have evaluated their own commonly used materials and assigned specific a-values to them. Some of the older studies which are mainly based on lab experimentation have shown that a-values are correlated with gradation, thickness, abrasion of aggregate and more important the strength or stability of asphalt mixtures [4]. Layer coefficient calibrations are conducted based on different methodologies which will be discussed briefly in this section.

2.4.1 PAVEMENT EQUIVALENT STRUCTURAL RESPONSE

Different methods have been investigated to use the concept of the equivalent structural response in calibrating the layer coefficients. In many instances, a reference mixture with a defined thickness is selected and the rest of the mixtures are compared to that. The comparison is conducted with respect to the required thickness of a given material to result in identical deflection to that of the reference mixture under similar loading conditions. Similarly, the identical maximum vertical stress on top of subgrade soil for different types of hot mix asphalt mixtures has widely been used to recalculate the a-values. Maximum

tensile strain at the bottom of asphalt layer has also been used to determine the layer coefficient of recycled mixes. The thickness of the recycled layer to result in the equivalent number of load repetitions to failure (N_f) of the standard reference hot mix asphalt on the same subgrade soil has been used to determine the layer coefficient since the SN is equal for both cases [4,5].

2.4.2 PAVEMENT PERFORMANCE

AASHTO pavement performance analysis has been used as a practical method for layer coefficient calibration. This method monitors the serviceability indicators (rut depth, cracks, patching, IRI and etc.) and calculates the PSI. The rate of change in serviceability for a given pavement structure with known thicknesses for different layers is then converted to SN value. Conducting the regression analysis on the SN (Equation 2.2) results in the new layer coefficients. This method has been successfully used by NCAT to calibrate the a-value of the asphalt mixtures used by Alabama Department of Transportation (ALDOT). Using the IRI value and converting that to PSI for the known cross sections, researchers at NCAT suggested a new layer coefficient of 0.54 instead of 0.44 for the hot mixed asphalt. This magnitude of change was shown to have the potential to reduce construction costs by approximately 18% [3, 6].

2.4.3 USE OF MECHANISTIC-EMPIRICAL PAVEMENT DESIGN GUIDE

The mechanistic-empirical design method (MEPDG) has also been used to calibrate the a-values. This is a highly data intensive method and has been used by states such as Washington State. This method is recommended only for agencies that are in the process of implementing a mechanistic-empirical design approach and have a large enough database available for the calibration. Once the database is available, the calibration can be simply performed by designing the required thickness using the MEPDG approach and then calibrating the a-value in the AASHTO empirical design method to obtain the same thickness for the structure. Using this method, the a-value of hot mixed asphalt increased from 0.44 to 0.50 for WSDOT which also resulted in significantly reduced construction costs for that agency [6].

2.4.4 MATERIAL CHARACTERIZATION

Among all the factors that influence the layer coefficient value, the material type and properties have the highest impact. To account for these factors, the AASHTO 1993 design guide uses the resilient modulus (M_r) of the material [2] since it is not only a measure of stiffness but also can be an indicator of strength of the material.

The relationship between the asphalt mixture's layer coefficient and the elastic resilient modulus at 70 °F was established in 1972. This relationship (Equation 2.3 and Figure 2-1) is valid for a dense graded asphalt mixture and can only be used if the elastic modulus is between 110,000 psi and 450,000 psi. It should be mentioned that when using Equation (2.3), the resilient modulus units should be in MPa. AASHTO 1993 design guide proposes the value of 0.44 as the layer coefficient for M_r corresponding to 450,000 psi, however caution is recommended for higher M_r values as stiffer mixtures can be more prone to cracking [1].

$a_i = 0.4 \log(M_r) - 0.951$ Equation (2.3)

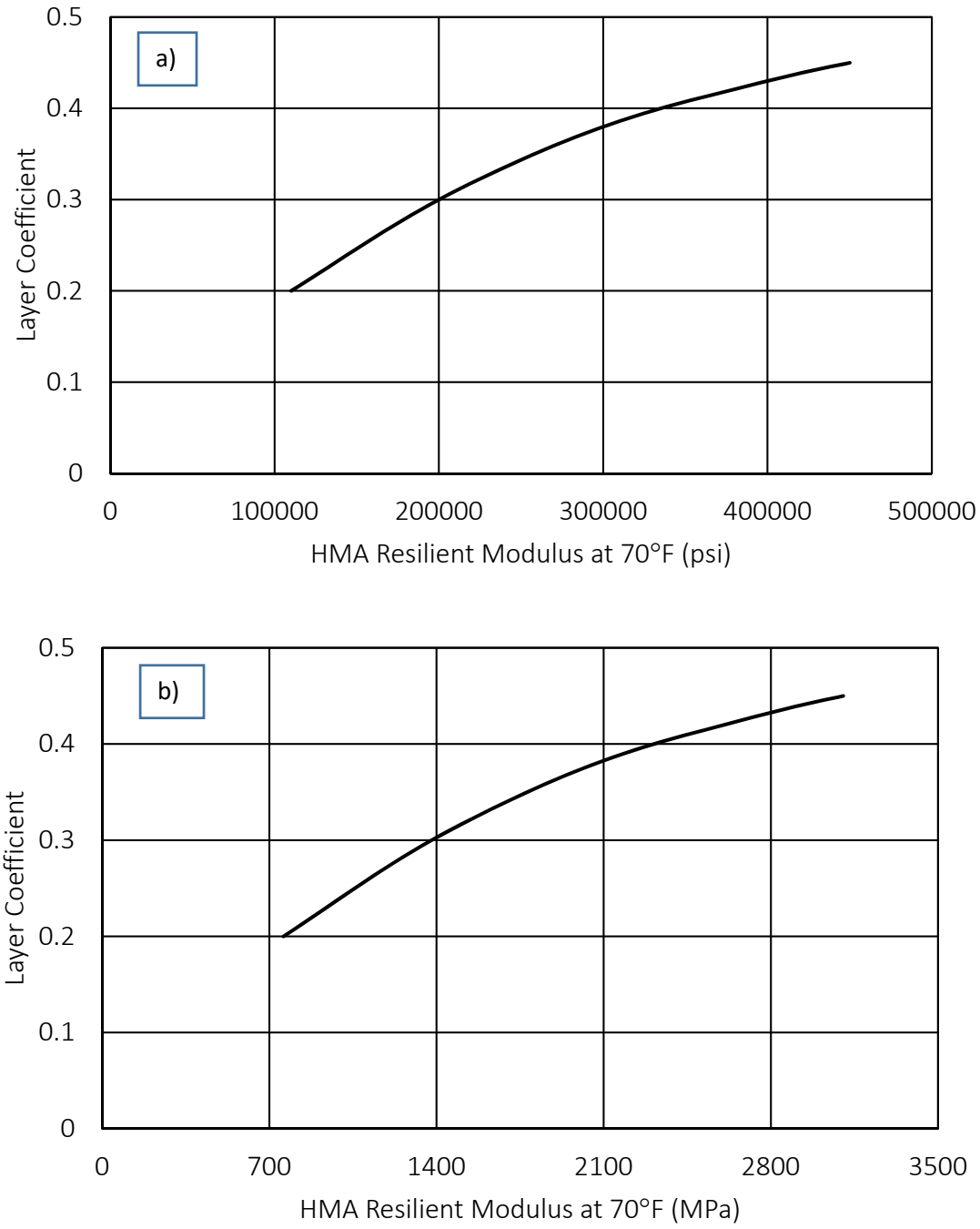

Figure 2-1 Estimating layer coefficient of dense-graded asphalt concrete based on elastic resilient modulus a) Resilient modulus unit as psi b)resilient modulus unit as MPa

Research conducted at the University of Wisconsin for calibrating the a-values of commonly used asphalt mixtures by Wisconsin Department of Transportation (WIDOT) implemented the M_r measurement in the

lab. The test was performed in accordance with the AASHTO T-294-94 standard (which is not the commonly used test method for M_r) at 20 °C. Using Equation 3.3, new layer coefficients were determined. The main concern stated by researchers was that the resilient modulus measurements for different types of mixtures at the aforementioned temperature were so close and as a result the a-values were nearly the same. To better differentiate the mixtures, a triaxial testing apparatus was used to measure the rutting at 52°C and 64°C. The researchers proposed the correlation of the a-value with the combination of resilient modulus, rutting performance and any other available damage factor to calculate the new a-values [7].

Among many state DOTs that use empirical design methods, South Carolina is using the AASHTO 1972 design guide and is trying to switch into the mechanistic-empirical (MEPDG) design method. Research was performed to enhance the precision of the a-values used for the asphalt base mixtures in South Carolina. The procedure included conducting the dynamic modulus test on the mixtures and prediction of the M_r value from the |E*| master curve at the frequency of 1.59 Hz at 68 °F which is equal to 0.1 second of loading on the specimen (same loading time for M_r test in accordance with ASTM D7369). Once the M_r was predicted, Equation 3.3 was utilized to calculate the new a-values which indicated an increase from the initial value of 0.34 to 0.44 and higher [8].

2.4.5 FALLING WEIGHT DEFLECTOMETER

According to the AASHTO 1993 design guide, a more reliable way to determine the layer coefficients is to back calculate the moduli from the Falling Weight Deflectometer (FWD) test on the road in lieu of lab testing. One reason could be related to possible variation between the lab made specimens and the mixture placed in the field [2]. In addition, FWD is considered to simulate the dynamic loading of a moving wheel in a wide range of loading levels, resulting in a more realistic loading.

New Hampshire Department of Transportation (NHDOT) was one of the first State DOTs in the nation to use FWD for calibration of layer coefficient values for its pavement materials. Research conducted in 1994 by Dr. Janoo on a segment of I-93 between exit 18 and 19 through construction of ten test sections with different combination of materials that resulted in the same structural number for the section. The primary purpose of testing was to evaluate the a-value used for the Reclaimed Stabilized Base (RSB) materials, since RSB resulted in higher surface deflections compared to other sections of the road. The results from FWD and back calculated moduli confirmed that incorrect a-value for this type of material was used in the design and the new a-value for RSB was established by decreasing from 0.17 to 0.14. The layer coefficients of the asphalt material used by NHDOT range between 0.34-0.38 and back calculations from FWD in this research resulted in an a-value of 0.37 for the wearing course [9].

2.5 REVIEW OF LAYER COEFFICIENTS USED BY OTHER AGENCIES

As part of the literature review, twenty-one (21) State DOTs that currently use the AASHTO empirical design methods (any version) were surveyed to determine what a-values they use for the surface and non-surface course asphalt mix materials. The survey was not limited to any specific region or climatic condition but the objective was to evaluate the current NHDOT's layer coefficients with respect to those

used elsewhere. Table 2-1 shows the results of the survey showing that New Hampshire is using one of the lowest a-values compared to other states, even compared to those in the New England region where the environmental and perhaps the traffic loading is not significantly different.

Table 2-1 Layer coefficients used by other agencies

Layer type	Layer coefficient(a_i)	State DOTs
Surface Course (HMA)	0.54	AL
	0.50	WS
	0.44	AR, CT, FL, GA, IA, MA, ME, MT, NJ, PA, SC, WI
	0.43	OH
	0.42	NY
	0.4	DE, IL
	0.38	**NH**
	0.35	NV, VT
Non-Surface Course (HMA)	0.44	FL, PA, SC
	0.42	NY
	0.4	DE,CT
	0.36	OH
	0.35	NV
	0.34	MA, ME, MT, **NH**
	0.33	VT
	0.31	WI
	0.30	GA, IL

2.6 LITERATURE REVIEW SUMMARY

As part of the project, a literature review was conducted to explore and discuss different aspects and design variables of the AASHTO 1993 pavement structure design guide which is the most commonly used pavement design standard in the nation and worldwide. The influential variables are listed below:

1- Equivalent Single Axle Load (ESAL)
2- Reliability
3- Present Serviceability Index (PSI)
4- Structural Number (SN)
5- Soil resilient modulus

Among these variables, the structural number of the pavement is the factor which directly relates the required structure configuration and thickness to the material quality and properties using the layer coefficient values (a-value).

As the definition provided by AASHTO design guide, layer coefficient is the empirical relationship between the structural number of a pavement structure and layer thickness, which indicates the relative ability of a material to function as a structural component of a pavement.

Factors affecting the layer coefficient are listed below:

1- Material type and properties
2- Layer thickness and location in the pavement structure
3- Failure criterion
4- Traffic loading level

The original layer coefficients derived in the AASHO road test were based on the material and environmental conditions and the limited traffic during this road test. As the material production and construction techniques evolve, it is necessary to calibrate the a-values by considering diverse material, climatic conditions and increasing traffic levels.

Researchers have used different methods to calibrate the a-values. These methods correlate some pavement structure or material attributes to the layer coefficient and derive new a-values on basis of that correlation. These methods were discussed in the literature review and are listed here:

1- Pavement Structural Response
2- Pavement Performance
3- Mechanistic-Empirical Design Approach
4- Material Properties Characterization
5- Falling Weight Deflectometer

All of these methods have shown to be reliable in calibration of a-values. AASHTO 1993 design guide recommends the use of Resilient Modulus (M_r) to determine the a-value of asphalt mixtures using a regression equation (Equation 2.3).

A survey of 21 state DOTs indicated that many states have adjusted the original a-values and are using values higher than those used by NHDOT, supporting the re-evaluation of a-values used in NH.

2.7 REFERENCES

[1]. Huang, Y. H. (2004). Pavement design and analysis. Pearson/Prentice Hall.

[2]. Transportation Officials. AASHTO guide for design of pavement structures, 1993. Vol. 1. AASHTO, 1993.

[3]. Davis, K., & Timm, D. (2010). Recalibration of the asphalt layer coefficient. Journal of Transportation Engineering, 137(1), 22-27.

[4]. Van Til, C. J. (1972). Evaluation of AASHO interim guides for design of pavement structures. Highway Research Board.

[5]. Van, W. A. (1984). Determination of the Structural Coefficients of a Foamed Asphalt Recycled Layer.

[6]. Timm, D. H., Robbins, M. M., Tran, N., & Rodezno, C. (2014). Recalibration Procedures for the Structural Asphalt Layer Coefficient in the 1993 AASHTO Pavement Design Guide (No. NCAT Report 14‐08).

[7]. Bahia, H. U. (2000). Layer coefficients for new and reprocessed asphaltic mixes. Wisconsin Department of Transportation, Division of Transportation Infrastructure Development, Bureau of Highway Construction, Technology Advancement Unit.

[8]. Prowell, B. D., James, T., Bennert, T., & Jordan, J. (2017). Evaluation of Moduli and Structural Coefficients of South Carolina's Asphalt Base Mixtures. Transportation Research Record, 2641(1), 21-28.

[9]. Janoo, V. C. (1994). Layer Coefficients for NHDOT Pavement Materials (No. CRREL-SP-94-30). COLD REGIONS RESEARCH AND ENGINEERING LAB, HANOVER, NH.

CHAPTER 3: PROJECTS, MATERIALS AND TEST METHODS

3.1 PROJECTS AND MATERIALS

To develop the experimental plan of the research study, a wide range of ongoing projects that use different types of rehabilitation methods and mixtures were evaluated for use in this study. The objective was to select a variety of the commonly used mixtures in New Hampshire that include diverse mixture design properties. In addition, the selected projects and mixtures needed to represent all the conventional traffic levels, climatic conditions, cross sectional designs, production methods, aggregate size and binder types, recycled asphalt pavement (RAP) amount and recycled binder ratio (RBR) as well as gyration levels. Based on the investigation and criteria, a set of 18 asphalt mixtures were selected. The mixtures include two asphalt rubber gap graded (ARGG), four cold central plant recycled (CCPR) mixtures as well as other different types of conventional and polymer modified hot mixed asphalt (HMA) mixtures used in wearing, binder, and base course layers. Table 3.1 shows the study mixtures as well as the projects and roadways from which the mixtures have been sampled.

The design properties of the study mixtures are summarized in Table 3-2. Recycled binder ratio (RBR) and RAP percentage by weight are used to define the recycled content for HMA and CCPR mixtures, respectively. All of the HMA mixtures are designed at a 4% air void level.

All the study mixtures were sampled in the production plants and stored in metal buckets. The buckets were then transported to the asphalt materials testing lab at the University of New Hampshire. To fabricate the HMA testing specimens, the buckets were directly placed into the oven for reheating. The oven temperature was set at the mixture's conventional mixing temperature of nearly 160°C for 2.5 hours with lids on the buckets. This resulted in an internal material temperature of nearly 135° which is in the conventional HMA discharge temperature range in the field. It is hypothesized that this method of reheating would result in less aging compared to the method described in AASHTO R35 due to less direct contact between the materials and circulating hot air in the oven. After reheating, the materials were placed into preheated molds and compacted using a standard Superpave gyratory compactor to the desired air void level of 6±0.5%.

The cold central plant recycled mixtures (denoted as CM-1 and CM-2) are produced by mixing recycled asphalt pavement (RAP) with MS-4 emulsion for 5 minutes using a Wirtgen twin-shaft pugmill mixer (model WLM30) in the laboratory. The MS-4 emulsion is an anionic medium setting emulsion which is specified by the New Hampshire Department of Transportation (NHDOT) [1]. In addition, two emulsions that did not meet the AASHTO T 59 minimum requirement of 2% oil distillate were included in the study to investigate the effect of the oil distillate percentage on performance. These two mixtures are denoted as CM-1-a (1% oil distillate emulsion) and CM-2-a (1.25% oil distillate emulsion). Two different sources of cold central plant recycled (CCPR) material with different nominal maximum aggregate size (NMAS) (19 mm for CM-1 and 12.5 mm for CM-2) were used in fabricating the CCPR mixtures in the lab. The RAP used in lab testing was sampled from the field and is representative of the material used in actual pavement construction at two sites. The age of the RAP is unknown. Based on the quality assurance (QA)

documentation, the binder content for RAP used in CM-1 and CM-1-a ranges from 4.8% to 5.45%, while the RAP source used for CM-2 and CM-2-a contains 6.3% binder.

Table 3-1 Selected projects and mixtures

Course	Mix Name	Binder Type	Project Number	Project Name	Roadway
Wearing	ARGG-1	Asphalt Rubber (AR)	13080A	Durham-Newmarket	NH 108
	ARGG-2	Asphalt Rubber (AR)	14966	Manchester	I-293
	T-1	PG 64-28	13933H	Salem-Manchester	I-93
	T-2	PG 58-28	40423	Belmont-Laconia	NH 106
	T-3	PG 58-34	29222	District 1 Rehab.	NH 26 (FDR)
	THS-1	PG 76-28	13933H	Salem-Manchester	I-93
	SHM-1	PG 70-34 PMA	40763	Manchester-Auburn	NH 101; (MM: 100.3-102.1)
	SHS-1	PG 76-28	40871	Statewide	NH 107 (Kingston); Section ID 17602
	S-1	PG 58-28	40863	Statewide	US 3 (Whitefield);Section ID 17108
	SV-1	PG 64-28	40871	Statewide	NH 111 (Kingston); Section ID 17601
Binder	B-1	PG 64-28	14633B	Salem-Manchester	I-93
	B-2	PG 58-34	29222	District 1 Rehab.	NH 26 (FDR)
	B-3	PG 58-28	40944	Grantham-Enfield	Smith Pond Road;(I-89 Exit 15)
Base	BB-1	PG 64-28	10044-G	Plaistow	NH 125
Cold Interlayer Mix	CM-1	Emulsion (MS-4) Peckham	40404	Thornton-Woodstock	I-93 NB Exits 29-30;(MM: 88.4-95.1) Passing Lane ONLY
	CM-1-a	Emulsion (MS-4) All States			
	CM-2	Emulsion (MS-4) Gorman	16164F	District IV Resurfacing	NH 63 (Hinsdale)
	CM-2-a	Emulsion (MS-4) All States			

The CCPR mixtures were made in a manner to replicate the mixtures produced for actual construction. The mix designs were conducted by pavement contractors for CM-1 and CM-2 using Marshall stability criteria to determine the optimum binder content. In the CCPR mixture design procedure, the moisture content of the RAP was not altered to achieve the maximum density, rather the design was conducted at the existing moisture level of about 1.75% for both mixtures.

The CCPR specimens were fabricated using a Superpave gyratory compactor to achieve 10±0.5% air void level to replicate typical air void content in the field for these materials. The specimens were cured for 7

days at room temperature and subsequently cured 3 days in an oven at 40°C. The 7-day room temperature curing assures that the specimen has gained enough strength before it is placed in the oven so that it will not fall apart during the second phase of the curing. The oven curing process follows the Wirtgen method that ensures specimens reach a constant mass before testing [2].

Table 3-2 Study mixtures design properties

Mix Name	Mix ID	Course	NMAS (mm)	Binder Grade/ Emulsion type	AC%	VMA %	V_{be}%	RBR(5)/ RAP(6)%	Gyration
ARGG-1	ARGG-1	Wearing	12.5	PG58-28	7.8	19.1	15.1	0.0	75
ARGG-2	ARGG-2			PG58-28	7.6	18.4	14.4	6.6	75
T-1	W-6428H-12.5			PG64-28	5.4	16.1	12.1	18.5	75
T-2	W-5828L			PG58-28	5.8	15	11	16.2	50
T-3	W-5834L			PG58-34	5.4	15.3	11.3	18.5	50
THS-1	W-7628H-12.5			PG76-28	5.4	16.1	12.1	18.5	75
SHM-1	W-7034PH			PG70-34	5.8	16	12.0	0.0	75
SHS-1	W-7628H-9.5		9.5	PG76-28	6.1	16.3	12.3	14.8	75
S-1	W-5828H			PG58-28	5.9	16.6	12.6	16.9	75
SV-1	W-6428H-9.5			PG64-28	6.4	17.1	13.1	0.0	75
B-1	B-6428H	Binder	19	PG64-28	4.8	14.3	10.3	20.8	75
B-2	B-5834L			PG58-34	4.6	14.1	10.1	21.7	50
B-3	B-5828H			PG58-28	4.8	14.9	10.9	20.8	75
BB-1	BB-6428L	Base	25	PG64-28	4.8	14.8	10.8	20.8	50
CM-1	CM-1(1)	Cold Mix Interlayer	19	MS-4(3)	4.0(4)	–	–	100.0	–
CM-1-a	CM-1-a(2)				4.0(4)	–	–	100.0	–
CM-2	CM-2(1)		12.5		4.0(4)	–	–	100.0	–
CM-2-a	CM-2-a(2)				4.0(4)	–	–	100.0	–

(1) Percentage of oil distillate in the emulsion equal to the minimum requirements of 2% as per NHDOT MS-4 requirements.
(2) Percentage of oil distillate in the emulsion below the minimum requirements of 2% as per NHDOT MS-4 requirements.
(3) MS-4 is a special type of emulsion that is specified by the NHDOT bureau of material
(4) Undiluted emulsion amount by weight of total mix
(5) Recycled binder ratio
(6) Recycled asphalt pavement

3.2 LABORATORY TEST METHODS

3.2.1 RESILIENT MODULUS TEST

The resilient modulus (M_r) test was conducted at 25°C on three disk-shaped replicates in accordance with ASTM D7369-11 standard test method [3]. The test method involves a haversine loading protocol with 0.1s of loading and 0.9s of rest period for 105 cycles where the last five cycles are used to calculate the resilient modulus. The test is conducted on 150 mm diameter disks that are 50±1mm in thickness and are conditioned at 25 °C. The deflection measurements are conducted on both sides of the replicates and the total resilient modulus is determined by averaging the individual modulus values from the two sides of the specimen. Equation 3.1 indicates the M_r calculations and variables. Figure 3-1 shows the test setup and one typical cycle of test data.

$$M_r = \frac{P_{cyclic}}{\delta_h t}(I1 - I2.\mu) \qquad \text{Equation (3.1)}$$

M_r: Instantaneous or total resilient modulus of elasticity, MPa (psi),

δ_h: Recoverable horizontal (instantaneous or total) deformation, mm (in.),

μ: Instantaneous or total Poisson's ratio,

I: Constant depending on the gauge length

t: Thickness of specimen, mm (in.),

P_{cyclic}: Cyclic load applied to specimen, N (lb),

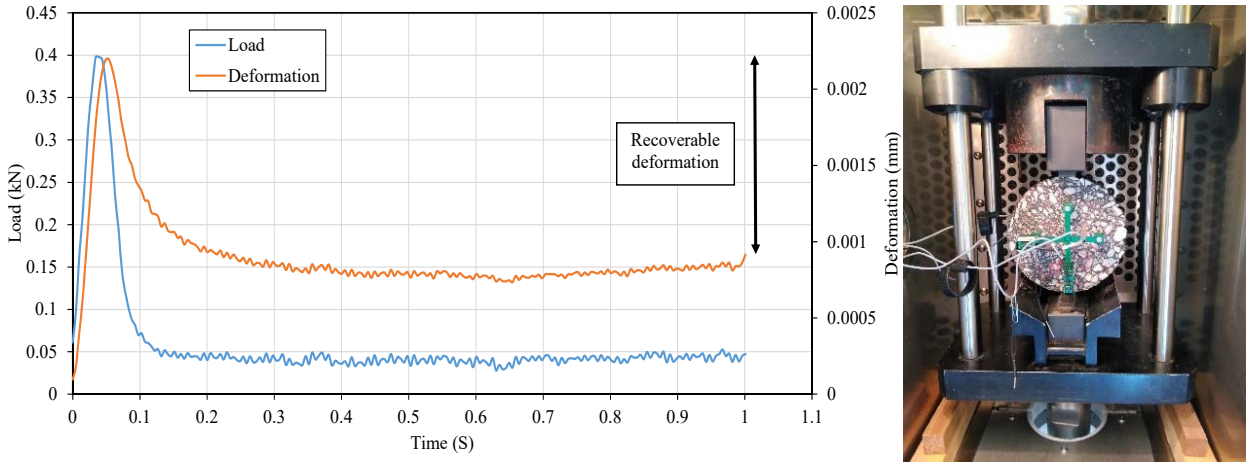

Figure 3-1 Resilient modulus test result and setup

3.2.2 COMPLEX MODULUS TEST

The complex modulus test is performed in accordance with AASHTO T342 standard [4] using an Asphalt Mixture Performance Tester (AMPT) machine on 150×100 mm cylindrical specimens. The test is conducted on three replicate specimens at different temperatures (4.4°C, 21.1°C and 37.8°C) and loading frequencies (25, 10, 5, 1, 0.5, 0.1 Hz) to characterize the linear viscoelastic properties of the asphalt mixtures: dynamic modulus |E*| and phase angle (δ). The test is conducted using a sinusoidal loading

protocol and three linear variable differential transformers (LVDT) are used to measure the on-specimen strains. To use the results of testing, the dynamic modulus and phase angle master-curves are constructed at a reference temperature of 21.1°C using time temperature superposition principle (TTSP) and appropriate shift factors. Equations 3.2 and 3.3 indicate the dynamic modulus and phase angle calculations. Figure 3-2 shows the test setup and a typical stress and strain related to one load cycle of the test data.

$$|E^*| = \frac{\sigma_{amp}}{\varepsilon_{amp}} \qquad \text{Equation (3.2)}$$

$$\delta = 2\pi f \Delta t \qquad \text{Equation (3.3)}$$

$|E^*|$: Dynamic modulus (psi),

σ_{amp}: Amplitude of applied stress (psi),

ε_{amp}: Amplitude of strain response (in/in),

δ: Phase angle (degrees),

f: Load frequency (Hz),

Δt: The time lag between stress and strain peak to peak.

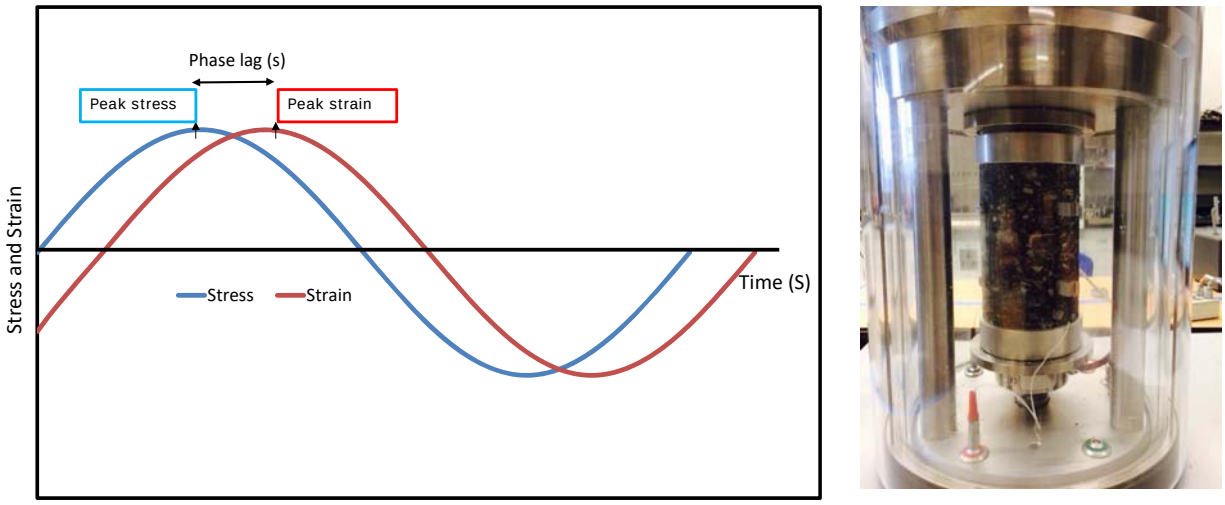

Figure 3-2 Complex modulus test result and setup

3.2.3 SEMI-CIRCULAR BEND (SCB) TEST

The Semi-Circular Bend test is performed to determine the intermediate temperature fracture properties of asphalt mixtures in accordance with AASHTO TP 124 standard [5]. The test is conducted in monotonic

loading conditions using a line-load displacement rate of 50mm/min at 25°C for 4 replicates. Fracture energy (G_f), defined as the amount of energy required to create unit fracture surface, is calculated from the area under the load-displacement curve (Equation 3.4). The Illinois flexibility index (FI), which normalizes the fracture energy by the post peak slope at the inflection point, is calculated using Equation 3.5 [4]. While the fracture energy of different mixtures can be the same, the inclusion of the post peak slope has been shown to better discriminate the fracture resistance of mixtures. Figure 3-3 shows the test setup and one typical result for semi-circular bend test.

$$G_f = \frac{Area\ under\ load{-}displacement\ curve\ (Farcture\ work)}{Fracture\ Area} \qquad \text{Equation 3.4}$$

$$FI = \frac{G_f}{Slope\ at\ post\ peak\ inflection\ point} \qquad \text{Equation 3.5}$$

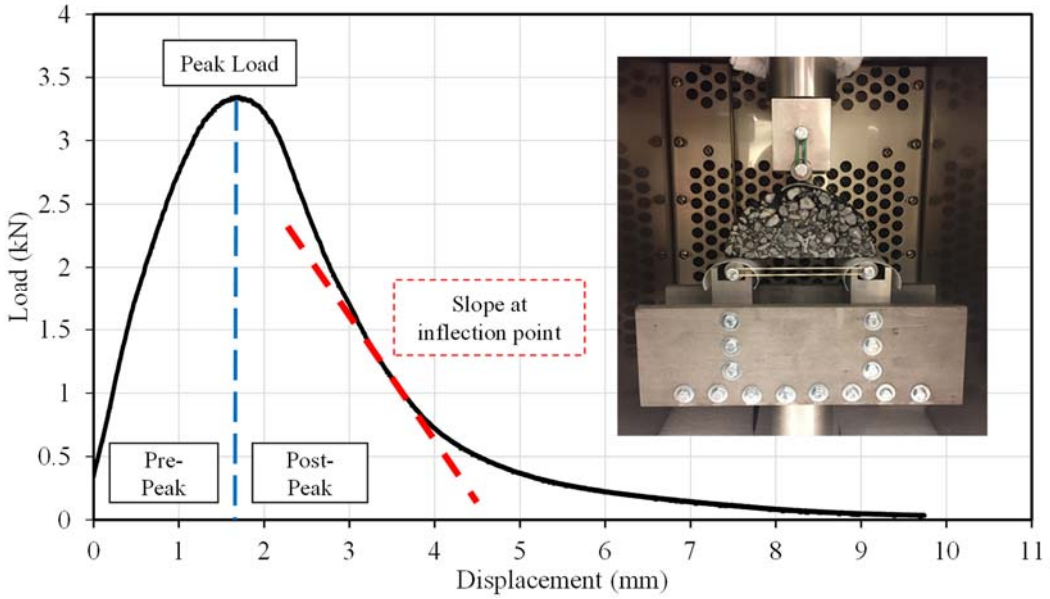

Figure 3-3 Semi-circular bend test result and setup

3.2.4 DIRECT TENSION CYCLIC FATIGUE TEST

The uniaxial fatigue test is performed in accordance with AASHTO TP 107 [6] in a direct cyclic tension mode and the analysis is conducted using Simplified Viscoelastic Continuum Damage (S-VECD) theory. The test is conducted on 130×100 mm specimens that are preconditioned with respect to binder performance grade at temperature equal to $(\frac{PGHT-PGLT}{2} - 3°C)$. The test is conducted on four replicates each at a different strain level under cyclic tension and constant crosshead testing mode. The main output of this test and analysis is the damage characteristic curve (DCC) which is a fundamental mixture property that is independent of loading mode and temperature and indicates the trend of reduction of pseudo stiffness

(C) as damage grows. Pseudo stiffness can be considered as the material's internal integrity and its capacity to resist fatigue. As the loading cycle is applied, damage in form of micro-cracks is induced in the whole body of the specimen. This results in reduction in material's capacity until micro-cracks are localized and form macro-cracks and specimen failure happens. Figure 3-4 indicates a typical DCC curve and the test setup.

Currently, there are three accepted fatigue criteria based on the S-VECD approach: G^R, D^R and S_{app}. G^R is the rate of averaged dissipated pseudo strain energy which indicates the decrease in the mixture's energy storage capacity due to each loading cycle [7]. These parameters are defined in Equations 3.6, 3.7 and 3.8 respectively. The number of cycles to failure at G^R equal to 100 (N_f @ G^R=100) is usually used to rank mixtures. D^R is the average reduction in pseudo stiffness per loading cycle and indicates the decrease in material's integrity in terms of stiffness as the load is applied. D^R values usually range from 0.3 to 0.7 with higher values indicating better fatigue resistance [8]. S_{app} is the accumulated damage when C is equal to 1-D^R [9].

$$G^R = \frac{\int_0^{N_f} w_c^R}{N^2{}_f} \qquad \text{Equation (3.6)}$$

$$D^R = \frac{\int_0^{N_f} (1-C)}{N_f} \qquad \text{Equation (3.7)}$$

$$S_{app} = \frac{1}{10000} \times \left(\frac{1}{C_{11}} \times D^R\right)^{\frac{1}{C_{12}}} \qquad \text{Equation (3.8)}$$

Where:W_C^R: Total released pseudo strain energy, *C*: Pseudo stiffness, N_f: number of loading cycles to failure, *C11* and *C12*: Model coefficients of the damage characteristic curve

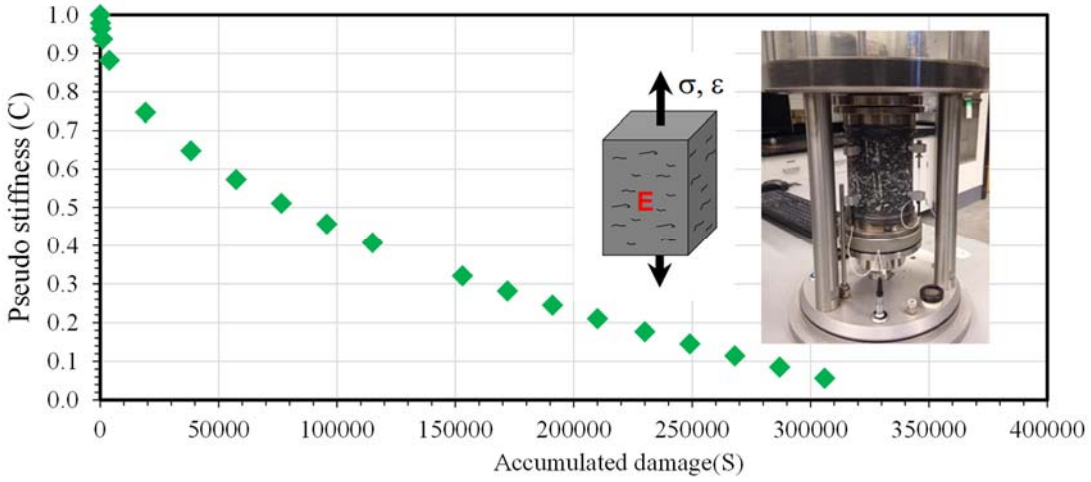

Figure 3-4 Damage characteristic curve and direct tension cyclic fatigue test setup

3.2.5 DISK-SHAPED COMPACT TENSION TEST (DCT)

The disk-shaped compact tension (DCT) test was performed in accordance with the ASTM D7313 standard testing method [10] on three replicates. The test is conducted in monotonic loading conditions and measures the low temperature fracture properties of the asphalt mixtures. As opposed to SCB, the displacement measurements in DCT are controlled by using the crack mouth opening displacement

(CMOD) which is perpendicular to the crack path and is conducted in a rate of 1 mm/min. In general, the testing temperature for DCT test is determined as 10°C warmer than the low temperature performance grade (10°C+PGLT) of the binder. However, in this study, the LTTPBind software was used to determine the testing temperature as 10°C warmer than the 98% reliability pavement low temperature without rounding to nearest 6°C increment. In other words, continuous PGLT value on basis of the pavement location was used in the test temperature calculation. The two index parameters that are used to analyze the DCT test results are the fracture energy (G_f) and the fracture strain tolerance (FST) where FST is determined by dividing G_f by the fracture strength (S_f) [12]. Figure 3-5 indicates a typical DCT test result and setup as well as the specimen geometry. Similar to SCB analysis, the fracture energy for DCT is calculated by normalizing the area under load-CMOD (Crack Mouth Opening Displacement) curve by the fracture area. Also, fracture strength is a geometry dependent parameter and is defined as the maximum stress that the specimen is able to withstand before crack is propagated. Equations 3.9 and 3.10 indicate the calculations of S_f and FST respectively.

$$S_f = \frac{2P(2W+a)}{t(w-a)^2}$$ Equation (3.9)

S_f : Fracture strength

P: Maximum load sustained by specimen

w and a M are indicated in Figure 3-5

t: Specimen thickness

$$FST = \frac{G_f}{S_f}$$ Equation (3.10)

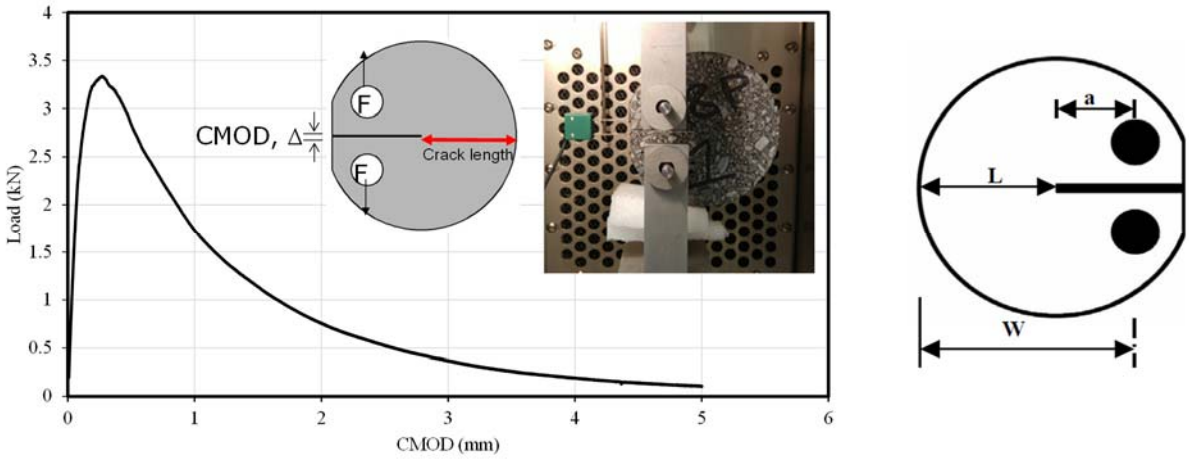

Figure 3-5 Disk-shaped compact tension test result, setup and specimen geometry

3.3 REFERENCES

[1]. New Hampshire Department of Transportation. Standard specifications for road and bridge construction. Section 702, Division 700. Edition 2010.

[2]. Macedo, A. L., Arsénio, E., Batista, F. A., Cardoso, J. L., Fortunato, E., Freire, A. C., ... & Roque, C. A. (2018). Programa de ID&I 2013-2020 do Departamento de Transportes do LNEC-Revisão Intercalar (2013-2017).

[3]. ASTM D7369-11: Standard Test Method for Determining the Resilient Modulus of Bituminous Mixtures by Indirect Tension Test, ASTM International, West Conshohocken, PA, 2011.

[4]. AASHTO, T. (2011). 342-11. Standard method of test for determining dynamic modulus of hot-mix asphalt concrete mixtures. Standard specifications for transportation materials and methods of sampling and testing. Washington (DC): AASHTO

[5]. AASHTO TP (2016). 124-16. Standard method of test for determining the fracture potential of asphalt mixtures using semicircular bend geometry (SCB) at intermediate temperature. Washington, DC: American Association of State Highway and Transportation Officials.

[6]. Ozer, H., Al-Qadi, I. L., Lambros, J., El-Khatib, A., Singhvi, P., & Doll, B. (2016). Development of the fracture-based flexibility index for asphalt concrete cracking potential using modified semi-circle bending test parameters. *Construction and Building Materials*, *115*, 390-401.

[7]. AASHTO TP 107. (2004): Determining the Damage Characteristic Curve of Asphalt Concrete from Direct Tension Cyclic Fatigue Tests, American Association of State and Highway Transportation Officials, Washington, D.C.

[8]. Zhang, J., Sabouri, M., Guddati, M. N., & Kim, Y. R. (2013). Development of a failure criterion for asphalt mixtures under fatigue loading. *Road Materials and Pavement Design*, *14*(sup2), 1-15.

[9]. Wang, Y., & Richard Kim, Y. (2017). Development of a pseudo strain energy-based fatigue failure criterion for asphalt mixtures. *International Journal of Pavement Engineering*, 1-11.

[10]. Wang, Y. D., Keshavarzi, B., & Kim, Y. R. (2018). Fatigue Performance Analysis of Pavements with RAP Using Viscoelastic Continuum Damage Theory. *KSCE Journal of Civil Engineering*, *22*(6), 2118-2125.

[11]. ASTM D7313–06. "Standard test method for determining fracture energy of asphalt-aggregate mixtures using the disk-shaped compact tension geometry." ASTM International, April (2007).

[12]. Zhu, Y., Dave, E. V., Rahbar-Rastegar, R., Daniel, J. S., & Zofka, A. (2017). Comprehensive evaluation of low-temperature fracture indices for asphalt mixtures. *Road Materials and Pavement Design*, *18*(sup4), 467-490.

CHAPTER 4: LABORATORY EVALUATION RESULTS AND ANALYSIS

4.1 INTRODUCTION

The performance of asphalt mixtures is a direct function of mixture design properties such as aggregate size and gradation, binder type and content, air void percentage and any additives in the mixture. Due to the viscoelastic nature of asphalt mixtures, the loading and climatic conditions will also significantly affect mixture performance. Therefore, it is important to examine the mixture performance through laboratory testing and apply the necessary adjustments to the mixture design to ensure the best possible field performance. For that reason, a thorough understanding of the effect of each of the mixture's components with respect to a specific type of distress is of high interest to pavement engineers. In general, asphalt mixtures may encounter three types of structural distresses; rutting, fatigue, and transverse cracking, each with specific failure mechanisms. Many studies have been conducted to determine the relationship between mixture design parameters and different types of distresses. The paragraphs below provide recent examples that evaluate similar parameters to those included in this study.

Work performed by Zhao [1] investigated the correlation of the aggregate gradation, voids of mineral aggregate (VMA), voids filled with asphalt (VFA) and asphalt film thickness (FT) with rutting. The results indicated that the effects of these parameters are considerably lower for a mixture with 4% air void content compared to one with 7% air voids.

Diab et al. [2] indicated the importance of the effect of fine aggregate source and dust to effective binder (d/be) ratio by means of conducting the indirect tensile strength and moisture susceptibility tests, where a combination of hydrated lime and 0.95 (d/b_e) resulted in improved mechanistic properties of the mixtures. In another study to demonstrate the effect of aging level, Rahbar showed that there may not be a strong correlation between binder and mixtures cracking properties [3]. Through statistical analysis during development of a balanced mix design for overlay mixtures in Texas, it was indicated that the binder performance grade (PG), effective binder volume (V_{be}), film thickness (FT) and aggregate surface area (SA) have a significant effect on the mixtures cracking performance, while air void content was shown to have minimal effect in the results of the Texas Overlay (OT) test [4]. Using a large dataset of more than 170 mixtures from New England and Minnesota, Oshone et al. showed high correlation of binder related properties such as binder content, film thickness and performance grade useful temperature interval (UTI) (UTI is the difference between PG high temperature (PGHT) and PG low temperature (PGLT)), with fracture energy (G_f) obtained from the disk-shaped compact tension (DCT) test [5]. A research study conducted by the National Center for Asphalt Technology (NCAT) on the refinement and validation of 4.75 mm Superpave mixtures examined the statistical correlation between the mixture design volumetric properties such as V_{be}, VMA, VFA, d/b_e and FT to the rut depth from the Asphalt Pavement Analyzer (APA) and G_f from the indirect tensile creep (IDT) test [6]. The Pearson's correlation coefficients indicated that d/b_e is the most significant factor followed by FT. The results also revealed the importance of V_{be} and its two-way interaction with the amount of natural sand in the mixture with regards to the rut depth. In a research study to develop predictive models for dynamic modulus (|E*|) and phase angle of asphalt

mixtures, Nemati and Dave implemented only the nominal mixture design properties such as recycled binder ratio (RBR), nominal maximum aggregate size (NMAS), air void percentage (AV%) and asphalt content (AC%) in construction of the models and indicated the significance of two-way interactions of these parameters in the linear viscoelastic behavior of asphalt mixtures [7]. There are many more examples of the research studies conducted on correlations between mixtures' properties and performance conducted by other researchers [8-12]. However, due to continuous improvements in asphalt material production and construction techniques, it is necessary to regularly evaluate the correlation of the distress index parameters with mixtures' nominal properties to identify the gaps between production and performance evaluation tools.

A variety of laboratory performance based testing and analysis methods are available to characterize mixture performance with respect to individual types of distresses. In order to simplify the application of these tests to rank and correlate the performance of the mixtures in the lab to that of the field, different failure criteria and performance indicator parameters have been proposed and evaluated. Many of the existing criteria are based on different mechanics of failure (i.e. fracture mechanics, continuum damage mechanics) and are designed to evaluate only one particular type of performance. Optimally, the mixture should be designed in a manner to tolerate multiple competing distresses such as rutting and cracking at the same time. In many instances laboratories are not equipped with all the required testing equipment and if so, the exhausting amount of time required for sample fabrication and testing in addition to the required number of trained technicians in the lab may not be feasible to conduct all tests. As a result, there is a need to investigate the correlation between laboratory test results and index parameters of different tests to determine if any of them can be used interchangeably or at least provide some preliminary estimate of the mixture's performance in laboratory tests that have not been performed. For instance, Na Chiangmai found a high correlation between the plateau value (PV) from the bending beam fatigue test and pre-peak fracture energy from the DCT test [13]. Also, Tang investigated the correlation between fracture and fatigue resistance of high RAP continued HMA mixtures [14]. However, there is generally very little available in the literature to investigate the correlations between the indices from different tests.

The following sections of this chapter will provide the testing results and discussions on the observations. Each subsection will briefly compare the mixtures for an individual test using the specific performance index parameter related to that test. Along with the performance tests, a forward direction step-wise linear regression statistical analysis is conducted between the mixture design properties and performance index parameters to determine the most significant design variables affecting the index parameters with aim of improving pavement performance to specific distresses. All the statistical analysis are conducted by means of JMP PRO statistical software. Moreover, the correlations between indices from different performance prediction tests will be determined to estimate other types of distress which can help in reducing the laboratory testing. Due to the limited number of CCPR mixtures in this research project and lack of volumetric properties of such mixtures, the statistical analysis will be limited to the hot mixed asphalt mixtures only. Table 4-1 indicates the mixture design properties (includes 10 design parameters) that were investigated for statistical analysis.

The statistical analysis includes the following parameters:

- The coefficient of estimate of linear regression where a positive estimate means that the variable and response are directly proportional, and a negative estimate value indicates that they are inversely proportional.
- The t-ratio which is the estimate divided by the standard error. Since the degree of freedom (DF) for the t-test analysis in this study is 10 (DF=number of variables-1), the t-ratios over 1.812 (in absolute value) at 90% confidence level, suggests that the coefficient is significantly different from the mean.
- The probability value (p-value) of a two tailed t-test analysis which reveals the influence of each mix design factor on the performance test where a lower p-value means a higher effectiveness of the factor. A significance level (α) of 0.1 equal to 90 percent confidence level was considered as the set p-value to discriminate the influential parameters.

Table 4-1 Mixture design properties used for statistical analysis

Mix ID	NMAS (mm)	Binder Grade	Useful Temperature Interval (UTI) (°C)	AC%	VMA %	V_{be}%	RBR%	%Passing 4.75mm	%Passing 0.075mm	Gyration
ARGG-1	12.5	PG58-28	86	7.8	19.1	15.1	0.0	40.0	3.5	75
ARGG-2		PG58-28	86	7.6	18.4	14.4	6.6	37.0	3.5	75
W-6428H-12.5		PG64-28	92	5.4	16.1	12.1	18.5	57.0	3.8	75
W-5828L		PG58-28	86	5.8	15	11	16.2	57.0	3.6	50
W-5834L		PG58-34	92	5.4	15.3	11.3	18.5	60.0	3.7	50
W-7628H-12.5		PG76-28	104	5.4	16.1	12.1	18.5	57.0	4.0	75
W-7034PH		PG70-34	104	5.8	16	12.0	0.0	59.0	3.7	75
W-7628H-9.5	9.5	PG76-28	104	6.1	16.3	12.3	14.8	68.0	4.9	75
W-5828H		PG58-28	86	5.9	16.6	12.6	16.9	70.0	4.5	75
W-6428H-9.5		PG64-28	92	6.4	17.1	13.1	0.0	69.0	5.2	75
B-6428H	19	PG64-28	92	4.8	14.3	10.3	20.8	46.0	3.5	75
B-5834L		PG58-34	92	4.6	14.1	10.1	21.7	43.0	3.2	50
B-5828H		PG58-28	86	4.8	14.9	10.9	20.8	47.0	3.2	75
BB-6428L	25	PG64-28	92	4.8	14.8	10.8	20.8	36.0	3.2	50

4.2 RESILIENT MODULUS (M_r)

The results from resilient modulus test are shown in Figure 4-1. The error bars on the graph show one standard deviation from the mean for the replicates that have been tested. The ARGG-2 has a higher M_r value compared to ARGG-1 which is mainly related to the RBR percentage difference. The other wearing courses show expected results such that stiffer binder PG grades have higher M_r values and mixtures with softer binders have lower M_r values. A noteworthy result from this test is related to W-6428H-12.5 and W-5828L. Although the two mixtures have significant differences in their mixture design properties (W-6428H-12.5 has a higher PGHT, number of gyrations and RBR content), both mixtures

indicate similar resilient modulus values. It is hypothesized that the intermediate testing temperature (25°C) may have not been capable of differentiating the viscoelastic properties of theses mixtures.

All the binder courses indicated expected results with B-6428H having a stiffer PG grade on both ends (PG64-28) and higher design gyration level compared to B-5834L indicated to be the stiffest among all. The only base course mixture in this research (BB-6428L) has one of the highest modulus values among all the mixtures. Even though the NMAS for this mixture is higher compared to B-6428H (25mm for BB-6428L and 19mm for B-6428H, with the same binder content (4.8%), the effect of design number of gyrations (50 for BB-6428L and 75 for B-6428H) is clearly obvious in stiffening the mixture matrix and increasing the load carrying capacity.

The CM-1 and CM-1-a mixtures have similar modulus values while the CM-2 mixture is softer than the CM-2-a mixture. The similar resilient modulus values for CM-1 and CM-1-a (despite different amount of oil distillate in emulsion), shows limited ability of M_r test in distinguishing mixtures. The effect of the distillate amount is different for the two mixtures and can be observed by comparing the graphs. Although CM-2 has a smaller NMAS and the RAP has more binder compared to CM-1, it has a higher M_r value. These results are likely due to differences in the RAP sources; other studies have shown that the chemical interaction between the emulsion and the RAP binder will be significantly different depending on the age and chemistry of the binder in the RAP [15]. This illustrates that the RAP age and binder chemistry can have a greater effect than other factors such as the emulsion's oil distillate percentage or even the maximum aggregate size on the CCPR mixture M_r values. While this is a pertinent observation, it should also be considered that M_r is a property that is measured at a single test temperature and loading frequency and thus, may not portray a full picture of material's response to traffic loading. In previous studies, M_r has shown to be correlated with rutting susceptibility [16], so the results from this test indicate that the CCPR mixtures can be expected to have lower rutting resistance than HMA mixtures.

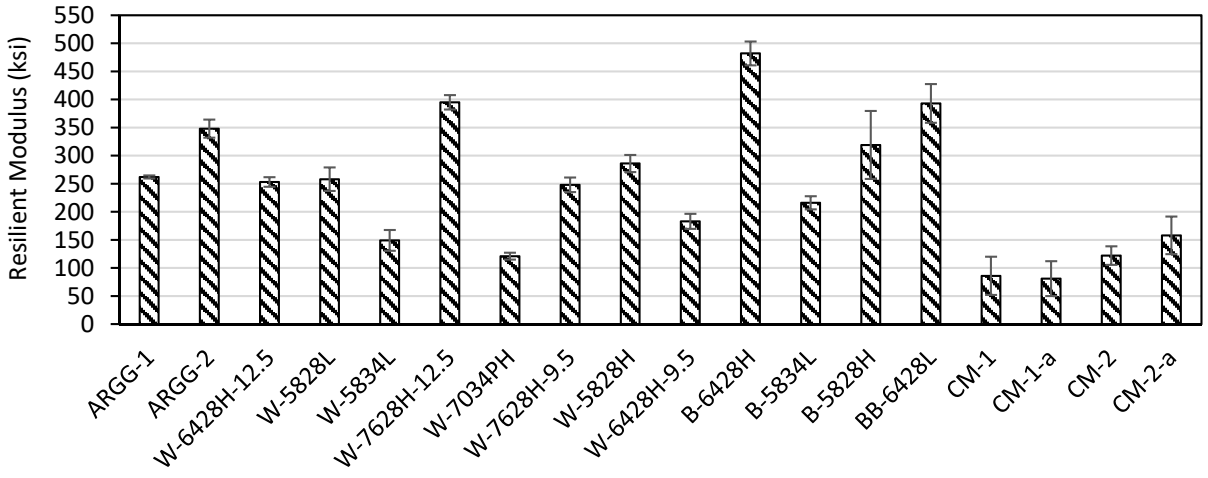

Figure 4-1 M_r test results (error bars represent one standard deviation interval)

The results from the statistical analysis on M_r test is depicted in Table 4-2. The results indicate that the % passing 4.75 mm sieve size and RBR are among the significantly effective factors on the resilient modulus.

Almost all volumetric parameters as well as gyration levels have less than 10% significance level when rutting is a concern. However, the NMAS with a positive estimate coefficient was seen to be close to the 0.10 significance level. Considering the results from statistical analysis on M_r, with an intention to mitigate the rutting issues, designers can simply change the binder type as an efficient adjustment to the mix design.

Table 4-2 Significant mix design properties affecting resilient modulus (M_r)

Index Parameter	Mix Property	Estimate	Std Error	t-Ratio	Prob>|t|
Resilient Modulus, M_r	PGHT	181.20	42.42	4.27	0.0021
	UTI	-156.22	40.84	-3.83	0.0041
	%Passing 4.75mm	-29.15	9.57	-3.05	0.0139
	RBR	32.15	12.38	2.6	0.0289

4.3 COMPLEX MODULUS (|E*| AND PHASE ANGLE)

The |E*| master-curve indicates the stiffness of the mix over a broad range of frequencies at the reference temperature. The master-curve is an excellent tool to compare different mixtures in terms of their stiffness and the rutting susceptibility of the mix. Also, the mixtures can be assessed and ranked in terms of their potential for fatigue and low temperature cracking based on their stiffness. The phase angle master-curve on the other hand reflects the relative proportions of viscous and elastic properties of the mix at a given temperature and frequency with higher phase angles indicating greater viscous response, which is indicative of better crack resistance. The results from the complex modulus testing are discussed in the following paragraphs. It should be noted that due to the continuous nature of complex modulus master-curves, it is not feasible to perform statistical analysis between the mixtures.

The dynamic modulus master-curves for all the mixtures are depicted in Figure 4-2. The results indicate that ARGG-2 is stiffer than ARGG-1 over a broad range of frequencies because of the RBR content in the ARGG-2. In terms of other wearing courses, W-7628H-12.5 is shown to be the stiffest mixture while W-7034PH which contains a polymer modified binder with 4% styrene butadiene styrene (SBS) and 4% aromatic oil is the softest. In terms of other wearing courses. As opposed to resilient modulus test that was not able to capture the difference between W-6428H-12.5 and W-5828L, the dynamic modulus master-curves indicate relatively higher stiffness for W-6428H-12.5 in higher frequencies and lower stiffness in lower frequencies. This observation confirms the previous hypothesis made on the resilient modulus results and its inability in differentiating the mixtures. The equivalent frequency on the master-curves (1.59Hz at 21°C) for resilient modulus testing conditions is close to where the two master-curves cross and as a result resilient modulus is not able to discriminate the performance of these mixtures.

Considering the wearing course mixtures, the phase angle master-curves in Figure 4.2 for the two ARGG mixtures are significantly different compared to other mixtures, especially along the mid to low frequencies. Generally, more elastic mixtures would have a lower peak phase angle value in the low frequencies. This trend can be seen for all other wearing courses such that W-7628H-12.5 with higher PGHT is more elastic whereas W-7034PH and W-5834L are more viscous.

With respect to hot mixed binder and base course mixtures and their dynamic modulus master-curves, the B-6428H mixture is the stiffest along all the frequencies whereas the B-5834L mixture is the softest through the middle frequencies. The BB-6428L mixture is softer than B-6428H and B-5828L mixtures even though it has larger NMAS with similar mixture asphalt content and effective binder volume. However, BB-6428L is designed in a lower gyration level which can be a result of such observations.

Similar trends exist with the phase angle master curves for binder and base course HMA mixtures. For instance, B-5828H has a softer binder, finer gradation and smaller NMAS compared to BB-6428L mixture. While all these factors should result in a softer mix, the higher design compaction level of B-5828H led to a lower binder content, resulting in a decreased phase angle and increased modulus. This shows that binder content (and design compaction level) can supersede the effects of larger aggregate size and coarser gradation when considering the mix stiffness.

The CCPR mixtures have comparable |E*| master-curves with CM-2-a being the stiffest of four. The amount of oil distillate percentage has consistent impact on changing mixture stiffness. The CCPR mixtures with higher oil distillate percent emulsions have lower stiffness, for example, at 21.1°C and 10 Hz, the |E*| of CM-1 mixtures is 20.3% lower than CM-1-a, whereas at same temperature and frequency, CM-2 has a 40% lower |E*| than CM-2-a. The oil distillate percent has a greater effect on the CM-2 complex modulus; this agrees with the M_r results. The difference in the response of the two mixtures is likely due to the effect of interaction between the RAP binder and emulsion.

The modulus values of CCPR mixtures are approximately half of HMA mixtures and the phase angles are higher in the mid to high frequency ranges. The higher relative viscous component of the response can be considered as a positive feature for CCPR mixtures as it can result in better fatigue performance. On the other hand, and as indicated from the M_r results, the low stiffness of the CCPR mixtures at high temperatures and low frequencies indicates a greater susceptibility to rutting.

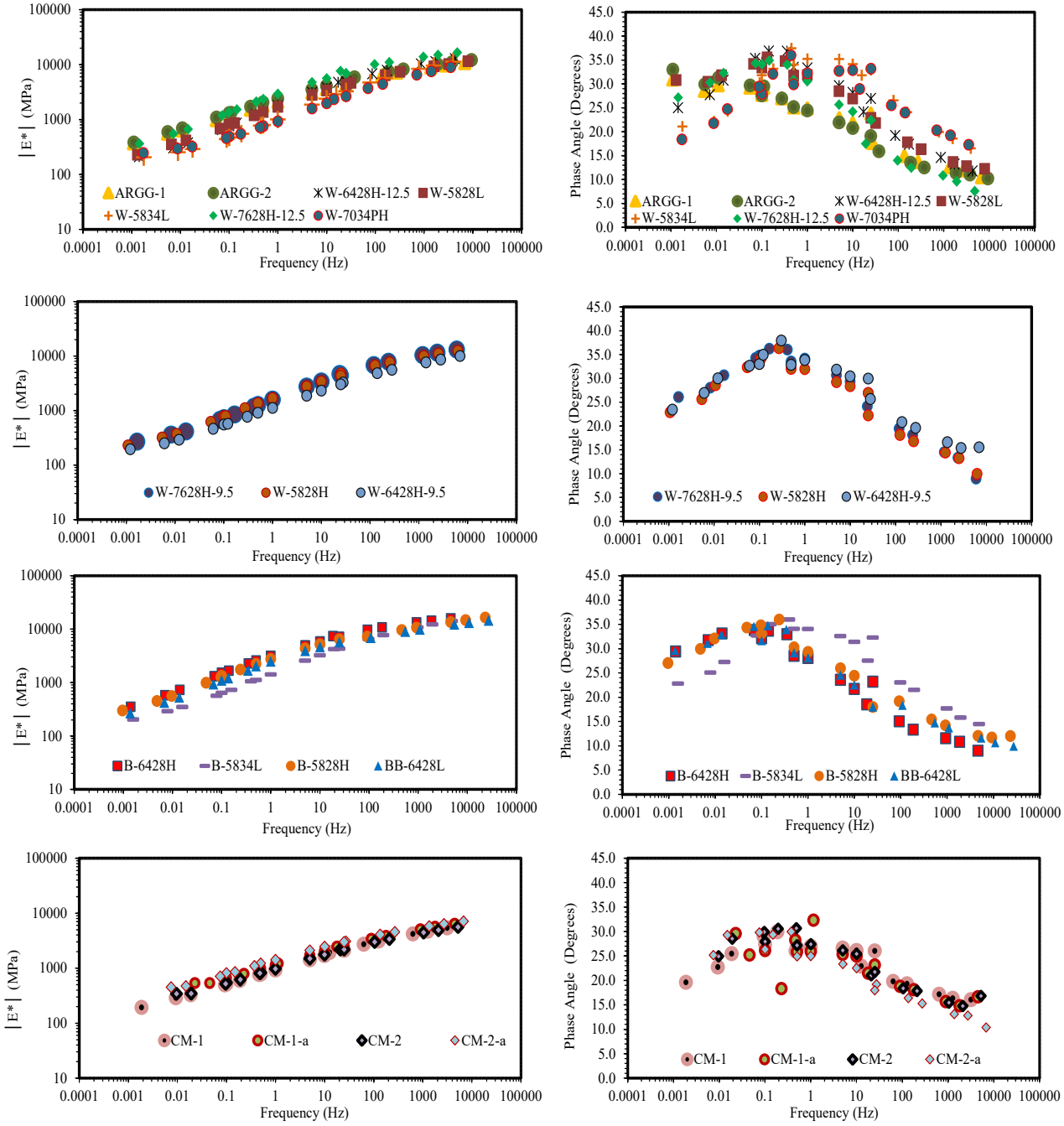

Figure 4-2 |E*|and phase angle master-curves constructed with shifted raw data

4.4 SEMI-CIRCULAR BEND TEST

The results from fracture energy determined from the SCB test are depicted in Figure 4-3. The results indicate that the fracture energy is not capable of differentiating the fracture properties of different mixtures. For example, the previous test results indicated that ARGG-2 is a stiffer mixture compared to ARGG-1 and it is expected to have a lower fracture resistance, but the two mixtures have very close fracture energy values. Also, according to the complex modulus results, W-7034PH and W-5834L are the

softest mixtures among all wearing courses and are expected to have a relatively high crack resistance while fracture energy values do not reflect this. The same observations are made for the binder and base course mixtures.

The flexibility index values (Figure 4-4) agree well with the other test results and crack resistance expectations. According to the results, W-7034PH is the most crack resistance mixture amongst all others. With respect to G_f, the higher PGHT and RBR result in a stiffer mixture and higher G_f values. However, it should be considered that higher fracture energy is not always about the higher stiffness and depending on the binder type and content a ductile mixture could also have a high fracture energy. This can be seen through a more in-depth investigation on a mixture such as W-7628H-9.5 which maintains high G_f and FI values at the same time, while it retains one of the highest binder contents among the study mixtures. Due to the general expectations from the cold mixtures and the observed dynamic modulus master-curves, it is not surprising that the fracture energy for these mixtures is relatively low compared to HMA mixtures. Nonetheless, they maintain high flexibility index compared to HMAs. It should be taken into consideration that the combination of SCB testing temperature (25°C) and relative softness of these mixtures can result in creep rather that real fracture happening during the test which could result in unrealistic flexibility index for these mixtures. Considering the test results, CM-1 did not show an inflection point on the post peak side of load-displacement curve and therefore the FI is not applicable for this mixture. The lack of inflection point on CM-1 specimen was mostly due to very brittle failures (which is also evident from very low fracture energy values for CM-1). In contrast, CM-1-a specimens (with only difference as the emulsion with lower oil-distillate amount), did exhibit a more typical quasi-brittle failure mode with presence of inflection point in the post-peak region.

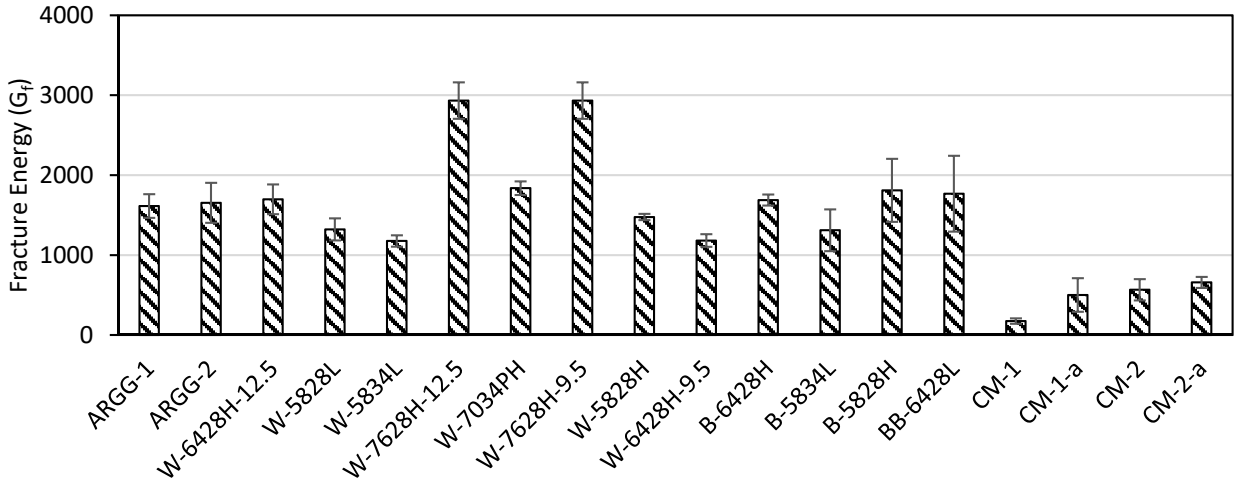

Figure 4-3 Fracture energy plots

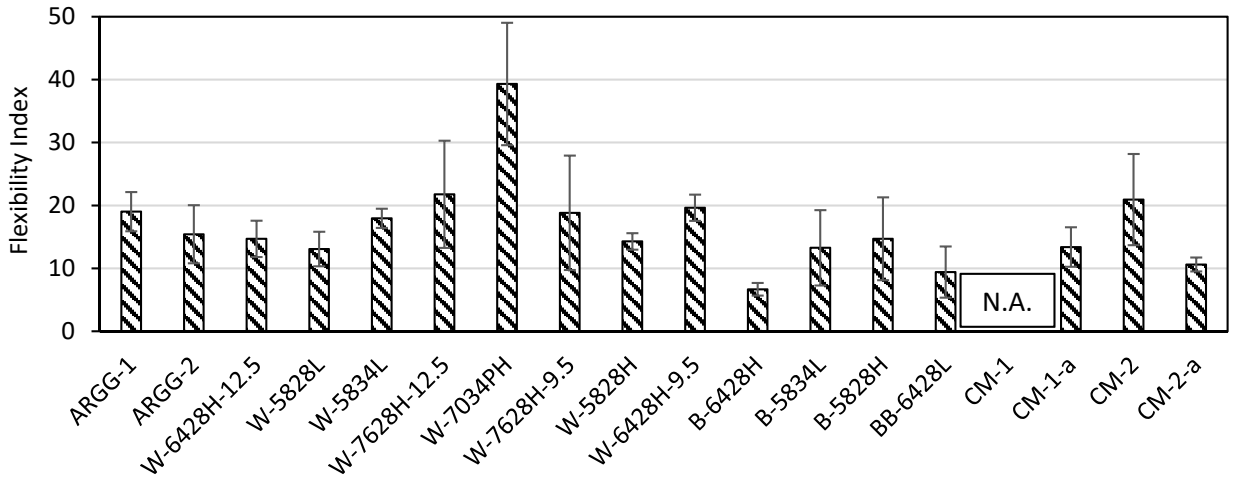

Figure 4-4 Flexibility Index plots

The effect of mix design properties on the SCB fracture energy and FI are shown in Table 4-3. With respect to G_f, the higher PGHT and RBR result in a stiffer mixture and higher G_f values. As discussed above, fracture energy is not analogous to higher stiffness, it depends substantially on the binder type (as evident from presence of PGHT as significant factor for G_f and UTI for FI) and binder content. One of the main intents of developing the FI has been to capture the effect of RBR on mixtures cracking [17], in this study this effect is also clearly seen with RBR impacting both G_f and FT (c.f. Table 4-3). The effective binder content and VMA also show as significant variables for FI, both of these quantities can be tied back to amount of available binder in the asphalt mixture.

Table 4-3 Significant mix design properties affecting SCB G_f and FI

Index Parameter	Mix Property	Estimate	Std Error	t-Ratio	Prob>|t|
Gf	PGHT	79.64	9.81	8.12	0.0001
	RBR	41.09	12.26	3.35	0.0074
	AC%	321.92	105.53	3.05	0.0122
FI	RBR	-0.79	0.15	-5.11	0.0006
	VMA	-5.69	1.67	-3.39	0.0080
	UTI	0.27	0.13	1.94	0.0843
	V_{be}	2.90	1.58	1.83	0.1008

4.5 DIRECT TENSION CYCLIC FATIGUE

The results from N_f @ G^R=100, D^R and S_{app} are shown in Figure 4-5, Figure 4-6 and Figure 4-7 respectively. The effect of addition of RAP is evident when comparing the fatigue performance of ARGG-1 to ARGG-2 as the latter mixture has significantly lower fatigue resistance. With respect to N_f @ G^R=100 and D^R results, the W-7034PH, shows very good fatigue performance compared to other mixtures. However, considering the S_{app} results, it is the W-7628H-12.5 followed by W-7628H-9.5 that indicate the best performance. As expected, the hot mixed binder and base course mixtures have lower fatigue resistance because of larger aggregate size, lower binder content, and higher RBR percentages. The three indices result in different mixture ranking, especially for mixtures such as W-6428H-12.5, W-7628H-12.5, W7628H-9.5, and B6428H. Also, the discrimination of the magnitude of difference between performances is shown to be quite different. For example, W-7034PH is indicated to have 4 times higher N_f @ G^R =100 value compared to W-7628H-9.5, however, their D^R and S_{app} values are relatively close. The three indices result in quite different performance prediction for the cold mixtures. It should be mentioned that some State DOTs such as Georgia have started using the S_{app} parameter as part of their mixture design specifications. All four cold mixtures are shown to have low fatigue resistance with respect to N_f @ G^R =100 and S_{app} while their D^R values are similar or even higher than most of the wearing course mixtures. In general, the results indicate that while these indices can discriminate the overall performance of the mixtures and their production methods, they may not consistently predict and rank the mixtures' performance as standalone parameters.

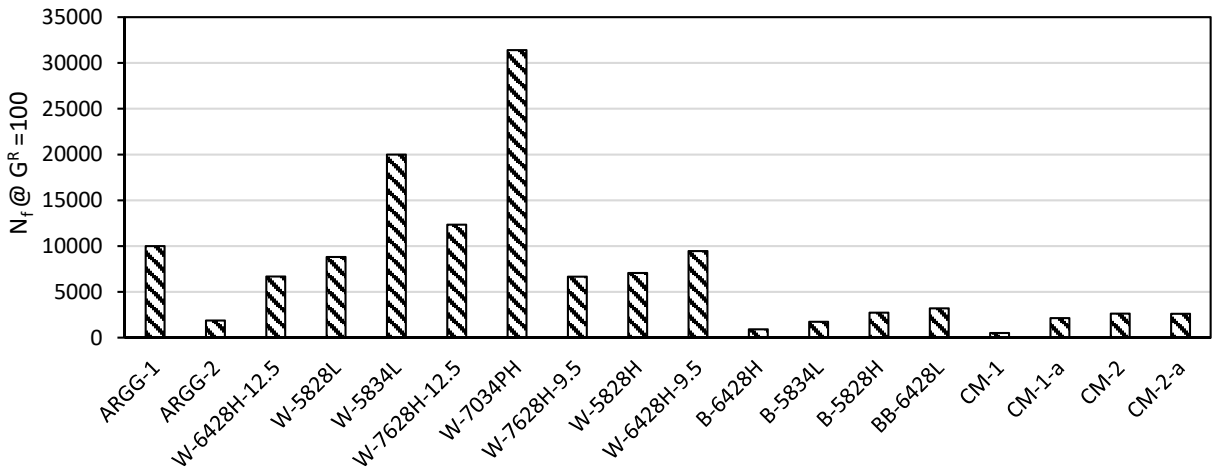

Figure 4-5 N_f @G^R=100 fatigue failure criterion plots

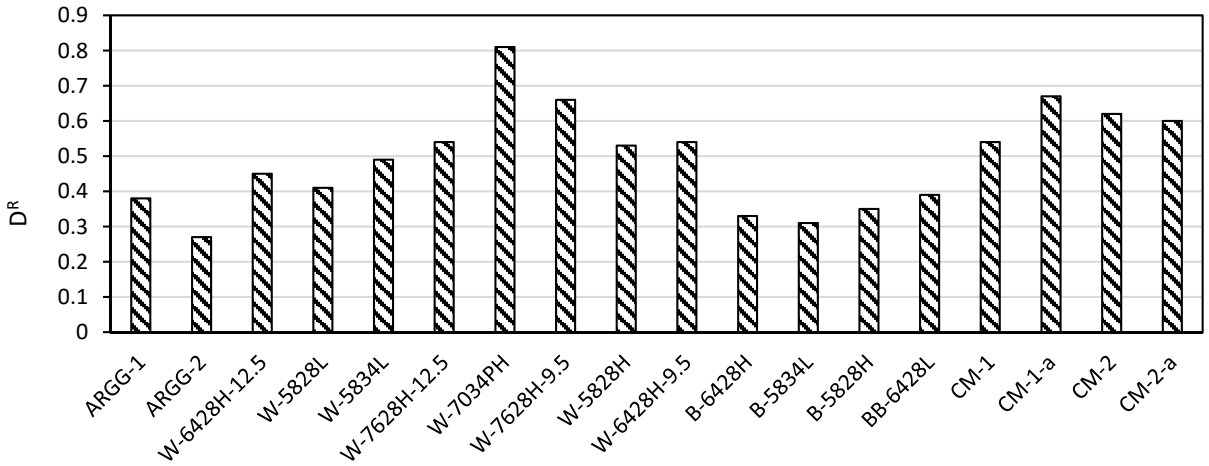

Figure 4-6 D^R fatigue failure criterion plots

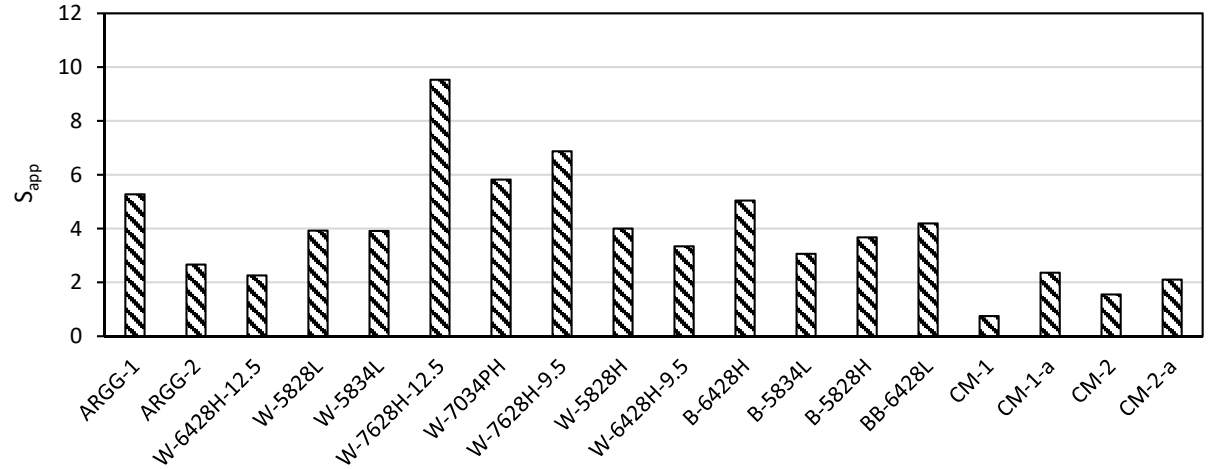

Figure 4-7 S_{app} fatigue failure criterion plots

The effect of mix design parameters on S-VECD based index parameters is shown in Table 4-4. The analysis indicated that S_{app} is only sensitive to the binder grade and UTI in 10% significance level for the mixtures evaluated in this study. However, with respect to G^R and D^R parameters, the analysis confirms the importance of fine aggregate and dust in the mixtures as both indices are highly dependent on the cumulative percent passing amounts on 4.75 mm and 75 µm sieves, where an increase in the dust amount causes a lower fatigue life. On the other hand, the increase in cumulative percent passing 4.75 mm results in lowering of non-uniform air void dispersion in the aggregate matrix and results in a better fatigue resistant mixture. The effect of UTI is apparent in both indices, with a larger value being better for fatigue resistance. Both indices show sensitivity to the changes in the amount of RBR with G^R being more influenced by the RBR content. The effect of gyration level could be the main noteworthy difference

between the two parameters where a higher level of gyration is shown to have a negative effect on the N_f @ G^R=100 parameter.

From an engineering perspective, higher VMA is required for a durable mixture to retain a satisfactory amount of binder, however the statistical analysis indicated a negative effective of VMA. It should be noted that throughout the analysis, wherever VMA is indicated as a negative effective factor, it is accompanied by the positive effect of either V_{be} or AC% as they are tied to each other. This means that a higher VMA in the mixture design is not a guarantee for a crack resistant mixture and the effective binder content to fill the void spaces in aggregate skeleton is critical. In general, the significant mixture design parameters on S-VECD based parameters are similar to those for Flexibility Index from SCB test, indicating that there could potentially be a high correlation between the two indices. Therefore, if a mixture is optimized for one of these tests then it is likely to meet the requirements for other one as well.

Table 4-4 Significant mix design properties affecting Simplified Viscoelastic Continuum Damage based fatigue performance indices (N_f @ G^R = 100, D^R and S_{app})

Index Parameter	Mix Property	Estimate	Std Error	t-Ratio	Prob>|t|
N_f @ G^R=100	RBR	-730.84	162.26	-4.5	0.0041
	% Passing 4.75 mm	469.03	187.52	2.5	0.0465
	%Passing 0.075mm	-9011.72	3748.20	-2.4	0.053
	UTI	372.52	170.75	2.18	0.0719
	VMA	-190.285	90.28	-2.11	0.0796
	Gyration	-5262.82	2511.85	-2.1	0.081
	V_{be}	4089.5	2004.01	2.04	0.0874
D^R	UTI	0.012	0.002	5.69	0.0007
	% Passing4.75 mm	0.021	0.005	4.29	0.0036
	%Passing 0.075mm	-0.156	0.051	-3.03	0.0191
	RBR	-0.006	0.002	-2.62	0.0343
	V_{be}	0.061	0.031	2.00	0.0850
S_{app}	UTI	0.225	0.055	4.11	0.0017

4.6 DISK-SHAPED COMPACT TENSION TEST

The results from G_f (including the test temperatures in degrees Celsius) and FST are shown in Figure 4-8 and Figure 4-9, respectively. The results indicate that the ARGG mixtures have better performance compared to other wearing courses such as W-6428H-12.5, W-5834L and W-7628H-9.5 that are tested in similar temperature range, that is, these mixtures may have better thermal cracking performance in similar climatic conditions. Identical to the SCB-IFIT test results, W-7034PH mixture indicates an outstanding performance with respect to low temperature cracking. The hot mixed binder course mixtures reveal comparable low temperature cracking performance to some of the wearing course mixtures such as W-6428H-12.5 and W-5828L with respect to specific projects and temperatures at which they have been tested. In general, the ranking from both G_f and FST are similar except for three mixtures (ARGG-2, W-5828L and, BB-6428L). At present, the Minnesota Department of Transportation (MnDOT) has implemented the DCT test in the mix design and acceptance processes. According to MnDOT specifications the minimum acceptable fracture energy is set to be 450J/m^2 and as it can be observed from the plots, all the common New Hampshire mixtures pass this threshold. Since MnDOT is the only entity to have fully implemented this test, the threshold values from their specifications is used here for comparison. In future similar threshold should be developed for NHDOT. The CCPR mixtures were not tested though DCT since these mixtures are generally used in relatively lower levels in the pavement cross sections and are covered with other wearing courses. Therefore, it is assumed that low temperature cracking may not be a structural distress for CCPR mixtures.

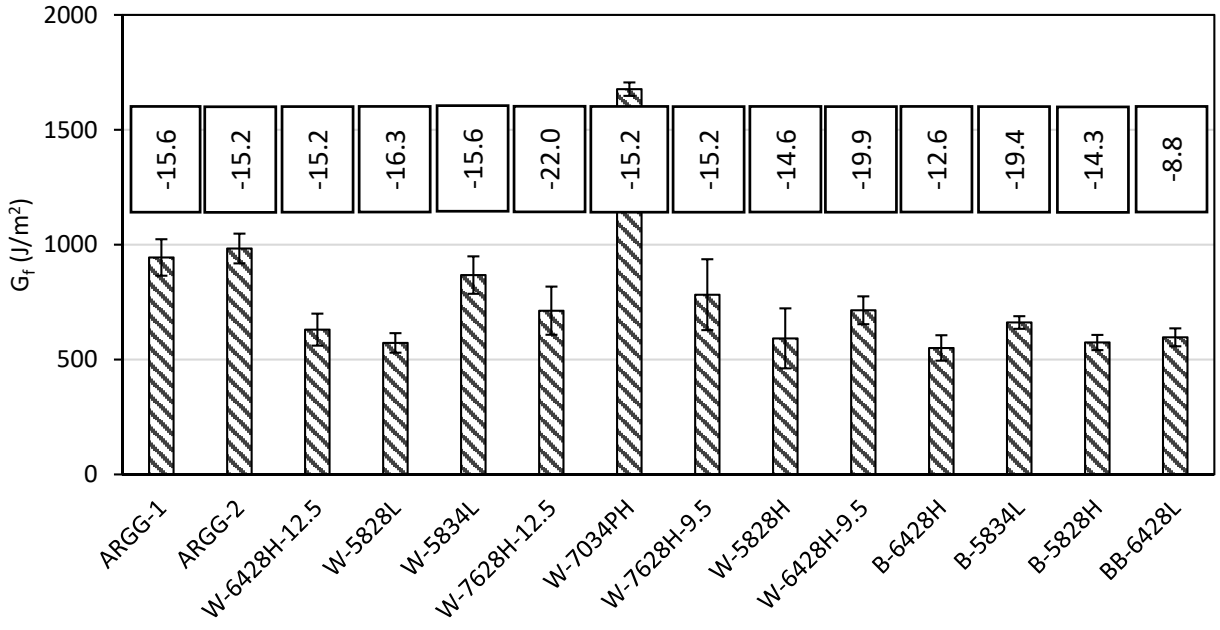

Figure 4-8 DCT Fracture Energy (G_f) plots (number in box indicate test temperature in ˚C)

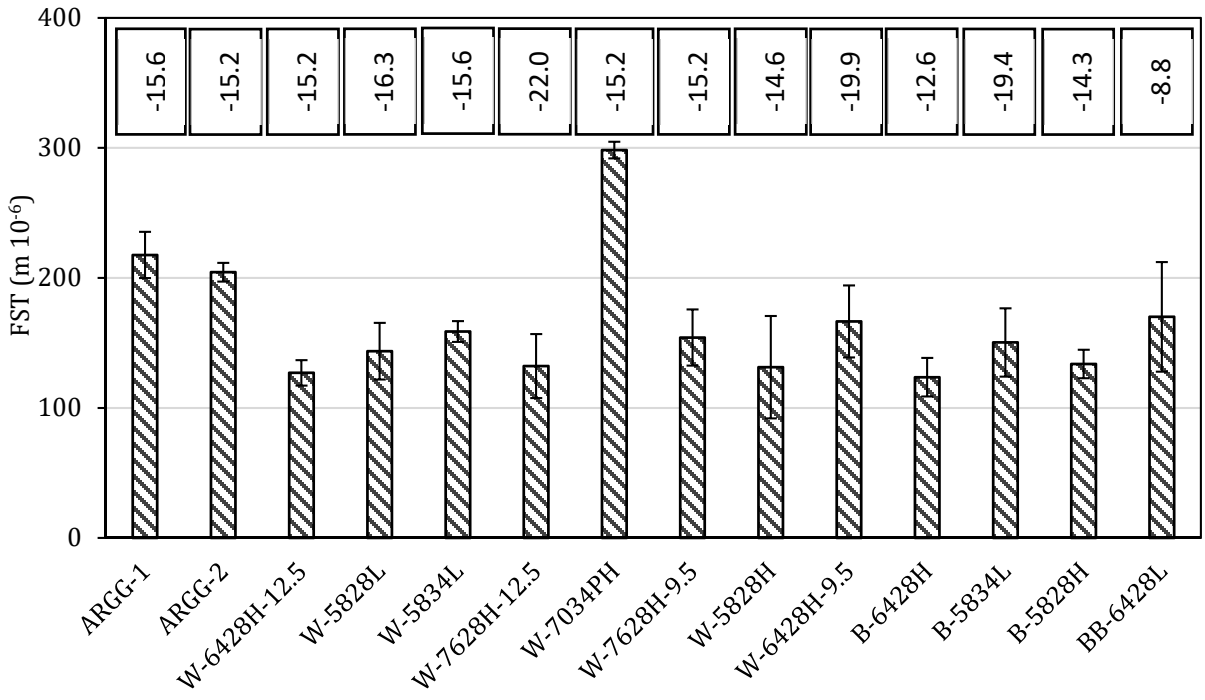

Figure 4-9 Fracture Strain Tolerance (FST) plots

Table 4-5 summarizes the significant mixture design properties on DCT index parameters. Similar to previous observations for FI and N_f @ G^R =100, higher VMA has a negative effect on G_f while accompanied with the positive effect of AC%. The statistical analysis confirms that a lower PGLT will result in higher fracture energy values, indicating the importance of selecting an appropriate binder type for mixtures to withstand low temperature cracking.

Similar to results from S-VECD fatigue indices (G^R and D^R), the % passing 75µm is considered as a significant mix design property for both G_f and FST. Higher amounts of dust can over-stiffen the mastic phase of mix and lower the asphalt film thickness which can lead to cracking. While the higher amount of RBR is shown to increase the cracking susceptibility, increase of UTI which, in general, can be translated into use of polymer-modified binders, mitigates the cracking. The positive effect of design gyration level in increasing the fracture energy is an interesting point in the statistical analysis. For both the low temperature fracture energy and N_f @ G^R =100, the four significant parameters are common, and they have similar type of effects on the performance (increasing cracking resistance); this indicates the potential for a high correlation between these two parameters.

Table 4-5 Significant mix design properties affecting disk-shaped compact tension test performance indices (G_f and FST)

Index Parameter	Mix Property	Estimate	Std Error	t-Ratio	Prob>|t|
G_f	**RBR**	-21.70	5.28	-4.11	0.0063
	VMA	-175.10	45.61	-3.84	0.0086
	UTI	47.19	12.50	3.77	0.0092
	%Passing 0.075mm	-157.88	45.69	-3.45	0.0136
	AC%	227.63	68.16	3.34	0.0156
	PGLT	-36.21	13.13	-2.76	0.033
	Gyration	6.54	2.62	2.49	0.0473
FST	**RBR**	-4.96558	0.78	-6.38	<0.0001
	%Passing 0.075mm	-44.16	11.55	-3.82	0.0034
	UTI	2.17	0.96	2.26	0.0474

4.7 STATISTICAL CORRELATION OF THE PERFORMANCE INDEX PARAMETERS

With respect to conventional volumetric mixture design, it is important for the designers to understand the significance of each mix design variable on the performance of the product. However, with changes in materials and loadings, asphalt mixture design is moving towards performance based design approaches such as the performance engineered mix design (PEMD). One of the main goals of the PEMD approach is to embed the mixture performance prediction tests within the structure of the volumetric based mixture design. The final product of the PEMD is a mixture that can withstand competing distresses such as rutting and cracking at the same time. However, such approaches need intensive testing to evaluate both rutting and cracking performance which may be time consuming and unaffordable in many settings. As a result, identifying the correlation among different distress index parameters could be a key factor in reducing the costs of performance based mixture design procedures.

Before determination of any correlation among the indices, it is important to verify the data and identify any outliers within the dataset which could cause biased or unrealistic correlations. Therefore, the Mahalanobis distance (MD) [18] analysis was performed to determine the outlier mixtures in the study. This analysis essentially identifies an overall mean as the centroid for multivariate data. In a multivariate space, this point is where all the averages from all variables intersect. Therefore, as a data point gets further away from the centroid, the MD for that data point becomes larger. In a dataset with different mixtures such as this study, the MD value is first calculated for the whole dataset and is called the MD threshold value. Then, for each individual mixture, a separate MD value is calculated; if it exceeds the

threshold MD value then that mixture is an outlier. As it can be seen from Figure 4-10, the W-7034PH and W-7628H-9.5 mixtures are very close to the calculated threshold value, however, they are below this point. Therefore, all the mixtures in the study can be used to establish the correlations.

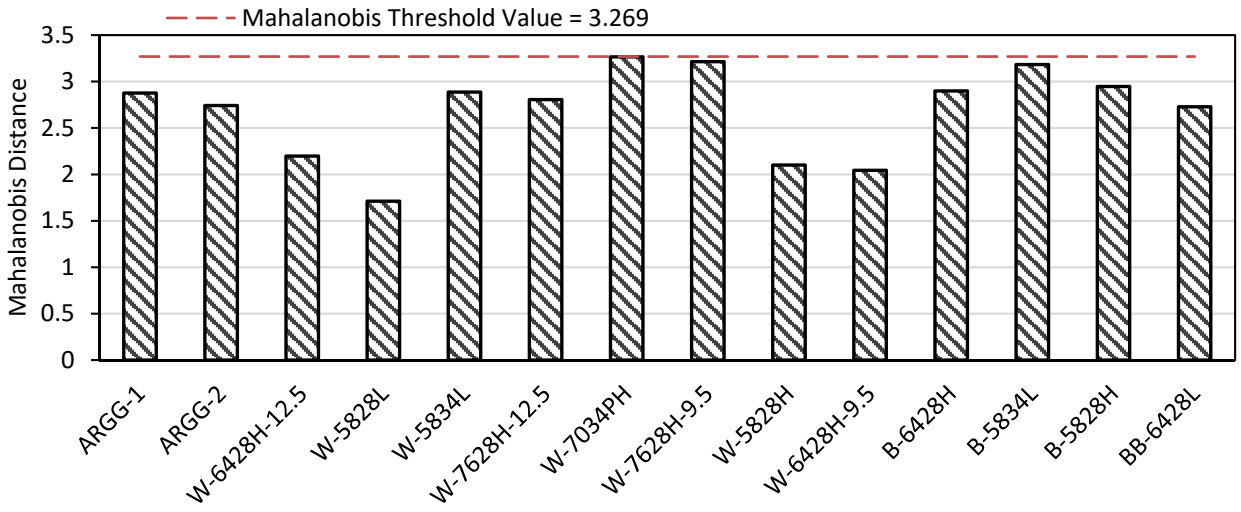

Figure 4-10 Mahalanobis distance of the study mixtures

To determine the correlations among the parameters, the Pearson's linear correlation coefficients (r) were calculated and depicted in Table 4-6. In general, the Pearson's coefficients range from -1 to 1 indicating a perfect negative and positive correlations, respectively. The strength of the correlations in this research are categorized into three categories defined as follows:

- Weak correlation (W), $|r| < 0.3$ (*indicated by italic font*)
- Medium correlation (M), $0.3 \leq |r| < 0.7$
- Strong correlation **(S)**, **$0.7 \leq |r| \leq 1$** (**indicated by bold font**)

M_r has a medium to high inverse correlation with N_f at G^R=100 and FI, indicating that increased stiffness may increase the cracking susceptibility. However, there is a weak positive correlation between M_r and S_{app} which may indicate that S_{app} can slightly increase with higher stiffness in intermediate temperatures. This hypothesis may be supported by the strong correlation that exists between S_{app} and SCB fracture energy. As expected, D^R and N_f @ G^R=100 are highly tied to each other and both of them are strongly correlated with the FI. The strong correlations between the N_f at G^R=100 and FI with DCT (G_f) are among the important observations in the table indicating that the proper adjustments to the mixture design properties can improve both fatigue and thermal cracking performance at the same time. However, it should be noted that the distress mechanism is substantially different between fatigue and thermal cracking and more in-depth analysis is required to discriminate the capability of the mixtures to withstand either of these distresses.

Table 4-6 Pearson's correlations among performance index parameters (Italics and (W) indicate weak correlation, (M) indicate medium correlation and, bold and (S) indicate strong correlation)

Distress								
Criterion	Rutting	Fatigue					Thermal cracking	
	M_r	D^R	N_f at G^R=100	S_{app}	SCB (G_f)	FI	DCT (G_f)	FST
M_r	1.00	-	-	-	-	-	-	-
D^R	-0.54 (M)	1.00	-	-	-	-	-	-
N_f at G^R=100	-0.65 (M)	**0.78 (S)**	1.00	-	-	-	-	-
S_{app}	*0.22 (W)*	0.49 (M)	0.33 (M)	1.00	-	-	-	-
SCB (G_f)	0.33 (M)	0.38 (M)	*0.02 (W)*	**0.81 (S)**	1.00	-	-	-
FI	-0.64 (M)	**0.80 (S)**	**0.87 (S)**	0.31 (M)	*0.17 (W)*	1.00	-	-
DCT (G_f)	-0.53 (M)	0.58 (M)	**0.79 (S)**	0.19 (W)	*0.07 (W)*	**0.91 (S)**	1.00	-
FST	-0.46 (M)	0.40 (M)	0.63 (M)	*0.05 (W)*	*-0.05 (W)*	0.83 **(S)**	0.93 **(S)**	1.00

4.8 SUMMARY OF TEST RESULTS AND STATISTICAL ANALYSIS

In order to evaluate and characterize the study mixtures, different mechanistic and performance based testing including resilient modulus (M_r), complex modulus (E*), semi-circular bend (SCB), direct tension cyclic fatigue (S-VECD) and disk shaped compact tension (DCT) were conducted. The main observations from each test are summarized as following:

- Resilient modulus:
  - Resilient moduli of wearing course mixtures depended on binder grades. Higher binder PG grades resulted in higher M_r values and mixtures with softer binders revealed lower M_r values.
  - The cold recycled mixtures indicated to be more susceptible to rutting compared to other hot mixed asphalt mixtures.
- Complex modulus:
  - The ARGG mixtures are relatively stiffer compared to most of other wearing course mixtures.
  - The cold recycled mixtures have lower stiffness (approximately 50% less) as compared to hot mixed binder and base course mixtures. However, considering the phase angle master-curves, these mixtures are more elastic compared to hot mixtures.
- Semi-circular bend:

    - While the ARGG mixtures indicated good fracture properties, the W-7034PH mixture indicated to have relatively higher FI value compared to rest of mixtures.
    - In general, the cold recycled mixtures have comparable FI values as to that of hot mixed binder and base course mixtures.
- Direct tension cyclic fatigue:
    - With respect to G^R and D^R failure criteria, the W-7034PH mixture has a better fatigue performance compared to rest of the mixtures. However, S_{app} fatigue criteria ranked the W-7628H-12.5 followed by the W-7628H-9.5 to be the best mixtures.
    - While Both G^R and S_{app} indicated the cold recycled mixtures to be more fatigue susceptible compared to hot mixed binder and base course mixtures, the inverse results were seen for the D^R criterion.
- Disk-shaped compact tension:
    - Both G_f and FST parameters indicated that the W-7034PH mixture has a better thermal cracking performance compared to other mixtures that were tested in similar temperature ranges.
    - All the NHDOT hot mixed mixtures passed the 450 J/m^2 threshold value of G_f the is currently put forth by MnDOT to protect against thermal cracking of wear course mixtures.

Using a forward stepwise statistical regression analysis, the most influential mixture design parameters on the performance index parameters were determined at 10% significance level. The main observations from these analyses are summarized as following:

- The cumulative percent passing 4.75 mm sieve size, binder type and RBR significantly affect the resilient modulus.
- While an increase in cumulative percent passing 4.75 mm sieve size improves the fatigue life, the percent passing 0.075 mm sieve size has an adverse effect on fatigue performance.
- The increase in binder useful temperature interval (UTI) improves the fatigue performance.
- Increase in the effective binder volume (V_{be}) and UTI improve the SCB flexibility index.
- The low temperature fracture energy is highly affected by mixture volumterics, binder type and cumulative percent passing 0.075 mm sieve.
- Although the statistical analysis did not indicate the significance of the NMAS, in general, this parameter should still be considered as one of the most important factors in determining the mixtures performance as the total gradation of the mixture is a function of this value. The significance of this parameter was determined when cumulative percent passing 4.75mm and cumulative percent passing 0.075mm sieve sizes were removed from the regression analysis.
- Resilient modulus has a medium negative correlation with all other index parameters of performance based destructive tests.
- There is a strong positive correlation between N_f @ G^R =100, FI, and low temperature fracture energy. This indicates that there may be a good correlation between resistance to various cracking modes for an asphalt mixture.

4.9 REFERENCES

[1]. Zhao, W. (2011). The effects of fundamental mixture parameters on hot-mix asphalt performance properties.

[2]. Diab, A., & Enieb, M. (2018). Investigating influence of mineral filler at asphalt mixture and mastic scales. International Journal of Pavement Research and Technology, 11(3), 213-224.

[3]. Rahbar-Rastegar, R., & Daniel, J. S. (2016). Mixture and production parameters affecting cracking performance of mixtures with RAP and RAS. In 8th RILEM International Conference on Mechanisms of Cracking and Debonding in Pavements (pp. 307-312). Springer, Dordrecht.

[4]. Zhou, F., Hu, S., & Scullion, T. (2006). Integrated asphalt (overlay) mixture design, balancing rutting and cracking requirements (No. FHWA/TX-06/0-5123-1). Texas Transportation Institute, Texas A & M University System.

[5]. Oshone, M., Ghosh, D., Dave, E. V., Daniel, J. S., Voels, J. M., & Dai, S. (2018). Effect of Mix design Variables on Thermal cracking performance parameters of asphalt mixtures. Transportation Research Record, 2672(28), 471-480.

[6]. West, R., Heitzman, M. A., Rausch, D., & Julian, G. (2011). Laboratory Refinement and Field Validation of 4.75 mm Superpave Designed Asphalt Mixtures. NCAT report, 11-01.

[7]. Nemati, R., & Dave, E. V. (2018). Nominal property based predictive models for asphalt mixture complex modulus (dynamic modulus and phase angle). Construction and Building Materials, 158, 308-319.

[8]. Abu Abdo, A. M., & Jung, S. J. (2016). Effects of asphalt mix design properties on pavement performance: a mechanistic approach. Advances in Civil Engineering, 2016.

[9]. Bonaquist, R. (2013). Impact of mix design on asphalt pavement durability. Enhancing the Durability of Asphalt Pavements, 1.

[10]. Dong, Y., & Tan, Y. (2011). Mix design and performance of crumb rubber modified asphalt SMA. In GeoHunan International Conference 2011American Society of Civil Engineers.

[11]. Esfandiarpour, S., Ahammed, M. A., Shalaby, A., Liske, T., & Kass, S. (2013, September). Sensitivity of pavement ME design predicted distresses to asphalt materials inputs. In Proceedings of the 2013 Conference and Exhibition of the Transportation Association of Canada-Transportation: Better-Faster-Safer (TAC/ATC'13).

[12]. Bazzaz, M., Darabi, M. K., Little, D. N., & Garg, N. (2018). A straightforward procedure to characterize nonlinear viscoelastic response of asphalt concrete at high temperatures. Transportation Research Record, 2672(28), 481-492.

[13]. Na Chiangmai, C. (2010). Fatigue-fracture relation on asphalt concrete mixtures.

[14]. Tang, S. (2014). Evaluate the fracture and fatigue resistances of hot mix asphalt containing high percentage reclaimed asphalt pavement (RAP) materials at low and intermediate temperatures. Ph.D. Thesis, Iowa State University, https://doi.org/10.31274/etd-180810-1886.

[15]. Du, S. (2015). Performance characteristic of cold recycled mixture with asphalt emulsion and chemical additives. Advances in Materials Science and Engineering, 2015.

[16]. Brown, E. R., Kandhal, P. S., & Zhang, J. (2001). Performance testing for hot mix asphalt. National Center for Asphalt Technology Report, (01-05).

[17]. Al-Qadi, I. L., Ozer, H., Lambros, J., El Khatib, A., Singhvi, P., Khan, T. & Doll, B. (2015). Testing protocols to ensure performance of high asphalt binder replacement mixes using RAP and RAS. Illinois Center for Transportation/Illinois Department of Transportation.

[18]. Mahalanobis, P. C. (1936). On the generalized distance in statistics. National Institute of Science of India.

CHAPTER 5: PERFORMANCE INDICIES FOR ASPHALT MIXTURES

5.1 INTRODUCTION

In order to develop mechanistically informed asphalt mix specific layer coefficients, it is necessary to utilize reliable pavement performance index parameters to evaluate different asphalt mixtures. Pavement performance index parameters here are defined as lab measured mechanical properties of asphalt mixtures that have shown to correlate well with field performance of those mixtures. These index parameters are usually distress specific. Thus an important aspect of the performance index parameter is the degree of correlation between the parameter and the long term field performance of the mixtures. The three main structural distresses of the asphalt pavements are rutting, fatigue and transverse cracking for which the mixtures are usually tested and evaluated. In Chapter 4, the result of the mixture testing and analysis through existing performance index parameters were discussed, however, it was necessary to determine the suitability of these indices with respect to traffic and climatic conditions in New Hampshire. Therefore, this study undertook research effort to assess the suitability of current lab based performance indices for use with New Hampshire flexible pavements and if necessary, develop improved performance indices to better distinguish between the mixtures and have better correlations with field performance. In order to accomplish this goal, the following tests were used to evaluate the mixtures for specific distresses and develop new indices:

- Rutting: Complex modulus
- Fatigue: Direct tension cyclic fatigue
- Transverse cracking: Semi-circular bend

The selection of these tests were on the basis of the mixture discrimination potential that is discussed in Chapter 4 as well as on the basis of observations that research team has made for asphalt pavements ad mixtures in New England region.

5.2 DEVELOPMENT OF A COMPLEX MODULUS BASED RUTTING INDEX PARAMETER FOR ASPHALT MIXTURES

5.2.1 INTRODUCTION AND BACKGROUND

Rutting as one of the major asphalt pavement structural distresses has long been investigated by researchers. This phenomenon is the permanent plastic strain due to repeated loads; rutting rate increases significantly due to overweight vehicles and traffic consistently moving below design speed. At warmer conditions, the asphalt mixtures tend to behave in a more viscous manner because of the softened binder which consequently results in creep and permanent deformations. There are different testing and analysis methods such as Hamburg wheel tracking test (HWTT), asphalt pavement analyzer (APA), flow number (FN), stress sweep rutting (SSR), Superpave shear tester (SST) etc. to evaluate the rut susceptibility of the asphalt mixtures. The majority of these tests need equipment specifically designed to evaluate only the rut performance and involve specimen fabrication and analysis methods which are often

relatively time consuming. Others, such as SST, while providing fundamental mixture properties, are substantially complicated to conduct and analyze the result while there is no acceptable model associated with the results from this test to predict performance [1].

One of the most widely accepted tests to determine the asphalt mixtures rutting and stripping susceptibility is the HWTT. The test is run in accordance to the AASHTO T-324 standard testing method in 52±2 cycles per minute at a temperature usually set in accordance with the PG high temperature. Based on the test track length (22.7 cm), number of loading cycles in time domain and the sinusoidal loading function of the wheel on the specimen, the applied loading frequency in the middle of the track length were the rut depth is measured can be calculated [2]. This frequency would be equal to 0.866 Hz. As the test is run in wet condition, the results not only indicate the rut susceptibility but are also used to determine the mixture stripping potential. The deformation versus loading cycles graph is generally divided into three distinguished parts. The initial part of the graph is related to the densification of the asphalt mixture due to loading which usually happens after about 1000 cycles [3]. The second portion of the curve with a constant creep slope can be used to evaluate the mixture rutting susceptibility. The third portion of the curve which can be distinguished through an inflection point and a steeper slope is related to mixture degradation due to stripping [1]. Although different destructive testing methods are available to specifically determine the mixtures rutting susceptibility, the specimen fabrication and conditioning as well as testing different replicates might be time consuming. In addition, many of these tests, require expensive testing equipment which may not be available in many labs.

It has been shown that rutting is directly correlated with the mixtures' stiffness [4], and as a result stiffness based measures can be used to evaluate the mixtures' rutting susceptibility. There are different tests such as resilient modulus (M_r) and complex modulus (E* and phase angle) to measure mixture stiffness. Although resilient modulus has been shown to have some correlations with rutting [1], it measures the recoverable strain of the mixture due to repeated loading whereas rutting is related to the mixture's plastic deformation (unrecoverable strain) which is a substantially different aspect of mixture performance. In other words, it is possible that a mixture with a higher resilient modulus could have a higher plastic deformation compared to a mix with a lower M_r value. Also, resilient modulus measures the stiffness at only one temperature and frequency (25°C at 10Hz). However, depending on the loading and climatic conditions, rutting can happen under different circumstances and not only in one specific condition.

The complex modulus test evaluates the mixture's performance at multiple frequency and temperature combinations. Using the dynamic modulus master-curves, the mixture's stiffness can be measured at different temperatures and frequencies. Therefore, it can be used to estimate the mixtures rutting performance in different conditions. Despite the fact that rutting is a plastic deformation with non-recoverable strains [5,6], the dynamic modulus as a linear viscoelastic property has been widely used in distress prediction models in many performance prediction tools such as Pavement ME because of the simplicity in conducing the test and analysis [7,8]. Also, because of the correlation between rutting and stiffness, the dynamic modulus can be used as an additional preliminary rutting performance screening tool. The NCHRP project 19-9 introduces dynamic modulus as one of the three main tests to discriminate the mixtures rutting performance where the other two are flow time and repeated loading permanent

performance tests [9]. Therefore, a dynamic modulus based index parameter can facilitate the mixture performance ranking and reduce the extensive specimen fabrication and lab work. Many studies have been conducted to relate the dynamic modulus to any one of the specific rutting tests. Research conducted by Apeagyei tried to develop a mathematical model between the FN as function of dynamic modulus at 38°C and 10, 1, 0.1Hz plus the mixture gradation [10]. Dynamic modulus at 38°C and 54°C and 5Hz has also been examined to investigate the relationship between the modulus and field rutting [11], but no consistent results with respect to different mix types were observed with consideration of only |E*| at this specific temperature and frequency. Nemati (2017) used the combination of |E*| at 37.8° and 1.59Hz to investigate the relationship between this parameter and resilient modulus for typically used mixtures in New Hampshire. This combination revealed promising correlation for majority of mixtures in the study [12]. However, since rutting is the measure of plastic deformation, it is important to consider the mixture's viscous properties along with the stiffness through incorporating the phase angle. The prevailing pre-peak behavior of the phase angle master-curve towards the lower frequencies is generally considered to be controlled with the aggregate (Figure 5-1). Theoretically, in this frequency range, the binder-aggregate interaction phase weakens and as the mixture overall load bearing capacity decreases, rutting happens.

A comprehensive study was conducted by Bhasin (2003) to evaluate the rut susceptibility of some of the commonly used asphalt mixtures in southern United States. Mixtures were tested using the APA, flow test and dynamic complex modulus. The mixtures were ranked and compared to APA as the baseline [13]. The results indicated that $|E^*|/\sin\delta$ at 1Hz was able to rank the mixtures similar to APA whereas the same criteria at 10 Hz revealed poor correlation to APA results. In general, there has not been much success in implementing the dynamic modulus at single temperature and frequency to relate to the rutting performance as mixtures with different gradation and characteristics behave differently in a predefined loading conditions [14]. Another problem with considering only one point on the master-curve is that there is a possibility that the master-curves of different mixtures would intersect at that specific point or may have similar stiffness and phase angle values which can make it difficult to distinguish between different mixtures. Therefore, there is need to investigate the complex modulus master-curves at more than one single point to evaluate the effect of temperature and frequency on the rutting mechanism.

Many state highway agencies such as NHDOT do not have any specific requirements for evaluating the rutting susceptibility of the mixtures other than the general ones put forth by the AASHTO R30 standard Superpave mixture design which specifies the minimum number of gyrations for a given traffic level. However, in general, the mixtures that are designed to have an acceptable cracking performance are softer and might be prone to rutting in warmer climatic conditions which can significantly affect the ride quality, highway safety and maintenance and rehabilitation costs. Considering the limitations of the equipment as well as the state agency requirements, there is need for a reliable index parameter to provide a preliminary evaluation of the mixtures' rutting susceptibility.

The main objective of this section of the report is to explore the possibility of development of a rutting index parameter using the complex modulus master-curves (dynamic modulus and phase angle). Such index parameter can be used as a screening tool to help reduce the required lab work during the mixture

design and evaluation procedure by narrowing down the number of mixtures that should be tested using destructive rutting tests.

The approach in this study uses three points on the master-curves to develop various index parameters. The first point (marked by subscript "A") is associated with the reduced frequency on the master-curves at which the peak phase angle happens. This point is selected because it indicates the highest potential for non-recoverable deformation within LVE response range of the asphalt mixtures. The selection of the second point (marked by subscript "B") is directly correlated to the HWTT testing temperature (regionally assigned temperature) and loading frequency (52 cycles per minute equal to 0.866 Hz) and its projected reduced frequency on the master-curves. The choice for this point is driven by need to capture asphalt mixture behavior in a low stiffness range, where greater compressive strains will be experienced by asphalt under traffic loading. As HWTT has shown to distinguish asphalt mixtures' rutting performance and correlate well to field performance, the loading frequency associated with that test was chosen. The third point (marked by subscript "C") corresponds to the average of phase angle and dynamic modulus values of points A and B on the master-curves. Please note that the frequencies used in this research are shifted as per the time-temperature superposition principle. Once the points are assigned, 5 different parameters are investigated to determine their correlations with rutting performance of asphalt mixtures. Figure 5-1 and Table 5-1 indicate and describe the selected points on the master-curves used to evaluate various complex modulus based rutting index parameters.

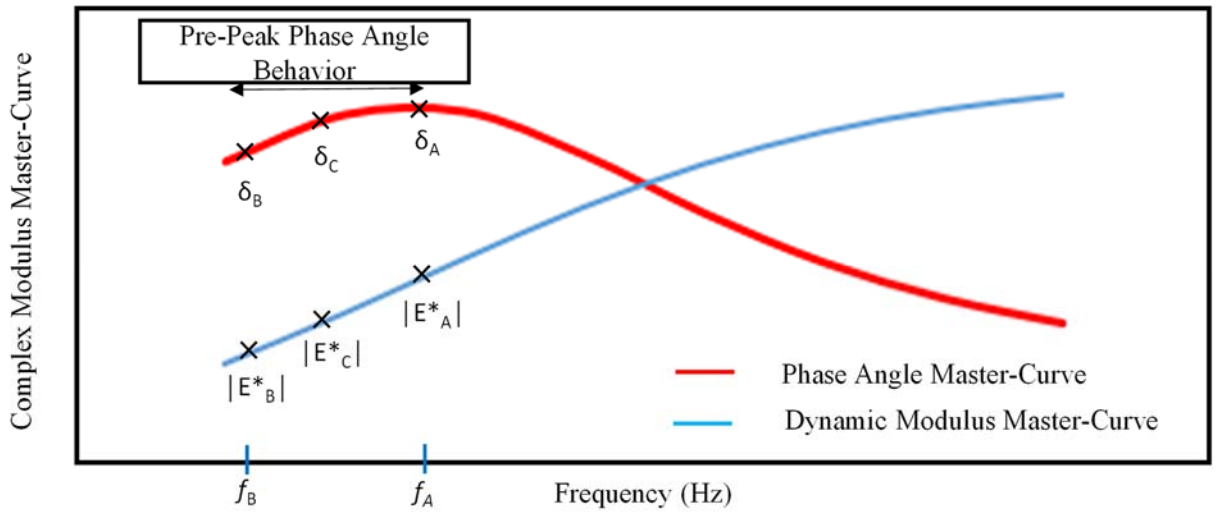

Figure 5-1 Typical dynamic modulus and phase angle master-curves for asphalt mixtures. Selected points on the master-curves to develop the rutting index parameters

Table 5-1 Description of the selected points on the master-curves for rutting assessment

Complex Modulus Master-Curve	Point	Description
Phase Angle (δ)	δ_A	Peak Phase Angle (δ)
	δ_B	(δ) corresponding to HWTT testing condition (45°C at 0.866Hz)
	δ_C	Estimated average phase angle between points A and B; $\delta_C = [\delta_A + \delta_B]/2$
Dynamic Modulus |E*|	$\|E^*_A\|$	$\|E^*\|$ corresponding to peak phase angle
	$\|E^*_B\|$	$\|E^*\|$ corresponding to the HWTT testing condition (45°C at 0.866Hz)
	$\|E^*_c\|$	Estimated average dynamic modulus between points A and B; $\|E^*_c\| = [\|E^*_A\| + \|E^*_B\|]/2$
(δ) and |E*|	f_A	Logarithm of frequency corresponding to Peak Phase Angle
	f_B	Logarithm of frequency corresponding to HWTT testing condition (45°C at 0.866Hz)

In order to develop, verify and validate a complex modulus based rutting index parameter (CMRI), three different sets of mixtures are evaluated. The first set includes 7 mixtures for which the HWTT results are available and 5 different complex modulus based indices are investigated to determine the best statistically correlating index parameter with the rut depth measurements. The second set of mixtures includes 6 hot mixed asphalt mixtures for which the field rut measurements are available and the index parameters will be evaluated in terms of mixture ranking and statistical correlations with the field performance. The third set includes 9 mixtures with the same gradation but varying air void and binder content. This set is used to verify the capability of the indices in determining the expected rutting performance of a mixture with respect to the mixture design properties. The material properties and test results will be discussed in the following subsections.

5.2.2 MATERIALS FOR MIX SET-1

As a preliminary step to explore the capability of master-curves in determining the mixtures rut susceptibility, a set of 7 different mixtures with diverse rheological properties were selected. These mixtures have been evaluated through the HWTT at 45°C as per the AASHTO T324 test specifications. All testing for these mixtures was conducted in submerged conditions. The rut depth and creep slope are primarily used to evaluate the mixture rutting susceptibility. Based on the literature, the 8000th cycle of loading has been usually used to distinguish the rutting susceptibility of asphalt mixtures [15]. However, in this study the rutting depth at 7000th pass in the test was selected to compare the mixtures with respect to rutting performance. The creep slope was not used for comparison purposes, since some of these mixtures start to reveal stripping related behavior after about 7000 test cycles [16].The design properties of this set of mixtures is summarized in Table 5-2. It should be mentioned that The MEP, MEM-1, MEW and VTG-1 are polymer modified mixtures. Also, an antistripping agent has been used in VTP-2 mixture production.

Table 5-2 Properties of the first set of mixtures used to develop the rutting index parameters

Mixture	Binder Grade	NMAS (mm)	RAP%	AC (%)	(VMA, %)	(VFA, %)	%Passing #200 (%)	(N_{des} gyrations)
MEP	64-28	12.5	10	5.9	Not Available	Not Available	5.1	50
MEM-1	64-28	12.5	20	5.6	Not Available	Not Available	5.0	50
MEW	64-28	12.5	20	5.8	Not Available	Not Available	4.5	50
VTP-1	58-28	9.5	20	6.0	16.5	76	4.8	50
VTP-2	58-28	9.5	20	6.0	16.5	76	4.8	50
VTG-1	70-28	12.5	15	4.9	15.5	74	4.4	80
CTG-1	64-22	12.5	0	5.0	15.5	72	2.5	50

The results from HWTT test is depicted in Figure 5-2. The plots and the rut depths are averaged measured values from two specimens in the HWTT test. The test results confirm the reasonability of selecting the 7000th pass of the HWTT test as the comparison reference point, where all the slopes remain steady before the stripping initiates. Also this point on the curve is significantly away from the post-compaction consolidation point which is happening after about 1000 cycles. On the other hand, this point is selected as such that mixtures like MEP and VTP-2 could be evaluated in terms of rutting performance only and the response is not overwhelmed by moisture induced stripping damage.

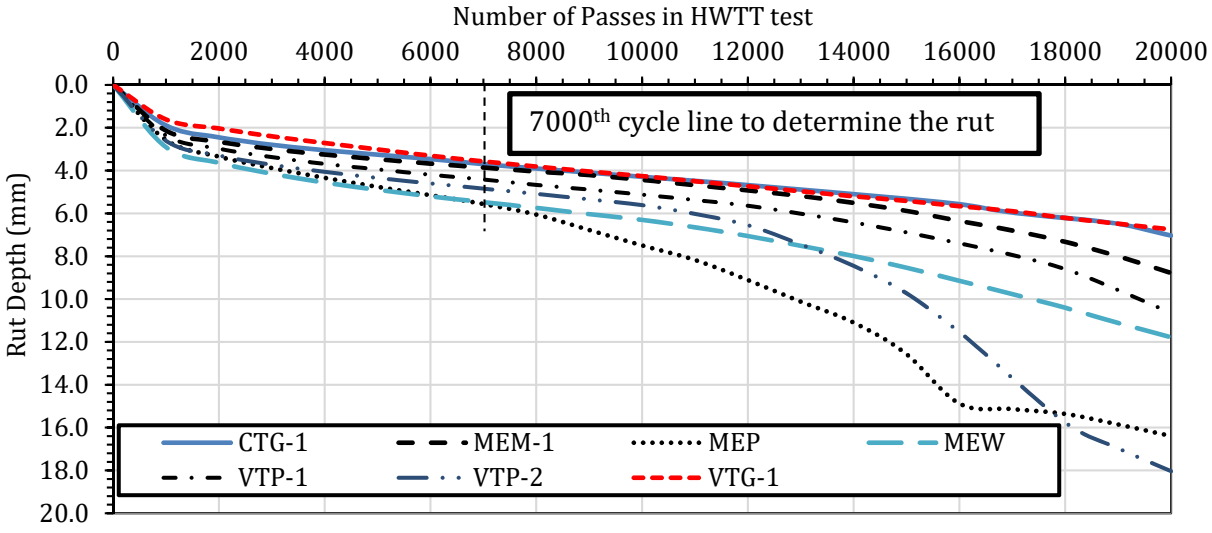

Figure 5-2 HWTT test results for the first set of study mixtures

5.2.3 COMPLEX MODULUS MASTER-CURVES

Complex modulus specimens were cored, cut and tested with respect to AASHTO T342 standard procedure in three temperatures 4.4°C, 21.1°C and 37.8°C and 6 loading frequencies as 0.1Hz, 0.5Hz, 1Hz, 5Hz, 10Hz and 25Hz. Then using the time temperature superposition principle (TTSP) master-curves were constructed at a reference temperature of 21.1°C.

In order to analyze the master-curves to develop the index parameters, Equations 5.1 and 5.2 were used to fit the dynamic modulus and phase angle graphs respectively [17].

$$Log\ (E^*) = c + \frac{[d-c]}{\left[1+e^{[-a[Log(f)-b]]}\right]} \qquad \text{Equation (5.1)}$$

Where:

f = Load Frequency

a = Growth Rate

b = Inflection Point

c = Lower Asymptote

d = Upper Asymptote

$$\delta = \frac{[a\times b^2]}{\left[\left[(Log(f))-c\right]^2+b^2\right]} \qquad \text{Equation (5.2)}$$

Where:

f = Load Frequency

a = Peak Value

b = Growth Rate

c = Critical Point

The fitted dynamic modulus and phase angle master-curves are depicted in Figure 5-3 and Figure 5-4 respectively. As discussed earlier the aim of this study is to implement the pre-peak behavior of phase angle master-curve (Figure 5-1) as a starting point for developing a rutting index parameter. The behavior of this portion of the phase angle master-curve is controlled with the aggregate stiffness and binder flow which is reflected as a drop in phase angle master-curve. The rate, magnitude and coordination of the phase angle and stiffness drop on the master-curves is deemed to be unique for different mixtures as mixtures have different rheological properties. The peak point on the phase angle is considered as the maximum extent of the viscous behavior of a mixture and depending on the aggregate size and gradation, binder type and content as well as other mixture properties the coordination of this peak point can change

significantly. It is hypothesized that after this peak point towards the lower frequencies, the combination of the low loading frequency and high temperature will cause the binder to flow into the mixture air voids and thinner asphalt film will be left around the aggregate resulting in a more elastic response. This phenomenon causes the aggregate to be the prevailing load bearing element in the mixture and because of that the phase angle starts to drop [18]. For the same aggregate gradation and different binder type, the faster the binder flows (softer binder) the faster the phase angle will drop and probably the higher amount of rutting will be observed.

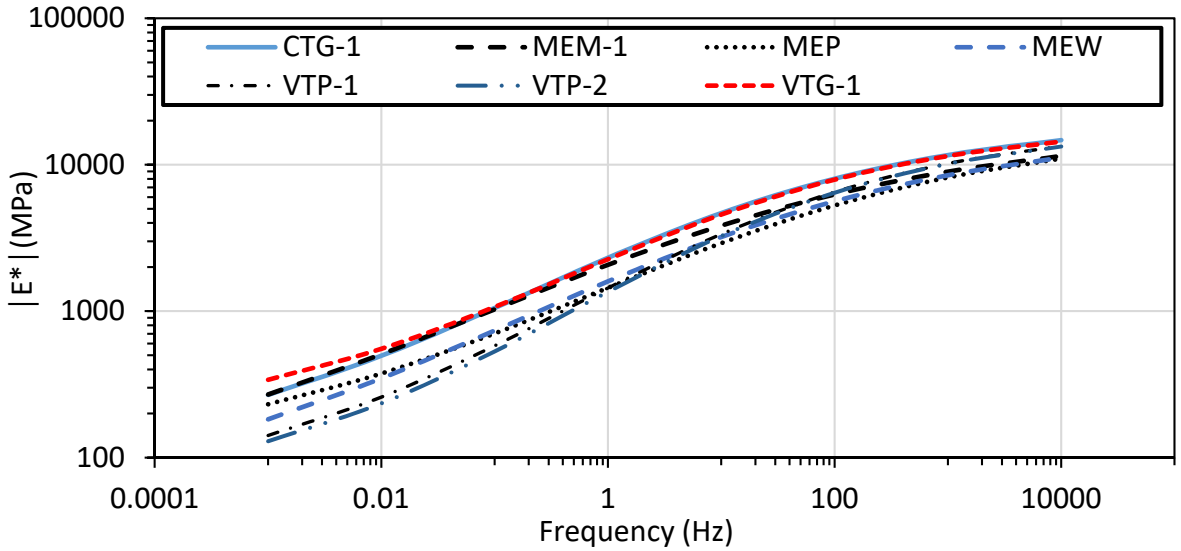

Figure 5-3 Fitted dynamic modulus master-curves of the first set of mixtures

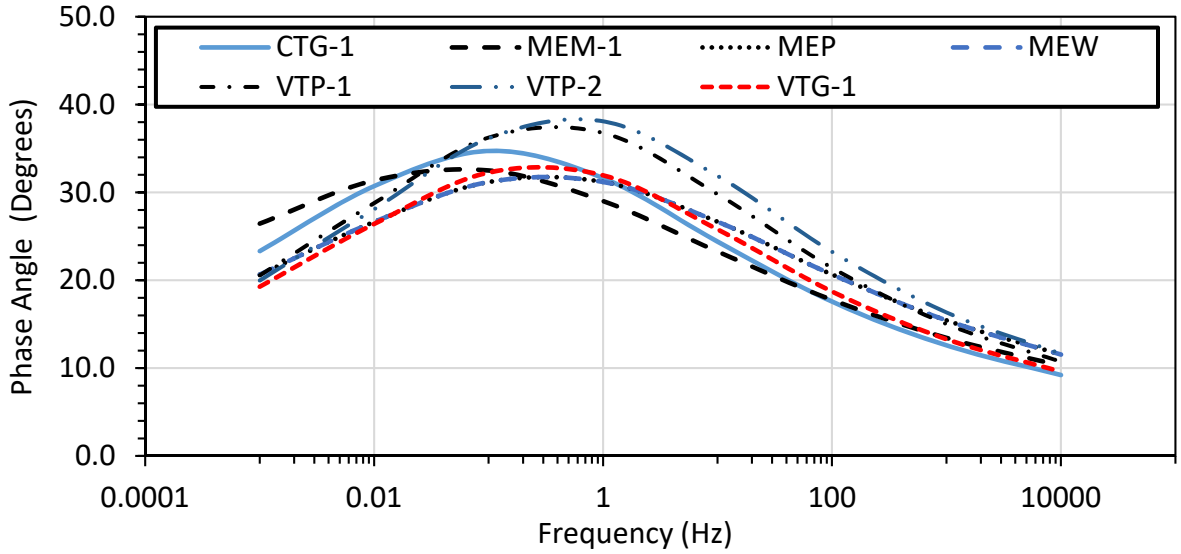

Figure 5-4 Fitted phase angle master-curves of the first set of mixtures

In order to establish any type of correlation between rutting and the observed performance, it is necessary to define and select the critical rutting related points on the master-curves and resume the analysis on

basis of them. As mentioned earlier the peak point on the phase angle master-curve can be physically interpreted and correlated to the mixture rut susceptibility but this point alone may not be enough to explain the mixture performance. For this reason, a second point on the pre-peak side of the phase angle master-curve should be selected for evaluation purposes. In this study, this second point on the master-curve is selected based on the HWTT loading and temperature conditions.

The HWTT test temperature is usually selected either with respect to binder high temperature performance grade (PGHT) or the regional climatic conditions needs. In New England area, this temperature is usually set at 45°C. Also, the frequency of the rolling wheel in HWTT is 52 passes per minute which is equal to 0.866 Hz. Thus, the second point on the master-curves is selected as such to be equivalent to 45°C at 0.866 Hz. The corresponding reduced frequency on the master-curves is calculated through using the appropriate shift factors for this temperature and frequency combination. The investigated indices and their calculation are described in Table 5-3. The subsequent text discusses each index individually.

Table 5-3 Proposed complex modulus based rutting index (CMRI) parameters to evaluate the rutting performance

CMRI Parameters	Calculation Method
I	$[\delta_A-\delta_B] / \lvert f_A - f_B \rvert$
II	$[\lvert E^*_A \rvert - \lvert E^*_B \rvert] / \lvert f_A - f_B \rvert$
III	$[\lvert E^*_A \rvert - \lvert E^*_B \rvert] / \lvert f_A - f_B \rvert^2$
IV	$\lvert E^*_c \rvert / [\delta_c \times \lvert f_A - f_B \rvert^2]$
V	$[\lvert E^*_A \rvert - \lvert E^*_B \rvert] / [[\delta_A-\delta_B] \times \lvert f_A - f_B \rvert^2]$

The first index (I) investigates the rheological properties of the mixtures by determining the rate of drop in phase angle with respect to changes in frequency without considering the effect of stiffness in the analysis. The second index (II), evaluates the dynamic modulus drop rate with respect to changes in frequency to investigate the effect of stiffness. The third index (III) is similar to the second index (II) in the context of using the rate of changes in dynamic modulus over the loading frequency. The main difference here is that Index (III) uses the squared effect of logarithm of frequency to increase the emphasis on the effect of loading rate on the rutting. Further analysis confirmed that the squared logarithm of frequency can improve the correlation between the rutting and the indices. Although it might seem that indices (II) and (III) do not consider the effect of phase angle in the parameters, the selection of the reduced loading frequencies in these parameters is a direct function of where the peak phase angle occurs. Indices IV and V incorporate the effect of modulus, phase angle and frequency at the same time. Generally, from the Superpave binder PG grading system, it is well known that shear modulus divided by the phase angle ($|G^*| / \sin \delta$) has been a good indicator of binder rutting properties and indices IV and V are developed based on this logic.

5.2.4 RESULTS AND DISCUSSION

5.2.4.1 EVALUATION OF THE RUTTING INDICIES THROUGH HWTT DATA

The calculated values and the ranking from each of the rutting index parameters are shown in Table 5-4 Calculated value and ranking of individual rutting index parameters for the first set of mixtures. A lower calculated value for Index (I) is more desirable indicating less decrease in phase angle due to loading/temperature whereas for indices (II), (III), (IV) and (V), a larger calculated value indicates a better rut resistant mixture.

5.2.4.2 MIXTURE RANKING

As it can be seen in Table 5-4, Index (I) is not capable of representing the mixtures performance because of merely focusing on the phase angle drop rate. Although Index (II) successfully predicts the ranking of 3 mixtures, in general it either over/underestimates the mixtures rutting performance. The ranking order indicates the promise of Index (III) in determining the mixtures rutting performance order with the only difference between the order of VTG1 and CTG1 mixtures. With respect to HWTT results, the difference between the measured rut for these two mixtures is less than 0.13mm or 3.5% which can be reasonably considered as negligible. The usefulness of Index (III) is clearer when considering mixtures like MEM1 and MEW. The two mixtures have similar properties in terms of binder type, RAP percentage, aggregate size and binder content. Considering these properties one may expect very similar rutting performance for the two mixtures while one is significantly more rut-resistant than the other. Similar to HWTT results, Index (III) has been able to predict this difference. Also considering the dynamic modulus master-curves for VTP-1 and MEP, the latter has a relatively higher stiffness in the lower end of the master-curve and a single point type index would indicate it to have a higher rutting resistance. However, the HWTT results show MEP to be a poor performer as compared to VTP-1 and this is correctly captured by Index (III). Indices (IV) and (V) resulted in same type of ranking compared to each other, but with respect to HWTT ranking, the results are not promising.

In summary, Index (III) has a better capability in ranking the mixtures with respect to HWTT for the mixtures evaluated. However, it is necessary to evaluate these parameters through the field rutting performance. The next subsection will evaluate parameters through ranking a set of 6 other mixtures for which the field rutting data is available after 5 years in service.

Table 5-4 Calculated value and ranking of individual rutting index parameters for the first set of mixtures

Mixture	HWTT Results		CMRI Parameter and Rank									
	HWTT Rut Depth (mm)	Rank	I	Rank	II	Rank	III	Rank	IV	Rank	V	Rank
MEP	5.5	**7**	4.1	**3**	387.3	**6**	173.5	**7**	5.6	**5**	20.6	**5**
MEM-1	3.8	**3**	2.9	**1**	353.5	**5**	302.0	**3**	11.9	**1**	80.7	**1**
MEW	5.5	**6**	4.0	**2**	314.1	**7**	194.3	**6**	5.9	**4**	30.0	**4**
VTP-1	4.4	**4**	6.3	**6**	396.6	**4**	207.6	**4**	5.0	**6**	17.4	**6**
VTP-2	4.8	**5**	6.5	**7**	417.0	**3**	205.5	**5**	4.7	**7**	15.6	**7**
VTG-1	3.6	**1**	5.0	**5**	590.9	**1**	339.2	**2**	11.3	**3**	38.8	**3**
CTG-1	3.7	**2**	4.6	**4**	505.7	**2**	353.4	**1**	11.7	**2**	53.7	**2**

5.2.5 EVALUATION OF THE RUTTING INDICES THROUGH FIELD RUTTING DATA (MIX SET-2)

As mentioned in the previous subsection, the introduced rutting index parameters will be further evaluated through comparing the index parameter based ranking to that of the field performance. The 6 investigated mixtures in this subsection are placed on I-93 as part of the North-East High RAP Pooled Fund Study. The field performance of this set of mixtures has been monitored yearly through construction of six test sections in 2011 on the southbound lanes on I-93 between exits 30 and 32 in Woodstock and Lincoln, New Hampshire. It is worth mentioning that the distresses have been measured through an automated pavement distress data collection van by New Hampshire DOT. Since the pavement structure, traffic and climatic condition is the same for these mixtures, it would be possible to compare and rank the mixtures independent from other variables that can affect the pavement overall response and performance. The mix design properties for this second set of mixtures are summarized in Table 5-5.

Table 5-5 Mixture design and properties of the second set of mixtures to verify the index parameters

Mixture	Binder Grade	NMAS (mm)	RAP (%)	AC (%)	VMA (%)	VFA (%)	Field Air Void (%)	Pavement Rut Depth (mm)
Virgin-58-28	58-28	12.5	0	5.9	16.8	74.0	5.4	4.15
15%RAP-58-28	58-28	12.5	15	5.6	16.9	74.2	5.3	5.24
25%RAP-58-28	58-28	12.5	25	5.8	16.7	75.3	5.9	3.96
25%RAP-52-34	52-34	12.5	25	6.0	16.5	79.0	5.3	3.73
30%RAP-52-34	52-34	12.5	30	6.0	16.4	78.1	6.2	3.84
40%RAP-52-34	42-34	12.5	40	4.9	17.0	75.2	4.5	2.85

As it can be seen from the table, the 15%RAP-58-28 mixture has the highest rut depth whereas the 40%-52-34 has the lowest. Unlike these two, the rest of the mixtures although possess different values of rut depth, their magnitude is generally very close to each other and one can reasonably consider them as similar rut performing mixtures at least in the first five years after construction. It should be noted that there is inconsistency among the mixtures' measured field air void which might seem to affect the rutting ranking and performance. However, the air voids of the first four mixtures in the table are close to each other and within one standard deviation of the mean for all the mixtures. The air void level of the last two mixtures in the table (30%RAP-52-34 and 40%RAP-52-34) are only marginally away from one standard deviation from the mean.

The other noteworthy point in the table is the higher rut depth of the mixture with stiffer binder PG grade with the same RAP content in the case of 25%-58-28 and 25%-52-34 mixtures. A possible reason for this observation is related to the binder properties and the binder's ΔT_{cr} parameter. A comprehensive study has been conducted on different aspects of properties of these mixtures and further discussion about these properties have been discussed in the High-RAP Pooled Fund Study Report [19]. The dynamic modulus and phase angle master-curves were constructed and fitted through the same procedure explained in Section 5.2.3 The fitted dynamic modulus and phase angle master-curves are depicted in Figure 5-5 and Figure 5-6 respectively.

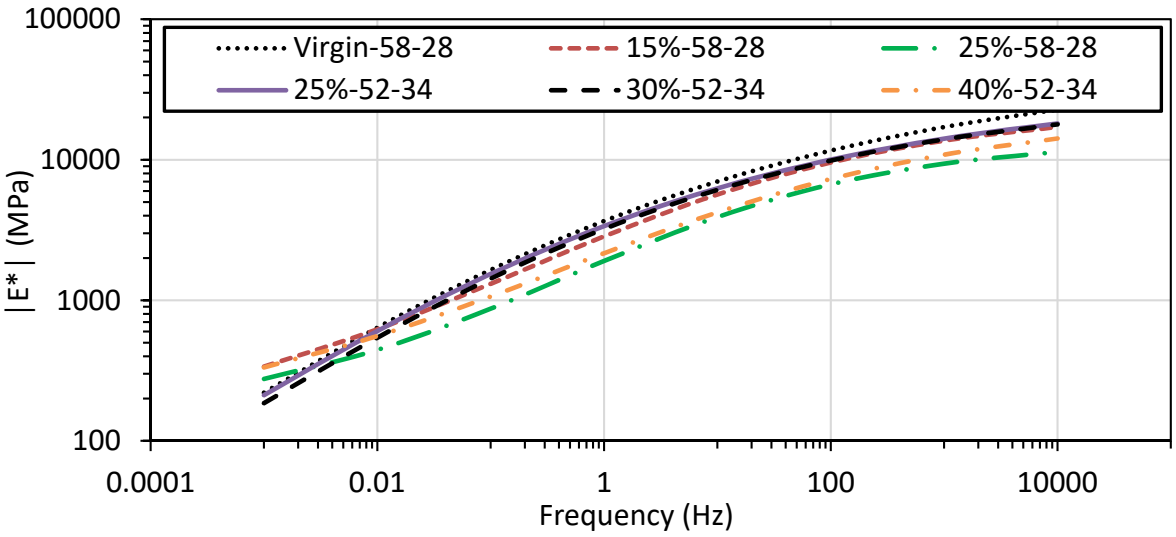

Figure 5-5 Fitted |E*| master-curves of the second set of mixtures

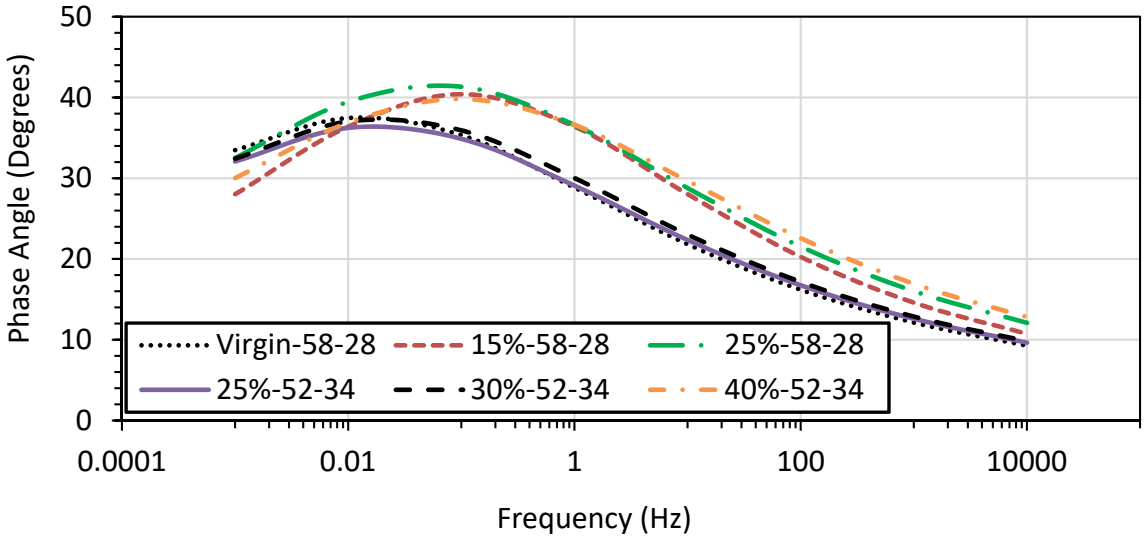

Figure 5-6 Fitted phase angle master-curves of the second set of mixtures

5.2.5.1 MIXTURE RANKING

The five different indices were calculated for the 6 mixtures in order to make comparisons to the field distress measurements. The calculated indices and the rankings have been depicted in Table 5-6. As it can be seen from the table, except for Index (II) all other indices have been able to capture the worst (15%-58-28) rut resistant mixture. Based on the results, Index (I) seems not be a good enough tool to indicate the rutting susceptibility. Also, Index (II) has not been able to predict the ranking of majority of the mixtures. With respect to Index (III), the ranking comparison indicates that this index has identical ranking to the field conditions. Also, a comparison between the calculated index parameters and the rut depths reveals that Index (III) is able to better distinguish the relative difference between the mixtures in addition

to ranking them. Index (IV) indicates to be incapable of ranking the mixtures which was also seen previously for the first set of the study mixtures dataset. On the other hand, Index (V) is showing promising results in terms of discriminating the mixtures rutting ranking with respect to field data.

Table 5-6 Values of Rutting Index Parameters for High RAP Pooled Fund Study Mixtures

Mixture	Field Results		CMRI Parameter and Rank									
	Field Rut Depth (mm)	Rank	I	Rank	II	Rank	III	Rank	IV	Rank	V	Rank
Virgin-58-28	4.1	**5**	3.1	**2**	351.8	**6**	355.6	**5**	12.5	**4**	117.3	**4**
15%-58-28	5.2	**6**	6.0	**6**	505.4	**1**	267.1	**6**	6.7	**6**	23.3	**6**
25%-58-28	4.0	**4**	3.1	**4**	358.6	**5**	397.1	**4**	17.5	**2**	141.4	**5**
25%-52-34	3.7	**2**	2.9	**1**	498.6	**2**	478.8	**2**	14.0	**3**	156.1	**2**
30%-52-34	3.8	**3**	3.2	**5**	469.3	**4**	425.4	**3**	11.4	**5**	117.7	**3**
40%-52-34	2.9	**1**	3.1	**3**	497.6	**3**	496.3	**1**	20.7	**1**	160.9	**1**

5.2.6 EVALUATION OF THE RUTTING INDICES THROUGH MIXTURE DESIGN PROPERTIES VARIATIONS (MIX SET-3)

One of the main goals of a complex modulus based rutting performance index parameter in this study is to estimate the mixtures performance and screen the mixtures based on the complex modulus results ahead of conducting a specific rutting test such as the HWTT. Therefore, it is necessary to examine the performance index parameters through a sensitivity analysis with respect to mixture design properties. In order to accomplish this goal, a third set of mixtures with the same gradation and varying design air void and asphalt content were selected to determine how each of the index parameters can capture these variations in the mix design and consequently the expected rutting performance. The mixtures were designed and compacted at three different levels of air void content and three binder contents (resulting in 9 different combinations). The mixture design and properties are summarized in Table 5-7. The complex modulus specimens were fabricated and tested in accordance to AASHTO T342 test method and the master-curves were constructed and fitted at 21.1°C. The dynamic modulus and phase angle master-curve plots are depicted in Figure 5-7 and Figure 5-8 respectively. It can be seen from the plots that for each set of binder content the dynamic modulus master-curves become relatively softer (indicate lower modulus values) with increasing air void but no specific trend is observed for phase angle master-curves which makes the overall performance prediction challenging through comparing only master-curves.

Table 5-7 Properties of the third set of mixtures used to examine the index parameters based on altering the mix design properties

Mixture	Binder Grade	NMAS (mm)	RAP (%)	AC (%)	AV (%)
5.9AC-4AV	64-28	9.5	0	5.9	4
5.9AC-7AV	64-28	9.5	0	5.9	7
5.9AC-9AV	64-28	9.5	0	5.9	9
6.3AC-4AV	64-28	9.5	0	6.3	4
6.3AC-7AV	64-28	9.5	0	6.3	7
6.3AC-9AV	64-28	9.5	0	6.3	9
6.8AC-4AV	64-28	9.5	0	6.8	4
6.8AC-7AV	64-28	9.5	0	6.8	7
6.8AC-9AV	64-28	9.5	0	6.8	9

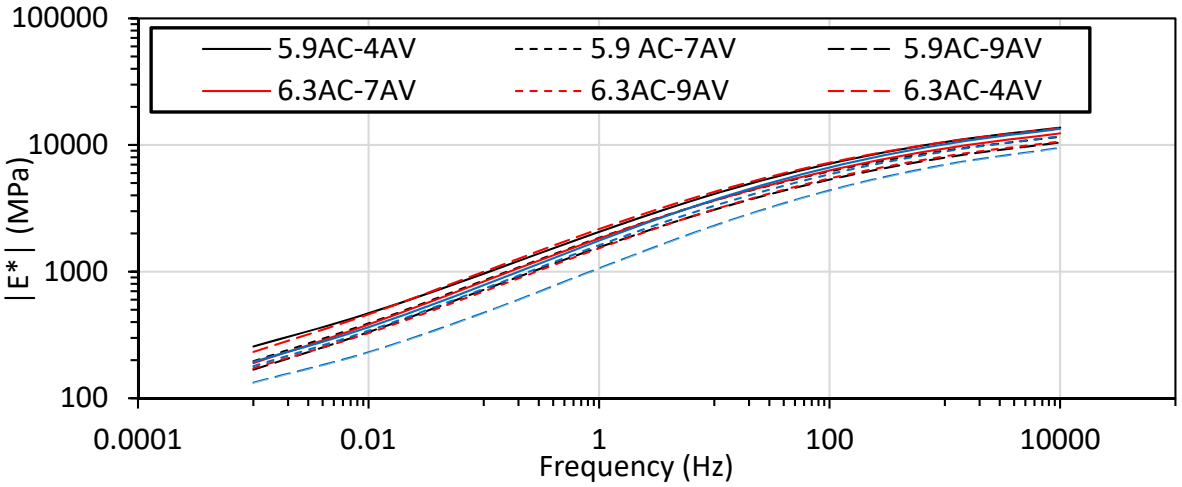

Figure 5-7 Fitted |E*| master-curves of the third set of mixtures

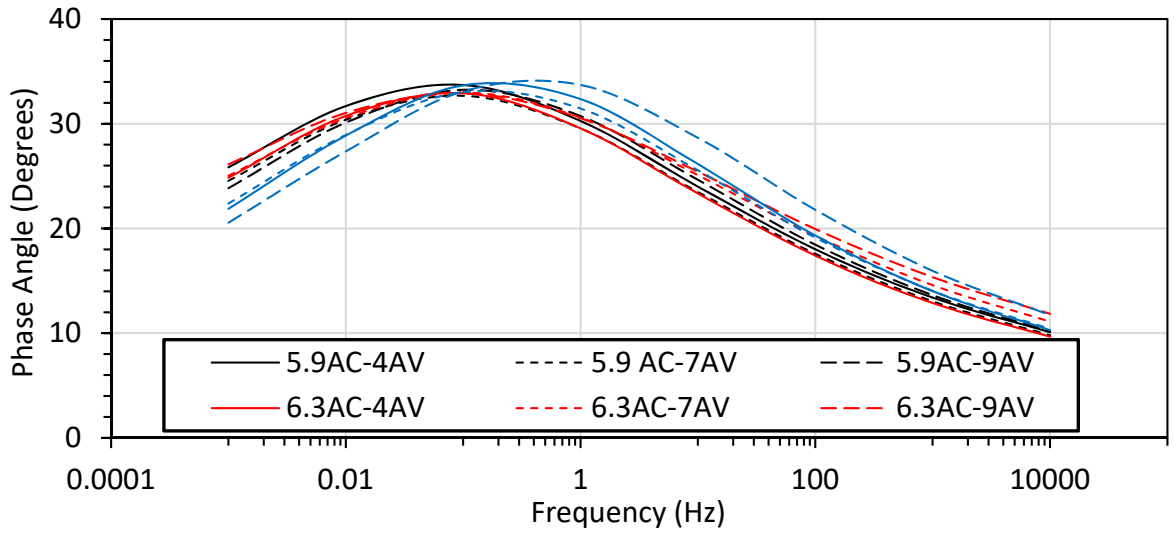

Figure 5-8 Fitted phase angle master-curves of the third set of mixtures

5.2.6.1 MIXTURE RANKING

To evaluate the capability of the index parameters to estimate the mixtures rutting performance, the ranking was conducted in three different categories for each variable separately. Based on the general expectations from volumetric point of view, a mix with lower binder content would be more rut resistant compared to one with higher binder content. In general, mixes with excessively high air void levels have potential for rutting due to lower stiffness and mixtures with a low air voids (typically below 4%) also have high propensity for rutting due to lack of sufficient air voids to allow expansion of binder during high temperatures. However, in the data-set used in this study, the air void levels are within 4 to 9% range and not sufficiently varied to draw conclusions regarding air void associated rutting performance prediction without performing lab test, such as HWTT. Nonetheless to make full comparisons for effects of both air-voids and asphalt binder contents, the mixtures are ranked in two ways; first, a constant air void level and varying binder content (Table 5-8) and second, a constant binder content and varying air void level (Table 5-9).

Table 5-8 Ranking is based on the varying binder content at constant air void level

Mixture	Volumetric based Expected Rank	CMRI Parameter and Rank									
		I	Rank	II	Rank	III	Rank	IV	Rank	V	Rank
5.9AC-4AV	**1**	3.1	**1**	366.5	**3**	239.5	**1**	8.1	**1**	41.2	**1**
6.3AC-4AV	**2**	4.0	**2**	385.7	**2**	229.5	**2**	7.0	**2**	33.7	**2**
6.8AC-4AV	**3**	4.8	**3**	409.1	**1**	224.7	**3**	6.4	**3**	25.7	**3**
5.9AC-7AV	**1**	3.4	**3**	379.6	**1**	281.7	**1**	9.8	**1**	61.2	**1**
6.3AC-7AV	**2**	3.6	**2**	359.3	**3**	212.4	**2**	6.3	**2**	34.9	**2**
6.8AC-7AV	**3**	4.4	**1**	360.0	**2**	197.4	**3**	5.7	**3**	24.4	**3**
5.9AC-9AV	**1**	3.9	**2**	336.5	**1**	218.1	**1**	6.9	**2**	36.2	**2**
6.3AC-9AV	**2**	2.8	**1**	304.5	**2**	217.7	**2**	7.5	**1**	55.4	**1**
6.8AC-9AV	**3**	5.1	**3**	266.9	**3**	117.0	**3**	3.1	**3**	10.0	**3**

Table 5-9 Ranking is based on the varying air void level at constant binder content

Mixture	Volumetric based Expected Rank	CMRI Parameter and Rank									
		I	Rank	II	Rank	III	Rank	IV	Rank	V	Rank
5.9AC-4AV	**1**	3.8	**2**	366.5	**2**	239.5	**2**	8.1	**2**	41.2	**2**
5.9AC-7AV	**2**	3.4	**1**	379.6	**1**	281.7	**1**	9.8	**1**	61.2	**1**
5.9AC-9AV	**3**	3.9	**3**	336.5	**3**	218.1	**3**	6.9	**3**	36.2	**3**
6.3AC-4AV	**1**	4.0	**3**	385.7	**1**	229.5	**1**	7.0	**2**	33.7	**3**
6.3AC-7AV	**2**	3.6	**2**	359.3	**2**	212.4	**3**	6.3	**3**	34.9	**2**
6.3AC-9AV	**3**	2.8	**1**	304.5	**3**	217.7	**2**	7.5	**1**	55.4	**1**
6.8AC-4AV	**1**	4.8	**2**	409.1	**1**	224.7	**1**	6.4	**1**	25.7	**1**
6.8AC-7AV	**2**	4.4	**1**	360.0	**2**	197.4	**2**	5.7	**2**	24.4	**2**
6.8AC-9AV	**3**	5.1	**3**	266.9	**3**	117.0	**3**	3.1	**3**	10.0	**3**

5.2.7 CORRELATION OF INDEX PARAMETERS WITH THE HWTT/FIELD RUT MEASUREMENTS

As it was seen in the previous section, some of the indices were able to rank the mixtures in a similar way to the ranking from the volumetric based expectations. However, the ability of the indices to differentiate

the mixtures performance would be different. Therefore, it is necessary to further investigate the correlation between the index values with the actual measurements from field and the HWTT test results. Figure 5-9 reveals the correlation and goodness of fit in terms of (R^2) between different index parameters and the measured rut depths for the first and second set of the study mixtures. Using the standard least squared method to determine the line of best fit the R^2 value was determined for both sets of data for individual index parameters. It can be seen that fairly good correlation exists between the indices and the rutting measurements except for Index (I) where there is no correlation between the index and the HWTT measurements. Amongst all the indices, Index (III) indicates a clearly strong linear correlation with both the field and HWTT rut depth measurements. Considering the ranking results from the previous sections, this index can reasonably determine the mixtures relative rutting performance difference in addition to ranking them. Also, with respect to Index (III), for most of the mixtures, the ratio of the two measured rut values and their calculated index parameter counterpart is closely comparable indicating the capability of this parameter in determining the relative difference in performance between mixtures.

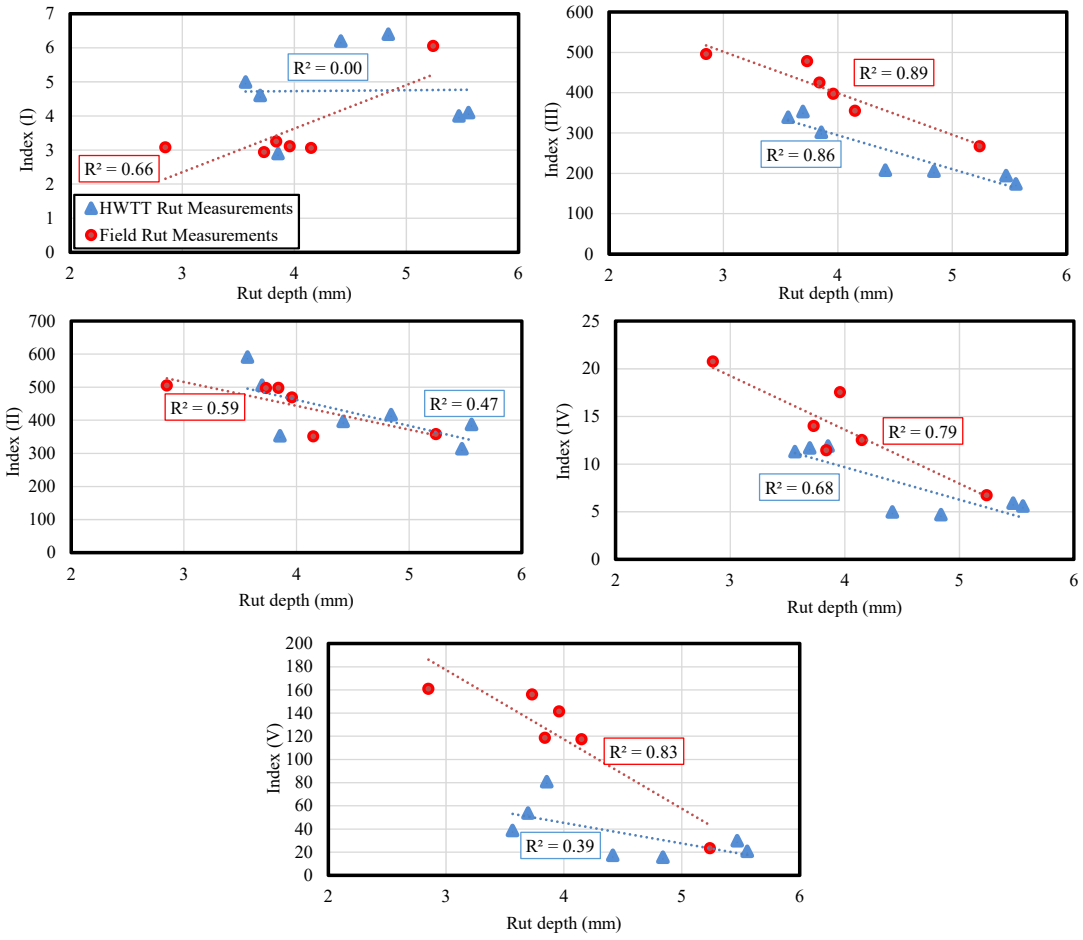

Figure 5-9 Correlation between the index parameters and the measured rut depths

5.2.8 EVALUATION OF THE NHDOT PROJECT MIXTURES THROUGH THE DEVELOPED RUTTING INDEX PARAMETER

The results from evaluation of the NHDOT project mixtures for development of layer coefficients are shown in Figure 5-10. The plots indicate that ARGG-2 is a significantly more rut resistant mixture compared to the rest of the mixtures. Among the rest of the wearing course mixtures, W-7628H-12.5 has the highest CMRI value while W-5834L followed by W-7034PH can be considered as relatively more rut susceptible mixtures. This indicates that the mixtures with colder PGLT may be more prone to rutting as both of these mixtures have the lowest PGLT (-34) among the others. As expected the binder and base course mixtures have relatively higher CMRI values compared to other mixtures. However, Similar to W-5834L and W-7034PH, the B-5834L has a PGLT of -34°C which could have contributed to a lower CMRI value for this mixture. On the other hand, The CCPR mixtures are indicated to be more prone to rutting compared to the hot mixed binder and base course mixtures. However, these mixtures indicate comparable rutting performance to some of the wearing course mixtures. It is evident from the plots that the lower distillated oil percentage in CCPR mixtures such as CM-1-a and CM-2-a has resulted in higher CMRI values which indicates a better rutting performance for these mixtures.

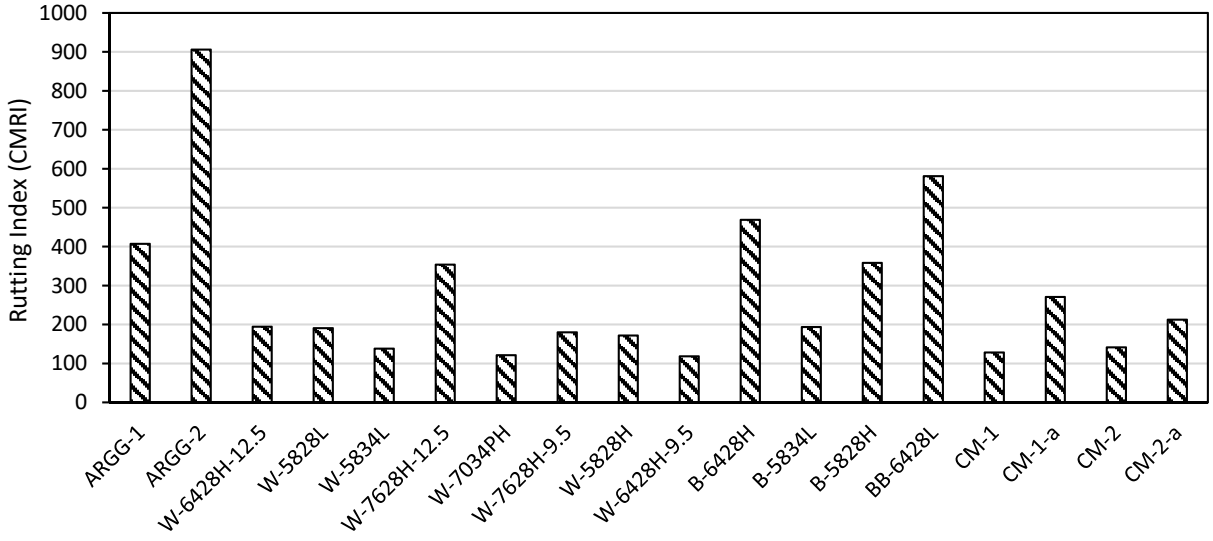

Figure 5-10 Evaluation of the NHDOT project mixtures through the developed rutting index parameter

5.2.9 SUMMARY AND CONCLUSIONS FOR RUTTING PERFORMNCE INDEX

Dynamic modulus |E*|as a measure of stiffness is generally considered as an indicator for asphalt mixtures rutting resistance where a mixture with higher modulus value frequency is generally considered to be less rut susceptible. However, this hypothesis ignores the viscoelastic behavior of the asphalt mixtures and the phase angle as the viscous part of the response. The research in this section of the report introduces and investigates 5 different complex modulus based index parameters to evaluate the asphalt mixtures' rutting susceptibility. These parameters implement the full linear viscoelastic properties of the asphalt mixtures (dynamic modulus and phase angle) at two specific points on the master–curves. The

first point is associated to the frequency at which the peak phase angle takes place. The second point is selected based on the Hamburg Wheel Tracking Test (HWTT) test loading frequency and temperature (52 passes/min equivalent to 0.866Hz at 45°C) and its equivalent reduced frequency on the master-curves.

The investigations were conducted on three different sets of mixtures (total of 22 mixtures). The first set includes 7 mixtures for which the HWTT test results are available to develop the parameters. The second set comprises from 6 mixtures for which the field rut depths in the 5th year after construction are used for verification of the introduced rutting index parameters. The third set of the mixtures is used to evaluate the index parameters with respect to volumetric variations in the mixture design where no rut measurements would be available. In addition to mixture ranking, the strength of correlation between the rut depths and the index parameters was evaluated through statistical analysis and the goodness of fit (R^2).

Amongst the 5 introduced parameters, Index (III) as $\left(\frac{|E_A^*|-|E_B^*|}{|f_A-f_B|^2}\right)$ revealed high capability in mixture ranking while maintaining high correlation with both the HWTT and field measured rut. The results indicated that this index can be used as a preliminary tool in evaluating and screening the mixtures rutting performance.

In order to implement the index parameters in this study, it is important to consider the regional mixture design properties (especially in southern United States) in selecting the HWTT related point on the master-curves. For stiffer mixtures, there is a possibility for the second critical point (f_b) to be projected on the post-peak side of the phase angle master-curve. In this situation, it is recommended to use the high binder PG grade temperature as opposed to the conventional HWTT test temperature to determine the reduced frequency on the master-curve.

5.3 DEVELOPMENT OF A DAMAGE GROWTH RATE-BASED FATIGUE FAILURE CRITERION FOR ASPHALT MIXTURES USING SIMPLIFIED-VISCOELASTIC CONTINUUM DAMAGE THEORY

5.3.1 INTRODUCTION AND BACKGROUND

The simplified viscoelastic continuum damage (S-VECD) theory has gained wide-spread attention among researchers as a promising asphalt fatigue cracking characterization tool [20-21]. The S-VECD theory uses a damage evolution law to determine the reduction in the pseudo stiffness (*C*) of material as a function of damage accumulation (*S*) due to loading cycle (*N*) [22]. The damage characteristic curve (DCC) reveals the disintegration of a mixture (decrease in pseudo stiffness) as the damage grows. However, the determination of the crack localization point from lab test results has been a major challenge in mixture characterization using the S-VECD approach. As discussed in section 3.2.4 in the report there are currently three different S-VECD based failure criteria called as N_f @ G^R =100, D^R and S_{app} that are used to indicate the mixture's fatigue performance. The pseudo-stiffness based criteria (D^R criterion) has originally been proposed to mitigate the extrapolation problems associated with the logarithmic scale of G^R [23]. However, mixtures with significantly different DCC curves could have similar D^R values as it only considers

the accumulated decrease in pseudo stiffness ($\int_0^{N_f}(1-C)\,dN$) and the number of loading cycles to failure (N_f) regardless of the total damage (S_f) prior to localization. In order to overcome this deficiency, the S_{app} was proposed to combine the effects of modulus and toughness in determining cracking susceptibility of asphalt mixtures. This parameter is defined as the damage accumulation (S) when pseudo-stiffness (C) is equal to $1\text{-}D^R$ [24]. While these parameters have tried to differentiate the asphalt mixtures' fatigue cracking performance in the lab, their strength in discriminating the mixtures' field performance through actual distress data needs to be assessed.

The main objectives of this section of the report are to:

- Evaluate the applicability of the existing S-VECD based fatigue failure criteria such as G^R, D^R and S_{app} in differentiating the field fatigue performance of the asphalt mixtures;
  and,
- Develop a new S-VECD based fatigue failure criterion that is better correlated with the field performance of asphalt mixtures in New Hampshire.

5.3.2 MATERIAL AND TESTING

In order to evaluate the asphalt mixtures' field performance with the S-VECD based fatigue failure criteria, a set 6 of mixtures for which the field fatigue performance is available were selected. This set of the mixtures is the same as the ones that were introduced in section 5.2.5 and their mixture design properties can be found in Table 5-5. As the mixtures have been placed on the same cross section with the same loading and climatic conditions, they can be used as a reliable source in indicating the capability of different index parameters in discriminating the mixture's performance with respect to different types of distresses. As the basis of comparison of the mix fatigue performance indices will be with respect to the field conditions, the testing and evaluation in this section of the report is conducted on the field cores taken after 1 year of construction. Moreover, testing the field cores will eliminate the difference between the production air voids which will lead to a more realistic assessment of the failure criterions. The field core air void of the mixtures is shown in Table 5-10.

Table 5-10 Field core air void of the mixtures

Mix	Virgin 58-28	15% RAP 58-28	25% RAP 58-28	25% RAP 52-34	30% RAP 52-34	40% RAP 52-34
Field core air void	3.5	2.5	2.2	2.5	3.7	3.4

5.3.3 FIELD CONDITIONS

Field performance of the sections has been monitored yearly since construction using an automated pavement distress data collection van by New Hampshire DOT. The fatigue cracking is tracked at three

severity levels. The weighted crack length for each section is calculated using the following equation (more details on use of this approach to characterize field performance can be found in Daniel et al., 2018 [19]:

$$Weighted\ crack\ length\ \left(\frac{m}{km}\right) = (Severity1\ crack\ length) + 2 \times (Severity2\ crack\ length) + 3 \times (Severity3\ crack\ length) + (Sealed\ crack\ length)$$

Equation (5.3)

The amount of fatigue cracking in each section is shown in Figure 5-11. In general, the mixtures with a lower RAP content indicates less cracking and the PG 58-28 binder appears to be performing better than the PG 52-34 binder (as seen from the two 25% RAP mixes). The 25% RAP PG52-34 section appears to have the worst performance overall, whereas the 15% RAP PG58-28 indicates the best fatigue performance among all other mixtures. While the virgin mixture reveals a relatively good and steady performance until the 4th year after construction, it indicates a relatively high rate of damage during the 5th year of service.

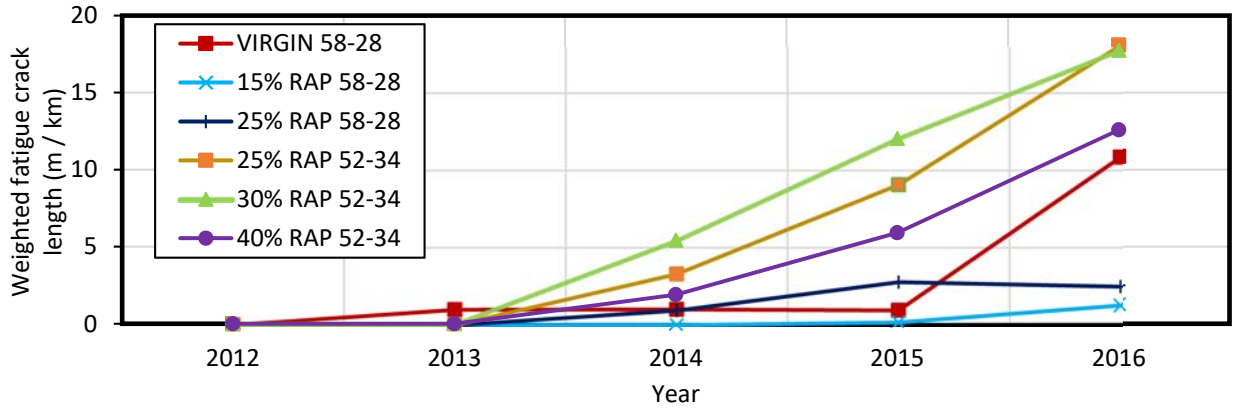

Figure 5-11 Normalized field fatigue cracking

5.3.4 RESULTS OF THE DIRECT TENSION CYCLIC FATIGUE

As mentioned before, the direct tension cyclic fatigue test was conducted in accordance to the AASHTO TP 107 standard method in order to determine the decrease in materials load bearing capacity through the averaged damage characteristic curves (DCC) plots tested for each mixture (Figure 5-12). Each curve is averaged from the test results conducted on 4 different replicates. The curves indicate the disintegration of the mixtures (decrease in pseudo stiffness) as the damage (*S*) grows [25]. However, with respect to DCC, a direct comparison between the mixtures may not be appropriate since the number of cycles to failure is missing between curves [26]. Therefore, the mixtures are ranked and evaluated with respect to different available failure criterion: (i) $N_f @ G^R=100$; (ii) D^R; and, (iii) S_{app}, which are plotted in Figure 5-13, Figure 5-14 and Figure 5-15 respectively. The plots indicate that the ranking of mixtures from the three indices are quite different such that the 40% RAP 52-34 is shown to have best fatigue performance with respect to $N_f @ G^R=100$ criteria whereas it holds one of the lowest D^R values and at the

same time it is ranked as the third best mixture in accordance to S_{app}. Similar observations can be made for other mixtures such as 25% RAP 52-34 indicating that none of the indices have been able to reliably predict this mixture's field performance. It can be seen from the results that the current failure parameters have not been able to rank the mixtures as compared to the actual field fatigue cracking as a standalone parameter. One main reason for this observation could be that with respect to continuum damage mechanics, it is the evolution and localization of micro-cracks that results in macro-cracks to form fatigue cracking. The magnitude and number of micro-cracks in the S-VECD analysis is quantified by the (S) value where neither G^R and D^R parameters explicitly take the amount of damage (S) into account. Although the S_{app} parameter tries to incorporate the magnitude of the damage in determination of fatigue resistance of the mixtures, it considers the damage at the average mixture's integrity (C at 1- D^R). However, since the accumulation of damage as well as decrease in capacity is a nonlinear phenomenon, the use of average C and corresponding (S) value may not be an appropriate indicator of fatigue failure. These results motivated the need to explore development of a new fatigue failure criterion based on S-VECD theory that can improve the reliability of predicting the field fatigue cracking performance.

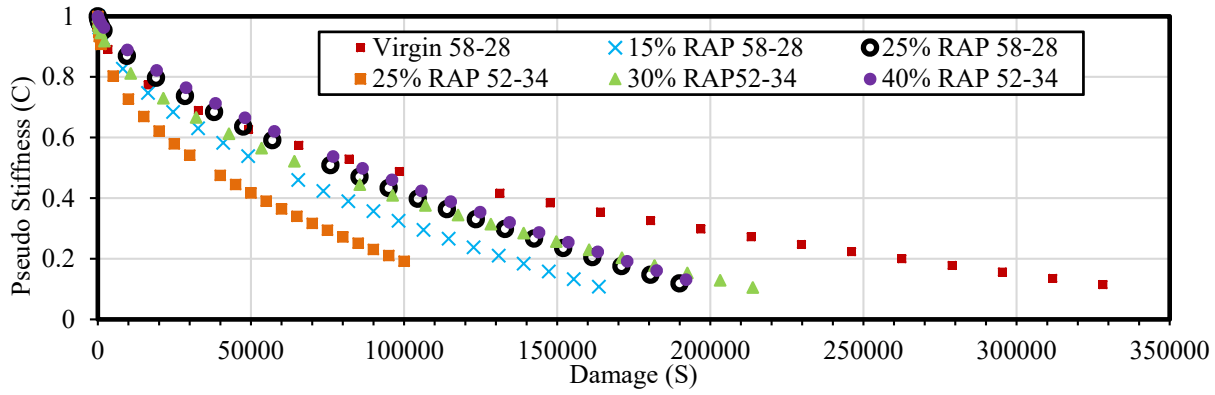

Figure 5-12 Damage characteristic curves (DCC)

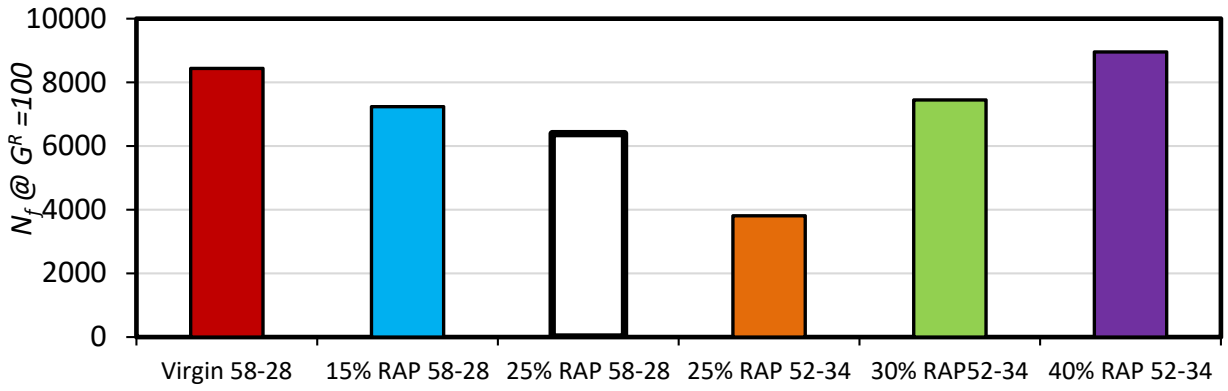

Figure 5-13 N_f @ G^R =100 fatigue failure criteria

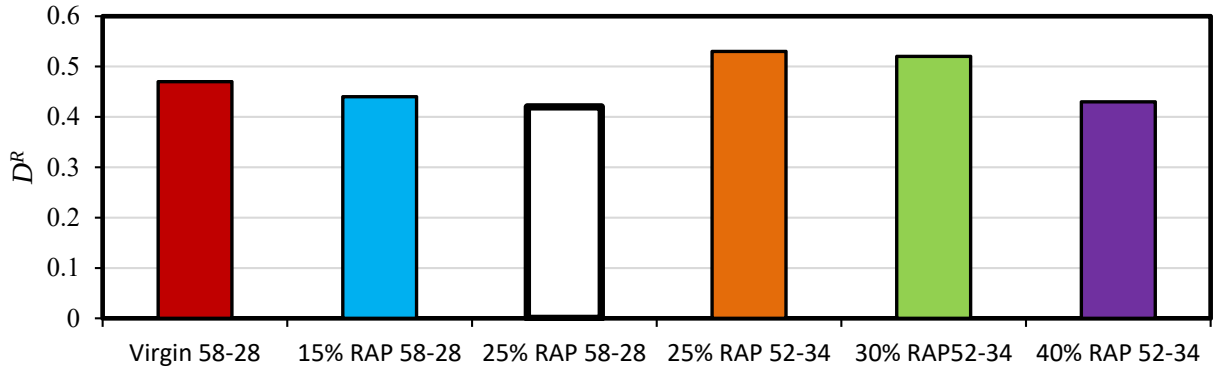

Figure 5-14 D^R fatigue failure criterion

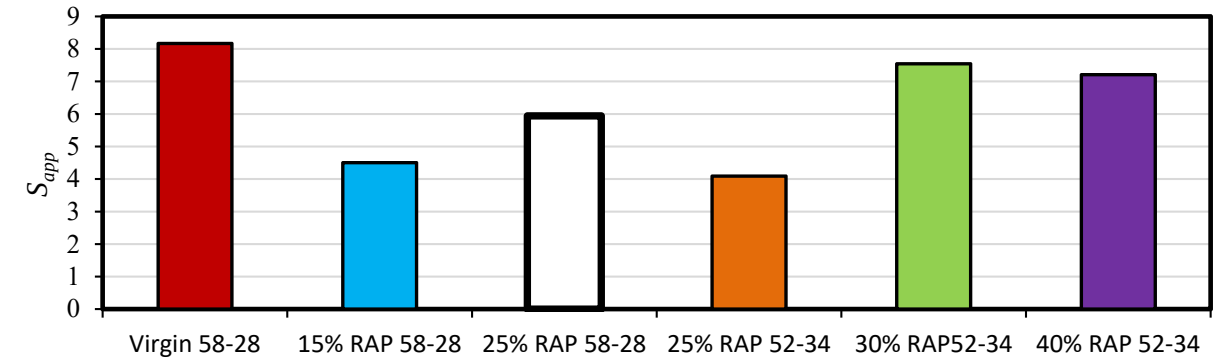

Figure 5-15 S_{app} fatigue failure criterion

5.3.5 DEVELOPMENT OF THE DAMAGE-GROWTH RATE BASED FATIGUE FAILURE CRITERION

As discussed in the previous section, neither of the currently available S-VECD theory based failure criterion were able to rank the mixtures on the I-93 test sections with respect to the actual field fatigue cracking performance which necessitates exploration of new failure criterion.

For a given test specimen in the direct tension cyclic fatigue test, the decrease in pseudo stiffness (C) can be explained through two separate graphs indicted in Figure 5-16. Figure 5-16(a) shows the damage characteristic curve where decrease in pseudo stiffness is associated with the accumulation of the damage (*C* vs *S*), and Figure 5-16(b) indicates the decrease in pseudo stiffness for the same test due to loading cycles (*C vs N*). In the cyclic fatigue test, the failure point of the test is determined through the peak phase angle [27]. This point in the test corresponds to the loading cycle at failure (N_f) and the accumulated damage at failure (S_f). The area above the *C vs N* curve indicates the accumulated decrease in material's capacity [28] and can be calculated through the following equation:

Accumulated decrease in material's capacity=$\int_0^{N_f}(1-C)\,dN$ Equation (5.4)

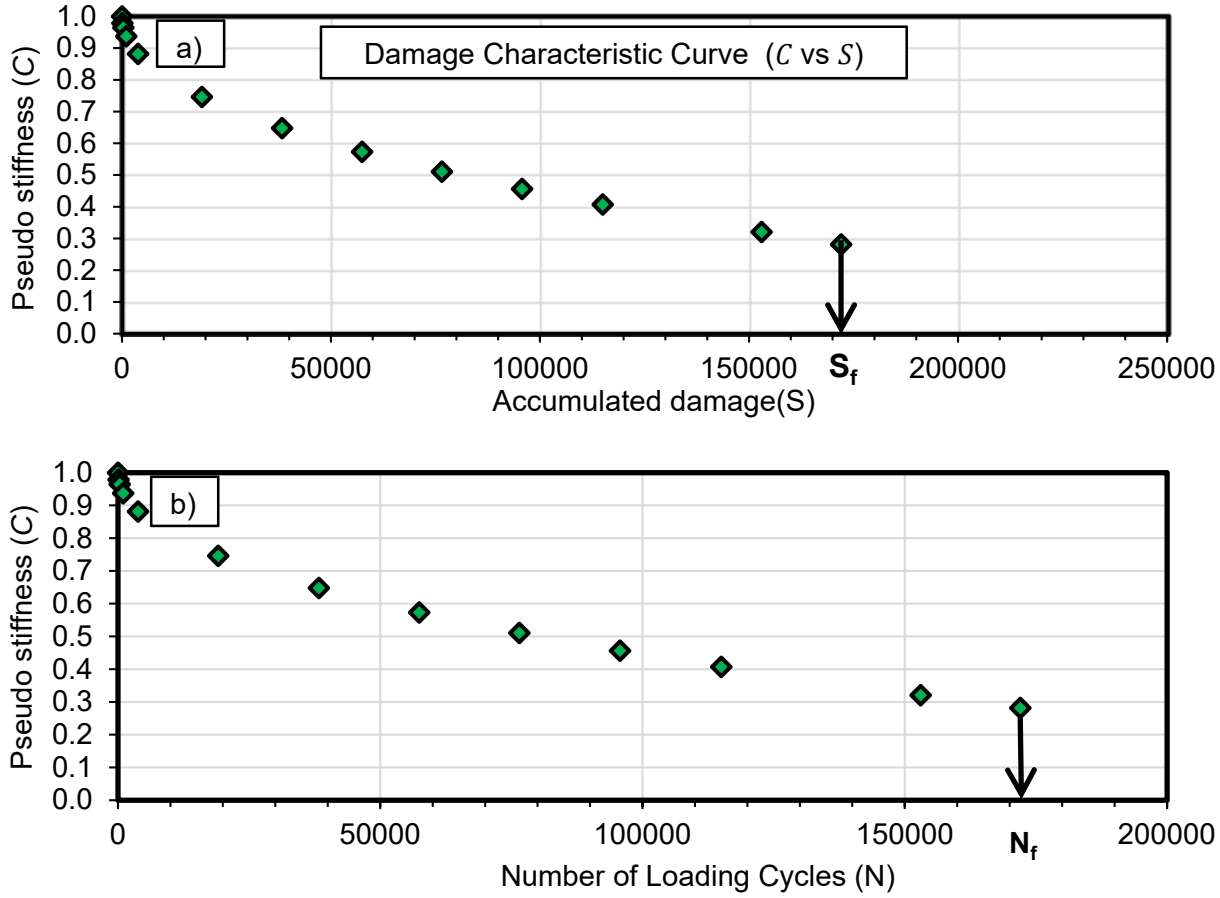

Figure 5-16 a) Pseudo stiffness versus damage accumulation (C vs S), b) Pseudo stiffness versus loading cycle (C vs N)

In order to develop a new fatigue failure criterion in this study, the correlations between these three components of S-VECD theory and analysis as the accumulated decrease in material's capacity ($\int_0^{N_f}(1-C)\,dN$), number of loading cycles to failure (N_f) and accumulated damage at failure(S_f) were investigated and incorporated to result in a damage growth rate based fatigue failure criterion. Using the test results for the 6 mixture from I-93 test section, Pearson's correlation coefficients were determined to investigate the relationships between the aforementioned parameters. These are shown in Table 5-11. The results indicate that as the number of cycles to failure increases, the magnitude of the accumulated damage at failure decreases. This correlation indicates that for different replicates of a same mixture, a higher level strain in the test may result in a lower amount of accumulated damage at the peak phase angle. In other words, at higher cyclic strains the rate of development of micro-cracks and their localization to form a macro-crack is high enough that the mixture is not able to use its full capacity to evenly disperse damage throughout the continuum to withstand the failure. This phenomenon is similar to a thermal shock occurrence for many other types of materials including asphalt mixtures where a sudden change in temperature results in premature cracks in the material before the material is able to reorganize its microscopic or even molecular structure to accommodate the temperature gradient. For the same reason and similarly, as the accumulated reduction in material's capacity ($\int_0^{N_f}(1-C)\,dN$)

increases due to higher strain levels the amount the accumulated damage at failure decreases. These observations indicate that not only the magnitude of the damage at failure is important but also the rate of increase in damage growth (governed by the strain levels at cyclic loading) is an important parameter that should be taken into consideration in development of a mixture fatigue performance index using the S-VECD theory.

Table 5-11 Pearson's correlation coefficients for the S-VECD based parameters.

S-VECD based parameters	N_f	S_f	$\int_0^{N_f}(1-C)\,dN$
N_f	1.00	-	-
S_f	-0.53	1.00	-
$\int_0^{N_f}(1-C)\,dN$	1.00	-0.53	1.00

With regards to the aforementioned discussion on the correlations between the investigated parameters, new fatigue failure criterion which is based on damage growth rate is proposed and indicated in Equation 5.5.

$$C_{N_f}^S = \frac{\int_0^{N_f}(1-C)\,dN}{S_f} \times m \qquad \text{Equation (5.5)}$$

Where:

$C_{N_f}^S$: Damage growth rate based fatigue failure criterion,

$\int_0^{N_f}(1-C)\,dN$: Accumulated decrease in pseudo stiffness,

S_f: Accumulated damage at failure

m: Unit correction factor set to 10^3 to increase the order of magnitude of the $C_{N_f}^S$ and for simplicity of comparisons between different mixtures

With respect to $C_{N_f}^S$, the higher S_f and lower $\int_0^{N_f}(1-C)\,dN$ are more desirable for fatigue performance as they indicate that material is able to withstand higher amounts of damage with less disintegration.

5.3.6 COMPARISON OF THE PROPOSED DAMAGE GROWTH RATE FATIGUE CRITERIA ($C_{N_f}^S$) WITH CURRENTLY AVAILABLE CRITERIA (N_f @ G^R=100, D^R AND S_{app})

In order to evaluate the reliability of the proposed failure criterion, the $C_{N_f}^S$ versus number of cycles to failure (N_f) graphs were plotted for each replicate tested for the six mixtures in Figure 5-17. The direct tension cyclic fatigue is usually conducted on four specimens each tested at a different strain level. The

accumulation of damage and decrease in material's capacity due to different strain levels is significantly non-linear which can result in wide ranges N_f value as can be seen in the figure. The results indicate a linear relationship in arithmetic scale between the proposed failure criterion and number of cycles to failure at each level of strain which eliminates the possible errors of the extrapolation that may occur in a logarithmic based relationship. In general, with respect to the graphs and definition of $C_{N_f}^S$,a lower slope of the fitted trend line between different mixtures is more desirable. For the purposes of simplicity in applying the $C_{N_f}^S$for comparing the mixtures' performance, a threshold parameter as $N_f@C_{N_f}^S = 100$ is suggested to be used in this study. This threshold parameter has been able to differentiate the mixtures performance with respect to field data. However, more investigation is required to confirm that this threshold is applicable to all types of mixtures and traffic levels. The ranking order from all the available failure criteria with respect to field performance is presented in Table 5-12. According to the rankings the $N_f@C_{N_f}^S = 100$ parameter has been able to rank all 6 mixtures, while other parameters such as N_f @ G^R *=100* and S_{app} have only predicted the worst mixture's performance among others. The results from the comparisons indicate the robustness of the newly proposed fatigue failure criteria in discriminating mixtures performance with respect to normalized field crack length 5 years after construction. It is worth mentioning that although a parameter such as D^R has not been able rank a mixture's performance, this parameter has been indicated to be a useful tool in discriminating the general properties of the mixtures with respect to production method and overall performance [26].

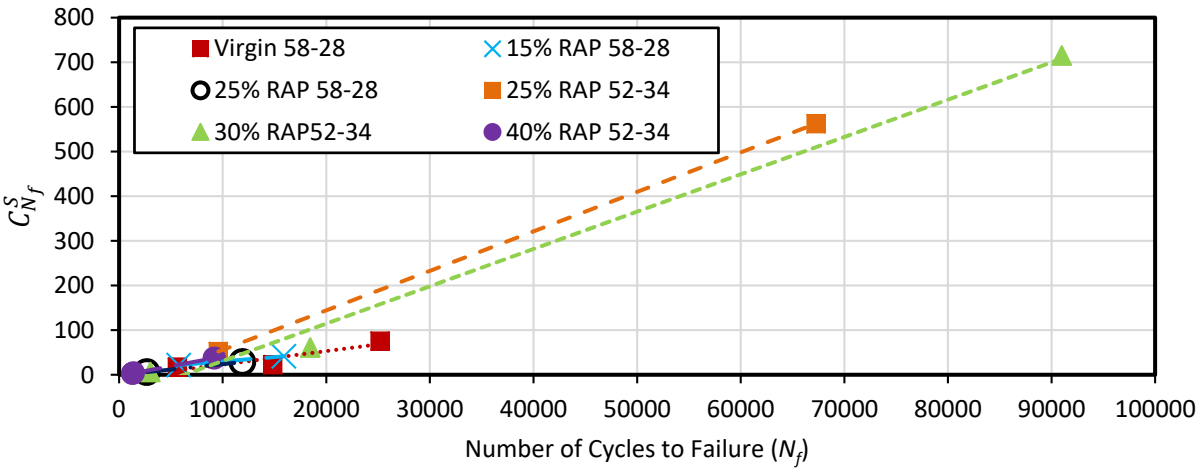

Figure 5-17 $C_{N_f}^S$ versus N_f plots

Table 5-12 Mixture ranking order in accordance to different failure criterion

Ranking with respect to different parameters (1;best , 6 worst)					
Mixture	**Field Rank (5years after construction)**	$N_f@C^S_{N_f} = 100$	$N_f@G^R = 100$	D^R	S_{app}
Virgin 58-28	3	3	2	3	1
15% RAP 58-28	1	1	4	4	5
25% RAP 58-28	2	2	5	6	4
25% RAP 52-34	6	6	6	1	6
30% RAP52-34	5	5	3	2	2
40% RAP 52-34	4	4	1	5	3

Although the mixture ranking is an important tool to discriminate the mixtures' performance, the statistical and mathematical correlation between the developed index parameter and the field data should be evaluated to examine if the parameter is capable of determining the order of magnitude, if different, between mixtures. For this reason, the normalized fatigue crack lengths were plotted versus the $N_f@C^S_{N_f} = 100$ parameter to determine the statistical correlation in terms of the R^2 goodness of fit parameter for the data. As it is shown in Figure 5-18, a power function fit with an R^2=0.73 was fitted to the data. The power function fitting is presumed to be suitable for fatigue as it can more realistically describe the boundary conditions of the crack length while it also can help in determining the appropriate threshold N_f value for a specific project during a performance based mixture design phase. Also, the power function has similar format as fatigue endurance limit where very poor mixtures have a very low N_f at the proposed threshold and similarly there is an asymptotic form for very good performers having fatigue life approaching infinity.

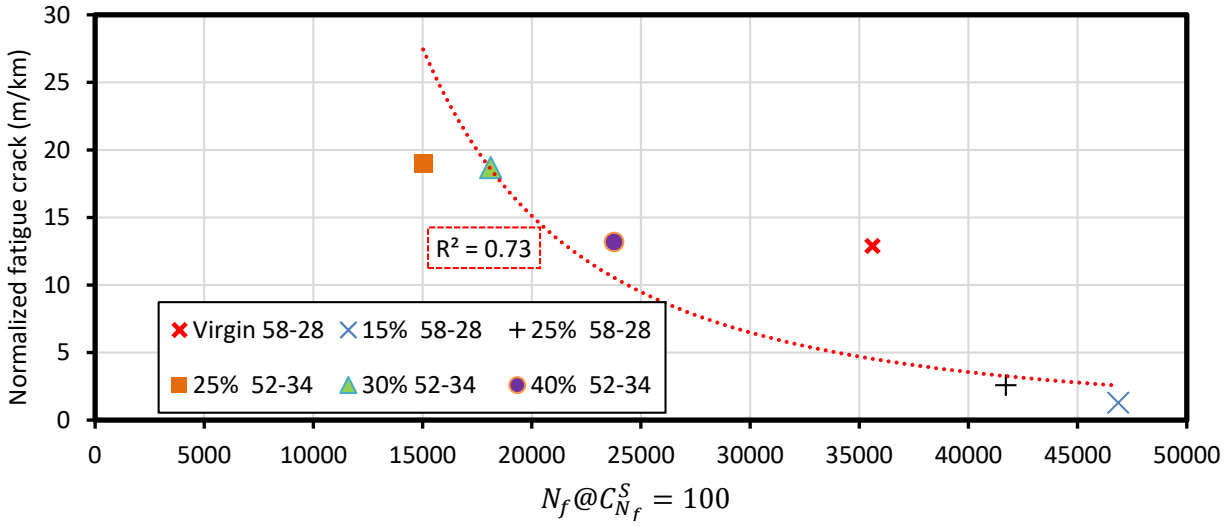

Figure 5-18 Statistical correlation between the field cracking length and the proposed fatigue criterion

5.3.7 EVALUATION OF THE NHDOT PROJECT MIXTURES THROUGH THE PROPOSED FAILURE CRITERION ($C^S_{N_f}$)

The results for the NHDOT project mixtures (c.f. Table 3-2) through the proposed fatigue failure criterion is shown in Figure 5-19. Similar to the results from D^R and N_f @ G^R =100 criteria as indicated in section 4.4, ARGG-1 has a better performance compared to ARGG-2. However, with respect to other wearing course mixtures, the ranking is different such that W-7628H-12.5 followed by W-5834L are shown to have the best performance. The other wearing course mixtures indicate similar fatigue performance with respect to $C^S_{N_f}$ criteria. With regards to hot mixed binder and base course mixtures, $C^S_{N_f}$ ranks B-5828H as a better mixture compared to other mixtures while D^R, N_f @ G^R =100, and S_{app} criteria had indicated the BB-6428L to be the best among these types of mixtures. However, these mixtures reveal to have acceptable fatigue performance when compared to wearing courses such as ARGG-2, W-6428H-12.5 and W-5828L mixtures. With an exception to ARGG-2, the CCPR mixtures are shown to be most susceptible to fatigue cracking among all the study mixtures. However, due to their use predominantly as base course materials, their propensity for fatigue cracking may not be of significant concern.

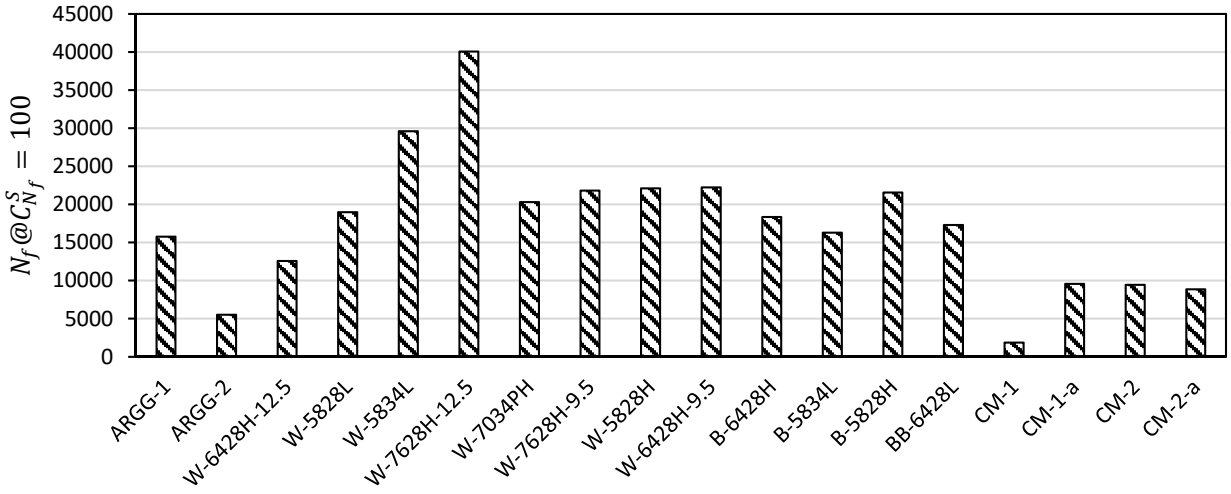

Figure 5-19 Evaluation of the NHDOT project mixtures through the developed fatigue index parameter $N_f@C^S_{N_f} = 100$

5.3.8 EVALUATING THE FIELD PERFORMANCE OF THE NHDOT PROJECT MIXTURES THROUGH THE PROPOSED FAILURE CRITERION ($C^S_{N_f}$)

In order to further evaluate the applicability of $C^S_{N_f}$ to different types of cross sections with different amount of traffic levels, a set of 6 wearing course mixtures from the NHDOT study mixtures were selected for more detailed evaluation. The mixtures have been used in different construction projects with different levels of traffic in New Hampshire and the field distress data for several years after construction are available for them. Using Equation 5.3, the normalized field crack lengths have been plotted in Figure 5-20. Since the cross sections, traffic volume and weather situations have been different for these

projects, the area under the curves normalized by the squared time after construction was used to unify the cracking performances for different mixtures as shown in Figure 5-21. This method of normalizing field cracking performance from different pavement sections has been developed and validated by previous work by Dave et al. 2016 [29]. As it is demonstrated in Figure 5-21, a power function fit has resulted in a very good correlation (R^2=0.80) between the fatigue index parameter and the amount of field cracking for different mixtures. These observations reaffirm the reliability and usefulness of the proposed fatigue failure criterion to be used as an indicator for the mixture's fatigue performance.

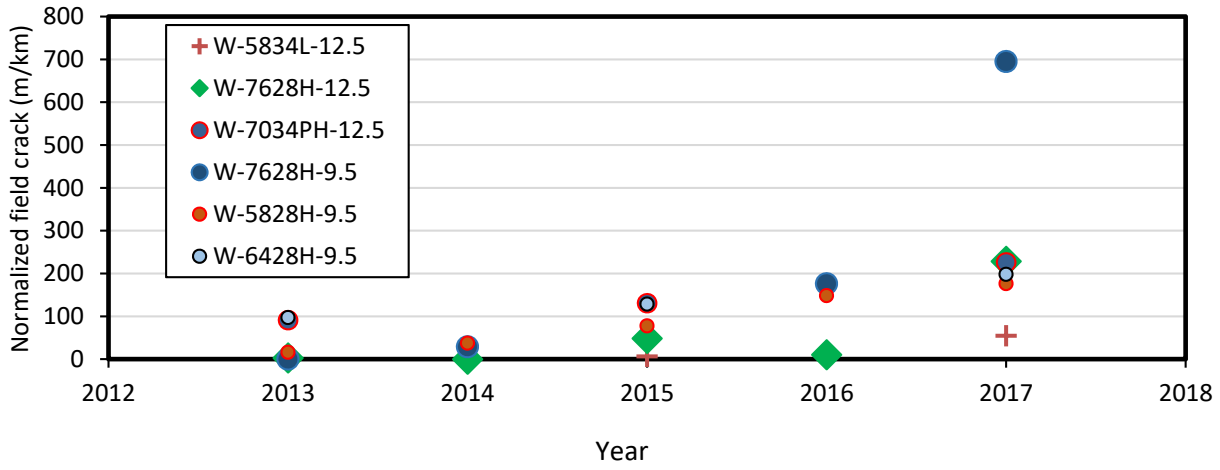

Figure 5-20 Normalized field crack length for different mixtures in terms of meter per kilometer

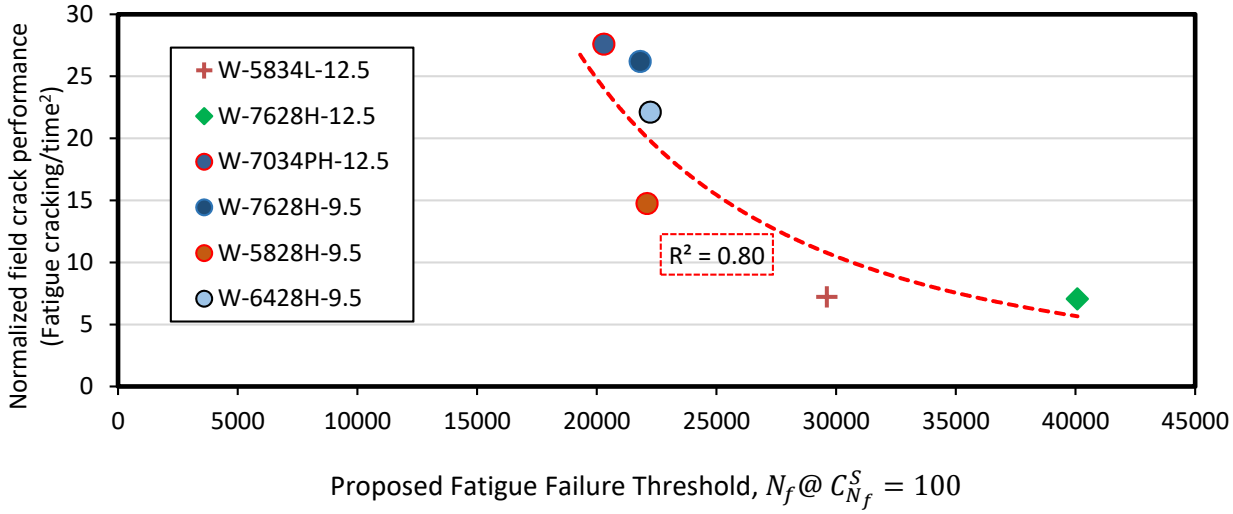

Figure 5-21 Normalized field fatigue cracking performance versus proposed fatigue failure threshold($N_f@\ C_{N_f}^S = 100$)

5.3.9 SUMMARY AND CONCLUSIONS FOR FATIGUE FAILURE CRITERION

There are currently three fatigue failure criterion that are commonly used to evaluate fatigue performance of asphalt mixtures that are tested through direct tension cyclic fatigue testing method and the S-VECD theory. However, because of the challenge of using logarithmic scale in defining G^R, insensitivity of D^R to the amount of damage growth prior to crack localization, and lack of S_{app} parameter in appropriately ranking mixtures as per field performance (as shown in this section), there is a need for a stand-alone fatigue threshold that can be reliably used to rank field performance. Therefore, a new failure criterion called as $C_{N_f}^S$ was developed and investigated. This criterion incorporates three components of the S-VECD theory ($\int_0^{N_f}(1-C)\,dN$, N_f and S_f) to capture the mixture's disintegration with respect to damage growth rate. In order to use this parameter for a given mixture, the $C_{N_f}^S$ is calculated for each tested replicate (minimum of two strain levels are required) and the results are plotted versus the number of cycles to failure (N_f).An index parameter called as $N_f@C_{N_f}^S = 100$ is determined for ranking purposes of different mixtures. The evaluations of the new parameter were conducted through investigations of two different sets of mixtures (each set combined of 6 mixtures) for which the field distress are available and $C_{N_f}^S$ indicated to be able to reliably rank the mixtures. This parameter indicated that it is not only able to rank the mixtures but it also has a high correlation with the magnitude of cracking in the field.

5.4 DEVELOPMENT OF A RATE-DEPENDENT CUMULATIVE WORK AND INSTANTANEOUS POWER BASED ASPHALT CRACKING PERFORMANCE INDEX

5.4.1 INTRODUCTION AND BACKGROUND

Cracking is one of the major structural distresses in asphalt mixtures and has been widely investigated by researchers. Based on different mechanistic theories, numerous laboratory testing methods have been proposed to characterize the cracking performance of asphalt mixtures. Fracture mechanics has extensively informed development of laboratory tests and as they relate to the formation and growth of cracks with respect to material's microstructure, loading rate and environmental circumstances. The application of fracture mechanics in characterizing the cracking performance of asphalt mixtures has been documented as early as the 1970s. Using a simple beam test under cyclic loading, a study by Majidzadeh et al. aimed to relate the stress intensity factor to the crack growth rate with respect to Paris' law for asphalt mixtures' fatigue performance [30, 31].

With respect to the fracture mechanics for heterogeneous composites such as asphalt mixtures, materials are assumed have a uniform distribution of pre-existing flaws. In order to conduct a laboratory test with stable crack growth and to hone in on the energy needed to propagate that crack, a specimen with a pre-existing crack or notch is needed. Using these concepts, Wagoner et al. explored the use of a single-edge notched beam (SENB) test to quantify the fracture properties of asphalt mixtures under repetitive loading [32]. The geometry of the SENB test is challenging in terms of obtaining field samples from existing pavements, so alternative testing methods such as disk-shaped compact tension (DCT) and semi-circular

bend (SCB) tests have been proposed [33-35]. Both of these geometries can be prepared using cored specimens from pavements or from cylindrical gyratory samples following the standard Superpave mix design and compaction approaches. While the DCT test is generally used to characterize low temperature fracture properties of asphalt mixtures, the SCB test has been used to determine both low and intermediate temperature cracking performance [36-38]. Since its first implementation in rock mechanics [39] and later application in asphalt performance testing, the SCB test has been shown to have acceptable sensitivity to mix design variables [40] as well as loading rate and testing temperatures [41]. Moreover, the SCB has also shown potential to be used for characterizing the mixed-mode fracture properties of asphalt mixtures [42].

In order to determine the fracture properties of asphalt materials using the SCB geometry, the force versus load-line displacement (LLD) curve under a monotonic loading protocol has been investigated by different researchers [37, 43]. Figure 5-22 indicates a typical SCB force-LLD curve.

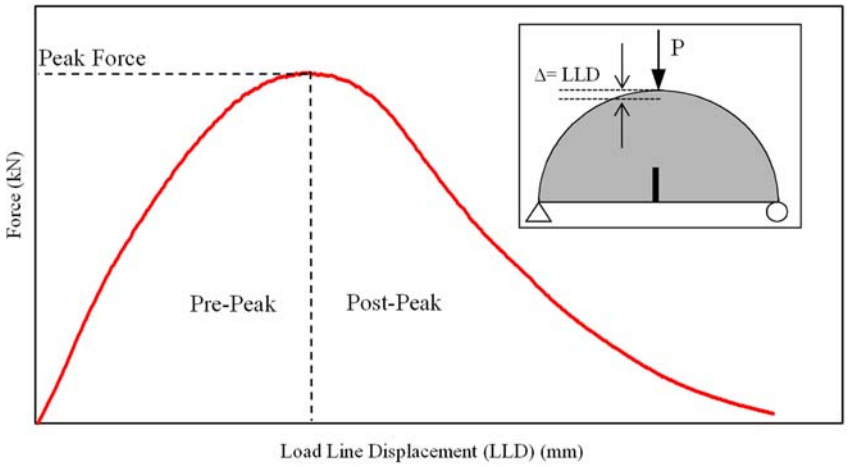

Figure 5-22 Typical Load-LLD curve

The curve can be divided into two distinct portions with respect to the required force for the crack to initiate (pre-peak) which is followed by a decrease in the force when the crack propagates along the specimen (post-peak). As the force is applied, the portion of the specimen below the neutral axis undergoes tensile strains, which result in the accumulation of tensile stresses in the notch tip vicinity. These stresses bring about the creation of a region of micro-cracks, namely the fracture process zone (FPZ), in front of the crack tip. Although the length of the fracture process zone can be considered as a material specific property [44], its determination requires either reliance on inverse analysis based modelling approaches or use of advanced laboratory characterization techniques, such as acoustic emissions [45].

Based on principles of fracture mechanics, the energy required for generation of a unit fracture surface area in a material is called the fracture energy (G_f) [46]. This energy is the sum of the positive surface energy (S) and the negative released strain energy (U). The surface energy is the energy absorbed during the crack growth because of the creation of newly made free surfaces as the atomic bonds break and the

specimen's bulk energy is converted into the surface energy. The surface energy increases linearly with respect to crack length. On the other hand, the released strain energy is related to the unloaded region of material adjacent to the free surfaces as the crack is growing. The strain energy is proportional to the squared length of the crack [46]. Considering the order of correlation of these energies to the crack length, the energy required for the crack to propagate decreases at a critical crack length where the peak resistive force occurs in the force vs LLD curve (Figure 5-22).

In order to use the SCB geometry to evaluate the cracking properties of asphalt mixtures in a relatively simple manner, different testing protocols and analysis methods have been proposed and investigated. For instance, in the work conducted by Louisiana Transportation Research Centre (LTRC) [38], the SCB test is conducted at a loading rate of 0.5 mm/minute at 25°C using three different notch depths on specimens 75 mm diameter and 57 mm thick. The analysis of the test results is performed through determination of the critical strain energy rate (J-integral) [47]. The low temperature SCB fracture test, developed by [48], utilizes a 25 mm thick specimen that is tested using the crack mouth opening displacement (CMOD) rate of 0.015 mm/minute at low temperatures (typically in range of -12 to -40°C) and determines asphalt mixture's fracture energy and stress-intensity factor. The third commonly used SCB testing method, which is of main interest in this study, is the protocol developed by the Illinois Centre for Transportation, commonly referred to as the Illinois Flexibility Index Test (I-FIT) [49]. The test is conducted using a 50 mm/minute LLD rate at 25°C on specimens 50 mm thick and 75 mm diameter. The notch depth is constant among all the replicates and is equal to 15 mm [50]. The I-FIT test was originally developed with the purpose of discriminating the cracking performance of mixtures with varying amounts of recycled asphalt pavement/shingles (RAP/RAS) [40]. In order to rank the mixtures through I-FIT results, the fracture energies (area under the force-LLD curve divided by the ligament area) of different mixtures were compared. The comparisons indicated the insufficiency of this parameter as mixtures with different rheological properties could result in similar fracture energy values. It should be noted that fracture energy here is a global fracture energy (not a material scale property) that is a function of the material's intrinsic fracture energy but dependent on specimen geometry and other testing factors (such as loading rate and test temperature). Due to poor discrimination between mixtures from fracture energy alone, other possible influential parameters from the force-LLD curve on the FPZ such as the peak load, the slope at the inflection point, and critical displacement were investigated [40]. As a result, the flexibility index (FI), which is an engineering parameter, was developed to correlate the crack growth velocity and the brittleness of the mixtures.

$$FI = A \times {G_f}\Big/_{abs\ (m)} \qquad \text{Equation (5.6)}$$

Where:

A= Unit correction coefficient taken as 0.01,

G_f = Fracture energy (J/m^2)

m = Slope at the inflection point

Although the flexibility index has generally been shown to be a good indicator of cracking performance, in many instances it results in relatively high coefficient of variation (COV) among the replicates, which can significantly reduce the practicality of using this parameter for routine use. The high COV results from the fact that the m-value is derived from the shape of the post-peak segment of the force-LLD curve and is highly sensitive to the gradation, density and air void distribution within the specimen, as well as other random variables such as operator variability etc. [40]. For the same reasons, the FI may not be able to discriminate the performance of brittle or long-term aged mixture, as these mixtures may exhibit steep post peak curves resulting in indeterminate or quite low FI values (as low as 1) [51]. Other studies have also indicated that the FI may not be sensitive to variations in asphalt content [52].

As an alternate to FI, [53] proposed the use of maximum load (P_{max}) to determine the fracture strength (S_f) from the DCT test. The fracture energy normalized by S_f resulted in an index parameter called Fracture Strain Tolerance (FST) which was introduced in section 3.2.5 in this report. FST was shown to lower the COV, while maintaining high discriminability among the mixtures. Researchers at the Texas A&M University also used the P_{max} as a normalizing factor for fracture energy and introduced the Crack Resistance Index (CRI) as an alternative to FI [51]. It should be noted that CRI does not account for specimen to specimen geometric differences, whereas FST does account for specimen geometry in the index calculation. The comparisons for CRI indicated a decrease in COV for the short-term oven aged (STOA) mixtures compared to FI. However, the study indicated a higher variability of CRI compared to FI for long-term oven aged (LTOA) mixtures with both indices indicating similar trends for different mixtures. Moreover, CRI may need further evaluation since the peak load as a normalization factor may not be physically interpretable in terms of fracture process. There could also be examples of polymer modified mixtures with high fracture energy and high peak load where the CRI and FST may not be capable of discriminating among them.

A study conducted at the University of Arkansas used the concept of Resistance Curve (R-Curve) to determine mixture fracture properties. The R-Curve indicates the cumulative fracture energy as a function of crack extension. In general, if the slope of R-Curve is zero then the material is brittle and if the slope maintains a gradual increment then the behavior is ductile [46]. The benefit of using the R-Curve is that it provides a dynamic trace of the strain energy with respect to crack growth and it can better explain the crack initiation and propagation mechanism. Therefore, the application of R-Curve can be supported by the fracture mechanics. In addition, The R-curve indicated a high potential for determining the effect of mixture properties as well as environmental factors on the cracking performance [54].

Most of the current approaches and parameters used in analyzing the SCB test focus merely on the characteristics of the force-LLD curve whether it is the slope, peak force, or the crack extension. However, the factor of loading rate is an equally important influential parameter in characterizing viscoelastic material; this has been neglected in the development of existing index parameters for discriminating the fracture properties of asphalt mixtures. Based on the rate dependency of the viscoelastic material, it can be hypothesized that the development and growth of the FPZ and consequently the crack propagation, could be significantly different for mixtures with similar G_f, P_{max} or even post-peak slopes at the inflection point. However, the displacement measured by means of the extensometers or clip-on gauges in most of the fracture tests is an average deformation value that could be far from the actual FPZ and may not be

appropriate to characterize the true fracture properties of viscoelastic materials at intermediate temperatures. A study conducted at the University of Nebraska indicated the importance of rate dependency of asphalt mixtures in capturing the local fracture processes and FPZ through analyzing the SCB test results at different loading rates (1, 5, 10 and 50 mm/minute) using a digital image correlation system and finite element modelling [55].

The objective of section of the report is to explore use of a rate dependent cracking index parameter based on the I-FIT testing method which can be used to describe the crack initiation and propagation process with respect to the fracture processes in viscoelastic materials. The ability of this index to discriminate cracking resistance of asphalt mixtures as well as for a mixtures at different aging levels will be evaluated and compared to the FI parameter. Furthermore, the resultant coefficient of variation for the new parameter (rate dependent cracking index, RDCI) will be compared to FI.

5.4.2 DEVELOPMENT OF THE RATE DEPENDENT CRACKING INDEX (RDCI)

Perhaps, the rate dependency and hereditary behavior are the main distinguishing characteristics for viscoelastic materials that delineate them from elastic solids. Multiple studies [56, 57] have indicated the importance of time dependency in the fracture mechanics of viscoelastic materials and indicate that the crack growth in viscoelastic materials originates from viscoelastic deformation in the process zone. This deformation provides the required energy for gradual propagation of the crack with respect to time as opposed to brittle materials such as metals [58]. For example, a study conducted by Chung and Williams [59] used a three-point bend notched specimen to evaluate the effect of time along with the load line displacement measurements in the cracking process. The results indicated that before crack growth initiates, the displacement as a function of time is caused by the viscoelastic deformation. As the crack growth commences, the viscoelastic constitutive relationships combined with compliance can be applied to calculate the crack size with respect to time and consequently the crack growth rate and stress intensity factor using only simple LLD versus time measurements.

In order to develop a simple, useful rate dependent cracking index in this study, three main parameters in the I-FIT test and the force-LLD curve were considered:

i. The cumulative work (W_c) as a function of time (t)
ii. The peak force (P_{max})
iii. Times to reach the peak force and 10% of the peak force (post-peak) on the force-LLD curve (t_c). (The use of these specific times is discussed in the following section of the report.)

The average fracture energy has been used as the main parameter in evaluating the mix crack resistance in the I-FIT test. However, it was indicated that a single average value may not be able to differentiate the behavior of the mixture during crack growth. Therefore, the cumulative work (accumulated area under the force-LLD curve, Figure 5-23) as a function of time is used to lower the challenge faced by use of the fracture energy value in terms of its inability to capture the crack velocity.

The cumulative work over time not only exhibits the history of the dissipated work during the crack growth, but it can also be used to indicate the crack resistance rate at any time during the loading period. From a mechanistic perspective, the rate of the work over time ($\frac{\Delta W}{\Delta t}$) is power (*P*), which simply indicates the amount of energy transferred per unit time. Thus, when evaluating a material's fracture resistance potential, it can be hypothesized that for a certain duration from the start of loading application (indicated by t_0), a material requiring more power will exhibit more brittle behavior due to a larger amount of stored potential strain energy. In the case of viscoelastic materials such as asphalt mixtures, while part of the energy is stored as a potential strain energy, a portion of the energy is spent towards the creep dissipation prior to the crack initiation. A coupled experimental and numerical simulation based analysis can provide the decomposition of the potential strain energy and creep dissipation [60]. However, for routine usage of a cracking index parameter such analysis is not feasible. Over a smaller range of time, such that when Δt approaches 0, it can be reasonably assumed that power is the rate of the work with respect to time, i.e. $\frac{\Delta W}{\Delta t} \approx \frac{\mathrm{d}W}{\mathrm{d}t}$. Typically, this slope is referred to as the instantaneous power (P_t), which is a scalar quantity that indicates the instantaneous energy dissipation rate and can be rewritten as follows:

$$P_t = \frac{\mathrm{d}W}{\mathrm{d}t} = \boldsymbol{F}.\frac{\mathrm{d}\boldsymbol{x}}{\mathrm{d}t}; \frac{\mathrm{d}\boldsymbol{x}}{\mathrm{d}t} = \boldsymbol{V} \qquad \text{Equation (5.7)}$$

Therefore:

$$P_t = \boldsymbol{F} \cdot \boldsymbol{V} \qquad \text{Equation (5.8)}$$

Where:

Pt = instantaneous power; ***F***= force; ***V***= instantaneous velocity

The instantaneous power is the scalar product of force and velocity at any time (*t*) during the test. During the crack initiation process, the rate of instantaneous power will change drastically; this is due to transition of the energy state of the material from predominantly controlled by potential strain and creep dissipation modes to fracture dissipation dominant mode. The crack initiation usually occurs in quasi-brittle materials such as asphalt mixtures when the internal stresses approach the tensile strength of the material [61]. This instance can be reasonably assumed to happen near the occurrence of the peak force in a fracture test. Therefore, the time required for the peak load to occur will be used as the first time point in this study; this is indicated by symbol t_{peak}. Defining a second critical point of time is necessary to consistently define the ending point of the I-FIT test where it is assumed that full crack propagation has happened and the test specimen has no more load carrying capacity. For test practicality purposes and to prevent damage to test equipment, tests are typically stopped at 10% peak force. Therefore, the time at which 10% of peak force occurs, in the post peak segment of the load-LLD curve, is chosen as the second time point of interest.

As a summary, in order to explore a rate dependent cracking index parameter the following variables have been introduced and described:

- Cumulative work with time, W_c

- Instantaneous power at the peak force, $P_{t = peak}$
- Two times of interest on the force-LLD curve;
    - Time at peak load, t_{peak}
    - Time at 10% peak load at post-peak, $t_{0.1peak}$

In order to calculate various parameters from the fracture test results, the cumulative work (W_c) and time data were fitted using a polynomial equation and the area under the curve from the t_{peak} to $t_{0.1peak}$ were calculated. In order to focus on the fracture work associated with propagation of the crack in the specimen, the area under the cumulative work and time from start of test to t_{peak} was excluded from the integration. The resulting area is then normalized by the product of the instantaneous power at peak force ($P_t = t_{peak}$) and the fractured ligament area (product of fracture width and length) to calculate an index referred to as the rate dependent cracking index (RDCI):

$$\boldsymbol{RDCI} = \frac{\int_{t_{peak}}^{t_{0.1peak}} \boldsymbol{W_c} \ . \boldsymbol{dt}}{\boldsymbol{P_{tpeak}} \times \boldsymbol{ligament\ area}} \times C \qquad \text{Equation (5.8)}$$

Where:

RDCI = rate dependent cracking index ($\frac{s^2}{m^2} \times 10^4$)

$\int_{t_{peak}}^{t_{0.1peak}} W_c \ . dt$= area under the cumulative work vs time

P_t= instantaneous power at peak force

C= Unit correction factor set to 0.01 to lower the order of magnitude of the RDCI and for simplicity of plotting

Ligament area = specimen thickness times the ligament length

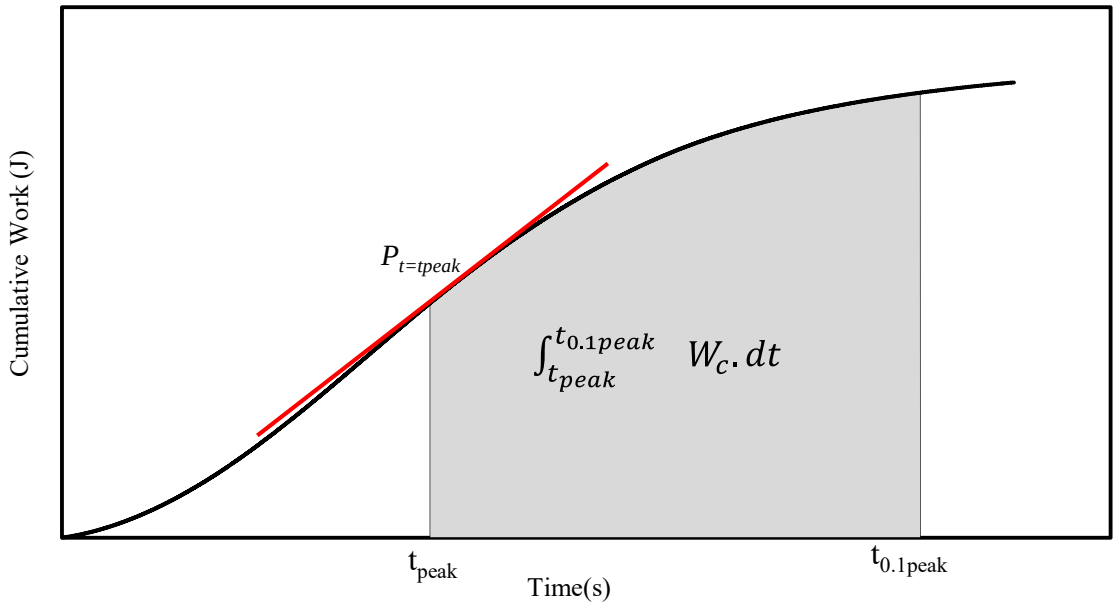

Figure 5-23 Determination of cumulative work between time at peak load and 0.1 of peak load

Comparing the RDCI to the FI, the area under the W_c curve and the $P_{t = tpeak}$ in RDCI replaced the fracture energy (Gf) and the post peak slope (m) at the inflection point on the force-LLD curve in FI respectively. Although it may appear that the area under the W_c curve is still a single average value, the expansion of the integral results in the product of impulse (J) and displacement as such:

$$\frac{\Delta W}{\Delta t} = \boldsymbol{F} \cdot \frac{\Delta \boldsymbol{x}}{\Delta t} \qquad \text{Equation (5.9)}$$

Multiplying both sides of above equation by $(\Delta t)^2$

$$\boldsymbol{\Delta W} \cdot \boldsymbol{\Delta t} = (\boldsymbol{F} \cdot \Delta t) \cdot \boldsymbol{\Delta x} \text{ such that } \Delta \boldsymbol{x} = \boldsymbol{x}_{0.1peak} - \boldsymbol{x}_{peak} \qquad \text{Equation (5.10)}$$

Where:

$\boldsymbol{F} \cdot \Delta t$= J or impulse (N.s)

$\boldsymbol{x}_{0.1\text{peak}}$= displacement at 0.1 peak load (post-peak segment)

$\boldsymbol{x}_{\text{peak}}$= displacement at peak load

Impulse in a fracture test can be interpreted as the capability of the material to tolerate force over a duration of time (similar in concept to momentum, however here in context of the formation of new fractured surfaces within the specimen). A material with higher impulse during the course of a fracture test will have more fracture resistance capacity and typically a more ductile response (due to ability of having greater fracture work potential during crack propagation). On the other hand, the instantaneous power at the peak load as a normalizing parameter indicates the rate at which the total work accumulation occurred until the point of crack initiation. A smaller rate is more desirable as it reveals a shallower

transition between pre-peak and post-peak energies, that is, a balance between potential strain energy accumulation, viscous creep dissipation and fracture dissipation. A major advantage of the above described parameters is that they inherently account for the rate dependency of the material.

One may argue that for a constant rate of displacement (in case of I-FIT 50 mm/min test), the instantaneous power will have a similar normalizing effect of peak load in parameters such as CRI. While this holds true for a test with a constant crack velocity, for tests controlled with constant LLD rate, often the crack velocity is not constant [54]. Furthermore, the field distress investigations often indicate a non-uniform crack growth rate [19], thus for these reasons, a rate dependent parameter such as instantaneous power can better describe the fracture processes in viscoelastic materials.

5.4.3 MATERIALS AND TESTING

To evaluate the proposed RDCI parameter in terms of distinguishing cracking resistance of different types of asphalt mixtures, 18 different plant-produced hot mixed asphalt (HMA) mixtures with varied designs, fabrication processes, and aging levels were selected from Minnesota (4 mixtures), New Hampshire (11 mixtures), and Virginia (3 mixtures). It should be mentioned that 10 mixtures from New Hampshire are the same wearing course mixtures that are selected for development of layer coefficients in this project (Table 3-2). However, in order to maintain consistency and ease of analysis and discussions with respect to source of mixtures throughout this part of the report, these mixtures will be labelled differently. Mixtures were tested using the I-FIT test in accordance with the AASHTO TP 124 test method at a test temperature of 25°C. Minnesota and New Hampshire mixtures were reheated and compacted in lab (referred to as plant-mixed lab compacted or PMLC) while the Virginia mixtures were sampled and compacted in the plant (plant mixed plant compacted, PMPC) without reheating. Using a Superpave gyratory compactor, the specimens were compacted to the typical target in-field construction air void level of 6±0.5% for New Hampshire and 7±0.5% for Minnesota and Virginia. The number of replicates from each source is 4, 24 and 3 for New Hampshire, Minnesota and Virginia respectively. Table 5-13 summarizes the mixture design and specimen fabrication methods. The RBR in the table is the percent replacement binder ratio for New Hampshire and Minnesota mixtures, however for the Virginia mixtures this is actually the amount of RAP in the mixture by weight of total mix.

There are five highlighted mixtures in the table which are selected for further evaluation of the cracking index parameter at different aging levels which will be discussed in the following sections.

Table 5-13 Summary of mixture used in RDCI development

Mixture name	Mixtures from Table 3.3	Mix Sampling Location	Specimen Fabrication Method	Nominal Maximum Aggregate Size (mm)	Air Void (%)	Gyration	Binder (PG)	Asphalt Content (%)	RBR/ RAP (%)
NH_ARGG-1	ARGG-1	New Hampshire	Plant Mixed-Lab Compacted (PMPC)	12.5	4.0	75	58-28	7.8	0.0
NH_ARGG-2	ARGG-2							7.6	6.6
NH_64-28	W-6428H-12.5						64-28	5.4	18.5
NH_70-34	W-7034PH						70-34	5.8	0.0
NH_76-28_1	W-7628H-12.5						76-28	5.4	18.5
NH_58-28_1	W-5828L					50	58-28	5.8	16.2
NH_58-34	W-5834L						58-34	5.4	18.5
NH_76-28_2	W-7628H-9.5			9.5		75	76-28	6.1	14.8
NH_58-28_2	W-5828H						58-28	5.9	16.9
NH_64-28_1	W-6428H-9.5						64-28	6.4	0.0
NH_64-28_2	-							6.3	18.5
MN_58-34	-	Minnesota	Plant Mixed-Lab Compacted (PMPC)	9.5	3.0	90	58-34	5.1	15.8
MN_58-28_1	-				4.0		58-28	5.8	17.2
MN_58-28_2	-							5.4	16.7
MN_58-28_3	-				5.0	50		5.8	12.1
VA_76-22	-	Virginia	Plant Mixed-Plant Compacted (PMPC)	9.5	4.0	75	76-22	5.6	0.0
VA_70-22	-						70-22	5.2	20.0
VA_64-22	-						64-22	5.4	40.0

5.4.4 RESULTS AND DISCUSSION

5.4.4.1 STATISTICAL ANALYSIS OF MEANS

The RDCI parameter was calculated and compared to the FI. A graphical comparison between the RDCI and FI is depicted in Figure 5-24. The error bars on the graph indicate one standard deviation from the mean. Although similar trends may be observed from the graphs, there are differences between the rankings from the two indices such as NH_58-28_2, NH_76-28_1 and MN_58-28_2 that have different orders of ranking from the two indices. A Spearman's rank-order statistical analysis [62] was conducted to determine the significance of difference in the ranking of mixtures using FI and RDCI. The correlation coefficient was determined to be 0.98, which indicates that there is only negligible difference between the ranks yielded by these two parameters.

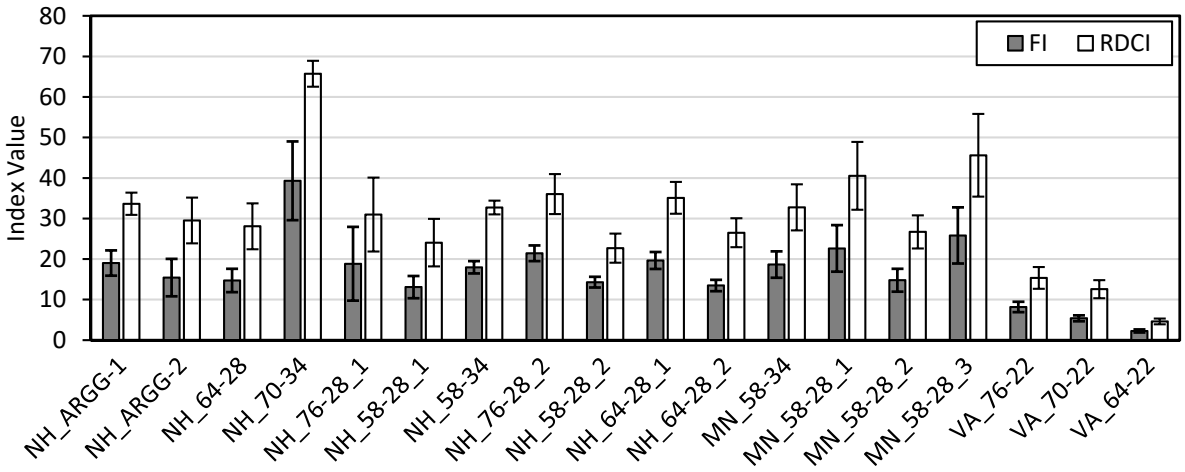

Figure 5-24 Comparison between RDCI and FI

In comparison of the two indices, the ability to discriminate mixture performance based on magnitude is also important. A student's t-test using 0.05 significance level was conducted to determine the statistical difference between the means for each mixture for each index. The results from this test are presented in Table 5-14. The mixtures that have the same letter in each column indicate that those mixtures are statistically similar in terms of mean and standard deviation, whereas the mixtures that are not connected by the same letter are significantly different. For example, considering the RDCI, MN_58-28_3 is not grouped with any of the other mixtures, while the analysis indicates that the FI for this mixture is similar to MN_58-28_1 and NH_76-28_2. It should be noted that the MN_58-28_3 mixture has same binder type and comparable aggregate gradation as the MN_58-28_1 mixture, however the volumetric properties and RBR between the two are substantially different, specifically the MN_58-28_3 mixture is designed using Superpave5 concept and has a significantly lower RBR. Also, with respect to RDCI the mixtures are categorized in slightly broader differentiated groups (A to K) as compared to that by FI (A to H). The t-test results and corresponding grouping demonstrate that the RDCI is either equal or better at discriminating different asphalt mixtures as compared to FI.

Table 5-14 Results from each pair of student's t-test at significance level of 0.05

FI										RDCI											
Mixture	Connecting Letters								Mean	Mixture	Connecting Letters										Mean
NH_70-34	A								39.3	NH_70-34	A										65.7
MN_58-28_3		B							25.8	MN_58-28_3		B									45.6
MN_58-28_1		B	C						22.6	MN_58-28_1			C								40.5
NH_76-28_2		B	C	D					21.4	NH_76-28_2			C	D							36.0
NH_64-28_1			C	D	E	F			19.6	NH_64-28_1			C	D	E						35.1
NH_ARGG-1			C	D	E	F			19.0	NH_ARGG-1			C	D	E	F					33.6
NH_76-28_1			C	D	E	F			18.8	MN_58-34				D	E						32.8
MN_58-34				D		F			18.6	NH_58-34				D	E	F	G				32.7
NH_58-34			C	D	E	F			18.0	NH_76-28_1				D	E	F	G	H			31.0
NH_58-28_2				D	E	F			15.7	NH_ARGG-2				D	E	F	G	H			29.5
NH_ARGG-2				D	E	F			15.4	NH_64-28				D	E	F	G	H			28.1
MN_58-28_2					E				14.8	MN_58-28_2						F	G	H			26.7
NH_64-28					E	F	G		14.7	NH_64-28_2					E	F	G	H			26.5
NH_64-28_2					E		G		13.5	NH_58-28_1							G	H	I		24.0
NH_58-28_1					E		G		13.1	NH_58-28_2								H	I	J	22.4
VA_76-22							G	H	8.2	VA_76-22									I	J	K	15.3
VA_70-22								H	5.4	VA_70-22										J	K	12.6
VA_64-22								H	2.2	VA_64-22											K	4.6

5.4.4.2 ANALYSIS OF REPLICATE VARIATIONS

The coefficient of variation (COV) of the test replicates demonstrates the extent of the variation between the replicates with respect to the mean and a lower COV is more desirable as it indicates higher repeatability of the test results as well as higher reliability in selecting the proper mixture to withstand cracking. Figure 5-25 indicates the COVs for FI and RDCI. It can be observed that except for a few cases, the COVs associated with RDCI are lower as compared to ones determined for FI. The results for Minnesota mixtures (MN_##-##_# mixtures) are of particular interest. As opposed to other mixtures that have been tested with three or four replicate specimens, these have been tested with 24 replicate specimens. Due to such high number of replication, the COVs of both indices for these mixtures are expected to be resulting from the material scale variability associated with the index itself and not

necessarily the variability in testing. For the four Minnesota mixtures, RDCI consistently showed a lower COV than FI.

Figure 5-26 indicates the relative percent difference in COV between FI and RDCI with respect to COV of FI. The range of relative differences is from 31% higher COV (VA_70-22) to 80.3% lower COV (NH_70-34) for RDCI as compared to FI. An overall average of 10.6% lowering of COV is observed as a combined average of all mixtures and tests.

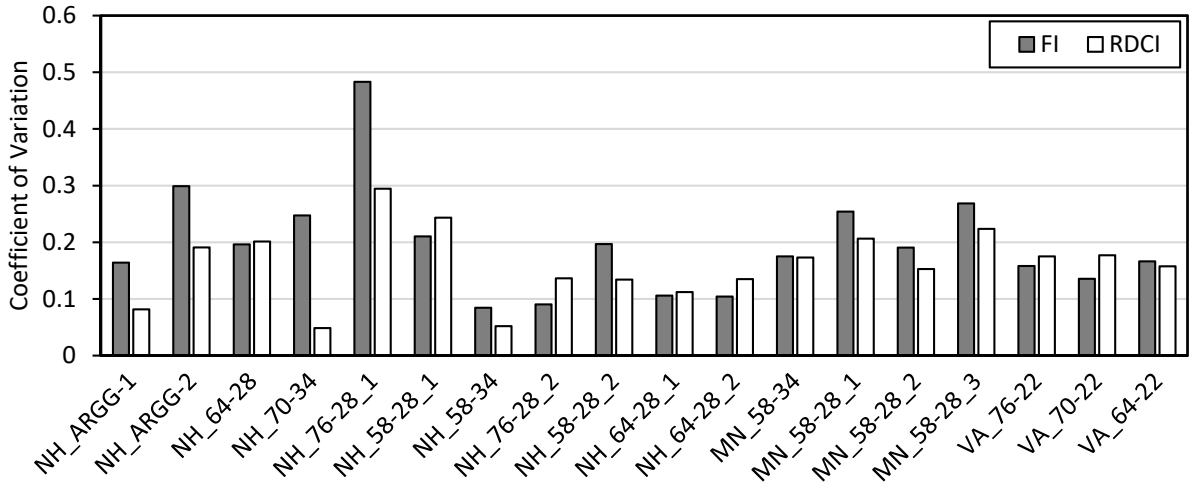

Figure 5-25 Comparison of coefficient of variations (COV) determined by cracking index parameters

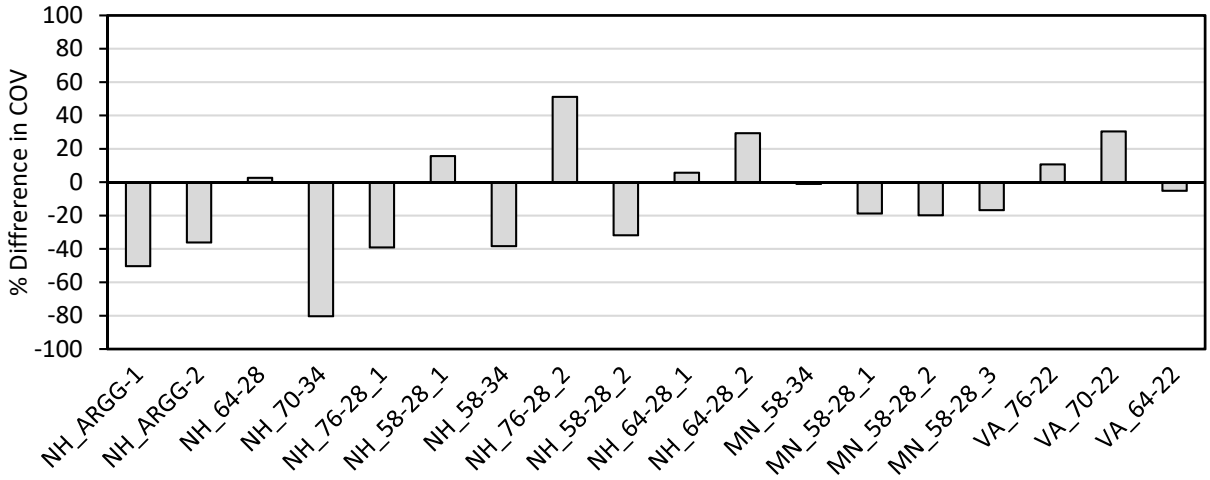

Figure 5-26 Percent difference in COV for RDCI and FI with respect to COV for FI

5.4.4.3 ANALYSIS OF EFFECT OF AGING

Mechanical properties of the asphalt mixtures can substantially change during production and in-service due to the volatilization and oxidation of asphalt binder. This typically results in a reduced relaxation

capability and increased brittleness and therefore greater susceptibility to cracking. Different laboratory aging methods have been proposed and investigated to simulate the short and long-term aging of the mixtures. However, proper analysis tools should also be available to distinguish the mixture performance at different levels of aging. A set of five plant-produced mixtures (previously indicted in Table 5-13) were selected to investigate the effect of aging at three different levels as following:

- STA: Short-term aged (aged during production and reheated for compaction)
- LTOA 5D: Long-term oven aged (loose mixture aged for 5 days at 95°C)
- LTOA 12D: Long-term oven aged (loose mixture aged for 12 days at 95°C)

The comparative FI and RDCI results from the analysis of the five mixtures at three aging levels is presented in Figure 5-27. In general, it can be seen that both indices follow a similar trend with respect to aging levels and the difference between the STA and 5 days at 95°C is relatively pronounced. However, there is not as perceptible a difference between the two LTOA levels. Therefore, each pair student's t-test at a 0.05 significance level (95% confidence interval) was used to determine if the two indices have been able to discriminate between different aging levels. The results from the statistical evaluation of cracking indices with respect to different aging levels is summarized in Table 5-15. Both indices have been able to easily determine the difference between STA and 5 days at 95°C aging levels for all five mixtures. For the LTOA conditions, the capability of the indices in discriminating the mixtures performance is different. Both indices have been able to differentiate the aging levels of NH_76-28_2, but considering the NH_70-34 mixture, only RDCI with a p-value of 0.0328 has been able to discriminate the two LTOA conditions. Although for the rest of mixtures in the table none of the indices have been able to statistically discriminate the LTOA levels at a reliability level of 95%, the p-values determined for RDCI are lower as compared to FI. Thus for the cases where neither index was able to confidently distinguish 5 and 12 days oven aging, RDCI has a greater probability of discrimination than FI. The results and discussions of test results for the five mixtures at different aging levels indicate that RDCI can distinguish effects of aging on cracking properties of asphalt mixtures as well or better than FI.

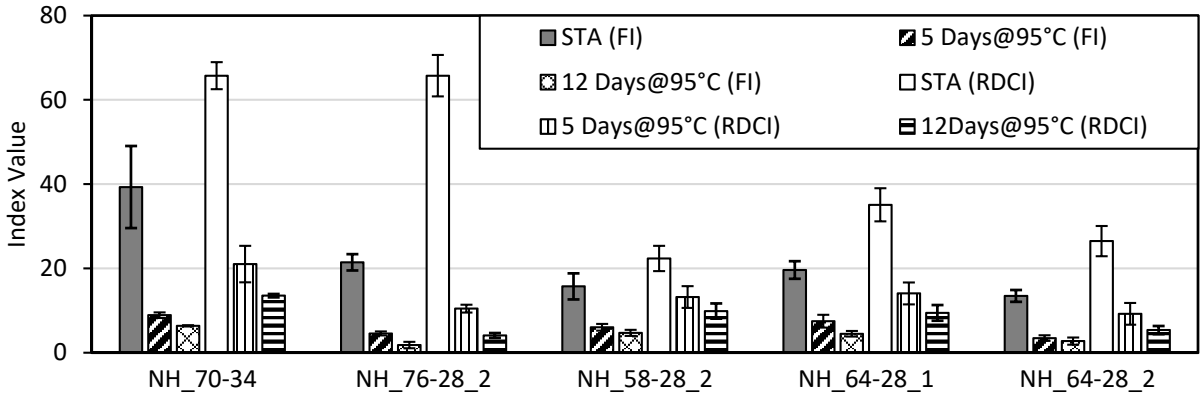

Figure 5-27 Evaluating the sensitivity of FI and RDCI to aging

Table 5-15 Statistical evaluation of cracking indices to distinguish the aging levels

Mixture	Compared Aging Levels		p-value (FI)	p-value (RDCI)
NH_70-34	NH_70-34_STA	NH_70-34_12D	0.0012	<0.0001
	NH_70-34_STA	NH_70-34_5D	0.0029	<0.0001
	NH_70-34_5D	NH_70-34_12D	0.6752	0.0328
NH_76-28_2	NH_76-28_2_STA	NH_76-28_2_12D	<0.0001	<0.0001
	NH_76-28_2_STA	NH_76-28_2_5D	<0.0001	<0.0001
	NH_76-28_2_5D	NH_76-28_2_12D	0.0409	0.0485
NH_58-28_2	NH_58-28_2_STA	NH_58-28_2_12D	<.0001	0.0001
	NH_58-28_2_STA	NH_58-28_2_5D	0.0002	0.0014
	NH_58-28_2_5D	NH_58-28_2_12D	0.406	0.1189
NH_64-28_1	NH_64-28_1_STA	NH_64-28_1_12D	<0.0001	<.0001
	NH_64-28_1_STA	NH_64-28_1_5D	<0.0001	<.0001
	NH_64-28_1_5D	NH_64-28_1_12D	0.1225	0.1092
NH_64-28_2	NH_64-28_2_STA	NH_64-28_2_12D	<0.0001	<0.0001
	NH_64-28_2_STA	NH_64-28_2_5D	<0.0001	<0.0001
	NH_64-28_2_5D	NH_64-28_2_12D	0.4545	0.1338

The COVs of the replicates at the two LTOA levels were evaluated and plotted in Figure 5-28. At the 5-day aging level, the COVs determined through the FI are indicated to be lower for most of the instances, whereas this trend is essentially reversed for the 12-day aging level with lower COVs determined through RDCI. In general, with the assumption of a 20% COV as an acceptable range of variation of results in one standard deviation from the mean (Ozer et al., 2017), there is only one case (NH_64-28_2 at 5D) that RDCI exceeds the threshold while there are three cases (NH_76-28_2 at 12D, NH_64-28_1 at 12D and NH_64-28_2 at 5D) where FI exceeds the threshold.

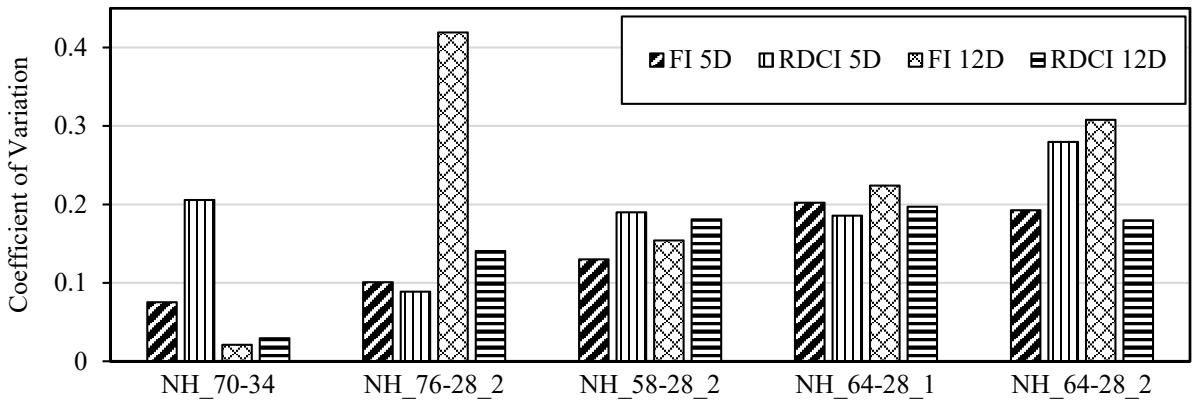

Figure 5-28 Comparison of coefficient of variations of the index parameters at different long-term oven aged levels

5.4.5 EVALUATION OF THE BINDER AND BASE COURSE MIXTURES FROM THIS STUDY USING RDCI PARAMETER

The results from analyzing the binder and base course mixtures with RDCI and FI are shown in Figure 5-29. While the mixture ranking is identical for the hot mixed asphalt mixtures, it is different for the CCPR mixtures. As the plots indicate, the RDCI has been able to determine the cracking performance of CM-1 while FI is inapplicable to this mixture as it did not indicate to have an inflection point in the post peak side of the Load-LLD curve. Also, with respect to FI, CM-1-a is a better mixture compared to CM-2, however, the inverse is seen using the RDCI analysis. With respect to COV analysis, both indices resulted in a very similar average value of 31%.

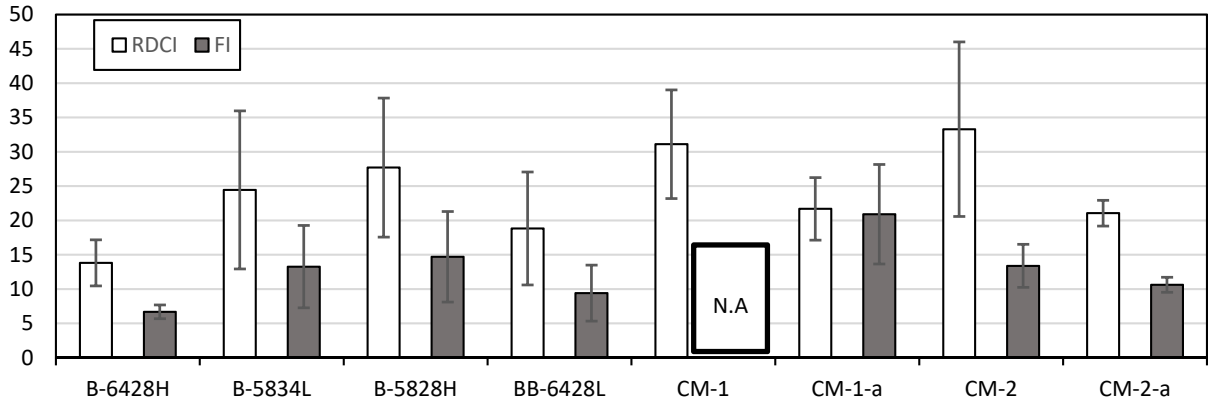

Figure 5-29 RDCI and FI comparison plots for NHDOT binder and base course mixtures from this study

5.4.6 SUMMARY AND CONCLUSIONS FOR TRANSVERSE CRACKING PERFORMANCE INDEX

A number of asphalt laboratory cracking performance tests have been proposed and investigated at different loading and temperature conditions. The semi-circular bending test is one of the simplest

geometries that has shown promising results with respect to field cracking. However, the Flexibility Index (FI) parameter associated with this test may not always be able to discriminate the performance between different mixtures, as it is highly dependent on the post-peak slope at the inflection point of the load-displacement curve. This can be a more significant problem for brittle or aged mixtures where the post-peak slope might be too steep resulting in significantly low or even undetermined FI values, which are sometimes followed by relatively high variations in FI values.

Based on the viscoelastic nature of asphalt mixtures, this study proposed a rate-dependent cracking index (RDCI) parameter to analyze the SCB-IFIT results. In order to develop this parameter, the time evolution of cumulative work curve (W_C) is used. Two critical time points on this curve are determined; the time associated with the peak force (t_{peak}) and the time associated with the 10% of the peak force on the post-peak portion ($t_{0.1peak}$). The instantaneous power at t_{peak} is used to normalize the area under W_f curve between t_{peak} and $t_{0.1peak}$. Through use of cumulative fracture work at different times and through use of instantaneous power, the RDCI parameter provides an estimate of the impulse associated with crack propagation in the specimen. Because rate is inherently included in the calculations, the RDCI parameter allows for better characterization for rate dependent fracture processes.

With respect to method of development of RDCI the following general observations can be made:

- The development of RDCI is supported by the combination of physics and fracture mechanics and is free from any type of empirical or undefinable variable within the parameter.
- The use of continuous cumulative work at various times can help with describing and evaluating the crack formation and propagation mechanisms at any given time during the test and due to inherent presence of time in all work and power terms of RDCI; it is expected to better capture the rate dependency of fracture in asphalt mixtures.

The statistical analysis of RDCI and FI for evaluated mixtures in this section of the report was used to assess the capability of each index in differentiating the cracking performance of mixtures. Further investigations were conducted on five select mixtures by evaluating the index parameters at three different aging levels. The findings of the analysis presented in this study are summarized as follows:

- The development of RDCI is supported by the combination of physics and fracture mechanics and is free from any type of empirical or undefinable variable within the parameter.
- The student's t-test analysis indicates RDCI has better discrimination between the mixtures at short and long-term oven aged conditions.
- RDCI resulted in an overall average reduction of 10.6% in the COV for the studied mixtures in this report.
- Results from statistical comparisons of the aging levels for 5 mixtures indicated that the RDCI is able to differentiate the effect of different aging levels at a reliability level of 86% whereas the FI is able to do so at a reliability level of only 32%.

5.5 SUMMARY OF PERFORMANCE INDICES FOR ASPHALT MIXTURES

In order to develop the mechanistically informed asphalt mixture layer coefficients, it is important to use reliable performance index parameters that can be highly correlated to the actual field performance of the mixtures. For this reason, three new performance index parameters for rutting (CMRI), Fatigue ($C_{N_f}^S$) and transverse cracking (RDCI) were developed in this project. All of these parameters are tailored for New Hampshire DOT mixtures and highways. These parameters were indicated to be able to rank the field performance/aging effect of mixtures and can be reliably used in development of mechanistically informed layer coefficients in this research. The following paragraphs summarize the method of development of each parameter:

- Complex modulus based rutting index parameter (CMRI):
  - Using the complex modulus master-curves, two important points on the master-curves were determined: Point A (corresponding to peak phase angle) and Point B (corresponding to the equivalent frequency of 0.866 at 45°C which is determined based on Hamburg Wheel Tracking Test (HWTT) testing condition). Based on the analysis of three set of asphalt mixtures, the CMRI parameter was developed as following:

    $$CMRI = \frac{|E_A^*| - |E_B^*|}{|f_A - f_B|^2}$$

    $CMRI$: Complex modulus based rutting index parameter

    $|E_A^*|$: | E*|corresponding to peak phase angle

    $|E_B^*|$: |E*| corresponding to the HWTT testing condition (45°C at 0.866Hz)

    f_A: Logarithm of frequency corresponding to Peak Phase Angle

    f_B: Logarithm of frequency corresponding to testing condition (45°C at 0.866Hz)

- Damage growth rate based fatigue failure criterion ($C_{N_f}^S$):
  - Using the simplified viscoelastic continuum damage theory (S-VECD), the damage characteristic curve (C vs S), the number of loading cycles to failure (N_f) and the accumulated damage at failure (S_f) for each tested replicate were investigated. On basis of these analyses, the rate of accumulated decrease in material's capacity ($\int_0^{N_f}(1-C)\,dN$) with respect to amount of damage at failure was shown to be highly correlated with the field fatigue performance. The fatigue failure criterion was developed as following:

    $$C_{N_f}^S = \frac{\int_0^{N_f}(1-C)\,dN}{S_f} \times m$$

    $C_{N_f}^S$: Damage growth rate based fatigue failure criterion,

    $\int_0^{N_f}(1-C)\,dN$: Accumulated decrease in pseudo stiffness,

    S_f: Accumulated damage at failure

    m: Unit correction factor set to 10^3 to increase the order of magnitude of the $C_{N_f}^S$ and for simplicity of comparisons between different mixtures

- Rate dependent cracking index parameter (RDCI):
  - Using the semi-circular bend test method at intermediate temperature (I-FIT), the accumulated fracture work versus time were plotted. Two important points on the curve were selected; the time corresponding to the peak load on the load-load line displacement (load-LLD) curve (t_{peak}) and time at 10 percent of the peak load on the post peak side of the load-LLD curve ($t_{0.1peak}$). In order to develop the parameter, the area under this portion of the curve ($\int_{t_{peak}}^{t_{0.1peak}} W_c \ .dt$) was normalized by the slope of the curve at t_{peak} which is called as P_{tpeak}. The RDCI parameter was developed as following:

    $$RDCI = \frac{\int_{t_{peak}}^{t_{0.1peak}} W_c \ .dt}{P_{tpeak} \times ligament\ area} \times C$$

    RDCI = rate dependent cracking index ($\frac{s^2}{m^2} \times 10^4$)

    $\int_{t_{peak}}^{t_{0.1peak}} W_c \ .dt$= area under the cumulative work vs time

    P_t= instantaneous power at peak force

    C= Unit correction factor set to 0.01 to lower the order of magnitude of the RDCI and for simplicity of plotting

    Ligament area = specimen thickness times the ligament length

5.6 REFERENCES

[1]. Brown, E. Ray, Prithvi S. Kandhal, and Jingna Zhang. (2001). "Performance testing for hot mix asphalt." NCAT report 1.05.

[2]. Mohammad, L., M. Elseifi, A. Raghavendra, & M. Ye. (2015). Hamburg Wheel-Tracking Test Equipment Requirements and Improvements to AASHTO T324, NCHRP Project 20-07/Task 361. Transportation Research Board, National Research Council, Washington, DC.

[3]. Yetkin, Y., and K. Stokoe. (2006). "Analysis of Hamburg wheel tracking device results in relation to field performance." CTR Technical Report 0-4185-5, Center for Transportation Research at the University of Texas at Austin.

[4]. Sivasubramaniam, S., and J. E. Haddock. (2006). "Validation of Superpave mixture design and analysis procedures using the NCAT test track." Publication FHWA/IN/JTRP-2005/24. Joint Transportation Research Program, Indiana Department of Transportation and Purdue University, West Lafayette, Indiana, https://doi.org/10.5703/1288284313375.

[5]. Bazzaz, Mohammad, et al. (2018). "A straightforward procedure to characterize nonlinear viscoelastic response of asphalt concrete at high temperatures." Transportation Research Record, https://doi.org/10.1177/0361198118782033.

[6]. Bazzaz, M. (2018). “Experimental and Analytical Procedures to Characterize Mechanical Properties of Asphalt Concrete Materials for Airfield Pavement Applications”, (Ph.D. thesis, University of Kansas).

[7]. Mohammad, L. N., Z. Wu., S. Obulareddy. (2006). "Permanent Deformation Analysis of Hot-Mix Asphalt Mixtures with Simple Performance Tests and 2002 Mechanistic–Empirical Pavement Design Software." Trans Res Rec1970.1: 133-142, https://doi.org/10.1177/0361198106197000114.

[8]. Nur Hossain E.I, and D. Singh. M. Zaman. (2013). "Dynamic modulus-based field rut prediction model from an instrumented pavement section." Procedia-Social and Behavioral Sciences104 129-138, https://doi.org/10.1016/j.sbspro.2013.11.105.

[9]. Witczak, M. W., H. L. Von Quintus, and C. W. Schwartz.(1997). "Superpave support and performance models management: Evaluation of the SHRP performance models system." Proc., 8th International Society of Asphalt Pavements.

[10]. Apeagyei, A. K., (2011). "Rutting as a function of dynamic modulus and gradation" J Mater Civil Eng 23.9: 1302-1310, https://doi.org/10.1061/(ASCE)MT.1943-5533.0000309.

[11]. Witczak, M. W. Kaloush, K., Pellinen, T., El-Basyouny, M., Von Quintus, H. (2002). “Simple performance test for Superpave mix design”. NCHRP Report No: 465. Transportation Research Board.

[12]. Nemati, R., Eshan V. Dave and J. S. Daniel. (2018). “Comparative Evaluation of New Hampshire Mixture Based on Lab Performance Tests” Proc., 19th International Society of Asphalt Pavements.

[13]. Bhasin, A, Button, J. W., and Arif Chowdhury. (2003). Evaluation of simple performance tests on HMA mixtures from the south central United States. USA: Texas Transportation Institute, Texas A & M University System. Report No: FHWA/TX-03/9-558-1.

[14]. Birgisson, B., Roque, R., Kim, J., Pham, L. V., (2004). "The use of complex modulus to characterize the performance of asphalt mixtures and pavements in Florida." Final report, University of Florida.

[15]. Kandhal, P. S., Cooley Jr, L.A. (2003). "Accelerated Laboratory Rutting Tests: Evaluation Of The Asphalt Pavement Analyzer", NCHRP Report No: 508, Transportation Research Board.

[16]. Decarlo, J. C. (2018). "Comparative evaluation of laboratory moisture susceptibility tests for asphalt mixtures in New England", (master's thesis, University of New Hampshire).

[17]. Nemati, R., and E. V. Dave. (2018). "Nominal property based predictive models for asphalt mixture complex modulus (dynamic modulus and phase angle)." Construction and Building Materials 158:308-319, https://doi.org/10.1016/j.conbuildmat.2017.09.144.

[18]. Zhao, Y., and Y. Kim. (2003). "Time-temperature superposition for asphalt mixtures with growing damage and permanent deformation in compression." Transportation Research Record, 1832:161-17, https://doi.org/10.3141/1832-20.

[19]. Daniel, J. S. M. Corrigan., C. Jaques., R. Nemati., E. V. Dave. (2018). "Comparison of asphalt mixture specimen fabrication methods and binder tests for cracking evaluation of field mixtures." Road Mater Pavement Des: 1-17, https://doi.org/10.1080/14680629.2018.1431148.

[20]. Babadopulos, Lucas Feitosa de Albuquerque Lima, Jorge Barbosa Soares, and Verônica Teixeira Franco Castelo Branco. (2015). "Interpreting fatigue tests in hot mix asphalt (HMA) using concepts from viscoelasticity and damage mechanics." Transportes 23.2: 85-94.

[21]. Daniel, J. S. and Y. R. Kim. (2002). "Development of a Simplified Fatigue Test and Analysis Procedure Using a Viscoelastic Continuum Damage Model." Journal of the Association of Asphalt Paving Technologists, Vol. 71, pp. 619-650.

[22]. Underwood, B. S., Kim, Y. R., & Guddati, M. N. (2010). Improved calculation method of damage parameter in viscoelastic continuum damage model. International Journal of Pavement Engineering, 11(6), 459-476.

[23]. Wang, Y. D., Keshavarzi, B., & Kim, Y. R. (2018). Fatigue Performance Prediction of Asphalt Pavements with FlexPAVETM, the S-VECD Model, and D^R Failure Criterion. Transportation Research Record, 0361198118756873.

[24]. Wang, Y. D., Keshavarzi, B., & Kim, Y. R. (2018). Fatigue Performance Analysis of Pavements with RAP Using Viscoelastic Continuum Damage Theory. KSCE Journal of Civil Engineering, 22(6), 2118-2125.

[25]. Park, S. W., Kim, Y. R., & Schapery, R. A. (1996). A viscoelastic continuum damage model and its application to uniaxial behavior of asphalt concrete. Mechanics of Materials, 24(4), 241-255.

[26]. Nemati, R. Dave, E. V., Daniel, J. S. (2019) Evaluation of Laboratory Performance and Structural Contribution of Cold Recycled Versus Hot Mixed Intermediate and Base Course Asphalt Layers in New Hampshire. Under publication. Transportation Research Board, Journal of Transportation Research Record.

[27]. Wang, C., Castorena, C., Zhang, J., & Richard Kim, Y. (2015). Unified failure criterion for asphalt binder under cyclic fatigue loading. Road Materials and Pavement Design, 16(sup2), 125-148.

[28]. Wang, Yizhuang, and Y. Richard Kim (2017). "Development of a pseudo strain energy-based fatigue failure criterion for asphalt mixtures." International Journal of Pavement Engineering : 1-11.

[29]. Dave, E.V., C. Hoplin, B. Helmer, J. Dailey, D. Van Deusen, J. Geib, S. Dai, and L. Johanneck (2016). Effects of Mix Design and Fracture Energy On Transverse Cracking Performance of Asphalt Pavements in Minnesota. Transportation Research Record, 2576, pp. 40-50.

[30]. Majidzadeh, K., Kauffmann, E., & Ramsamooj, D. (1971). Application of fracture mechanics in the analysis of pavement fatigue. Paper presented at the Association of Asphalt Paving Technologists Proc, 40.

[31]. Paris, P. C., & Sih, G. C. (1965). Stress analysis of cracks. Fracture toughness testing and its applications, ASTM International.

[32]. Wagoner, Buttlar, & Paulino. (2005). Development of a single-edge notched beam test for asphalt concrete mixtures. Journal of Testing and Evaluation, 33(6), 452-460.

[33]. Molenaar, A., Scarpas, A., Liu, X., & Erkens, S. (2002). Semi-circular bending test; simple but useful? Journal of the Association of Asphalt Paving Technologists, 71.

[34]. Molenaar, J., & Molenaar, A. (2000). Fracture toughness of asphalt in the semi-circular bend test. Paper presented at the Proceedings of the Papers Submitted for Review at 2nd Eurasphalt and Eurobitume Congress, Held 20-22 September 2000, Barcelona, Spain. Book 1-Session 1.

[35]. Wagoner, Buttlar, Paulino, & Blankenship. (2005). Investigation of the fracture resistance of hot-mix asphalt concrete using a disk-shaped compact tension test. Transportation Research Record: Journal of the Transportation Research Board, (1929), 183-192.

[36]. Elseifi, M. A., Mohammad, L. N., Ying, H., & Cooper III, S. (2012). Modeling and evaluation of the cracking resistance of asphalt mixtures using the semi-circular bending test at intermediate temperatures. Road Materials and Pavement Design, 13(sup1), 124-139.

[37]. Li, X., & Marasteanu, M. (2010). The fracture process zone in asphalt mixture at low temperature. Engineering Fracture Mechanics, 77(7), 1175-1190.

[38]. Mohammad, L. N., Kim, M., & Elseifi, M. (2012). Characterization of asphalt mixture's fracture resistance using the semi-circular bending (SCB) test. Paper presented at the 7th RILEM International Conference on Cracking in Pavements, 1-10.

[39]. Chong, K., & Kuruppu, M. (1984). New specimen for fracture toughness determination for rock and other materials. International Journal of Fracture, 26(2), R59-R62.

[40]. Al-Qadi, I. L., Ozer, H., Lambros, J., El Khatib, A., Singhvi, P., Khan, T., Doll, B. (2015). Testing Protocols to Ensure Performance of High Asphalt Binder Replacement Mixes using RAP and RAS.

[41]. Haslett, K. E., Dave, E. V., & Daniel, J. S. (2017). Exploration of temperature and loading rate interdependency for fracture properties of asphalt mixtures.

[42]. Im, S., Ban, H., & Kim, Y. (2014). Characterization of mode-I and mode-II fracture properties of fine aggregate matrix using a semicircular specimen geometry. Construction and Building Materials, 52, 413-421.

[43]. Saha, G., & Biligiri, K. P. (2016). Fracture properties of asphalt mixtures using semi-circular bending test: A state-of-the-art review and future research. Construction and Building Materials, 105, 103-112.

[44]. Bažant, Z. P., & Kazemi, M. (1990). Determination of fracture energy, process zone longth and brittleness number from size effect, with application to rock and conerete. International Journal of Fracture, 44(2), 111-131.

[45]. Li, X., Marasteanu, M. O., Iverson, N., & Labuz, J. F. (2006). Observation of crack propagation in asphalt mixtures with acoustic emission. Transportation Research Record, 1970(1), 171-177.

[46]. Anderson. (2005). Fracture mechanics fundamentals and application. New York: Taylor and Francis.

[47]. AASHTO TP105.105-13. (2013). Determining the Fracture Energy of Asphalt Mixtures using the Semicircular Bend Geometry (SCB).

[48]. Li, X., & Marasteanu, M. O. (2005). Cohesive modeling of fracture in asphalt mixtures at low temperatures. International Journal of Fracture, 136(1-4), 285-308.

[49]. Ozer, H., Al-Qadi, I. L., Lambros, J., El-Khatib, A., Singhvi, P., & Doll, B. (2016). Development of the fracture-based flexibility index for asphalt concrete cracking potential using modified semi-circle bending test parameters. Construction and Building Materials, 115, 390-401.

[50]. AASHTO TP124.124, 2016. AASHTO TP 124: Standard Method of Test for Determining the Fracture Potential of Asphalt Mixtures using Semicircular Bend Geometry (SCB) at Intermediate Temperature.

[51]. Kaseer, F., Yin, F., Arámbula-Mercado, E., Martin, A. E., Daniel, J. S., & Salari, S. (2018). Development of an index to evaluate the cracking potential of asphalt mixtures using the semi-circular bending test. Construction and Building Materials, 167, 286-298.

[52]. Zhou, F., Im, S., Hu, S., Newcomb, D., & Scullion, T. (2017). Selection and preliminary evaluation of laboratory cracking tests for routine asphalt mix designs. Road Materials and Pavement Design, 18(sup1), 62-86.

[53]. Zhu, Y., Dave, E. V., Rahbar-Rastegar, R., Daniel, J. S., & Zofka, A. (2017). Comprehensive evaluation of low-temperature fracture indices for asphalt mixtures. Road Materials and Pavement Design, 18(sup4), 467-490.

[54]. Yang, S., & Braham, A. (2018). R-curves characterization analysis for asphalt concrete. International Journal of Pavement Engineering, 19(2), 99-108.

[55]. Im, S., Kim, Y., & Ban, H. (2013). Rate-and temperature-dependent fracture characteristics of asphaltic paving mixtures. Journal of Testing and Evaluation, 41(2), 257-268.

[56]. Bažant, Z. P., & Li, Y. (1997). Cohesive crack with rate-dependent opening and viscoelasticity: I. mathematical model and scaling. International Journal of Fracture, 86(3), 247-265.

[57]. D'Amico, F., Carbone, G., Foglia, M., & Galietti, U. (2013). Moving cracks in viscoelastic materials: Temperature and energy-release-rate measurements. Engineering Fracture Mechanics, 98, 315-325.

[58]. Bradley, W., Cantwell, W., & Kausch, H. H. (1997). Viscoelastic creep crack growth: A review of fracture mechanical analyses. Mechanics of Time-Dependent Materials, 1(3), 241-268.

[59]. Chung, W. N., & Williams, J. G. (1991). Determination of J IC for polymers using the single specimen method. Elastic-plastic fracture test methods: The user's experience (second volume), ASTM International.

[60]. Song, S. H., Paulino, G. H., & Buttlar, W. G. (2006). A bilinear cohesive zone model tailored for fracture of asphalt concrete considering viscoelastic bulk material. Engineering Fracture Mechanics, 73(18), 2829-2848.

[61]. Dave, E. V., & Behnia, B. (2018). Cohesive zone fracture modelling of asphalt pavements with applications to design of high-performance asphalt overlays. International Journal of Pavement Engineering, 19(3), 319-337.

[62]. Spearman C (1904). "The proof and measurement of association between two things". American Journal of Psychology. 15 (1): 72–101. Doi:10.2307/1412159. JSTOR 1412159.

CHAPTER 6: DEVELOPMENT OF LAYER COEFFICIENTS

6.1 INTRODUCTION

As discussed in Chapter 2, different approaches have been investigated by researchers and practitioners to update the layer coefficients for the asphalt concrete pavement layers within the AASHTO 1993 empirical pavement design system. In this chapter, the main aim would be to establish a generalized methodology to develop mechanistic performance incorporated layer coefficients for asphalt mixtures and for this reason, the performance index parameters for rutting (section 5.2), fatigue cracking (section 5.3) and transverse cracking (section 5.4) that were previously developed in this research will be used as the primary material inputs in development of layer coefficients. It should be mentioned that in the original AASHO road test and layer coefficients associated with that, the pavement rutting was only considered to be due to plastic deformation of the subgrade soil, however, it is well-known that part of the overall rutting could result from the asphalt mixtures and for this reason, the mixtures' rutting performance will be incorporated in development of layer coefficients in this research.

The layer coefficient, as an indicator of structural contribution of each layer, may not be a constant value for a pavement structure during its design life as material properties and climatic conditions are ever changing, resulting in different overall pavement response, possibly even in relatively small time interval of a day. As a result, determining a continuously evolving layer coefficient, might be a significantly challenging task. Moreover, the establishment of a direct correlation between the performance index parameters such as the ones reviewed and developed in this research and layer coefficients, may not be appropriate since the resulting layer coefficients will be solely dependent on the material properties which ignores other effective variables in determining a realistic layer coefficient. As a result, it is necessary to incorporate the field distress conditions in the development of layer coefficients to account for other types of variables such as traffic level and climatic circumstances. Therefore, among different types of distress index parameters such as PSI and PCI, in this research project, the International Roughness Index (IRI) as a standardized distress index parameter was selected to be used as the primary tool in evaluating the field distress data. Although the pavement functionality measures such as IRI include different types of non-structural degradation such as raveling and potholes, a significant portion of them is related to structural distresses such as rutting and cracking. In addition, among the available functional distress index parameters, the IRI is more popular since it is measured by a standard vehicle's accumulated suspension motion and therefore it is less affected by external variables such as visual observations that can reduce the reliability of a functional distress index parameter. Moreover, there are different regression-based equations that relate IRI to PSI which is one of the variables in the AASHTO 1993 equation. Besides, many state highway agencies such as NHDOT gather yearly IRI data for different highways as part of their pavement management system.

Using the NHDOT'S Pavement Management System data base, the field distress data for a set of 17 cross sections which have been constructed by similar mixtures to the ones in this research were obtained from NHDOT and utilized to develop the layer coefficients. Through integration of performance index parameters with the field distress based back-calculated layer coefficients, a set of new mix specific layer

coefficients called as performance incorporated a-values were developed and proposed to be used at different levels of reliability.

6.2 RESILIENT MODULUS BASED LAYER COEFFICIENTS

As mentioned in Chapter 2, the resilient modulus has been conventionally used to back-calculate the layer coefficients of asphalt mixtures through Equation 6.1. For this reason, it was decided to first explore use of this equation to determine layer coefficients for the study mixtures prior to incorporating the distress data and other laboratory test results in development of layer coefficients. The results are plotted in Figure 2. As expected from the resilient modulus based a-value equation, the stiffer mixtures with higher resilient modulus have higher layer coefficient values whereas most of the wearing course mixtures such as W-7034PH, W7628H-9.5 and W-5834L as well as the cold mixtures are indicated to have relatively lower a-values. The results reveal the fact that resilient modulus alone may not be an appropriate tool to determine the layer coefficients of asphalt mixtures as some polymer modified mixtures such as W-7034PH with a comparable fatigue performance and relatively better transverse cracking performance compared to many other wearing courses in this study has the lowest resilient modulus based a-value.

$a_i = 0.4 \log(M_r) - 0.951$ Equation (6.1)

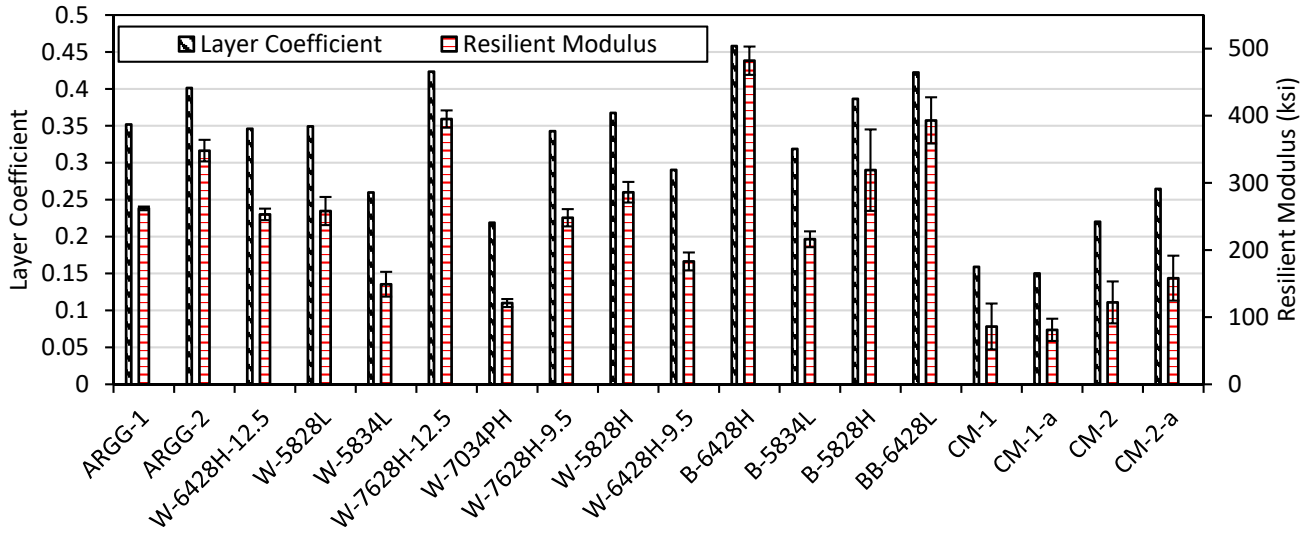

Figure 6-1 Resilient modulus based layer coefficients

6.3 FIELD DISTRESS DATA ANALYSIS

As one of the important steps in evaluating the structural contribution of the mixtures in form of layer coefficients, it is necessary to assess the field distress data of the study mixtures after construction. However, at this point of time in this research, there is not enough field data available for the study mixtures as they have been placed during 2016, 2017 and 2018 construction seasons. For this reason, a set of yearly measured distress data including IRI, rutting, fatigue and transverse cracking for similar

mixtures to those tested and analyzed in this project were provided by the New Hampshire Department of Transportation from their pavement management system. Similar mixtures in this work are defined as those that have same NHDOT mixture designation, that is, same application (wear, binder or base course), NMAS, gyration level, recycled binder amount and binder PG grade.

A total of 17 cross sections were investigated and the average yearly IRI values were plotted versus the pavement service time. The distress measurements are available only for a maximum of 5 years after construction for different mixtures and cross sections. However, the investigations indicated that at least for the first 5 years after construction, the yearly increase of the IRI has been following a linear trend for almost all of the mixtures and cross sections. While it is acknowledged that there is likelihood that the life-time IRI performance trends will not be linear in shape and will most likely follow a sigmoidal shaped response, due to limitations of the amount of data availability in NHDOT's PMS with respect to the time, this process used linear shape. Furthermore, use of linear shape is expected to have an overall higher deterioration rate and thus can provide some added reliability in the analysis. With use of linear fitting of IRI with time, the field IRI values after 20 years in service were determined for each cross section separately. It is well known that the initial IRI values immediately after construction can vary significantly among different cross sections with similar traffic and climatic situations due to differences in the construction quality as well as the conditions of the underlying layers. Also the increasing trend of the IRI right after construction up to the first year may not necessarily follow the trend after the first year and beyond. Nonetheless, determination of initial IRI immediately after construction is important as it translates into the Initial Serviceability (P_i) value for use in the AASHTO 1993 design process. The initial serviceability is deducted from the Terminal Serviceability (P_t) to obtain the ΔPSI value as the allowable serviceability loss at the end of design life. ΔPSI is a key input in the AASHTO 1993 design equation which can significantly affect the layer coefficient back calculation using the field data.

Research performed by Al-Omari [1] investigated the correlation between IRI and PSI using distress data of over 370 cross sections including flexible, rigid and composite pavements from 6 different states such as Indiana, Louisiana, Michigan, New Mexico, New Jersey and Ohio. The results indicated that IRI and PSI are highly correlated (R^2 =0.81) and their relationship can be described using a nonlinear model. Equations (6.2) and (6.3) indicate the relationship between IRI and PSI for flexible pavements.

$$PSI = 5e^{(-0.0038*IRI)}$$ Equation (6.2)

Where IRI is in inches per mile

$$PSI = 5e^{(-0.24*IRI)}$$ Equation (6.3)

Where IRI is in meters per kilometer

Considering the nature of the power function type of equation, the initial serviceability can significantly vary based on the initial IRI value. However, an initial value of 52 inches per mile is considered to be acceptable [2]. Based on this value, it was decided to divide the quality of the construction and initial IRI values into three categories. These categories are defined based on the construction quality and field measurement of IRI values after construction (which in most instances is at about one year in service after

construction). Table 6-1 indicates these categories and their criteria. As it can be seen from the table when the first year IRI is above 55 inch/mile the extrapolated IRI from the linear fit will be used to determine the initial IRI and consequently Equation 6. 2 or 6.3 (depending on the units used for IRI) will be used to determine the P_i. However, when IRI is below 45, a fixed P_i value of 5, and when IRI is between 45 and 55 inch/mile, a fixed P_i value of 4.5 will be used for the analysis.

Table 6-1 Defining the initial serviceability value based on construction quality and IRI values one year after construction.

Construction quality	Range of field IRI, one year after construction (inch/mile)	Assumption of Initial Serviceability (P_i)	Remarks
High	IRI < 45	5	-
Medium	45 ≤ IRI ≤ 55	4.5	-
Low	IRI > 55	Varied	Use the extrapolated linear fit from the measured IRI values to determine the initial IRI and back-calculate PSI using Equation 12

Figure 6-2 indicates the increase of IRI with time after rehabilitation for different mixtures that are placed on different projects in New Hampshire. The first point for each mixture and project is related to the IRI after one year of construction. As it can be seen from the figure, the mixtures with smaller aggregate size (indicated in Figure 6-2 (c)) generally have a higher IRI in the first year whereas the ARGG mixtures (Figure 6-2(a)) which are relatively stiffer compared to rest of the mixtures have lower IRI values. It should be noted that in general the IRI measurements are better correlated with rutting rather than cracking since even minor rutting results in deflections along the roadway while minor or medium cracking may not indicate high deflections. Therefore, it might be necessary to directly incorporate the cracking performance in the back-calculated layer coefficients from the field data.

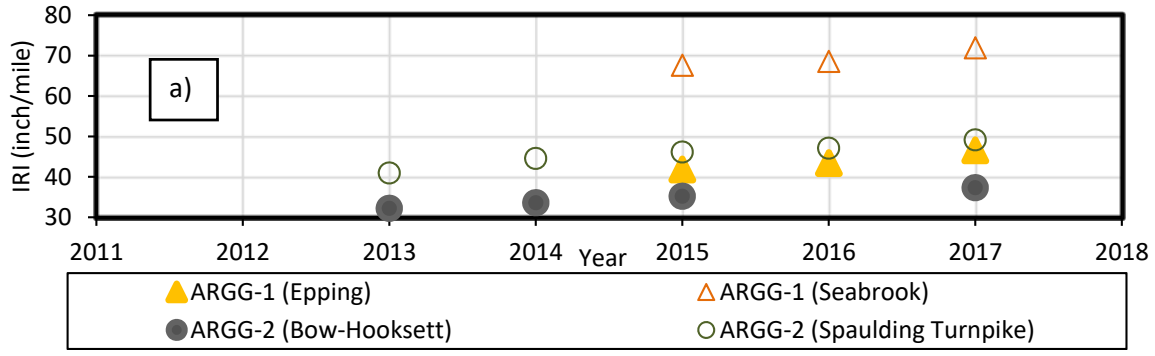

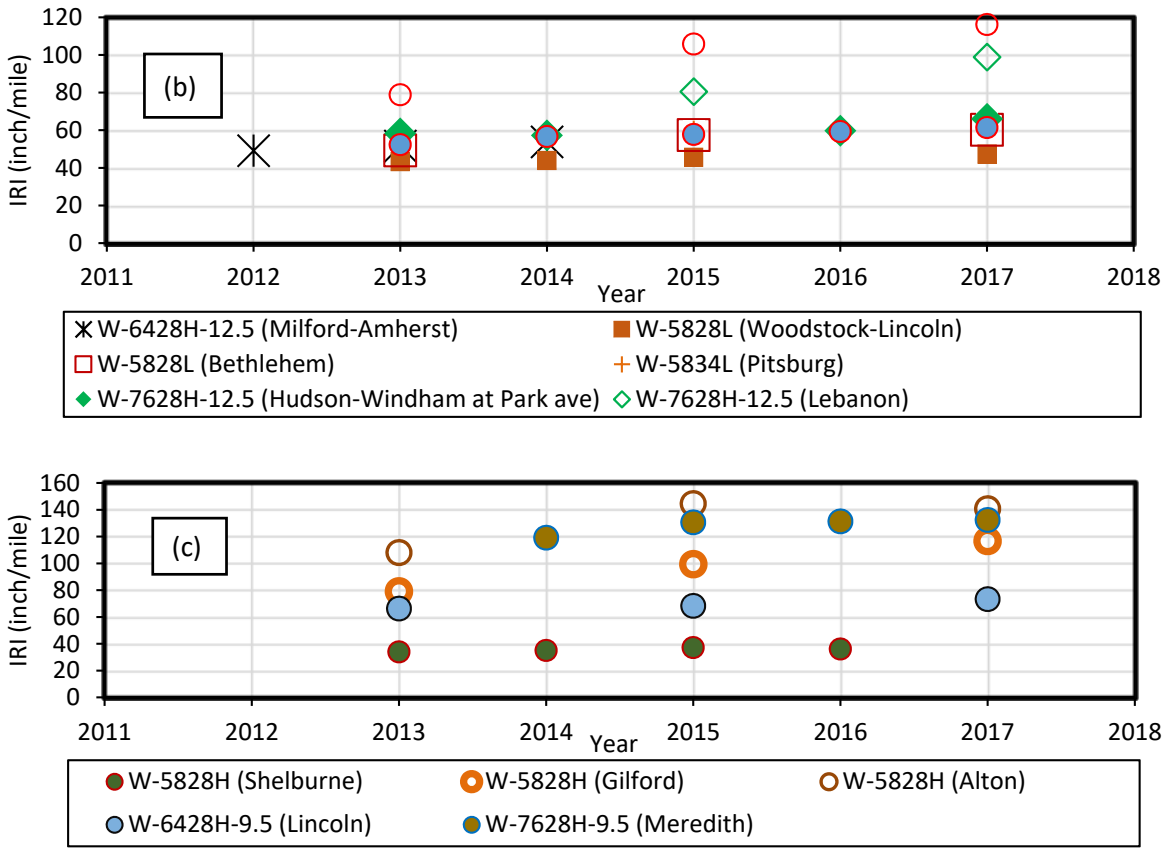

Figure 6-2 IRI versus time for different mixtures and projects: a) ARGG mixtures, b) 12.5mm NMAS mixtures, c) 9.5 mm NMAS mixtures

6.4 BACK-CALCULATION OF LAYER COEFFICIENTS FROM FIELD IRI MEASUREMENTS

In order to back-calculate the layer coefficients from the field IRI measurements, it is essential to have the cross section and traffic information of the road sections where mixtures similar to ones in this research are placed. The pavement management data provided by NHDOT included the original pavement cross sectional information as well as the thickness of the overlays conducted using mixtures with similar characteristic to the study mixtures. The traffic information was gathered using the NHDOT's online transportation data management system [3]. This GIS (Geographical Information System) based online tool provides a comprehensive traffic information including the annual average daily traffic as well as truck percentage for different roadways within the state. After analyzing the traffic data, the total design traffic in terms of equivalent single axle load (ESALs) was calculated for each cross section for 20 years after reconstruction or major rehabilitation. Since not all the structural design information of several of the pavements were available, some general assumptions were made and applied to all the cross sections regardless of the type of road, to facilitate the back-calculation of layer coefficients through the AASHTO 1993 design equation. These assumptions are summarized in Table 6-2. It should be pointed out that IRI provides the amount and severity of distresses of the surface layers only and there is no direct information about the type and magnitude of distress originating from the underlying layers, if any. However, with

respect to general functionality of binder and base course asphalt mixtures and considering that these type of mixtures are usually used to improve the load bearing capacity of the pavement structure through improving the rutting susceptibility due to their relatively higher stiffness, it can be reasonably concluded that a stiffness based layer coefficient such as the ones determined through resilient modulus in Figure 6-1 can be used to indicate the structural contribution of such mixtures in the pavement. Therefore, in back-calculating the layer coefficients of wearing course mixtures from the field data, the layer coefficients of hot mixed binder and base course mixtures will be based on resilient modulus only. For the cross sections that include cold recycled mixtures, the conventional layer coefficient of 0.22 (Table 1-1) will be used. The performance-based a-values for these types of mixtures are explored using the approach developed in this research and are discussed in section 6.8. Through the process of back-calculations, the layer coefficients of the granular material are based on the values that are conventionally used by the NHDOT pavement design approach [4]. Also, the subgrade soil resilient modulus is a typical average modulus value in New Hampshire which is determined based on the research conducted by Janoo in 1994 [4]. The level of reliability is selected such that it includes almost all the roadway categories with respect to their functionality.

Table 6-2 General design assumptions to back-calculate a-values from field data

Design Reliability	Standard deviation	z-statistic	Actual ΔPSI	Resilient Modulus of the subgrade soil (psi)	Traffic (ESALs)	Layer coefficients for granular material	Layer coefficient for binder and base course asphalt mixtures
95%	0.45	-1.645	Varied among the sections based on back-calculations from Equation (2.1)	8000	Varied among the sections based on the location	Cold recycled mix=0.22 Crushed stone=0.14 Crushed gravel=0.10 Gravel=0.07 Sand=0.05	Back-calculated from resilient modulus from Equation (6.1)

Table 6-3 summarizes the layer coefficients of the hot mixed binder and base course mixtures. However, since there are multiple types of binder course mixtures used in New Hampshire, each with a varying layer coefficient, it is important to determine what layer coefficient value should be used for these mixtures within a given pavement structure. For this reason, a binder performance grade recommendation map (Figure 6-3) provided by the NHDOT was utilized to determine the proper binder course mixture for a specific project with respect to its location in the state of New Hampshire.

Table 6-3 Layer coefficients of the binder and base course mixtures used in back-calculations (resilient modulus based for HMA and conventional NHDOT value for CCPR mixtures)

Mixture	B-6428H	B-5834L	B-5828H	BB-6428L	CCPR
Layer coefficient	0.46	0.32	0.39	0.42	0.22

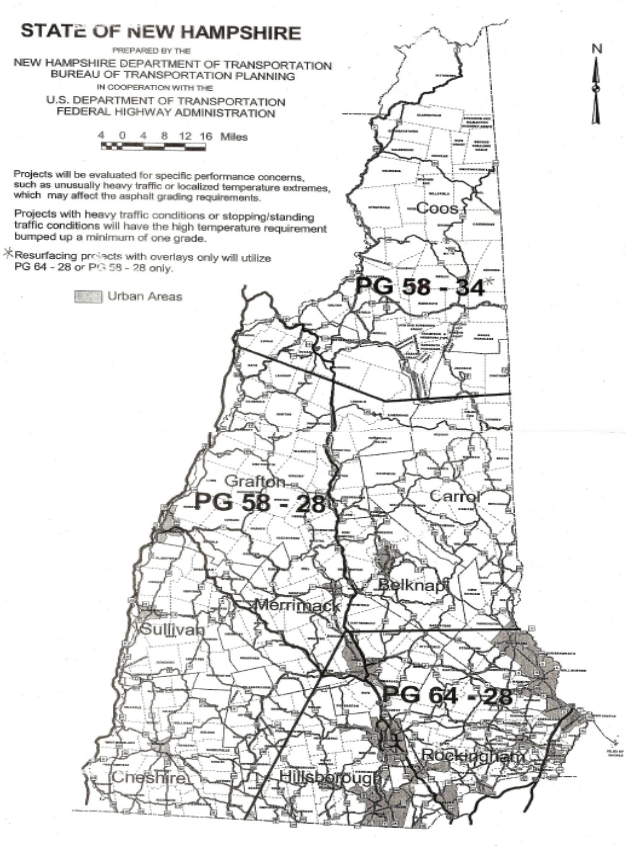

Figure 6-3 Binder performance grade specification map for New Hampshire

For a given cross section and a wearing course mixture, once all the required data in Table 6-2 is provided, the overall structural number (SN overall) based on the back-calculated ΔPSI value can be determined using the AASHTO 1993 design equation. Then, the structural number of the granular material as well as other base and binder course asphalt mixtures can be simply determined using their thickness and layer coefficients. This structural number is related to all the non-wearing course material and is called $SN_{non\text{-}wearing}$. The structural number of the wearing course asphalt mixtures ($SN_{wearing}$) can be determined through Equation (6.4) and the layer coefficient of the wearing course mixtures can be determined using Equation (6.5).

$$SN_{wearing} = SN_{overall} - SN_{non\text{-}wearing} \quad \text{Equation (6.4)}$$

$$a - value = \frac{SN_{wearing}}{Wearing\ course\ thickness} \quad \text{Equation (6.5)}$$

The following flowchart (Figure 6-4) is used to summarize the procedure of back-calculation of IRI based wearing course layer coefficients. As it is shown in the flowchart, the first step is to fit a linear function to the distress measurements which will result in determining the initial (right after construction) and terminal (20 years after construction) IRI values. The conditions to determine the initial IRI value will be based on the magnitude of IRI in the first year after construction as described in Table 6-1. Once the initial

and terminal IRI values are determined the initial and terminal serviceability values (P_i and P_t respectively) can be determined using either Equation (6.2) or (6.3) depending on the units of IRI. Once these values are determined the ΔPSI as one of the inputs in AASHTO 1993 design equation can be determined. The other input variables are assumed based on the values provided in Table 6-2. The back-calculations from this equation will result in the overall structural number ($SN_{overall}$) value which includes all types of materials in the cross section. To determine the structural number of the non-wearing course materials, the layer coefficients of the granular and non-wearing course asphalt mixtures determined from Table 6-2 and Table 6-3 respectively. Ultimately, the layer coefficient of the wearing course is determined through dividing the $SN_{wearing}$ by the thickness of the layer.

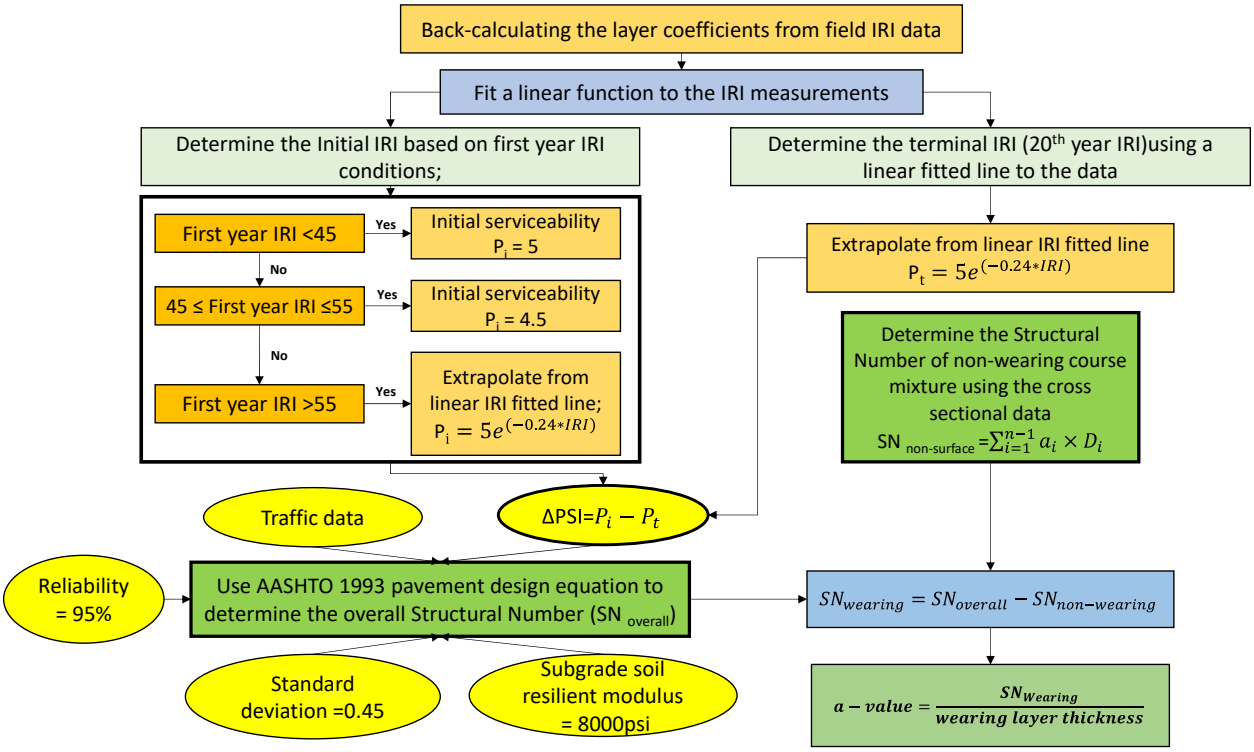

Figure 6-4 Flowchart to back-calculate the layer coefficients from field IRI data

Table 6-4 indicates the back-calculated wearing course layer coefficients from the field IRI data (a_{IRI}-value) using the aforementioned approach. According to the table, ARGG-2 has an extraordinary high a-value compared to the rest of the mixtures. This mixture has previously been indicated (section 4.2) to have a higher modulus value compared to rest of the wearing course mixtures except for W-7628H-12.5 mixture. However, both ARGG mixtures in this study have much lower phase angle values compared to all others including the binder and base course mixtures. The high stiffness and flexibility (and simultaneously a low creep deformation potential) of these mixtures which is associated to the asphalt rubber could have resulted in their outstanding performance with respect to IRI measurements, considering the high traffic volume of the projects where they have been placed. In general, based on field IRI data, all of the mixtures with an average layer coefficient value of 0.58 are indicated to have a considerably higher layer coefficient compared to the original value of 0.38 that is currently being used by the NHDOT pavement design

manual. Although in most cases, a similar mixture from different project sites (if applicable) have relatively close a-values, there are some cases such as ARGG-2, W-5828L, and W7628H-12.5 where the a-values from different projects are significantly different. Closer inspection of the pavement sections in these cases indicated that this could be a result of over designed non-wearing course material or difference between the assumed subgrade soil resilient modulus and actual modulus value. Since the actual design data is not available for every single project, it is not possible to definitively conclude the effects of subgrade modulus. Due to presence of instances where a-values for a mix type varied significantly, a one tailed t-test was conducted and based on the average and standard deviation of the whole dataset (all mixtures and all pavement sections), layer coefficients at two levels of reliability for all wearing courses (85% and 90%) used by NHDOT are suggested for the pavement design purposes based on IRI data. Based on the statistical analysis the suggested layer coefficients are 0.43 and 0.39 for 85% and 90% reliability levels respectively. It is important to note that based on the laboratory as well as field performance of ARGG mixtures and considering their significantly different production methods, they can be reasonably separated from other wearing course mixtures. Table 6-5 indicates the average layer coefficients, as well as layer coefficients at different levels of reliability for ARGG and non-ARGG wearing course asphalt mixtures. The results from separating ARGG mixtures from the rest of the wearing course mixtures indicate that an a-value of 0.43 at 90% reliability level can be used for non-ARGG mixtures whereas this value would be 0.41 for ARGG mixtures due to the higher standard deviation in these types of mixtures.

Table 6-4 Back-calculated layer coefficients from the field IRI data

Mix	Project	Traffic (ESALs)	P_i	P_t	ΔPSI	$SN_{overall}$	$SN_{non\text{-}surface}$	$SN_{surface}$	a_{IRI}-value
ARGG-1	Epping	5,344,563	5.0	3.6	1.4	4.919	3.789	1.130	**0.56**
	Seabrook	3,741,194	5.0	3.3	1.7	4.431	3.610	0.821	**0.55**
ARGG-2	Bow-Hooksett	3,741,194	5.0	4.0	1.0	5.096	3.525	1.571	**1.05**
	Spaulding turnpike	3,343,302	5.0	3.7	1.3	4.764	3.692	1.072	**0.71**
W-6428H-12.5	Milford-Amherst (NH101)	4,489,433	5.0	3.5	1.5	4.701	4.014	0.687	**0.46**
W-5828L	Woodstock-Lincoln (I-93 NB)	823,063	5.0	3.9	1.1	3.903	2.713	1.190	**0.40**
	Bethlehem	411,531	4.5	3.4	1.1	3.350	2.490	0.860	**0.57**
W-5834L	Pittsburg (US3)	328,500	4.5	3.2	1.3	3.130	2.560	0.570	**0.46**
W-7628H-12.5	Hudson-Windham - (Park Ave)	1,624,854	4.5	3.5	1.0	4.570	2.547	2.023	**0.67**
	Lebanon NH120	2,338,169	3.7	1.9	1.8	4.080	3.202	0.878	**0.44**
W-7034PH	Barrington	213,783	3.8	1.9	1.9	2.758	2.288	0.470	**0.63**
	Bethlehem-Carroll (US 302)	619,969	4.5	3.5	1.0	3.756	3.288	0.468	**0.62**
W-7628H-9.5	Meredith (US 3)	1,389,586	3.9	1.9	2.0	3.681	3.081	0.600	**0.60**
W-5828H	Shelburne (US 2)	383,846	5.0	4.1	0.9	3.502	2.778	0.724	**0.48**
	Gilford	1,192,296	3.8	1.8	2.0	3.584	3.054	0.530	**0.53**
	Alton	794,049	3.5	1.7	1.8	3.443	2.913	0.530	**0.53**
W-6428H-9.5	Lincoln (NH 112)	300,471	4.1	3.4	0.7	3.526	2.913	0.613	**0.63**
General layer coefficient for all types of wearing course mixture	**Average a-value for all wearing course mixtures (50% reliability)**								**0.58**
	Standard deviation of the layer coefficients for all wearing course mixtures								**0.15**
	a_{IRI}-value at 85% reliability								**0.43**
	a_{IRI}-value at 90% reliability								**0.39**

Table 6-5 Layer coefficients at different reliability levels for ARGG and non-ARGG wearing course asphalt mixtures based on field IRI data

a_{IRI}-value at different reliability levels	ARGG wearing course mixtures	Non-ARGG wearing course mixtures
50% reliability	0.72	0.54
85% reliability	0.48	0.45
90% reliability	0.41	0.43

6.5 INCORPORATING THE LABORATORY PERFORMANCE TEST RESULTS IN DEVELOPMENT OF LAYER COEFFICIENTS FOR WEARING COURSE MIXTURES

Although a layer coefficient developed based on field performance data (such as IRI) is expected to have greater reliability, it may not explicitly represent the structural contribution of the mixtures with respect to individual structural distress types such as rutting, fatigue and transverse cracking due to following reasons:

1. IRI includes functional distresses such as raveling, stripping, patching, potholes etc. which may not necessarily be related to structural deficiency of the asphalt mixtures.
2. With respect to structural distresses, IRI is more correlated to rutting than fatigue and transverse cracking, however actual pavement service lives are controlled by first dominant failure, which could be fatigue or transverse cracking.

Due to these reasons, it is necessary to incorporate the laboratory performance results in development and refining the field IRI based layer coefficients (a_{IRI}-value). For this purpose, the previously developed index parameters for rutting, transverse cracking, and fatigue cracking will be statistically incorporated with the field IRI based a-values to develop mechanistically informed layer coefficients. To develop such layer coefficients, this research work undertook the following steps:

1. Determine the individual performance index parameter value for each mixture on the basis of laboratory performance tests.
2. Determine the average and standard deviation of layer coefficients for all mixtures (including ARGG and non-ARGG wearing course mixtures) for each performance index parameter.
3. Using a normal distribution function, determine the z-statistic (number of standard deviations from average) and level of reliability of each mixture under each performance index category.
4. Using the average a-value and standard deviation of IRI based layer coefficients indicated Table 6-4, calculate the layer coefficient for each mixture under each performance index category at the specific level of reliability that was determined in step 3. Figure 6-5 indicates a visual summary of steps 2,3 and 4.

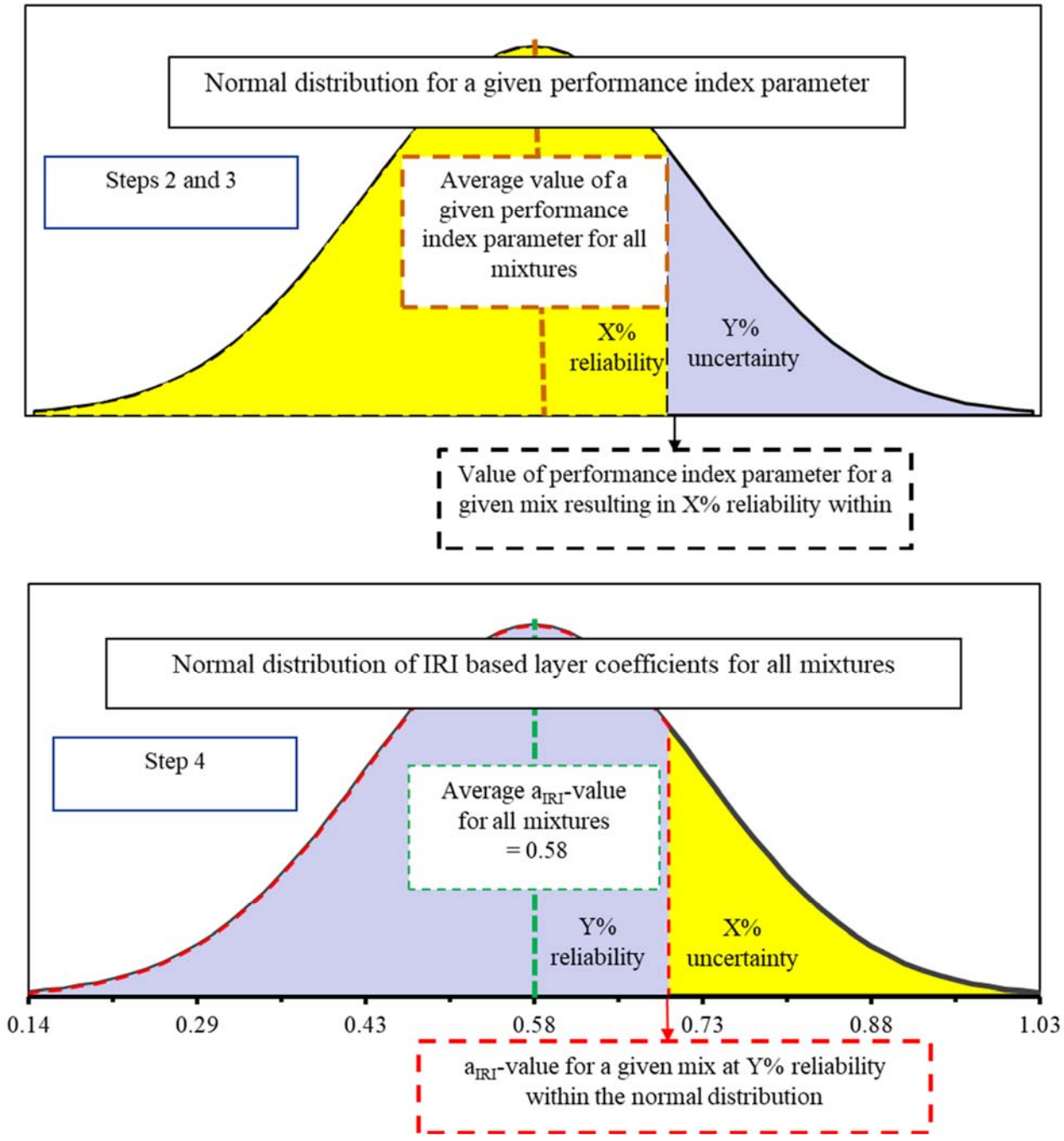

Figure 6-5. Schematic summary of steps 2,3 and 4 to incorporate performance index parameters in development of layer coefficients

5. Determine the performance-based a-value by averaging the layer coefficients determined under individual performance index category for each mixture. It is acknowledged that in present work it is an assumption to use average of layer coefficients from each of the three primary structural distresses, future studies should further explore a weighted average approach that is based on the performance data of New Hampshire's highways that can provide details on the distress

modes that control the service lives. For this reason, another set of layer coefficients combined of minimum performance based a-values for each mixture is generated for investigations.

6. Determine the average and standard deviation of the new sets of layer coefficients (both average and minimum layer coefficients).
7. Select the a-value at 90% reliability as the finalized layer coefficient.

Following the aforementioned steps, the levels of reliability and specific distress-based layer coefficients as well as the averaged performance based incorporated a-values are determined and summarized in Table 6-6.

As expected, the ARGG mixtures have the highest reliability and consequently highest a-values with respect to rutting index while they are indicated to have the lowest reliabilities as well as a-values with respect to fatigue criterion. However, these mixtures reveal a medium range of reliability (between 30% and 50% reliability) with respect to transverse cracking. Among other mixtures, W-7628H-12.5 indicates a good rutting (between 50% to 70% reliability) and excellent fatigue (above 70% reliability) performance while having a medium performance with respect to transverse cracking. In general, the non-ARGG wearing course mixtures are shown to have medium to weak reliability (below 50% reliability) with respect to rutting and transverse cracking while having good performance with respect to fatigue cracking. An averaged a-value (a_{ave}-value) from each performance index was determined for each mixture without assigning any weight factor to individual a-values driven from specific distresses since at the present time it is assumed that all three distresses are equally important in the overall performance of a given mixture within the pavement structure. According to the analysis, a layer coefficient equal to 0.50 at the reliability level of 90% can be used for all wearing course mixtures. The table also includes a minimum individual performance incorporated a-value (a_{min}-value) which essentially uses the minimum of the three a-values determined from each index parameter (bolded in each individual performance-based a-value column). Based on the minimum layer coefficients an a-value of 0.39 at 90% reliability level is determined. This conservative a-value results in a thickness design that covers all the three distresses at the same time. It should be noted that due to the limited number of ARGG mixtures, separation of these mixtures from the rest of the wearing course mixtures may not be statistically appropriate at this point in the analysis. In other words, determination of a separate average index value for the two ARGG mixtures will result in constant reliability levels of 24% and 76% for every single index parameter which may not be realistic and appropriate.

Table 6-6 Development of averaged and minimum performance base incorporated a-values for the wearing course mixtures

Mixture	Rutting			Fatigue cracking			Transverse Cracking			(a_{ave}-value)	(a_{min}-value)
	Index value (CMRI)	Reliability (%)	a-value	Index value ($N_f@C^s_{N_f} \times 1000 = 100$)	Reliability (%)	a-value	Index value (RDCI)	Reliability (%)	a-value		
ARGG-1	407.2	70	0.66	15764	29	**0.50**	33.64	49	0.58	0.58	0.50
ARGG-2	905.9	99	0.97	5523	5	**0.34**	29.52	36	0.53	0.61	0.34
W-6428H-12.5	194.2	37	0.53	12563	19	**0.45**	28.08	32	0.51	0.50	0.45
W-5828L	190.6	36	0.53	18985	42	0.55	24.05	20	**0.46**	0.51	0.46
W-5834L	138.1	29	**0.50**	29611	82	0.72	32.71	46	0.57	0.59	0.50
W-7628H-12.5	353.6	62	0.63	40069	98	0.89	30.97	41	**0.55**	0.69	0.55
W-7034PH	121.2	26	**0.49**	20301	48	0.57	65.72	99	0.97	0.68	0.49
W-7628H-9.5	180.0	36	**0.52**	21815	53	0.60	36.03	57	0.61	0.58	0.52
W-5828H	171.9	33	0.52	22104	55	0.60	22.36	18	**0.44**	0.52	0.44
W-6428H-9.5	118.5	26	**0.48**	22237	56	0.60	35.10	53	0.60	0.56	0.48
Average										**0.58**	**0.47**
Standard deviation										**0.06**	**0.06**
Layer coefficients at 90% reliability										**0.50**	**0.39**

6.6 CORRELATION OF LAYER COEFFICIENTS WITH MIXTURE PROPERTIES

As a summary up to the current point of this chapter, three different types of layer coefficients have been developed:

1. a_{IRI}-value: determined through the back-calculations of the filed IRI measurements
2. a_{ave}-value: determined through averaging the performance incorporated a-values
3. a_{min}-value: determined through the minimum performance incorporated a-value for each mixture

To determine which a-value is more reasonable for the purpose of application in the pavement design, it is necessary to evaluate the strength of correlations between the a-values, mixture properties and performance index parameters. For this reason, the Pearson's correlation coefficient is selected to be used to assess the correlations between these three components. In general, the final selected a-value needs to indicate a positive correlation with the performance index parameters while it should maintain a reasonable correlation (either positive or negative) with the mixture properties.

Table 6-7 and Table 6-8 indicate the Pearson's correlation matrix between the mixture properties and performance indices along with the various a-values. As mentioned before, ARGG mixtures have significantly different mix properties and performance and for that reason and in order to better discriminate and evaluate the effect of mixture properties on a-values, separate tables were generated. Table 6-7 includes all the wearing course mixtures, and the mixture properties include the performance grade high temperature (PGHT), performance grade low temperature (PGLT), performance grade useful temperature interval (UTI), nominal maximum aggregate size (NMAS), asphalt content (AC), level of gyration and recycled asphalt pavement (RAP). The main noteworthy observations with respect to the highlighted cells of Table 6-7 are as follows:

1. While a_{IRI}-value does not reveal any significant correlations with the binder grade properties (PGHT, PGLT and UTI) or the aggregate size, the a_{ave}-value indicates much higher sensitivity to these properties. However, this observation is reverse for a property such as asphalt content, whereby a_{IRI}-value indicates a relatively high positive correlation with asphalt content. On the other hand, a_{min}-value indicates similar correlations to that of the a_{ave}-value with respect to binder grade properties while unlike the a_{IRI}-value, it is negatively correlated with the asphalt content. Another important observation is the insensitivity of a_{ave}-value to the asphalt content which may be a result of existence of the ARGG mixtures with relatively higher binder contents in the dataset while their individual a_{ave}-value is notably close to the overall average a_{ave}-value which neutralizes the effect of binder, considering that the rest of the mixtures have close asphalt contents in general.
2. With regards to correlation of different types of a-values with the developed index parameters in this research it is shown that the a_{IRI}-value has an expected high positive correlation to the rutting index due to the relatively high correlation between the IRI and rutting distresses in general. However, a_{IRI}-value is negatively proportional to the fatigue index. This observation confirms that a_{IRI}-value needs to be refined through incorporating the lab performance tests in the analysis and as a result the a_{ave}-value is positively correlated to all three of the performance index parameters.

On the other hand, a_{min}-value reveals a reverse trend as compared to a_{IRI}-value when considering the correlations to rutting and fatigue indices. Since there is negative correlation between fatigue and rutting index parameters, the a_{IRI}-value and a_{min}-value indicate negative correlations with respect to fatigue and rutting indices. This is primarily associated to the ARGG mixtures' performance with respect to these types of distresses in the lab.

3. As a general conclusion with respect to Table 6-6 and Table 6-7 due to the aforementioned results and discussions on the correlations, the a_{ave}-value is recommended to be a better measure to indicate the structural contribution of the mixtures when all types of mixtures (ARGG and non-ARGG) are included in the analysis. However, a_{min}-value is a more conservative selection which may also increase the initial construction costs while it will probably result in less pavement maintenance and rehabilitation costs due to added redundancy.

Table 6-7 Correlation matrix including ARGG mixtures

Variables	PGHT	PGLT	UTI	NMAS	Asphalt Content	Gyration	RAP	Rutting index	Fatigue index	Transverse Cracking index	a_{IRI}-value	a_{ave}-value	a_{min}-value
PGHT	1.0	-	-	-	-	-	-	-	-	-	-	-	-
PGLT	0.00	1.0	-	-	-	-	-	-	-	-	-	-	-
UTI	0.95	-0.32	1.0	-	-	-	-	-	-	-	-	-	-
NMAS	-0.18	-0.33	-0.07	1.0	-	-	-	-	-	-	-	-	-
Asphalt Content	-0.38	0.34	-0.47	0.02	1.0	-	-	-	-	-	-	-	-
Gyration	0.42	0.38	0.28	-0.33	0.34	1.0	-	-	-	-	-	-	-
RAP	0.09	0.11	0.05	0.04	-0.67	-0.40	1.0	-	-	-	-	-	-
Rutting index	-0.23	0.32	-0.32	0.35	0.69	0.25	-0.18	1.0	-	-	-	-	-
Fatigue index	0.50	-0.23	0.54	-0.09	-0.61	-0.19	0.38	-0.47	1.0	-	-	-	-
Transverse Cracking index	0.42	-0.67	0.62	0.15	-0.04	0.24	-0.58	-0.22	0.04	1.0	-	-	-
a_{IRI}-value	**0.03**	**0.14**	**-0.02**	**-0.03**	**0.65**	**0.44**	**-0.52**	**0.77**	**-0.47**	**0.21**	1.0	-	-
a_{ave}-value	**0.56**	**-0.43**	**0.67**	**0.30**	**0.02**	**0.26**	**-0.29**	**0.23**	**0.43**	**0.64**	0.39	1.0	
a_{min}-value	**0.61**	**-0.20**	**0.64**	**-0.08**	**-0.45**	**-0.06**	**0.13**	**-0.64**	**0.80**	**0.26**	-0.59	0.33	1.0

Table 6-8 Correlation matrix including only non-ARGG mixtures

Variables	PGHT	PGLT	UTI	NMAS	Asphalt Content	Gyration	RAP	Rutting index	Fatigue index	Transverse Cracking index	a_{IRI}-value	a_{ave}-value	a_{min}-value
PGHT	1.0												
PGLT	0.12	1.0											
UTI	0.94	-0.24	1.0										
NMAS	-0.05	-0.45	0.11	1.0									
Asphalt Content	0.05	0.30	-0.06	-0.81	1.0								
Gyration	0.60	0.33	0.47	-0.45	0.30	1.0							
RAP	-0.15	0.28	-0.25	0.24	-0.65	-0.34	1.0						
Rutting index	0.48	0.44	0.31	0.29	-0.50	0.16	0.56	1.0					
Fatigue index	0.36	-0.11	0.39	0.14	-0.29	-0.06	0.22	0.63	1.0				
Transverse Cracking index	0.43	-0.67	0.66	0.20	0.12	0.27	-0.72	-0.35	-0.05	1.0			
a_{IRI}-value	**0.61**	**-0.01**	**0.61**	**-0.48**	**0.71**	**0.60**	**-0.80**	**-0.18**	**0.10**	**0.63**	1.0		
a_{ave}-value	**0.67**	**-0.47**	**0.83**	**0.29**	**-0.18**	**0.24**	**-0.31**	**0.33**	**0.68**	**0.67**	0.52	1.0	
a_{min}-value	**0.78**	**-0.15**	**0.81**	**0.14**	**-0.16**	**0.10**	**0.03**	**0.53**	**0.78**	**0.28**	0.39	0.8	1.0

In context of correlations for wearing course mixture without ARGG in the population (shown in Table 6-8), following key observations can be made:

1. All three a-value types (a_{IRI}, a_{ave} and a_{min}) indicate similar correlations regarding the binder grading properties with exception of a_{min}-value which is nearly insensitive to the PGLT. The table indicates that the a_{ave}-value and a_{min}-value have uncommon correlation directions with NMAS and asphalt content such that mixtures with larger aggregate size and lower asphalt content have higher a-values.
2. The elimination of the ARGG mixtures from the database resulted in improved correlations with respect to direction and magnitude of the correlations between all three types of a-values with fatigue and transverse cracking index. Also, both a_{ave}-value and a_{min}-value indicate higher positive correlations with the rutting index for non-ARGG mixtures. However, the a_{IRI}-value indicates a negative correlation with the rutting index which reaffirms the necessity of incorporating performance-based indices in development of a reliable a-value.
3. As a general conclusion with respect to Table 6-6 and Table 6-8, considering the previous discussions, both of the a_{ave}-value and a_{min}-value based layer coefficients can be reasonably used for the pavement structural design and the selection of the proper a-value should be based on the level of importance and reliability of a specific project.

Based on the discussions in this section a generalized non-mix specific a_{ave}-value and a_{min}-value for non-ARGG mixtures is recommended in Table 6-9.

Table 6-9 a_{ave}-value and a_{min}-value for non-ARGG mixtures

a-value	Level of reliability	Non-ARGG wearing course mixtures
a_{ave}-value	50% reliability	0.58
	90% reliability	0.48
a_{min}-value	50% reliability	0.49
	90% reliability	0.44

6.7 MIXTURE PROPERTY BASED PREDICTIVE MODEL FOR LAYER COEFFICIENTS

In many instances and due to the limitations in time and laboratory equipment as well as the unavailability of field distress data, it may not be possible to determine an accurate performance incorporated layer coefficient for the pavement design. Therefore, a predictive model based on nominal properties of the mixtures can help mixture and pavement design engineers to have an acceptable level of estimation of the structural contribution of the mixtures within the pavement structure. For this reason, the database created in this thesis in terms of mixture properties and layer coefficients are used to develop a simple

model to predict the performance incorporated layer coefficients (a_{ave}-value) for all the wearing course mixtures including ARGG and non-ARGG mixtures used in New Hampshire.

In order to develop the model, the nominal mixture properties including PGHT, PGLT, NMAS, AC, gyration level, and RAP content were selected as the initial variables in the model. These parameters are readily available before the mixture design and can help the design engineers with an initial estimation of the structural contribution of the mixture in the pavement system. A second-degree factorial variable selection was performed to determine the significance of possible two-way interactions in the model. To build the model, the stepwise regression analysis was utilized to determine the influential mixture properties and two-way interactions on the a_{ave}-value at 0.25 significance level which is equal to 75% confidence interval. This level of significance was determined through performing trial and error efforts to determine what level can result in the best possible fit for the available data. However, it should be noted that this level of significance can change based on the level of accuracy and importance of the project. Table 6-10 indicates the terms and resultant statistics of the developed model. The lower p-value and higher t-ratio indicate the significance of the variable in the prediction equation. As it can be seen the PGHT with the lowest p-value and the NMAS with the highest p-value are the most and least significant variables in the models. Although the p-value for NMAS is higher than the threshold value of 0.25, its interaction with the PGHT is a significant and for that reason NMAS is kept in the model. The results from the prediction are indicated in Figure 6-6. A strong correlation close to the line of equality is achieved through the developed model. In using any predictive equation including the one provided in this section, it is important to consider the constraints of the variables in terms of the input value as not every single value may result in a reasonable prediction. Also, as this predictive equation results in the a_{ave}-value (50% reliability level) it would be necessary to increase the level of reliability by calculating the layer coefficient at an increased reliability level by using a standard deviation of 0.06 (determined from Table 6-6) depending on the importance of a given design project.

Table 6-10 Prediction model for a_{ave}-value

Term	Statistics			
	Estimate	Standard Error	t-Ratio	Prob>|t|
Intercept	-1.09659	0.25611	-4.28	0.0505
PGHT	0.011663	0.00177	6.61	0.0222
PGLT	-0.017115	0.00415	-4.13	0.054
NMAS (mm)	0.000691	0.00618	0.11	0.9212
AC%	0.100468	0.02156	4.66	0.0431
Gyration level	-0.003087	0.00133	-2.33	0.1453
RAP%	0.002695	0.00158	1.71	0.2294
(PGHT-64)*(NMAS-11.6)	0.004462	0.00103	4.33	0.0494

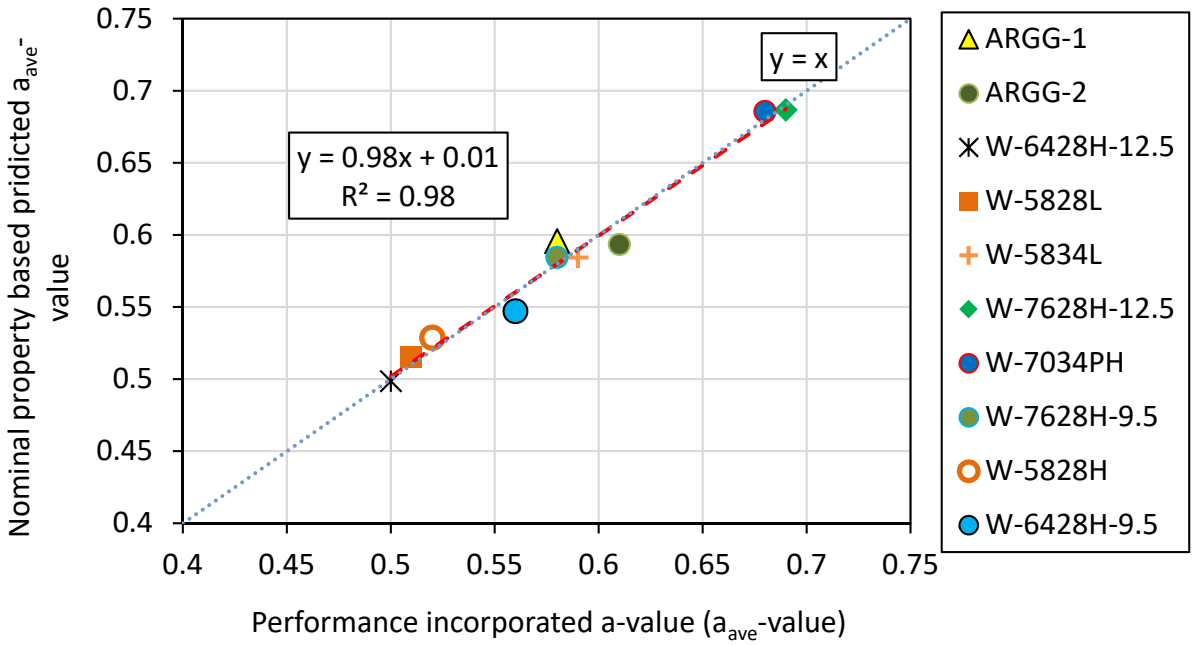

Figure 6-6 Nominal property based predicted a_{ave}-value for all the study surface mixtures

6.8 DEVELOPMENT OF LAYER COEFFICIENTS FOR BINDER AND BASE COURSE MIXTURES

Using the methodology developed in section 6.5, the layer coefficients of the binder and base course mixtures in the study (both hot and cold mixtures) were developed in this section. Table 6-11 indicates the results from the analysis. It can be seen from the table that while the CCPR mixtures have relatively similar rutting-based layer coefficients to that of wearing course mixtures, the hot mixed mixtures have relatively higher a-values with respect to rutting performance. However, while the fatigue-based a-values of binder and base mixtures is relatively lower than wearing course mixtures, the hot mixed mixtures indicate better fatigue resistance (higher a-values) compared to CCPR mixtures. On the other hand, both type of mixtures resulted in relatively lower transverse cracking-based a-values with CM-1 and CM-2 being the best among all the binder and base course mixtures.

In general, the expected functionality of the two types of productions (hot and cold) are the same and it is to serve as a foundation for wearing course mixtures. Therefore, it was decided to combine these types of mixtures for the a-value analysis. The table includes two different levels of reliability at 90% and 95% for the combined set of hot mixed and cold recycled mixtures. The overall averaged a_{ave}-value and a_{min}-value at 90% reliability are calculated to be 0.43 and 0.30 at 90% reliability. These values were calculated to be 0.41 and 0.28 at 95% reliability.

It should be noted that a direct field distress evaluation with respect to IRI measurements for the binder and base course mixtures has not been feasible. Therefore, a higher level of uncertainty should be considered when using the layer coefficients of the binder and base course mixtures developed based on IRI measurements. However, it should be mentioned that among all the evaluated cross sections there was only one constructed with CCPR mixtures. Therefore, it would be more appropriate to use the minimum developed a-value for CCPR mixtures. Considering the above discussions, it is recommended to use an averaged a-value of 0.41 at 95% reliability for the hot mixed binder and base course mixtures and a minimum a-value of 0.28 at 95% reliability for the CCPR mixtures in design of flexible pavements in New Hampshire.

Table 6-11 Development of averaged and minimum performance base incorporated a-values for the binder and base course mixtures

Mixture	Rutting			Fatigue cracking			Transverse Cracking			(a_{ave}-value)	(a_{min}-value)
	Index value (CMRI)	Reliability (%)	a-value	Index value ($N_f@C^s_{N_f} \times 1000 = 100$)	Reliability (%)	a-value	Index value (RDCI)	Reliability (%)	a-value		
B-6428H	468.7	78	0.70	18343	40	0.54	13.8	5	**0.34**	0.53	0.34
B-5834L	193.7	36	0.53	16282	31	0.51	24.4	22	**0.47**	0.50	0.47
B-5828H	358.3	63	0.63	21551	53	0.59	27.7	31	**0.51**	0.58	0.51
BB-6428L	580.7	89	0.77	17302	35	0.52	18.8	11	**0.40**	0.56	0.40
CM-1	128.3	27	0.49	1862	2	**0.28**	31.1	41	0.55	0.44	0.28
CM-1-a	271.0	49	0.58	9571	11	**0.40**	21.7	15	0.43	0.47	0.40
CM-2	141.2	29	0.50	9448	11	**0.40**	33.3	48	0.58	0.49	0.40
CM-2-a	212.5	40	0.54	8843	10	**0.39**	21.1	15	0.43	0.45	0.39
Average										**0.50**	**0.40**
Standard deviation										**0.05**	**0.07**
Layer coefficients at 90% reliability										**0.43**	**0.30**
Layer coefficients at 95% reliability										**0.41**	**0.28**

6.9 REFERENCES

[1] Al-Omari, B., & Darter, M. I. (1994). Relationships between international roughness index and present serviceability rating. Transportation Research Record, (1435).

[2]. Smith, K. D., & Ram, P. (2016). Measuring and Specifying Pavement Smoothness: [techbrief] (No. FHWA-HIF-16-032). United States. Federal Highway Administration.

[3]. https://nhdot.ms2soft.com/tcds/tsearch.asp?loc=Nhdot&mod=

[4]. Janoo, V. C. (1994). Layer Coefficients for NHDOT Pavement Materials (No. CRREL-SP-94-30). COLD REGIONS RESEARCH AND ENGINEERING LAB HANOVER NH.

CHAPTER 7: SUMMARY, CONCLUSIONS AND RECOMMENDATIONS

7.1 SUMMARY

Perhaps, one the major challenges in use of performance based specifications and design in pavement engineering is the discontinuity between the mixture and pavement designs. Since different asphalt mixtures have a wide range of variety with respect to their nominal properties and production methods, they can perform very differently under comparable loading and climatic conditions. For this reason, in many instances the pavements' failures are primarily associated with the improper design due to lack of knowledge about the structural contribution and performance of different mixtures within the pavement system, this is especially true when the design is based on empirical approaches. Although pavement design system is in transition from purely empirical approaches to mechanistic empirical design based methods, many State highway agencies are continuing to use empirical methods as their primary pavement structural design approach due to challenges associated with extensive experimentation needs and local calibrations.

Currently, New Hampshire Department of Transportation (NHDOT) employs the AASHTO empirical method for structural design of highways. This method uses material specific coefficients (layer coefficients) to quantify the structural capacity provided by each pavement layer. The current layer coefficients (a-value) used by NHDOT are based on original values suggested by AASHTO in 1960s. These coefficients are experimentally developed values based on simple statistical regressions and almost no fundamental or engineering mixture property or explicit failure criterion has been used in their original development. On the other hand, the evolutions in the mixture design, application of recycled materials and the growing traffic demand etc. requires the reevaluation of the existing layer coefficients.

In order to evaluate and compare the current NHDOT asphalt mixture layer coefficients, a comprehensive literature review on the topic along with a survey from other State DOTs that are using the AASHTO design method was performed to determine the most recent approaches that have been implemented in development of new layer coefficients. The survey confirmed that NHDOT is using one of the lowest values (0.38 for wearing course and 0.34 for binder and base course mixtures) amongst other States, even those with similar climatic and traffic conditions. Since the layer coefficients govern the required thickness of the pavement layers, they can significantly affect the construction costs. In addition, lower a-values can lead to unnecessarily overdesigned cross sections which will result in substantial financial burden. Therefore, it is important to develop new reliable layer coefficients for New Hampshire pavement designs that reflect the mixture's long term performance determined from mechanistic and performance based laboratory testing rather than simple regression based methods.

In order to fulfill this aim, a variety of pavement construction and rehabilitation projects were investigated to determine the most conventionally used mixtures in New Hampshire. As a result, 18 different types of asphalt mixtures including two asphalt rubber gap graded, four cold central plant recycled as well as ten conventional and polymer modified mixtures that are commonly used in New Hampshire were selected

for investigations and performance testing. The laboratory testing plan included resilient modulus (M_r), complex modulus (E*), direct tension cyclic fatigue (S-VECD), semi-circular bend (SCB) and disk-shaped compact tension (DCT) tests. The results of the tests and analysis were utilized to evaluate the effect of mixture design properties on performance prediction indices through statistical analysis, correlations between different performance index parameters from each test were also conducted. Furthermore, the effect of production methods (cold versus hot) was evaluated through predicted performances from mechanistic approaches. The correlations of the existing performance index parameters were compared to available field distress data for the study mixtures to evaluate the strength of correlations between the field and laboratory predicted performances. On the basis of the observations from these correlations, it was determined that there is need to develop new index parameters that can better reflect the field performance for New Hampshire roadways. Therefore, three index parameters for rutting (based on complex modulus, fatigue cracking (based on S-VECD) and transverse cracking (based on SCB) were developed. The rutting and fatigue index parameters were shown to be highly correlated with the field distress data while the transverse cracking index was shown to be able to reduce the variation among results from different replicates and better discriminate the aging effect on the mixtures.

In order to develop the layer coefficients, the designated approach in this research was to incorporate the performance test results with the appropriate failure distress criteria such as International Roughness Index (IRI). Therefore, the IRI data for a set of seventeen cross sections on which similar mixtures to the study mixtures (similar binder type and mix design properties) have been placed, were selected for evaluations. Based on these analysis, and using available equations in the literature, the IRI data were converted into the Present Serviceability Index (PSI). Using the AASHTO 1993 design equation, and the available cross sections, the pavement structural number (SN) and consequently the IRI base layer coefficients (a_{IRI}-values) for wearing course mixtures were back-calculated. Using a normal distribution function, the average and standard deviation for wearing course a_{IRI}-values were determined to be 0.58 and 0.15 respectively. In order to incorporate the developed performance based index parameters with the IRI based layer coefficients, the values of the index parameters were calculated for each mixture separately. Then, using the normal distribution function, the average, standard deviation and consequently the level of reliability within each performance index was calculated for individual mixtures. This level of reliability was incorporated with the normal distribution of the a_{IRI}-values and performance based a-values were determined for each mixture. Based on the analysis, a set of average and minimum a-values at different levels of reliability have been proposed for future New Hampshire pavement designs.

7.2 CONCLUSIONS

Over the course of this research project, a number of significant findings were inferred. Specific conclusions and findings from each component of research are discussed in previous chapters. A high-level summary of key conclusions from the research efforts are as following:

- Since rutting in asphalt is predominantly a viscoplastic distress, the phase angle of asphalt mixtures plays an important role in mechanism of rutting formation. Therefore, in this research a complex modulus based rutting index parameter (CMRI) is developed which takes into account the effect of phase angle and stiffness at the same time. This index is indicated to be highly

correlated with the field data as well as Hamburg wheel tracking test (HWTT) results for different mixtures in New Hampshire. This index parameter can also help reducing the specimen fabrication and testing time required to conduct a separate destructive testing such as HWTT, flow number etc.

- The development of a rate dependent cracking index (RDCI) in this research is supported by fundamental fracture mechanics, it is free from any type of empirical or undefinable variable within the parameter. The use of continuous cumulative work at various times can help with describing and evaluating the crack formation and propagation mechanisms at any given time during the test. Due to inherent presence of time in all work and power terms of RDCI; it is expected to better capture the rate dependency of fracture in asphalt mixture.
- The current fatigue failure criteria within S-VECD analysis framework did not indicate to be able to reliably rank the field performance of the mixtures as a stand-alone parameter. Therefore, a new failure criterion called as $C_{N_f}^{S}$ was developed and investigated. This criterion incorporates three components of the S-VECD theory (cumulative pseudo-strain, number of cycles to failure at strain level and amount of continuum damage in material at failure) to capture the mixture's disintegration with respect to damage growth rate. The parameter indicated that it is not only able to rank the mixtures but it also well correlated with the magnitude of fatigue cracking in the field.
- The application of performance index parameters has mostly been limited to differentiating the mixtures' lab performance as well as performance based mixture design approaches. However, the use of these indices to influence the pavement design has been limited. The new layer coefficients developed in this research incorporate the lab measured performance indices and reflect the expected performance of asphalt mixtures in the field. Thus, pavement structures designed with the proposed layer coefficients are expected to have higher reliability in terms of performance and service life. This will result in reduced initial construction and routine maintenance costs since the pavements structure is designed based on reliable performance parameters that the pavement deterioration time can be estimated on basis of them.

7.3 RECOMMENDATIONS

With advancements in laboratory testing equipment and scientific theories to capture constitutive behavior of asphalt mixtures, the performance-based material characterization and pavement design is becoming reality. These approaches are preferred as they can result in major savings through prolonging of pavement service lives. Therefore, it is necessary to develop appropriate testing and performance index parameters to determine the mixtures' distress susceptibility. The performance index parameters should not only be able to differentiate the mixtures in lab, but they also need to provide acceptable correlations with the field distress data. Ultimately, these parameters can be used in evaluation of structural contribution of the mixtures within the pavement cross section. For this reason, the recommendations in this section will be provided under two categories as following:

- Mixture design and performance index parameters; and,

- Structural contribution of mixtures in terms of layer coefficients for AASHTO empirical pavement design.

7.3.1 RECOMMENDATIONS FOR MIXTURE DESIGN AND PERFORMANCE INDEX PARAMETERS

The recommendations for mixture design and performance index parameters are listed below:

- An important parameter in design of the pavement structures and consequently the appropriate mixture for the structure is the prevailing failure criterion. The results and analysis from laboratory performance testing in this research indicated that while a mixture such as W7034-PH can be reliability used to reduce the thermal cracking potential, it may also increase the rutting susceptibility of the pavement structure. However, among all the study mixtures, the W7628H-12.5 indicated the most reliable performance with regards to rutting, fatigue and transverse cracking. In general, mixtures with higher useful temperature interval and smaller aggregate size indicated to have better fatigue and transverse cracking performance.
- In evaluating the performance of cold recycled mixtures in this project, the mixtures with lower distillated oil percentage (CM-1-a and CM-2-a) indicated to have a better rutting and fatigue cracking performance. Therefore, it is recommended to reevaluate the standard specifications for production of MS-4 emulsions through performing a more comprehensive research on the performance of cold recycled mixtures used in New Hampshire.
- In order to use the performance index parameters developed in this research during the mixture design procedure, it is necessary to develop preliminary threshold values for these indices. The performance index parameters for rutting (CMRI) and Fatigue cracking ($C_{N_f}^{S}$) introduced in this research were primarily developed based on the field performance of the mixtures placed on I-93 as part of the High RAP Pool Fund Research study. Therefore, the threshold values for these indices will be based on the correlations determined between those mixtures and the index parameters. In order to determine the correlations between the field cracking and mixture's performance, a power based function was fitted to the data which is deemed to be able to more appropriately explain the boundary conditions of rutting and fatigue with respect to actual field performance.
    - Figure 7-1 show plot between CMRI and rut depth and the power function curve fitted to the data. Three levels of rut depth were selected to determine the preliminary CMRI values for projects with different levels of importance (traffic level/functionality etc.) during the mixture design procedure. These levels are 12.5 mm (low criticality), 6.25 mm (medium criticality) and 3.12 mm (high criticality) rut depths at the end of the 5th year after construction. These levels result in CMRI values of 114.7, 239.2 and 498.7 respectively.

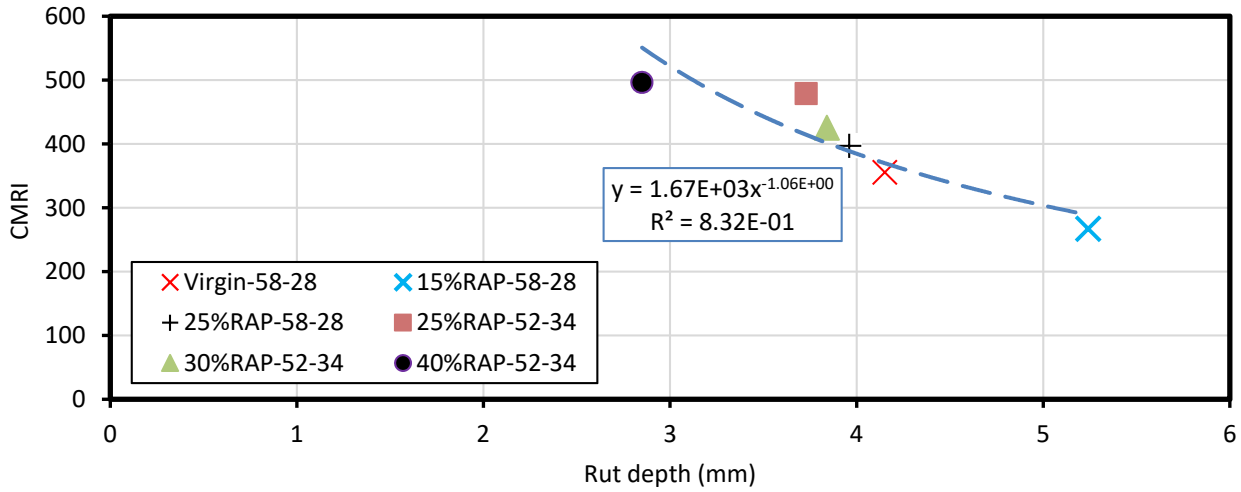

Figure 7-1 CMRI versus rut depth for I-93 study mixtures

- Figure 7-2 shows the normalized cracking length versus $N_f@C_{N_f}^S = 100$ and the power function fitted to the data. With respect to the default values in the AASHTOWare PavementME, the acceptable default value for top-down cracking at the end of pavement design life in 20 years is 375m/km (2000ft/mile). Based on this value, three levels of cracking length in the 5th year after construction were selected to establish the preliminary threshold values for fatigue cracking. These levels are determined at 12.5% (46.8m/km for low criticality), 6.25% (23.4 m/km for medium criticality), and 3.12% (11.7 m/km for high criticality) of the total allowable cracking length of 375m/km. These percentages result in $N_f@C_{N_f}^S = 100$ values of 11700, 16300 and 22800 for low, medium and high critically designs respectively.

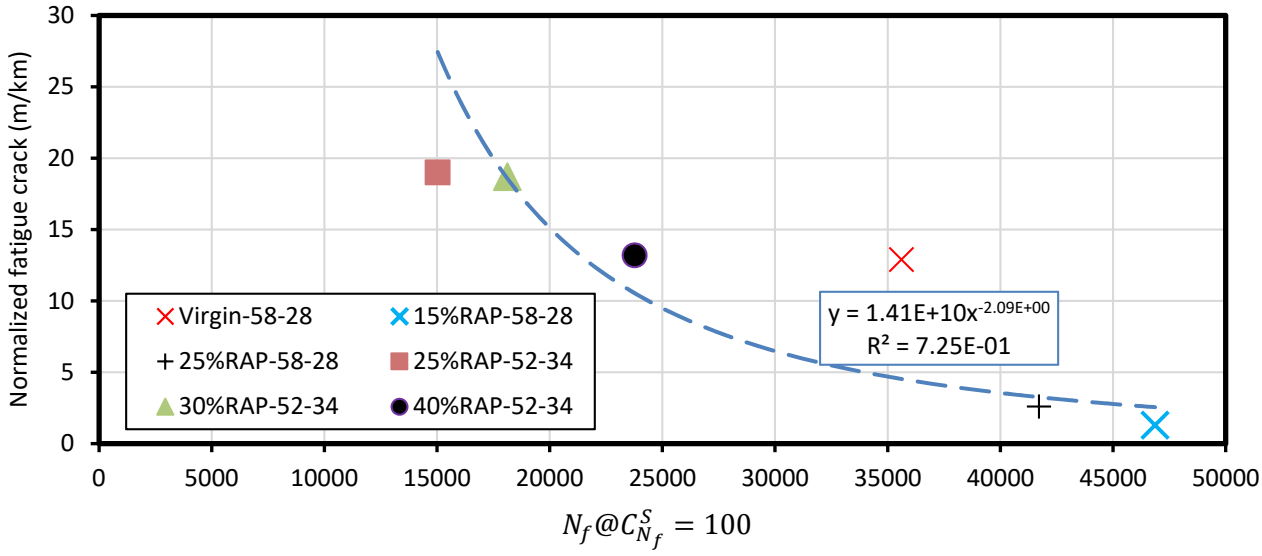

Figure 7-2 Normalized Crack length vs $N_f@C_{N_f}^S = 100$ for I-93 study mixtures

- In order to develop a threshold value for transverse cracking and RDCI parameter the correlations between this parameter and Flexibility Index for wearing course mixtures were investigated. As it can be seen from Figure 7-3 the two indices are highly correlated with a R^2=0.98. The minimum acceptable FI value put forth by Illinois Department of Transportation is 8.5 and using the correlating equation indicated in the figure, the preliminary acceptable RDCI value will be equal to 16.5. Although, this value can be used in initial mixture screening, more field data analysis is required to establish a firm minimum acceptable value for RDCI.

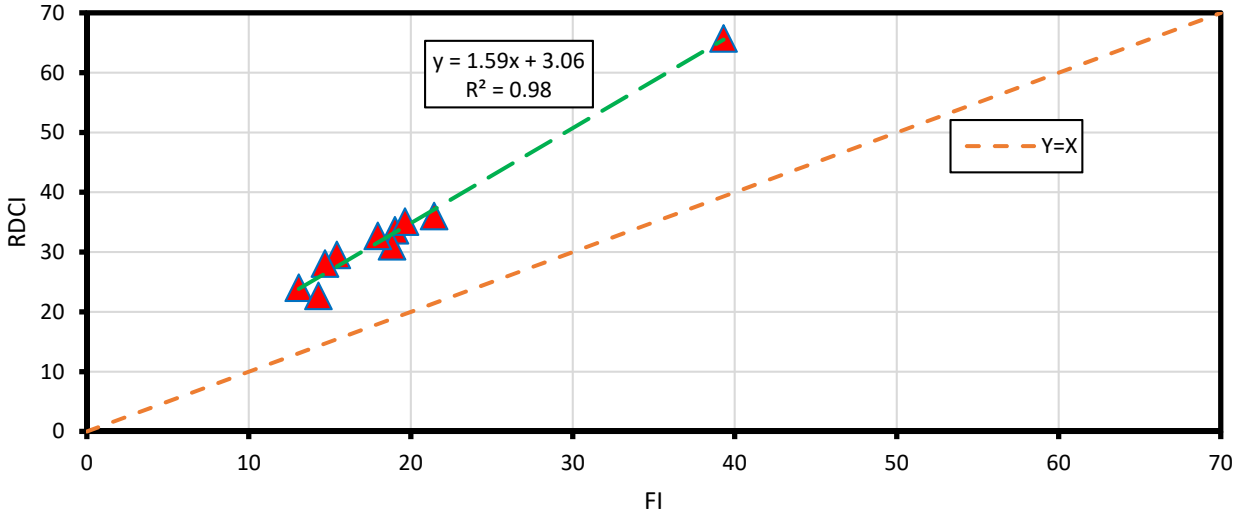

Figure 7-3 Correlation between RDCI and FI

Based on the recommended minimum threshold values at different traffic levels a performance space diagram (PSD) for study mixtures in this project is developed (c.f. Figure 7-4). As it can be seen from the figure, all the NHDOT mixtures studied in this project pass the minimum requirement for the rutting. Also all of the wearing and hot mixed binder and based course mixtures pass the minimum fatigue threshold value. However, the cold recycled mixtures do not meet the minimum requirement for fatigue cracking. Although the PSD indicates a satisfaction of the mixture design with respect to cracking for medium traffic level, rutting is expected to be a problem for mixtures such as W7034PH and W-6428H-9.5. For this reason, it is recommended that in future a performance engineered mixture design (PEMD) be used instead for full reliance on volumetric design for the mixtures used in New Hampshire.

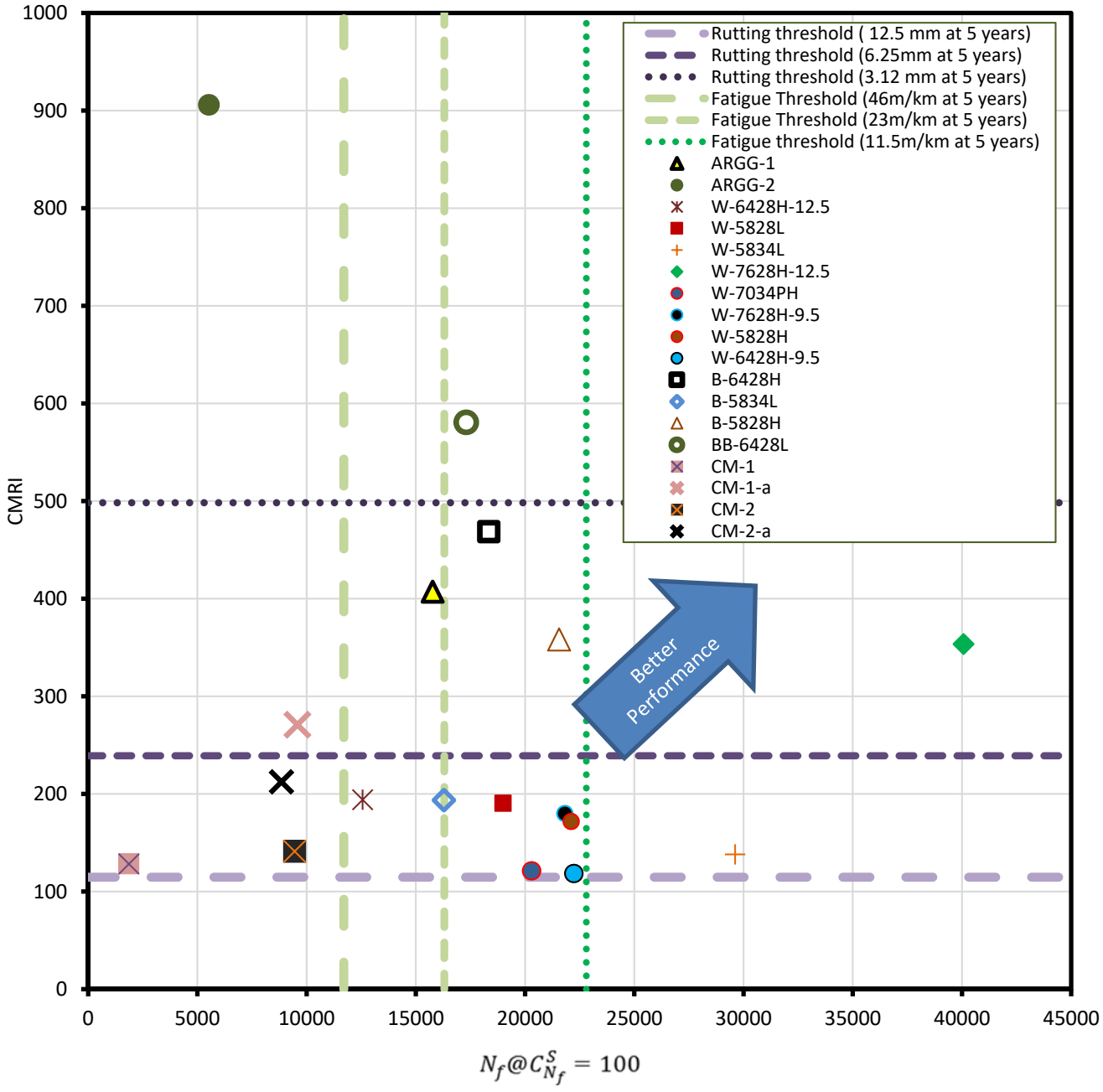

Figure 7-4 Performance space diagrams for NHDOT mixtures

7.3.2 RECOMMENDATIONS FOR LAYER COEFFICIENTS

The layer coefficients proposed in this research study are based on combination of field performance and performance based laboratory evaluations and can be reliably used in design of pavement structures in New Hampshire. Due to the availability of average and standard deviation for each category of mixtures (wearing, hot mixed binder and base as well as cold recycled mixtures), the recommend layer coefficients

can be adjusted with respect to specific project requirements and anticipated levels of reliability. This can result in a more efficient pavement structural design and major savings in construction costs. It should be mentioned that due to the direct applicability of IRI measurements to wearing course mixtures, the overall a-value developed for these mixtures can be used at 10% confidence interval (90% reliability). However, due to inapplicability of IRI as a direct distress measurement tool for base and binder course mixtures as well as limited number of mixtures in the evaluated cross sections (especially CCPR mixtures), the overall a-values developed for these mixtures should be preferably used at lower confidence interval. Therefore, it is recommended to use a 5% confidence interval (95% reliability) for a-values developed for these types of mixtures.

The non-mix specific (mix specific values are provided in Chapter 6) recommendations for layer coefficients are summarized as following:

- Wearing course mixtures:
  - ARGG mixtures:
    - a_{min}-value= 0.47 at 50% reliability
    - a_{min}-value= 0.39 at 90% reliability
  - Non-ARGG mixtures:
    - a_{ave}-value= 0.58 at 50% reliability
    - a_{min}-value= 0.49 at 50% reliability
    - a_{ave}-value= 0.48 at 90% reliability
    - a_{min}-value= 0.44 at 90% reliability
- Binder and base course mixtures:
  - Hot mixed:
    - a_{ave}-value= 0.50 at 50% reliability
    - a_{ave}-value= 0.41 at 95% reliability
  - Cold recycled mixtures:
    - a_{min}-value= 0.40 at 50% reliability
    - a_{min}-value= 0.28 at 95% reliability

APPENDIX A TESTING RESULT

Table A.1 SCB Test Results (Flexibility Index)

Flexibility Index (FI)																		
REPLICATE	**ARGG-1**	**ARGG-2**	**W-6428H-12.5**	**W-5828L**	**W-5834L**	**W-7628H-12.5**	**W-7034PH**	**W-7628H-9.5**	**W-5828H**	**W-6428H-9.5**	**B-6428H**	**B-5834L**	**B-5828H**	**BB-6428L**	**CM-1**	**CM-1-a**	**CM-2**	**CM-2-a**
N1	21.8	19.4	12.3	15.6	19.3	31.6	38.1	22.8	13.3	18.3	6.8	11.7	7.7	14.7	-	10.2	14.1	10.5
N2	15.7	8.8	18.1	15.1	19.2	16.2	49.6	23.3	-	17.7	6.5	5.6	20.2	9.6	-	16.5	30.2	10.4
N3	21.6	17.2	12.3	9.8	16.6	17.5	30.3	20.6	15.8	20.3	7.9	19.3	10.4	8.4	-	13.4	16.4	9.5
N4	17.0	16.5	16.2	11.9	16.7	-	-	19.1	13.8	22.3	5.5	16.5	20.4	4.9	-	-	23.0	12.1
Average	19.0	15.4	14.7	13.1	18.0	21.8	39.3	18.8	14.3	19.6	6.7	13.3	14.7	9.4	-	13.4	20.9	10.6
STDEV	3.1	4.6	2.9	2.8	1.5	8.5	9.7	9.1	1.3	2.1	1.0	6.0	6.6	4.1	-	3.1	7.2	1.1

Table A.2 SCB Test Results (Fracture Energy)

Fracture Energy (G_f)																		
REPLICATE	**ARGG-1**	**ARGG-2**	**W-6428H-12.5**	**W-5828L**	**W-5834L**	**W-7628H-12.5**	**W-7034PH**	**W-7628H-9.5**	**W-5828H**	**W-6428H-9.5**	**B-6428H**	**B-5834L**	**B-5828H**	**BB-6428L**	**CM-1**	**CM-1-a**	**CM-2**	**CM-2-a**
N1	1504.4	1992.6	1417.9	1311.6	1082.8	2998.8	1790.1	2393.1	1513.3	1207.4	1660.6	1332.1	1280.0	2254.5	135.0	737.1	490.0	753.0
N2	1553.7	1454.5	1788.0	1429.3	1210.5	3036.9	1784.9	2233.9	-	1150.3	1765.0	946.0	2221.6	2011.4	-	429.4	724.1	657.0
N3	1832.9	1474.6	1790.4	1415.2	1245.9	3100.1	1936.2	1959.1	1434.8	1278.5	1606.6	1560.7	1795.8	1638.6	194.0	335.2	429.0	633.0
N4	1566.0	1694.6	1792.4	1129.7	1166.6	2596.4	-	1914.1	1480.5	1092.1	1720.6	1404.2	1941.7	1167.0	194.0	-	621.0	590.5
Average	1614.2	1654.1	1697.2	1321.4	1176.4	2933.0	1837.1	2933.0	1476.2	1182.1	1688.2	1310.7	1809.8	1767.9	174.3	500.6	566.0	658.4
STDEV	148.2	250.5	186.2	138.2	70.4	228.3	85.9	228.3	39.4	79.7	69.2	261.2	394.9	474.0	34.1	210.2	132.4	68.8

Table A.3 Resilient Modulus Test Results (Mr)

Resilient Modulus (M_r) (psi)																		
REPLICATE	**ARGG-1**	**ARGG-2**	**W-6428H-12.5**	**W-5828L**	**W-5834L**	**W-7628H-12.5**	**W-7034PH**	**W-7628H-9.5**	**W-5828H**	**W-6428H-9.5**	**B-6428H**	**B-5834L**	**B-5828H**	**BB-6428L**	**CM-1**	**CM-1-a**	**CM-2**	**CM-2-a**
N1-0Deg	-	-	261643	277994	143998	410538	121904	250810	294224	168053	483621	204072	276152	396378	78968	78359	119130	136868
N1-90Deg	-	333684	249332	275950	131265	392804	-	256999	281013	197594	488216	220481	283785	361559	44434	72908	168054	207678
N2-0Deg	264010	365175	262703	238647	-	375009	116583	242351	314392	193849	475986	234657	326165	400793	74789	105772	85011	162092
N2-90Deg	260166	358815	-	234405	168935	389062	131887	227174	275263	171290	489267	-	422852	352980	64580	69325	91628	188190
N3-0Deg	-	-	250596	277433	176656	403600	120822	264825	280621	-	512361	213916	290946	450017	127358	-	140925	125826
N3-90Deg	-	335361	242630	244934	150003	403600	117815	250398	274078	188776	447571	209690	-	397950	128020	-	130767	130740
Average	262088	348258	253381	258227	154172	395769	121803	248759	286598	183912	482837	216563	319980	393279	86358	81591	122586	158566
STDEV	2718	16087	8586	20982	18501	12849	6038	12960	15380	13420	21134	11758	60611	34460	34167	16543	31154	33523

Table A.4 DCT Test Results (Fracture Energy)

Fracture Energy (G_f)														
REPLICATE	**ARGG-1**	**ARGG-2**	**W-6428H-12.5**	**W-5828L**	**W-5834L**	**W-7628H-12.5**	**W-7034PH**	**W-7628H-9.5**	**W-5828H**	**W-6428H-9.5**	**B-6428H**	**B-5834L**	**B-5828H**	**BB-6428L**
N1	998.7	1056.1	555.7	523.7	843.1	674.6	1664.0	849.3	684.5	651.6	508.8	652.1	582.0	1194.3
N2	980.6	932.7	641.2	597.4	801.2	632.3	1710.4	891.7	442.9	719.4	613.5	692.6	538.0	569.2
N3	853.4	961.3	694.0	596.8	959.0	831.6	1656.8	606.0	649.1	772.6	529.5	640.0	603.0	624.4
Average	944.3	983.4	630.3	572.6	867.8	712.8	1677.1	782.4	592.2	714.5	550.6	661.6	574.3	596.8
STDEV	79.2	64.6	69.8	42.4	81.7	105.0	29.1	154.2	130.5	60.7	55.4	27.5	33.2	39.1

Table A.5 DCT Test Results (Fracture Strain Tolerance)

Fracture Strain Tolerance (FST)														
REPLICATE	**ARGG-1**	**ARGG-2**	**W-6428H-12.5**	**W-5828L**	**W-5834L**	**W-7628H-12.5**	**W-7034PH**	**W-7628H-9.5**	**W-5828H**	**W-6428H-9.5**	**B-6428H**	**B-5834L**	**B-5828H**	**BB-6428L**
N1	212.6	212.6	115.7	118.7	157.5	124.4	296.1	170.9	167.8	148.4	110.9	140.8	134.3	218.7
N2	237.4	201.7	132.2	153.6	151.5	112.4	293.2	161.7	89.6	152.8	139.8	180.1	122.6	147.1
N3	202.9	198.9	133.0	158.7	167.2	159.8	305.6	129.8	136.7	198.4	120.1	130.2	144.5	144.4
Average	217.6	204.4	127.0	143.7	158.7	132.2	298.3	154.1	131.4	166.5	123.6	150.4	133.8	170.1
STDEV	17.8	7.2	9.8	21.8	8.0	24.6	6.5	21.6	39.4	27.7	14.8	26.3	11.0	42.2

Table A.6 SVECD Test Results

MIX		ARGG-1	ARGG-2	W-6428H-12.5	W-5828L	W-5834L	W-7628H-12.5	W-7034PH	W-7628H-9.5	W-5828H	W-6428H-9.5	B-6428H	B-5834L	B-5828H	BB-6428L	CM-1	CM-1-a	CM-2	CM-2-a
	$N_f@G^R = 100$	15765	5524	12563	18985	29611	40069	20302	21815	22104	22238	18343	16282	21552	17303	1863	9571	9448	8844
Parameter	D^R	0.38	0.27	0.45	0.41	0.49	0.54	0.81	0.66	0.53	0.54	0.33	0.31	0.35	0.39	0.54	0.67	0.62	0.60
	S_{app}	5.27	2.66	2.26	3.92	3.91	9.53	5.82	6.87	4.00	3.34	5.04	3.06	3.67	4.19	0.75	2.36	1.55	2.10
	$\boldsymbol{N_f@C^S_{N_f} = 100}$	15764	5523	12563	18985	29611	40069	20301	21815	22104	22237	18343	16282	21551	17302	1862	9571	9448	8843

Figure A.1 Damage Characteristic Curves

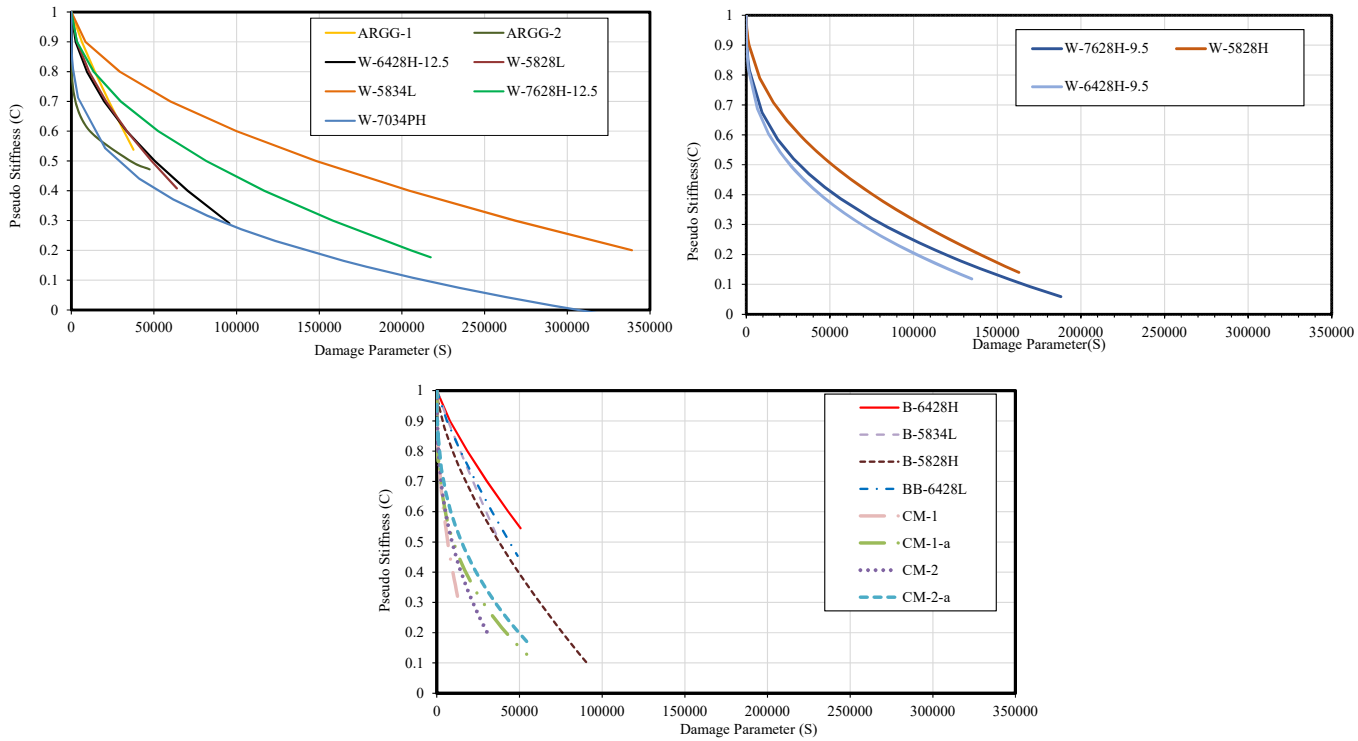

Table A.7 Dynamic Modulus Master-Curves

Pt. (No.)	Test Temperature (°C)	ARGG-1			ARGG-2			W-6428H-12.5			W-5828L		
		Shifted Frequency (Hz)	Complex Modulus (MPa)	Phase Angle (Degrees)	Shifted Frequency (Hz)	Complex Modulus (MPa)	Phase Angle (Degrees)	Shifted Frequency (Hz)	Complex Modulus (MPa)	Phase Angle (Degrees)	Shifted Frequency (Hz)	Complex Modulus (MPa)	Phase Angle (Degrees)
1	4.4	27.3	5014.9	17.6	37.6	5869.4	15.9	17.2	4774.4	24.2	31.8	4658.4	21.8
2	4.4	136.6	6477.4	14.9	188.1	7492.2	13.5	86.2	6863.8	19.2	159.3	6452.3	17.8
3	4.4	273.2	7148.4	13.6	376.2	8251.2	12.5	172.4	7887.4	17.4	318.7	7392.8	16.4
4	4.4	1366.4	8927.7	12.6	1881.4	10190.0	11.4	862.4	10325.7	14.6	1593.5	9368.9	13.7
5	4.4	2732.9	9703.3	11.9	3762.8	11094.0	11.0	1724.8	11403.0	13.2	3187.0	10309.5	12.8
6	4.4	6832.3	10750.9	10.4	9407.1	12138.9	10.2	4312.0	12852.5	11.8	7967.5	11576.6	12.3
7	21.1	0.10	1175.0	27.7	0.10	1319.9	27.6	0.10	768.6	34.6	0.10	809.0	33.5
8	21.1	0.50	1788.5	25.0	0.50	2044.3	25.2	0.50	1403.3	33.5	0.50	1375.8	31.7
9	21.1	1.0	2094.7	24.9	1.0	2416.6	24.4	1.0	1807.7	33.4	1.0	1707.6	31.9
10	21.1	5.0	3092.3	22.8	5.0	3535.6	21.9	5.0	3130.6	29.7	5.0	2810.0	28.5
11	21.1	10.0	3598.7	21.8	10.0	4117.5	20.8	10.0	3847.6	28.2	10.0	3398.8	26.9
12	21.1	25.0	4383.2	23.8	25.0	4984.0	19.1	25.0	4937.3	27.0	25.0	4310.8	22.9
13	37.8	1.09E-03	369.4	30.9	1.11E-03	383.5	33.0	1.43E-03	210.4	25.0	1.30E-03	227.6	30.8
14	37.8	5.46E-03	552.0	28.5	5.53E-03	593.4	29.9	7.13E-03	307.7	27.8	6.51E-03	353.5	30.5
15	37.8	1.09E-02	633.7	29.7	1.11E-02	694.1	31.3	1.43E-02	374.4	30.8	1.30E-02	418.9	31.9
16	37.8	5.46E-02	978.8	29.2	5.53E-02	1092.3	29.7	7.13E-02	659.5	35.3	6.51E-02	685.1	34.2
17	37.8	0.109216	1174.3	29.2	0.110504	1330.1	29.5	0.142513	862.8	36.9	0.130264	864.5	35.6
18	37.8	0.273039	1512.6	27.0	0.276259	1714.2	27.0	0.356283	1233.6	36.9	0.325661	1190.4	34.8

Pt. (No.)	Test Temperature (°C)	W-5834L			W-7628H-12.5			W-7034PH			W-7628H-9.5		
		Shifted Frequency (Hz)	Complex Modulus (MPa)	Phase Angle (Degrees)	Shifted Frequency (Hz)	Complex Modulus (MPa)	Phase Angle (Degrees)	Shifted Frequency (Hz)	Complex Modulus (MPa)	Phase Angle (Degrees)	Shifted Frequency (Hz)	Complex Modulus (MPa)	Phase Angle (Degrees)
1	4.4	15.7	2886.6	31.8	19.29468	7726.6	17.5	14.1	2356.5	28.9	23.8	4703.5	24.1
2	4.4	78.82	4727.7	26.5	96.47341	10176.4	14.0	70.6	3726.0	25.5	119.3	6784.0	19.4
3	4.4	157.6	5687.8	24.1	192.9468	11152.2	12.4	141.2	4443.7	24.0	238.6	7809.3	18.1
4	4.4	788.2	8400.5	19.9	964.7341	13887	10.8	706.2	6572.6	20.3	1193.4	10407.5	14.5
5	4.4	1576.4	9624.5	18.5	1929.468	15118.4	9.6	1412.5	7592.7	19.2	2386.9	11518.1	13.3
6	4.4	3941.1	11359.0	16.5	4823.67	16637.5	7.5	3531.4	8991.1	17.3	5967.4	13163.7	8.9
7	21.1	0.1	472.0	31.8	0.1	1365.1	34.1	0.1	494.7	27.9	0.1	724.2	34.7
8	21.1	0.5	796.5	34.0	0.5	2376.9	30.8	0.5	759.3	29.9	0.5	1260.2	33.5
9	21.1	1.0	1008.8	35.2	1.0	2949.8	30.5	1.0	930.2	32.2	1.0	1583.1	34.1
10	21.1	5.0	1872.7	35.2	5.0	4772.3	25.7	5.0	1593.3	32.7	5.0	2744.0	30.6
11	21.1	10.0	2404.7	34.1	10.0	5657.5	24.2	10.0	1988.7	32.8	10.0	3407.3	29.3
12	21.1	25.0	3275.8	32.9	25.0	6999.2	22.4	25.0	2665.4	33.2	25.0	4431.9	26.9
13	37.8	1.78E-03	207.5	21.1	1.44E-03	363.7	27.1	1.74E-03	246.0	18.4	1.65E-03	269.5	26.1
14	37.8	8.89E-03	254.1	22.1	7.22E-03	550.7	30.3	8.70E-03	296.4	21.8	8.27E-03	361.2	28.0
15	37.8	1.78E-02	292.6	24.3	1.44E-02	671.3	32.2	1.74E-02	321.8	24.7	1.65E-02	414.8	30.6
16	37.8	8.89E-02	440.5	30.2	7.22E-02	1195.0	34.3	8.70E-02	459.7	29.4	8.27E-02	675.4	34.2
17	37.8	0.177783	554.5	33.2	0.144376	1527.9	34.9	0.173913	550.0	32.0	0.16536	845.9	36.2
18	37.8	0.444459	778.4	37.4	0.360939	2118.8	34.0	0.434783	726.2	36.0	0.413401	1173.8	36.0

Pt. (No.)	Test Temperature (°C)	W-5828H			W-6428H-9.5			B-6428H			B-5834L		
		Shifted Frequency (Hz)	Complex Modulus (MPa)	Phase Angle (Degrees)	Shifted Frequency (Hz)	Complex Modulus (MPa)	Phase Angle (Degrees)	Shifted Frequency (Hz)	Complex Modulus (MPa)	Phase Angle (Degrees)	Shifted Frequency (Hz)	Complex Modulus (MPa)	Phase Angle (Degrees)
1	4.4	25.0	4831.3	22.2	27.8	3272.0	25.7	18.4	7448.2	18.5	19.48	4231.9	27.5
2	4.4	125.3	6763.0	18.1	139.0	4841.6	20.8	92.4	9808.7	15.1	97.44	6536.6	23.0
3	4.4	250.7	7675.3	16.8	278.1	5600.8	19.6	184.9	10810.5	13.3	194.8	7703.3	21.5
4	4.4	1253.9	10010.0	14.4	1390.9	7645.9	16.6	924.8	13380.9	11.6	974.4	10829.0	17.7
5	4.4	2507.9	11077.4	13.2	2781.9	8630.3	15.4	1849.7	14529.9	10.8	1948.8	12305.2	15.8
6	4.4	6269.8	12451.2	10.0	6954.8	9974.8	15.6	4624.3	15947.9	9.0	4872.0	14192.0	14.5
7	21.1	0.1	794.1	33.1	0.1	554.5	33.0	0.1	1535.4	32.1	0.1	642.7	33.0
8	21.1	0.5	1367.9	32.0	0.5	907.0	32.8	0.5	2595.4	28.5	0.5	1119.1	34.1
9	21.1	1.0	1697.1	31.9	1.0	1115.5	33.9	1.0	3185.3	28.1	1.0	1423.9	34.0
10	21.1	5.0	2807.0	29.2	5.0	1872.0	31.9	5.0	4975.3	23.6	5.0	2563.2	32.6
11	21.1	10.0	3431.8	28.4	10.0	2308.5	30.5	10.0	5888.4	21.7	10.0	3244.8	31.4
12	21.1	25.0	4387.3	27.0	25.0	3024.0	30.0	25.0	7203.5	23.2	25.0	4305.8	32.3
13	37.8	1.08E-03	229.7	22.9	1.21E-03	194.5	23.4	1.40E-03	351.8	29.4	1.58E-03	203.8	22.8
14	37.8	5.38E-03	320.0	25.7	6.05E-03	251.3	27.0	7.02E-03	580.4	31.8	7.91E-03	289.1	25.1
15	37.8	0.010764	375.0	28.6	1.21E-02	290.4	30.0	1.40E-02	734.4	33.1	1.58E-02	348.0	27.3
16	37.8	5.38E-02	622.4	32.4	6.05E-02	462.3	32.7	7.02E-02	1313.4	33.8	7.91E-02	563.9	32.7
17	37.8	0.107639	795.4	34.1	0.120951	571.0	35.0	0.140417	1676.6	33.7	0.158184	732.4	35.0
18	37.8	0.269098	1107.1	36.3	0.302378	769.4	38.0	0.351043	2284.8	33.0	0.39546	1053.1	36.0

Pt. (No.)	Test Temperature (°C)	B-5828H			BB-6428L			CM-1			CM-1-a		
		Shifted Frequency (Hz)	Complex Modulus (MPa)	Phase Angle (Degrees)	Shifted Frequency (Hz)	Complex Modulus (MPa)	Phase Angle (Degrees)	Shifted Frequency (Hz)	Complex Modulus (MPa)	Phase Angle (Degrees)	Shifted Frequency (Hz)	Complex Modulus (MPa)	Phase Angle (Degrees)
1	4.4	92.2	7265.0	19.2	108.5	6916.7	18.4	12.6	1928.1	22.9	17.9	2464.9	21.5
2	4.4	461.0	9728.1	15.4	542.6	9018.2	14.7	63.3	2730.3	19.8	89.5	3416.6	18.8
3	4.4	922.0	10753.4	14.2	1085.3	9912.5	13.7	126.7	3113.3	19.3	179.1	3881.3	18.1
4	4.4	4610.0	13620.3	12.1	5426.9	12302.8	11.6	633.8	4193.2	17.2	895.8	5094.1	15.7
5	4.4	9220.0	14790.9	11.7	10853.9	13230.3	10.6	1267.6	4703.5	16.3	1791.6	5664.3	14.8
6	4.4	23050.2	16537.5	12.0	27134.8	14595.8	9.9	3169.1	5423.6	16.1	4479.0	6431.8	16.6
7	21.1	0.1	1337.4	33.1	0.1	1098.7	31.7	0.1	514.8	27.4	0.1	670.4	26.1
8	21.1	0.5	2258.8	30.3	0.5	2038.2	29.2	0.5	776.8	26.7	0.5	988.4	25.8
9	21.1	1.0	2776.0	29.3	1.0	2505.3	28.1	1.0	921.3	27.0	1.0	1156.1	25.9
10	21.1	5.0	4382.9	26.0	5.0	3946.9	24.6	5.0	1420.4	26.6	5.0	1736.9	25.3
11	21.1	10.0	5249.5	24.4	10.0	4676.2	22.5	10.0	1692.8	26.1	10.0	2051.7	25.0
12	21.1	25.0	6476.5	18.0	25.0	5761.8	18.0	25.0	2103.3	26.0	25.0	2522.8	23.1
13	37.8	9.62E-04	300.5	27.1	1.37E-03	270.7	29.6	1.87E-03	193.4	19.6	2.29E-02	534.6	29.6
14	37.8	4.81E-03	452.4	30.0	6.84E-03	424.5	31.1	9.34E-03	290.1	22.7	4.57E-02	534.9	25.2
15	37.8	9.62E-03	564.5	32.1	1.37E-02	530.4	33.0	1.87E-02	326.9	25.4	0.22863	789.6	18.3
16	37.8	4.81E-02	992.1	34.4	6.84E-02	941.6	34.6	0.093389	493.6	29.0	0.457259	969.3	28.2
17	37.8	9.62E-02	1271.5	34.8	0.136735	1212.5	34.7	0.186779	594.8	30.0	1.143148	1212.7	32.3
18	37.8	0.240563	1759.6	36.0	0.341838	1681.4	33.9	0.466947	767.8	26.0	-	-	-

Pt. (No.)	Test Temperature (°C)	CM-2			CM-2-a		
		Shifted Frequency (Hz)	Complex Modulus (MPa)	Phase Angle (Degrees)	Shifted Frequency (Hz)	Complex Modulus (MPa)	Phase Angle (Degrees)
1	4.4	20.9	2185.9	21.0	27.1	3067.1	19.2
2	4.4	104.4	2996.3	18.4	135.5	4087.8	16.4
3	4.4	208.9	3376.0	17.8	271.1	4570.1	15.3
4	4.4	1044.3	4442.2	15.5	1355.5	5828.7	13.1
5	4.4	2088.6	4941.2	14.7	2711.0	6385.7	12.8
6	4.4	5221.5	5621.8	16.8	6777.4	7157.8	10.4
7	21.1	0.1	548.9	27.9	0.1	820.2	26.3
8	21.1	0.5	828.3	27.2	0.5	1223.7	24.9
9	21.1	1.0	976.4	27.4	1.0	1423.1	25.0
10	21.1	5.0	1492.8	26.2	5.0	2113.3	23.4
11	21.1	10.0	1760.6	25.4	10.0	2467.7	22.5
12	21.1	25.0	2185.3	21.7	25.0	3007.1	18.0
13	37.8	9.61E-03	344.3	24.9	7.45E-03	450.9	25.2
14	37.8	1.92E-02	345.7	28.5	1.49E-02	475.4	29.3
15	37.8	9.61E-02	517.8	29.9	7.45E-02	709.9	29.8
16	37.8	0.192213	621.6	30.6	0.149093	855.8	29.4
17	37.8	0.480531	805.5	30.7	0.372734	1095.6	30.0
18	37.8	-	-	-	-	-	-

Table A.8 New Developed Performance Index Parameters

MIX		ARGG-1	ARGG-2	W-6428H-12.5	W-5828L	W-5834L	W-7628H-12.5	W-7034PH	W-7628H-9.5	W-5828H	W-6428H-9.5	B-6428H	B-5834L	B-5828H	BB-6428L	CM-1	CM-1-a	CM-2	CM-2-a
Parameter	CMRI	407.2	905.9	194.2	190.6	138.1	353.6	121.2	180.0	171.9	118.5	468.6	193.7	358.3	580.7	128.3	270.9	141.2	212.5
	$N_f@C^S_{N_f} = 100$	15764	5523	12563	18985	29611	40069	20301	21815	22104	22237	18343	16282	21551	17302	1862	9571	9448	8843

RDCI																		
REPLICATE	ARGG-1	ARGG-2	W-6428H-12.5	W-5828L	W-5834L	W-7628H-12.5	W-7034PH	W-7628H-9.5	W-5828H	W-6428H-9.5	B-6428H	B-5834L	B-5828H	BB-6428L	CM-1	CM-1-a	CM-2	CM-2-a
N1	34.2	33.2	23.4	22.3	33.49	37.6	63.8	29.3	19.6	31.0	16.2	20.5	16.21	29.0	22.8	26.2	22.4	-
N2	31.4	21.1	34.4	32.5	34.4	30.9	69.4	41.2	26.6	32.9	12.1	10.9	39.36	20.9	38.6	21.6	-	20.9
N3	37.2	32.5	23.1	19.2	30.4	37.1	63.9	36.6	21.7	36.6	17	28.2	23.15	15.5	31.8	17.1	-	18.8
N4	31.6	31.0	31.2	21.9	32.4	18.0	-	36.8	-	39.8	9.9	30.0	32.06	9.7	-	-	40.6	23.4
Average	33.64	29.52	28.08	24.05	32.71	30.97	65.72	36.03	22.36	35.1	13.82	24.44	27.7	18.82	31.0	21.6	31.5	21.1
STDEV	2.7	5.6	5.7	5.9	1.7	9.1	3.2	4.9	3.6	3.9	3.4	11.5	10.1	8.2	7.9	4.6	12.9	2.3

Table A.9 Field IRI Performance

Year	ARGG-1 (Epping)	ARGG-1 (Seabrook)	ARGG-2 (Bow-Hooksett)	ARGG-2 (Spaulding Turnpike)	W-6428H-12.5 (Milford-Amherst)	W-5828L (Woodstock-Lincoln)	W-5828L (Bethlehem)	W-5834L (Pittsburg)	W-7628H-12.5 (Hudson-Windham at Park ave)	W-7628H-12.5 (Lebanon)	W-7034PH (Bethlehem-Carroll)	W-7034PH (Barrington-Rochester)
	IRI (inch/mile)											
2012	-	-	-		49.15	-	-	-	-	-	-	-
2013	-	-	32.20	40.91	51.62	43.29	49.22	-	58.30	-	52.28	78.79
2014	-	-	33.59	44.51	53.85	43.94	-	-	57.27	-	56.64	-
2015	41.80	67.59	35.17	46.09	-	45.58	57.37	59.43583	-	80.53	57.70	105.81
2016	43.40	68.55	-	47.05	53.71	-	-	-	59.75	-	59.28	-
2017	46.55	71.94	37.29	49.10	-	47.28	60.18	65.32143	66.00	98.91	61.43	116.16

Year	W-7628H-9.5 (Meredith)	W-5828H (Shelburne)	W-5828H (Gilford)	W-5828H (Alton)	W-6428H.9.5 (Lincoln)
	IRI (inch/mile)				
2012	-	-	-	-	-
2013	102.71	33.94	79.12	108.05	66.30
2014	119.19	34.95	-	-	-
2015	130.61	37.15	99.43	144.62	68.35
2016	131.37	36.11	-	-	-
2017	132.40	37.91	116.78	140.85	73.28

Table A.10 Cross Sections

ARGG-1 (Epping)	ARGG-1 (Seabrook)	ARGG-2 (Bow-Hooksett)	ARGG-2 (Spaulding Turnpike)	W-6428H-12.5 (Milford-Amherst)
2" ARGG-1	1.5" ARGG-1	1.5" ARGG-2	1.5" ARGG-2	1.5" wearing asphalt
1" binder asphalt	1.5" Macadam	0.5" binder asphalt	3" Macadam	3" binder asphalt
2.5" base asphalt	4" crushed stone (coarse)	2.5" base asphalt	4" crushed stone (coarse)	12" crushed gravel
6" crushed stone (fine)	28" gravel	14" crushed gravel	28" gravel	12"gravel
6" crushed stone (coarse)	Subgrade	12"gravel	Subgrade	12" sand
12"-30.5" sand		Subgrade		Subgrade
Subgrade				

W-5828L (Woodstock-Lincoln)	W-5828L (Bethlehem)	W-5834L (Pittsburg)	W-7628H-12.5 (Hudson-Windham at Park ave)	W-7628H-12.5 (Lebanon)
3" wearing asphalt	1.5" wearing asphalt	1.25" wearing asphalt	3" wearing asphalt	2" wearing asphalt
2" binder asphalt	3" wearing (existing)	0.5" leveling course	1.5" binder asphalt	1" binder asphalt
11" crushed gravel	21"gravel	4" cold mixture	8"crushed gravel	2.5" base asphalt
12"gravel	Subgrade	12" reclaimed base course	8"gravel	8"crushed gravel
Subgrade		Subgrade	20" sand	8"gravel
			Subgrade	8" sand

W-7034PH (Bethlehem-Carroll)	W-7034PH (Barrington-Rochester)	W-7628H-9.5 (Meredith)	W-5828H (Shelburne)	W-5828H (Gilford)
0.75" PMA overlay	1" wearing	1" wearing (SHS)	1" overlay	1" overlay
1.5" hot in-place recycled	4"crushed gravel	3" Macadam surface course	0.5" Leveling	3" binder course
1.5" binder	12"gravel	4" crushed stone base course	1" wearing asphalt	24" gravel
8" crushed gravel	Subgrade	18" gravel	2" binder asphalt	Subgrade
12"gravel		Subgrade	8" crushed gravel	
12" sand			8" gravel	
Subgrade			8"sand	
			Subgrade	

W-5828H (Alton)	W-6428H.9.5 (Lincoln)
1" Overlay	1"overlay
0.5" Leveling	1" wearing asphalt
1.25" wearing asphalt	2" binder asphalt
1.75" binder asphalt	8" crushed gravel
8" crushed gravel	8" gravel
8" gravel	8" sand
8" sand	Subgrade
Subgrade	